CONCRETE BEAMS with OPENINGS

Analysis and Design

M. A. Mansur
Kiang-Hwee Tan

CONCRETE BEAMS with OPENINGS

Analysis and Design

New Directions in Civil Engineering

Series Editor

W. F. CHEN
Purdue University

Zdeněk P. Bažant and Jaime Planas
Fracture and Size Effect in Concrete and Other Quasibrittle Materials

W.F. Chen and Seung-Eock Kim
LRFD Steel Design Using Advanced Analysis

W.F. Chen and E.M. Lui
Stability Design of Steel Frames

W.F. Chen and K.H. Mossallam
Concrete Buildings: Analysis for Safe Construction

W.F. Chen and S. Toma
Advanced Analysis of Steel Frames: Theory, Software, and Applications

W.F. Chen and Shouji Toma
Analysis and Software of Cylindrical Members

Y.K. Cheung and L.G. Tham
Finite Strip Method

Hsai-Yang Fang
Introduction to Environmental Geotechnology

Yuhshi Fukumoto and George C. Lee
Stability and Ductility of Steel Structures under Cyclic Loading

Ajaya Kumar Gupta
Response Spectrum Method in Seismic Analysis and Design of Structures

C.S. Krishnamoorthy and S. Rajeev
Artificial Intelligence and Expert Systems for Engineers

Boris A. Krylov
Cold Weather Concreting

M.A. Mansur and Kiang-Hwee Tan
Concrete Beams with Openings: Analysis and Design

Pavel Marek, Milan Gustar and Thalia Anagnos
Simulation-Based Reliability Assessment for Structural Engineers

N.S. Trahair
Flexural-Torsional Buckling of Structures

Senol Utku
Theory of Adaptive Structures: Incorporating Intelligence into Engineered Products

Jan G.M. van Mier
Fracture Processes of Concrete

S. Vigneswaran and C. Visvanathan
Water Treatment Processes: Simple Options

CONCRETE BEAMS with OPENINGS

Analysis and Design

M. A. Mansur
Department of Civil Engineering
National University of Singapore

Kiang-Hwee Tan
Department of Civil Engineering
National University of Singapore

CRC Press
Boca Raton London New York Washington, D.C.

Library of Congress Cataloging-in-Publication Data

Mansur, M. A.
Concrete beams with openings : analysis and design / M.A. Mansur, Kiang-Hwee Tan.
p. cm.
Includes bibliographical references and index.
ISBN 0-8493-7435-9
1. Concrete beams—Design and construction. 2. Prestressed concrete beams—Design and construction I. Tan, Kiang-Hwee. II. Title.
TA683.5.B3M36 1999
624.1'83423—dc21 98-51792
CIP

International Standard Book Number 0-8493-7435-9
Library of Congress Card Number 98-51792
Printed in the United States of America 1 2 3 4 5 6 7 8 9 0
Printed on acid-free paper

Preface

Transverse openings in concrete beams represent, from a practical viewpoint, a means of accommodating utility services in a building structure. The ability to accommodate such services through a member instead of below or above the member results in a compact design and an overall saving in terms of total building height.

Provision of openings through a beam, however, changes its simple mode of behavior to a more complex one. Therefore, the design of such beams needs special treatment, which currently falls beyond the scope of the major building codes. Only the Architectural Institute of Japan provides some guidelines for the design of concrete beams with web openings. Nevertheless, the treatment is far from being complete, and most of the information on concrete beams with openings that has been generated around the world since the early 1960s remains scattered and is not readily accessible to the designers.

The purpose of this book is to compile the state-of-the-art information on the behavior, analysis, and design of concrete beams that contain transverse openings through the web. The behavior of such beams under bending, shear, and torsion is treated in this book. Design methods based on plastic hinge mechanism, plasticity truss and strut-and-tie models, and skew-bending theory are described and illustrated with numerical examples. Suitable guidelines on the detailing of beams with web openings are also included. This information would not only give valuable guidance to the designers and consultants of concrete structures but also would help researchers in the planning and proper execution of future research programs in this area.

In writing this book, it is presumed that the reader is familiar with the fundamentals of reinforced and prestressed concrete design. No specific code of practice has been followed. The main emphasis is on the basic underlying principles for the treatment of openings through beams.

The text is organized into six chapters. Chapter 1 introduces the topic of openings through beams by illustrating the need for openings, effects of introducing an opening, classification of openings, and the general requirements that need to be fulfilled in design. Chapters 2 – 5 give a comprehensive coverage on reinforced

concrete beams. While Chapter 2 provides a complete treatment of a beam with small openings under different loading combinations, Chapter 3 mainly deals with large rectangular openings in beams under the most commonly encountered loading case of combined bending and shear. The effects of torsion in such beams are treated in Chapter 4. Large openings in continuous beams, their effects on possible redistribution of internal forces and, general guidelines, and procedure for the complete design of such beams are presented in Chapter 5. Chapter 6 deals with the effect of prestressing.

While we have put in our best effort to compile the state-of-the-art knowledge on openings through concrete beams, the readers must exercise their engineering judgment in applying the principles laid out in this book.

We would like to take this opportunity to express our sincere thanks and appreciation to our families, friends and colleagues for their inspiration and encouragement to write this book. In particular, we wish to thank Farooq, Iftekhar, Mandal, Rashid, B.C. Sit, K.L. Tan, and B.K. Teoh, who proofread and assisted in the preparation of the camera-ready manuscript, and Roni, who drew many of the figures. We also thank ACI, AIJ, ASCE, PCI, CI-Premier, Elsevier Science Ltd., and Nem Chand & Bros. for granting permission to reproduce some of the figures and tables from their publications.

We believe that *Concrete Beams with Openings: Analysis and Design* will be a valuable source of information and a useful guide, especially to designers and practicing engineers as little or no provisions or guidelines are currently available in most codes of practice.

M.A. Mansur
Kiang-Hwee Tan
National University of Singapore

To
the memory of my parents
and
Shireen and Roni
for their love, care, and understanding

Mansur

To
my beloved wife, Yoke Lin
and children, Hui Leng, Siah Hong, and Hui Xing

Kiang-Hwee

Contents

PREFACE v

NOTATION xiii

CHAPTER 1. INTRODUCTION

1.1 GENERAL INTRODUCTION 1
1.2 CLASSIFICATION OF OPENINGS 3
1.3 ELASTIC STRESS DISTRIBUTION AROUND OPENINGS 4
1.4 DESIGN CONSIDERATIONS 6

CHAPTER 2. BEAMS WITH SMALL OPENINGS

2.1 GENERAL INTRODUCTION 7
2.2 PURE BENDING 7
2.3 BENDING AND SHEAR 12
2.3.1 Behavior of Beams in Shear 12
2.3.2 Traditional Design Approach 16
2.3.3 AIJ Approach 26
2.3.4 Plasticity Truss Method 28
2.4 EFFECT OF TORSION 37
2.4.1 Behavior of Beams in Torsion 37
2.4.2 Analysis for Ultimate Strength 40
2.5 DESIGN FOR TORSION 51
2.5.1 Design for Beam-Type Failure 52
2.5.2 Design for Frame-Type Failure 55
2.5.3 Considerations for Detailing 56

2.6 EFFECT OF CREATING OPENINGS IN EXISTING BEAMS 61
2.6.1 Cracking and Crack Widths 63
2.6.2 Stiffness and Deflection 66
2.6.3 Ultimate Strength 68
2.6.4 Remarks 68

CHAPTER 3. BEAMS WITH LARGE RECTANGULAR OPENINGS

3.1 GENERAL INTRODUCTION 71
3.2 BEAM BEHAVIOR UNDER BENDING AND SHEAR 77
3.3 ANALYSIS AT COLLAPSE 80
3.3.1 Limit Analysis 80
3.3.2 Plasticity Truss Model 94
3.3.3 Strut-and-Tie Model 97
3.4 DESIGN FOR ULTIMATE STRENGTH 100
3.4.1 Plastic Hinge Method 100
3.4.2 Plasticity Truss Method 113
3.4.3 Strut-and-Tie Method 115
3.5 CRACK CONTROL 119
3.6 CALCULATION OF DEFLECTIONS 124
3.7 MULTIPLE OPENINGS AND DESIGN OF POSTS 127

CHAPTER 4. TORSION IN BEAMS WITH RECTANGULAR OPENINGS

4.1 GENERAL INTRODUCTION 131
4.2 PURE TORSION 132
4.2.1 Behavior of Beams in Pure Torsion 132
4.2.2 Outline of Analysis 135
4.2.3 Analysis for Ultimate Torque 138
4.2.4 Experimental Verification 147
4.2.5 Simplified Design Method 149
4.3 TORSION COMBINED WITH BENDING 152
4.4 COMBINED TORSION, BENDING, AND SHEAR 158

CHAPTER 5. CONTINUOUS BEAMS

5.1 GENERAL INTRODUCTION 161
5.2 ELASTIC ANALYSIS 162
5.2.1 Equivalent Flexural Stiffness 164
5.2.2 Equivalent Shear Stiffness 164
5.2.3 Member Stiffness and Transfer Matrix 166
5.2.4 Analysis Procedure 167
5.2.5 Comparison with Test Data 167

5.3 DESIGN PROCEDURE AND RECOMMENDATIONS 171
5.3.1 General Guidelines 171
5.3.2 Recommended Design Procedure 172

CHAPTER 6. EFFECT OF PRESTRESSING

6.1 GENERAL INTRODUCTION 187
6.2 STRESS CONCENTRATION AND STRESS DISTRIBUTION 188
6.2.1 Normal Stresses 189
6.2.2 Shear Stresses 190
6.3 TYPES OF CRACKING AND CRACK CONTROL 191
6.3.1 Cracking Due to Prestressing Force at Transfer 192
6.3.2 Cracking Around the Openings at Service Load 196
6.4 DEFLECTIONS 206
6.5 DESIGN AND DETAILING FOR ULTIMATE STRENGTH 207
6.5.1 General Detailing Requirements and Recommendations 207
6.5.2 Check for Ultimate Strength 208

REFERENCES 213

INDEX 217

Notation

All symbols are defined in the text where they first appear. The more frequently used symbols and those that appear throughout the book are listed below for ready reference.

a	=	depth of equivalent rectangular stress block
A	=	cross-sectional area
A_c	=	area enclosed by the perimeter of the section following the shape of stirrups
A_d, A_{sd}	=	area of diagonal reinforcement
A_ℓ	=	area of total longitudinal reinforcement to resist torsion
A_s, A'_s	=	area of bottom and top longitudinal steel, respectively, in a section
$A_{t,min}$	=	area (one leg) of minimum closed stirrup for torsion
A_v, A_{sv}	=	area of stirrups per stirrup spacing
A_w	=	area of one leg of stirrup
b	=	width of beam
b_w	=	web width
C	=	compressive stress resultant
c	=	distance from extreme compression fiber to neutral axis
d	=	effective depth
d_o	=	diameter of circular opening or depth of rectangular opening
d_v, d_{vs}	=	distance between the top and bottom longitudinal steel, respectively, in a section
e, e_o	=	eccentricity of an opening with respect to the longitudinal axis of the beam
E_c, E_s	=	modulus of elasticity of concrete and steel, respectively
F	=	prestressing force
f'_c	=	cylinder compressive strength of concrete
f_r	=	modulus of rupture of concrete
f_s	=	stress in reinforcement or allowable stress in steel
f_t	=	maximum vertical tensile stress
f_y, f_{yd}	=	yield strength of longitudinal, diagonal steel, respectively

f_{yv} (or f_{yw})	=	yield strength of transverse steel (stirrups)
G	=	modulus of rigidity
h	=	overall depth of a section
I	=	moment of inertia
I_g	=	gross moment of inertia
jd	=	level arm
k	=	effective length factor for compression member
ℓ_e	=	effective length of an opening
ℓ_o	=	length of opening
ℓ_u	=	unsupported length of compression member
M	=	bending moment
M_b, M'_b	=	moments at balanced failure under positive and negative bending, respectively
M_m	=	applied moment at center of opening
M_n	=	nominal moment of resistance
M_o, M'_o	=	nominal (ultimate) moment of resistance in positive and negative bending, respectively
M_u	=	factored moment
M_1, M_2, M_3	=	nominal strength of a section in positive, lateral, and negative bending, respectively
m	=	M/M_o
N	=	axial load
N_b, N'_b	=	axial compressive loads at balanced failure corresponding to M_b and M'_b, respectively
N_o, N'_o	=	ultimate strength of a section in axial compression and axial tension, respectively
N_u	=	factored axial load
n	=	N/N_o or modular ratio
p_c	=	perimeter of section following the shape of stirrups
P	=	axial load or point load
P_c	=	critical axial load
P_n	=	nominal axial load strength at given eccentricity
P_o	=	nominal axial load strength at zero eccentricity
P_u	=	factored axial load at given eccentricity
r	=	radius of gyration
s	=	spacing of stirrups in direction parallel to longitudinal reinforcement
T	=	torsional moment or tensile stress resultant
T_s	=	vertical splitting tensile force
T_n	=	nominal torsional strength
T_o	=	strength of a section under pure torsion
T_u	=	factored torsional moment at a section
T_1, T_2, T_3	=	nominal torsional strength in Mode 1, Mode 2, and Mode 3 failure, respectively
t	=	T/T_o

t_f = flange thickness
V = shear force
V_c = nominal shear strength provided by concrete
V_n = nominal shear strength
V_m = applied shear force at center of opening
V_o = strength of a section under pure shear
V_s = nominal shear strength provided by shear reinforcement
V_u = factored shear force at section
v = V/V_o
w = uniform load
x = shorter dimension of a rectangular section
x_1 = shorter center-to-center dimension of closed rectangular stirrup
y = longer dimension of a rectangular section
y_1 = longer center-to-center dimension of closed rectangular stirrup
z = distance between the plastic centroids of the chord members
α = angle of inclination of diagonal bars (stirrups) or web reinforcement to longitudinal axis
β_1 = factor for depth of equivalent rectangular stress block
δ = deflection
ν = effectiveness factor
ρ_v = web reinforcement ratio
ρ_w = reinforcement ratio
υ = Poisson's ratio
ϕ = capacity (strength) reduction factor
ψ = shear reinforcement index

Subscripts

b = bottom chord
t = top chord

Reinforcement designation

Two numerals and the letters *M* or *T* are used to designate the reinforcing steel bars. The letter *M* stands for mild steel bars, while *T* refers to high-yield steel bars. The numerals preceding and following the letter symbols designate the number and diameter (in mm) of bars, respectively.

1 Introduction

1.1 GENERAL INTRODUCTION

In the construction of modern buildings, many pipes and ducts are necessary to accommodate essential services like water supply, sewage, air-conditioning, electricity, telephone, and computer network. Fig. 1.1 shows a view of the typical layout of pipes for a high-rise building. Usually, these pipes and ducts are placed underneath the soffit of the beam and, for aesthetic reasons, are covered by a suspended ceiling, thus creating a "dead space." In each floor, the height of this dead space that adds to the overall building height depends on the number and depth of ducts to be accommodated. The depth of ducts or pipes may range from a couple of centimeters to as much as half a meter.

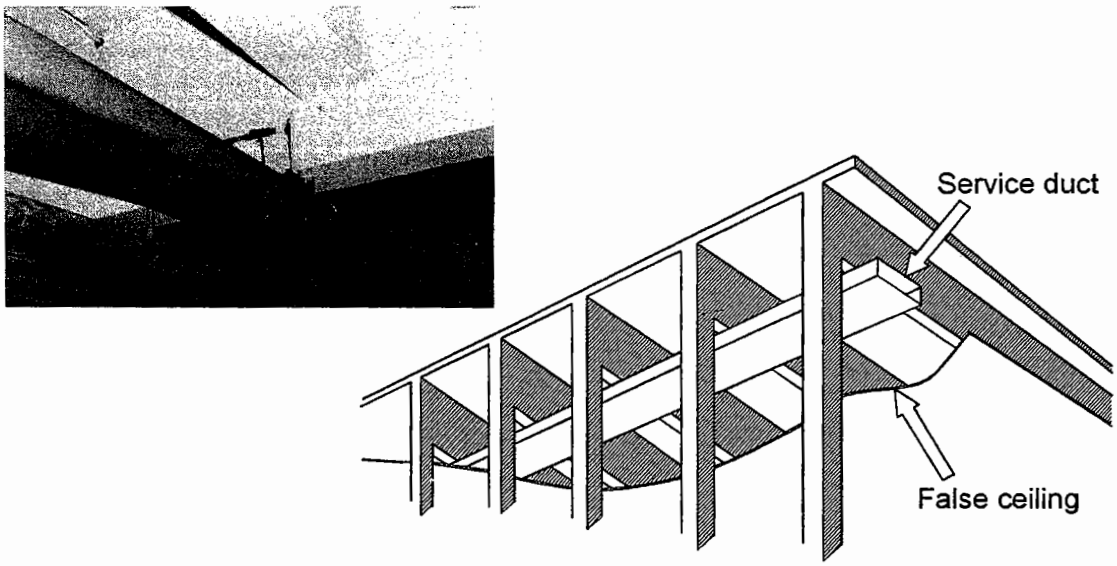

Figure 1.1 Typical layout of service ducts and pipes.

An alternative arrangement is to pass these ducts through transverse openings in the floor beams. As shown in Fig. 1.2, this arrangement of building services leads to a significant reduction in the headroom and results in a more compact design. For small buildings, the savings thus achieved may not be significant compared to the overall cost. But for multistory buildings, any saving in story height multiplied by the number of stories can represent a substantial saving in total height, length of air-conditioning and electrical ducts, plumbing risers, walls and partition surfaces, and overall load on the foundation.

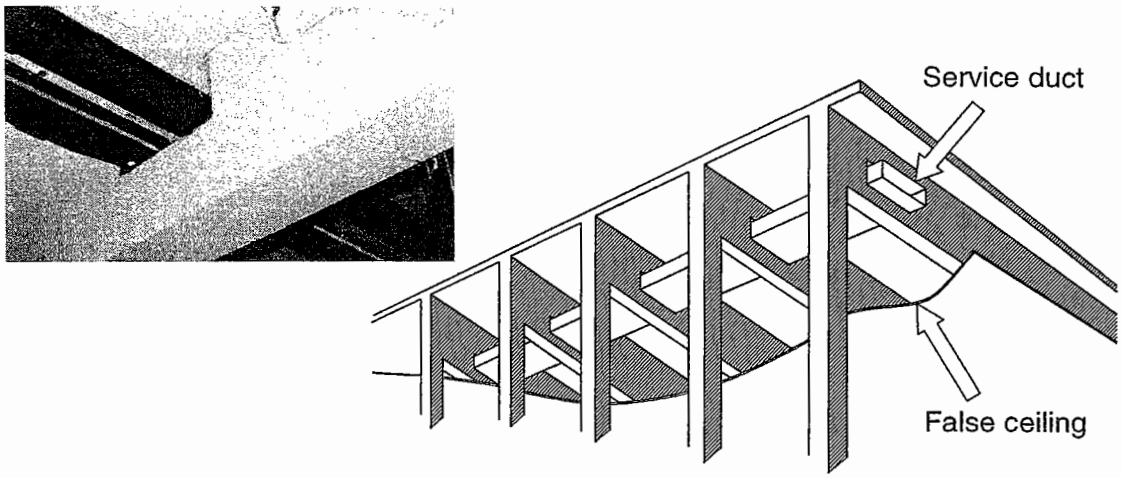

Figure 1.2 Alternative arrangement of service ducts and pipes.

It is due to economy and a growing trend toward the use of systems approach to building design that structural engineers are often required to keep provisions for transverse openings in beams. Most engineers permit the embedment of small pipes, provided some additional reinforcement is used around the periphery of the opening. But when large openings are encountered, particularly in reinforced or prestressed concrete members, they show a general reluctance to deal with them because adequate technical information is not readily available. There is also a lack of specific guidelines in building codes of practice (ACI, 1995; BS 8110-97), although they contain detailed treatment of openings in floor slabs. As a result, designs are frequently based on intuition, which may lead to disastrous consequences. There is at least one case on record, described by Merchant (1967), in which the failure of a large building was averted when severe distress at a large opening in the stem of a beam was discovered and mitigated in time.

It is obvious that inclusion of openings in beams alters the simple beam behavior to a more complex one. Due to an abrupt change in the cross-sectional dimensions of the beam, the opening corners are subject to high stress concentration that may lead to wide cracking that is unacceptable from aesthetic and durability viewpoints. The reduced stiffness of the beam may also give rise to excessive deflection under service load and result in a considerable redistribution of internal forces and moments in a continuous beam. Unless special reinforcement is provided in sufficient quantity, the strength of such a beam may be reduced to a critical degree.

1.2 CLASSIFICATION OF OPENINGS

Transverse openings in beams may be of different shapes and sizes. Prentzas (1968), in his extensive experimental study, considered openings of circular, rectangular, diamond, triangular, trapezoidal and even irregular shapes, as shown in Fig. 1.3. Although numerous shapes of openings are possible, circular and rectangular openings are the most common ones. Circular openings are required to accommodate service pipes, such as for plumbing and electrical supply. On the other hand, air-conditioning ducts are generally rectangular in shape, and they are accommodated in rectangular openings through beams. Sometimes the corners of a rectangular opening are rounded off with the intention of reducing possible stress concentration at sharp corners, thereby improving the cracking behavior of the beam in service.

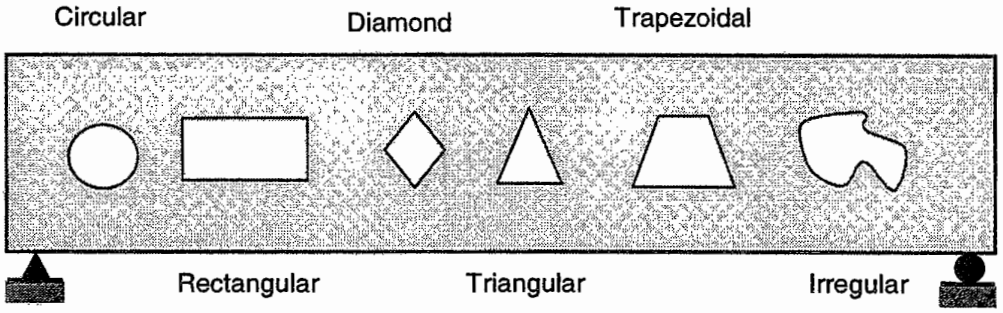

Figure 1.3 Opening shapes considered by Prentzas (1968).

With regard to the size of openings, many researchers use the terms *small* and *large* without any definition or clear-cut demarcation line. Mansur and Hasnat (1979) have defined openings circular, square, or nearly square in shape as small openings, whereas, according to Somes and Corley (1974), a circular opening may be considered as large when its diameter exceeds 0.25 times the depth of the beam web. However, the authors consider that the essence of classifying an opening as either small or large lies in the structural response of the beam. When the opening is small enough to maintain the beam-type behavior or, in other words, if the usual beam theory applies, then the opening may be termed a small opening. When beam-type behavior ceases to exist due to the provision of openings, then the opening may be classified as a large opening.

According to the above criterion, the definition of an opening being small or large depends on the type of loading. For example, if the opening segment is subject to pure bending, then beam theory may be assumed to be applicable up to a length of the compression chord beyond which instability failure takes place. Similarly, for a beam subject to combined bending and shear, test data reported in the literature (Prentzas, 1968; Mansur et al., 1985, 1990; Nasser et al., 1967) have shown that the beam-type behavior transforms into a Vierendeel truss action as the size of opening is increased. Some guidelines for identifying whether an opening is large or small are given in subsequent chapters when dealing with different types of loading and load combinations.

1.3 ELASTIC STRESS DISTRIBUTION AROUND OPENINGS

The distribution of stresses and, hence, the problem of stress concentration around an opening has been treated analytically by a number of investigators, notably by Savin (1951), Heller (1951, 1953), and Bower (1966a, 1966b). They used the method of elasticity, which assumes that the material is homogeneous and isotropic, and follows Hook's Law. Typical results for circular openings are presented in Fig. 1.4.

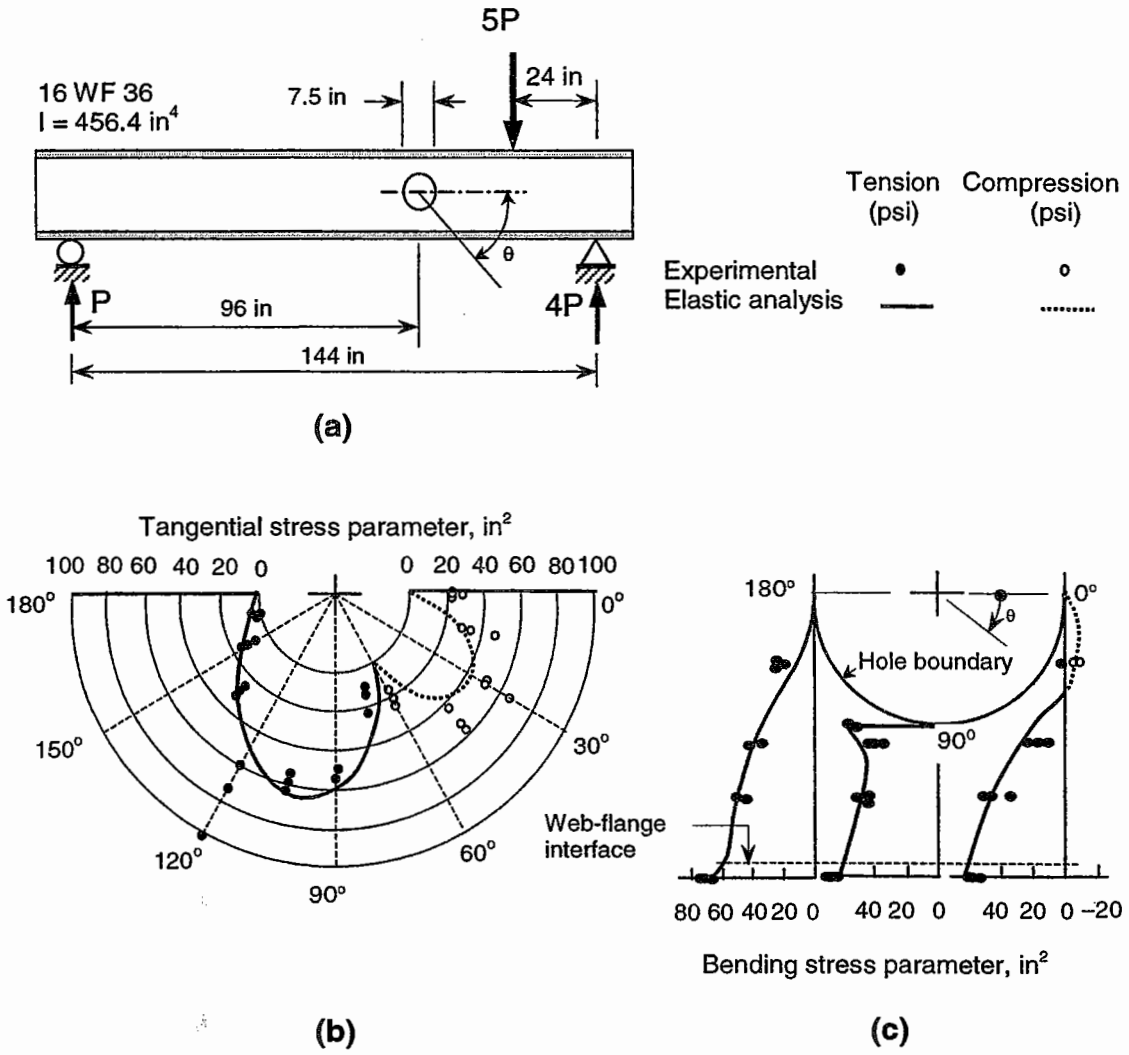

Figure 1.4 Stress distribution around a circular opening at a bending-shear ratio of 7.2 (a) test beam; (b) tangential stress parameter; and (c) bending stress parameter (Bower, 1966b).

Savin (1951) dealt specifically with the stresses around small openings in beams subject to pure bending. Heller (1951, 1953) extended the same concept to oval-shaped holes and later to square holes in beams subject to bending and shear. Bower (1966a) applied the elasticity approach to the case of relatively large

openings, both circular and rectangular, in flanged steel beams. They all employed the same basic technique in which a semi-inverse function, expressed as a complex variable, is first derived and then solved to give mathematically correct stresses at opening boundaries.

Bower (1966a, 1966b) obtained the results for circular opening in the beam shown in Fig. 1.4(a). Fig. 1.4(b) shows the distribution of tangential stress parameter together with test data while the variation of the bending stress parameter with distance from the hole boundary at three different cross sections are shown in Fig. 1.4(c). These figures are valid for a bending-shear stress ratio of 7.2 at the center of opening. It may be seen that tensile stresses of considerable magnitude occur at the hole boundary. Similar results for rectangular openings (Douglas and Gambrell, 1974) are presented in Fig. 1.5.

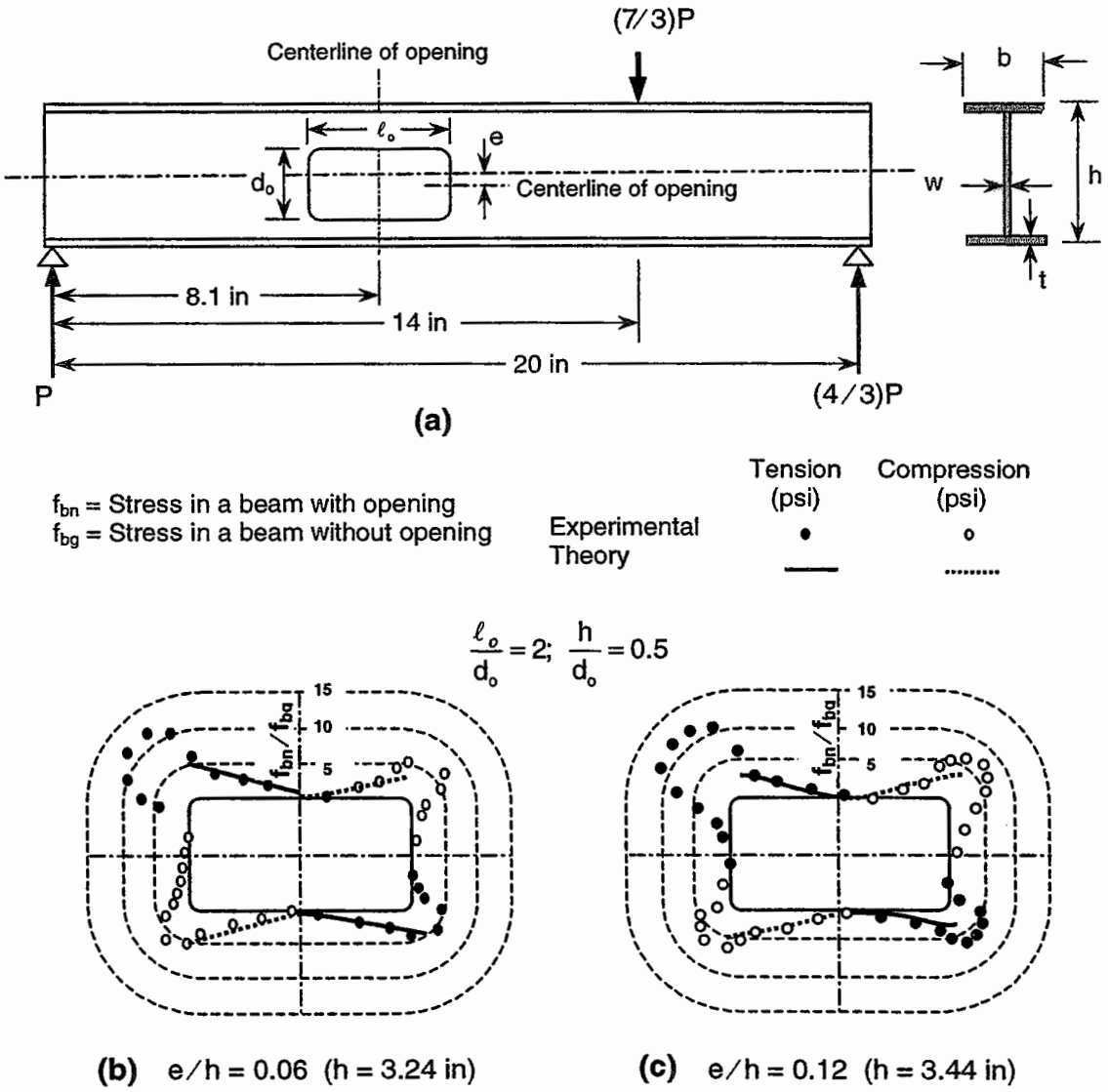

Figure 1.5 Stress distribution around a rectangular opening (a) test beam (b) and (c) normal stress tangent to opening (Douglas and Gambrell, 1974).

Although these results are not directly applicable to reinforced concrete once cracking occurs, they do provide a qualitative picture of the distribution of stresses that would exist prior to cracking, because at this stage concrete may be assumed to behave in an elastic manner with a reasonable degree of accuracy. This helps to identify the location and direction of potential cracking, which eventually leads to the development of an effective reinforcement scheme for the opening region. For example, the existence of high tensile stresses in the diagonally opposite corners of the opening calls for the use of diagonal reinforcement perpendicular to the direction of principal tensile stresses at those corners for effective control of cracking and to avoid possible premature failure of the beam.

1.4 DESIGN CONSIDERATIONS

In the design of a concrete beam with web openings, the usual acceptance criteria for structural members should apply. These are basically the strength and serviceability requirements. An accurate assessment of ultimate strength is necessary to provide adequate safety against possible collapse. Serviceability, in general, requires that the deflection produced under working loads be sufficiently small and cracking, if any, be controlled with maximum crack width not exceeding some tolerable limits. However, due to the provision of transverse openings, the usual design procedure for solid beams is not applicable to beams with openings. For example, the indirect way of satisfying the serviceability requirement of maximum deflection by ensuring a minimum span-to-effective depth ratio is not valid for beams with openings.

In a statically determinate structure, bending moment and shear force distributions are uniquely defined by statics alone. In statically indeterminate structures, however, the distribution of internal forces and moments depends on the relative stiffness of each individual member. Provision of openings through a member reduces its stiffness relative to others and causes a redistribution of internal actions from what is obtained by analyzing the structure, assuming prismatic members. This possible redistribution due to the provision of openings should be taken into account in the analysis of a statically indeterminate structure.

In prestressed concrete beams, it is also necessary to evaluate the effects of prestress on cracking around the opening to fulfill the crack control requirements both at transfer of prestress and at full service load. All the above aspects need to be addressed properly before a satisfactory design method for beams with transverse openings can evolve.

2
Beams with Small Openings

2.1 GENERAL INTRODUCTION

As discussed in Chapter 1, openings that are circular, square, or nearly square in shape may be considered as small openings provided that the depth (or diameter) of the opening is in a realistic proportion to the beam size, say, about less than 40% of the overall beam depth. In such a case, the beam action may be assumed to prevail. Therefore, analysis and design of a beam with small openings may follow the course of action similar to that of a solid beam. The provision of openings, however, produces discontinuities or disturbances in the normal distribution of stresses, thus leading to stress concentration and early cracking around the opening region. Special reinforcement should therefore be provided in sufficient quantity to contain the width of cracks to tolerable limits and prevent possible premature failure of the beam.

In this chapter, the simplest case of pure bending is treated first. This is followed by the most commonly encountered loading case of combined bending and shear. The effects of torsion are brought up at a later stage when considering the general case of combined torsion, bending, and shear. The problem is then reduced to combined torsion and bending by eliminating the effects of shear and, finally, to pure torsion by dropping the effects of bending moment and shear force. The last section in this chapter highlights the effects of creating an opening in existing beams.

2.2 PURE BENDING

Let us consider a solid beam that is subject to pure bending. At ultimate, the beam will exhibit a well-developed pattern of cracks, as shown in Fig. 2.1(a). Being initiated at the tensile face when the extreme fiber stress exceeds the flexural tensile strength of the concrete, the cracks would propagate vertically upward and extend up to the neutral axis, as shown. According to the usual flexural strength theory, the strain and stress distributions across a section at collapse are shown in

Fig. 2.1(b). The tensile stress resultant, T, and the compressive stress resultant, C, form a couple exactly equal to the applied moment at collapse.

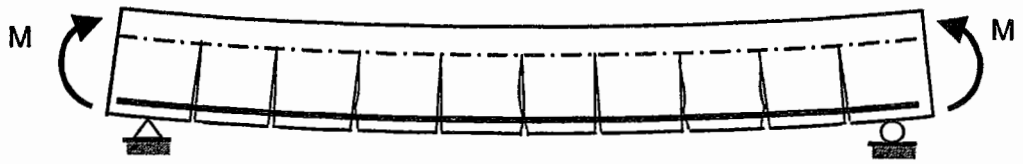

(a) Beam without openings

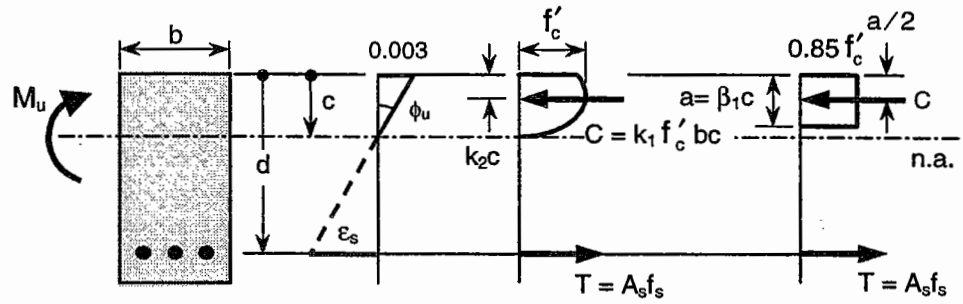

(b) Conditions at collapse

Figure 2.1 Beam subject to pure bending.

If the beam section shown in Fig. 2.1(b) is assumed to be under-reinforced, that is, the steel reinforcement yields at failure, and if the actual compressive stress block at nominal bending strength is replaced by Whitney's equivalent rectangular stress block, then T and C may be obtained as follows:

$$T = A_s f_y \tag{2.1}$$

$$C = 0.85 f'_c ba \tag{2.2}$$

where A_s = area of tensile reinforcement; f_y = yield strength of tensile reinforcement; f'_c = cylinder compressive strength of concrete; b = width of the section; and a = depth of rectangular compressive stress block.

The horizontal equilibrium, that is, $C = T$ gives

$$a = \frac{A_s f_y}{0.85 f'_c b} \tag{2.3}$$

With this value of a, the assumption that steel reinforcement yields at failure (that is, the assumption of an under-reinforced section) may be checked from Bernoulli's

hypothesis of plane sections before bending remaining plane after bending. The nominal flexural strength, M_n, is then obtained from moment equilibrium as

$$M_n = A_s f_y \left(d - \frac{a}{2} \right) \tag{2.4}$$

which, on substituting Eq. (2.3), reduces to

$$M_n = A_s f_y \left(d - 0.59 \frac{A_s f_y}{f_c' b} \right) \tag{2.5}$$

Eq.(2.5) may be rewritten as

$$\frac{M_n}{b d^2 f_c'} = q_s (1 - 0.59 q_s) \tag{2.6a}$$

in which

$$q_s = \frac{A_s}{bd} \frac{f_y}{f_c'} \tag{2.6b}$$

Now consider that a transverse opening of any shape is introduced in the same beam, as shown in Fig. 2.2(a). It is obvious that the provision of opening will not alter the load-carrying mechanism as long as the opening remains within the tension zone of the beam because concrete there would have cracked anyway in flexure at ultimate. As a result, the ultimate strength of the beam will not be affected by the presence of opening. This has been confirmed by several researchers in the past (Salam, 1977; Tan et al., 1996) who have noted that the strength of a beam with openings would remain the same as that of the corresponding solid beam provided that the openings do not reduce the concrete area necessary for the development of the compressive stress block at ultimate. Due to reduced moment of inertia at a section through the opening, however, cracks will initiate at an earlier stage of loading; however, such early initiation of cracking has only marginal effect on crack widths and deflection.

It follows from the preceding discussion that there will be no reduction in the ultimate moment capacity of the beam if the minimum depth of the compression chord, h_c, is greater than or equal to the depth of compressive stress block, a, that is, when

$$h_c \geq \frac{A_s f_y}{0.85 f_c' b} \tag{2.7}$$

If the opening is placed in such a way that it cuts material from the compression zone and thereby reduces the concrete area required for the development of the full compressive stress block at ultimate, that is, when the depth of the compression chord, $h_c < a$, the reduced area of concrete in compression should be taken into account in design. Example Problem 2.1 illustrates the strength analysis of such a beam.

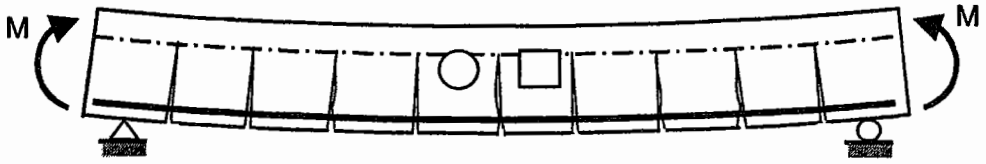

(a) Beam with small openings

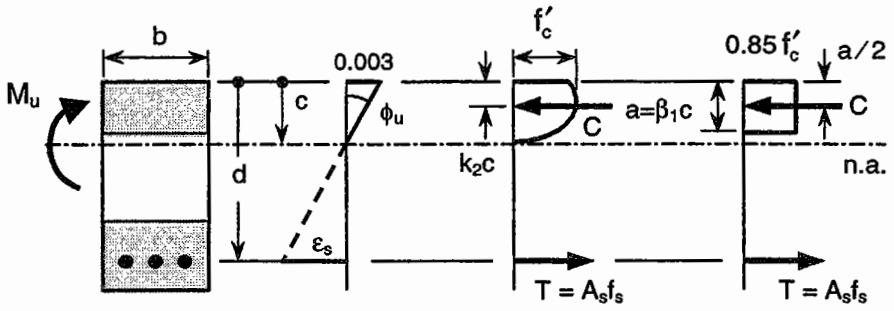

(b) Conditions through the opening at collapse

Figure 2.2 Beam with openings under pure bending.

EXAMPLE PROBLEM 2.1

The reinforced concrete beam segment of Fig. E2.1.1 contains a 200 mm-diameter circular opening located 100 mm above the centroidal axis of the beam. It is subject to pure bending. The sectional dimensions of the beam together with the amount and arrangement of reinforcement are shown in Fig. E2.1.1. Calculate the nominal flexural strength of (a) the solid section, and (b) the section through the opening. Assume f'_c = 25 MPa, f_y = 460 MPa, and E_s = 200 GPa.

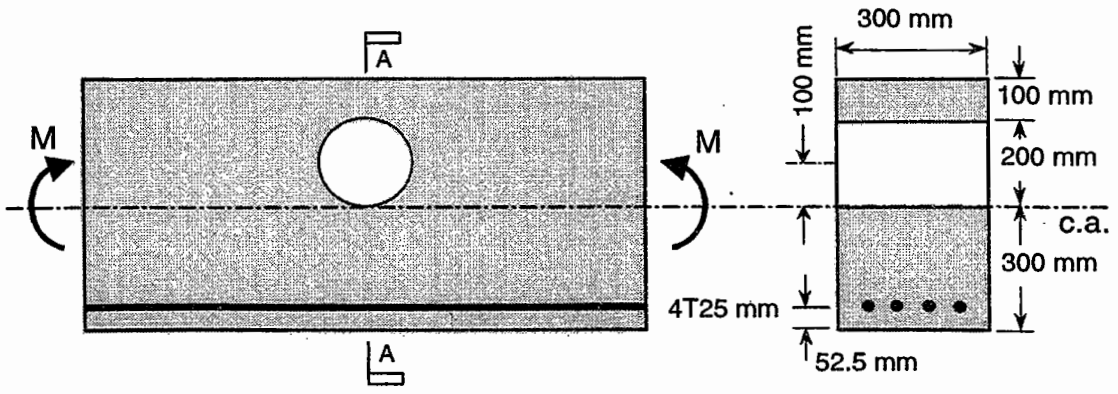

(a) Beam segment (b) Section A-A

Figure E2.1.1 Beam in Example Problem 2.1.

SOLUTION

(a) Solid Section

Assume that the steel bars have already yielded when the nominal ultimate strength is reached. The internal stress resultants C and T may be obtained as follows:

$$C = 0.85 f_c' ba = 0.85 \times 25 \times 300 \times a = 6375\, a$$

$$T = A_s f_y = 1960 \times 460 = 901.6 \times 10^3 \text{ N}$$

For equilibrium, $C = T$; therefore,

$$a = 901.6 \times 10^3 / 6375 = 141 \text{ mm}$$

$$\beta_1 = 0.85 \text{ for } f_c' = 30 \text{ MPa} \quad \text{[Refer to ACI Code (1995)]}$$

The neutral axis position is

$$c = a/\beta_1 = 141/0.85 = 166 \text{ mm}$$

The strain in the tensile steel when the compressive strain of 0.003 is reached at the extreme fiber is

$$\varepsilon_s = 0.003\left(\frac{d-c}{c}\right)$$

$$= 0.003\left(\frac{547.5-166}{166}\right) = 0.069$$

The yield strain of steel reinforcement is given by

$$\varepsilon_y = f_y / E_s = (460/200)\ 10^{-3} = 0.0023 < \varepsilon_s = 0.069$$

When the nominal flexural strength is reached ε_s is about 3 times ε_y, the yield strain of reinforcing bars. This means that the beam will deflect considerably before it finally fails by crushing of the concrete. The assumption that steel yields at failure is, therefore, valid.

The nominal flexural strength, therefore, is given by

$$M_n = C(d - a/2) \text{ or } T(d - a/2)$$
$$= 901{,}600\ (547.5 - 141/2)/10^6 = 430 \text{ kNm}$$

(b) Section through Opening

In this case, minimum depth of the compression chord is 100 mm, which is less than the depth, a (=141 mm) of rectangular stress block required for yielding of steel [Refer to Part (a)].

The compressive stress resultant is

$$C = 0.85\, f'_c\, b\,(100) = 0.85 \times 25 \times 300 \times 100 = 637.5 \times 10^3 \text{ N}$$

For equilibrium, $T = C$

$$T = A_s f_s = 637.5 \times 10^3 \text{ N}$$

Therefore, the stress in steel is

$$f_s = 637.5 \times 10^3 / 1960 = 325 \text{ MPa}$$

Since $f_s < f_y$, the section through the opening will be over-reinforced in flexure despite the equivalent solid section being under-reinforced.

The nominal flexural strength is

$$M_n = C(d - h_c/2) \text{ or } T(d - h_c/2)$$
$$= 637.5 \times 10^3\,(547.5 - 100/2)/10^6 = 317 \text{ kNm}$$

The beam thus will fail at the opening section. Evidently, the beam will exhibit much smaller curvature and, hence, smaller deflection, prior to reaching the full potential capacity of the solid section. Had the opening been located leaving 141 mm deep concrete above the opening, there would not have been any reduction either in strength or in ductility of the section through the opening.

2.3 BENDING AND SHEAR

2.3.1 BEHAVIOR OF BEAMS IN SHEAR

In a beam, shear is always associated with bending moment, except for the section at inflection point. In a homogeneous elastic beam, such as a concrete beam prior to cracking, the presence of shear changes the direction of principal tensile stress from a horizontal direction to a direction inclined to the longitudinal axis of the beam. Since concrete is weak in tension, this diagonal tensile stress eventually leads to what is basically known as diagonal tension failure of a beam. When the beam is provided with too much shear reinforcement, failure may also occur by crushing of the concrete in a diagonal direction, known as diagonal compression failure. The full details of the behavior of a solid beam in shear can be found in any standard textbook on structural concrete.

When a small opening is introduced in the web of a beam under-reinforced in shear, test data reported by Hanson (1969), Somes and Corley (1974), Salam (1977), and Weng (1998) indicate that the mode of failure remains essentially the same as that of a solid beam. Since the opening represents a source of weakness, however, the failure plane always passes through the center of the opening, except when the opening is very close to the support so as to bypass the potential inclined failure plane. Fig. 2.3 shows schematically some typical shear failures of beams containing square and circular openings as reported by Hanson (1969) and Somes and Corley (1974), respectively, and summarized by Mansur (1998).

Hanson (1969) at PCA laboratory tested a series of longitudinally reinforced T-beams representing a typical joist floor. The specimens contained square openings and were tested in an inverted position under a central point load to simulate the joists on either side of a continuous support. The major parameters considered in the study were the size, d_o, and horizontal (from the edge of the central stub) and vertical (from the compression face of the beam) locations, X and Y, respectively, of the opening. A similar study was reported by Somes and Corley (1974) but, in that case, the openings were circular in shape.

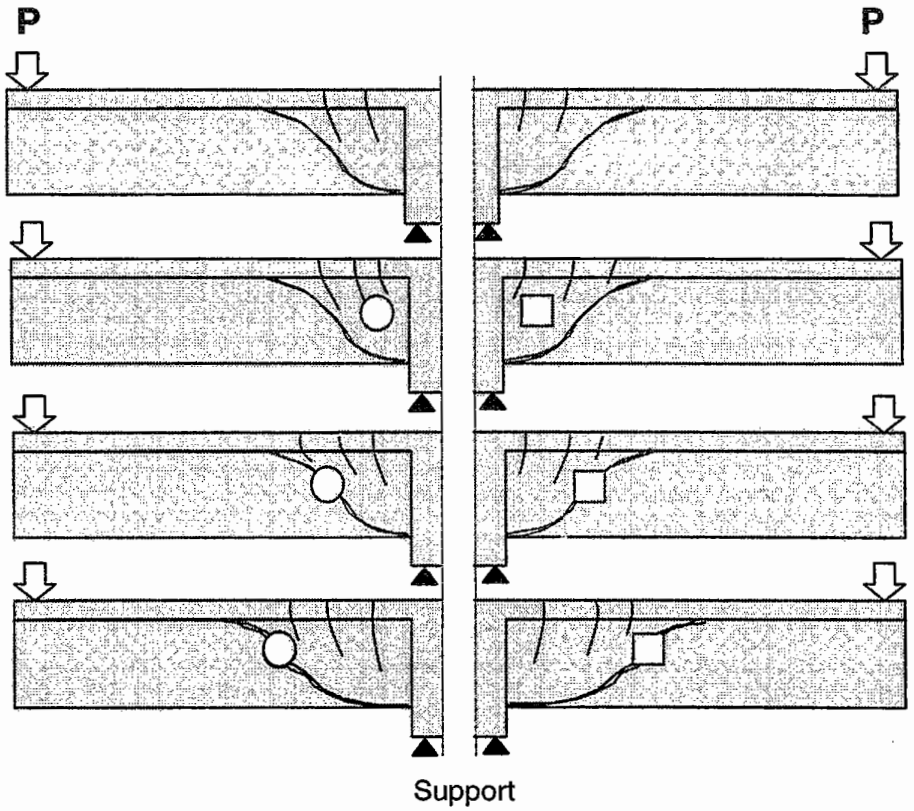

Figure 2.3 Typical shear failure of a beam without shear reinforcement (Mansur, 1998).

The effect of horizontal location, X, of an opening on nominal shear strength, $V_u / (\sqrt{f'_c}\, b_w d)$, of the beam in these investigations is summarized in Fig. 2.4(a), in which V_u is the ultimate shear strength of the beam in kN, f'_c is the concrete cylinder strength in MPa, b_w is the width of the web in mm, and d is the effective depth in mm. An opening located adjacent to the simulated continuous support produced no reduction in strength. As the opening is moved away from the support, gradual reduction in strength occurs until it levels off to a constant value. Test data suggests that the vertical position of opening has no significant effect, while an increase in the size of opening leads to an almost linear reduction in strength [Fig. 2.4(b)]. However, there appears to be a size of opening below which

no reduction in shear strength occurs. This size corresponds to about 20% and 30% of the beam depth for square and circular openings, respectively. They have also noted that the strength of such a beam may be fully restored by providing stirrups on either side of the opening.

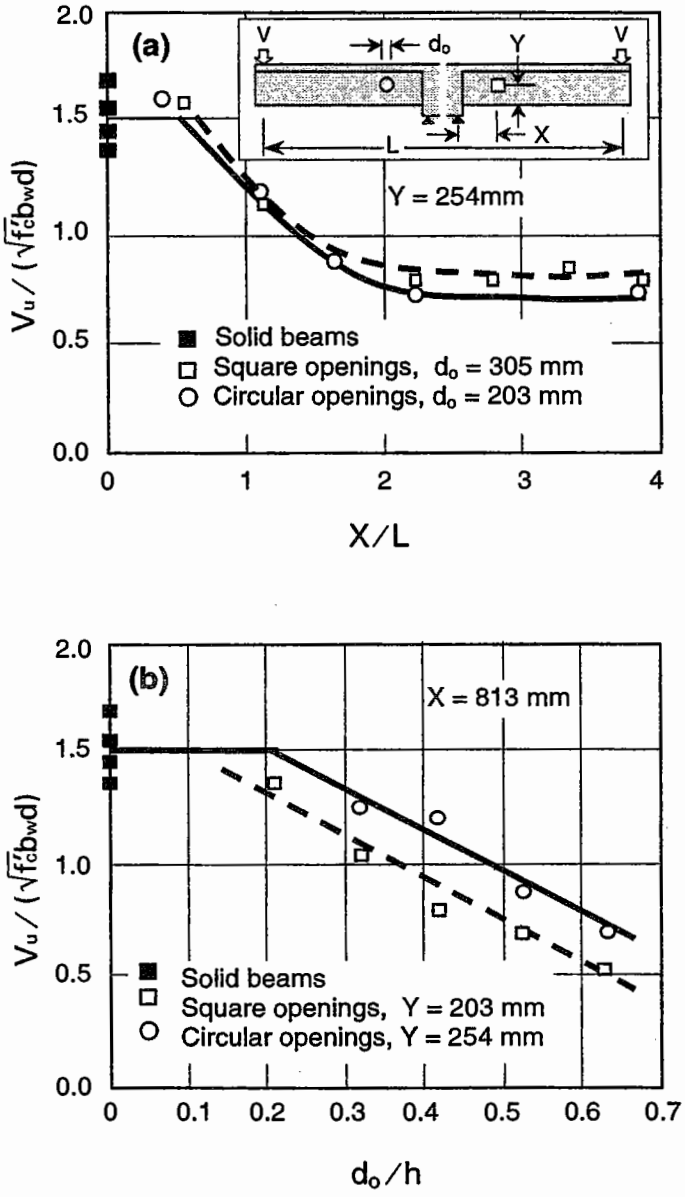

Figure 2.4 Effects of (a) horizontal location and (b) size of opening on shear strength of a beam without shear reinforcement (Mansur, 1998).

Salam (1977) conducted an investigation on reinforced concrete perforated beams of rectangular cross section tested under two symmetrical point loads. The study was mainly aimed at devising a reinforcement scheme suitable for restoring the strength to the same level as that of the corresponding solid beam. The

reinforcement schemes and the beam details employed are shown in Fig. 2.5. Salam found that, in addition to the longitudinal reinforcement above and below the opening and full depth stirrups by its sides, short stirrups in the members both above and below the opening (as in Beam B6) are necessary to eliminate the weakness due to the provision of opening. In his study, Salam (1977) also noted that when sufficient reinforcement (as in Beam B4) is provided to prevent a failure along a diagonal crack passing through the center of opening and traversing the entire depth (see Fig. 2.3), the failure is then precipitated at the minimum section. In such a case, formation of two independent diagonal cracks in the members above and below the opening splits the beam into two separate segments, thus leading to the final failure. Fig. 2.6 shows the cracking pattern of Beam B4 that failed in this manner.

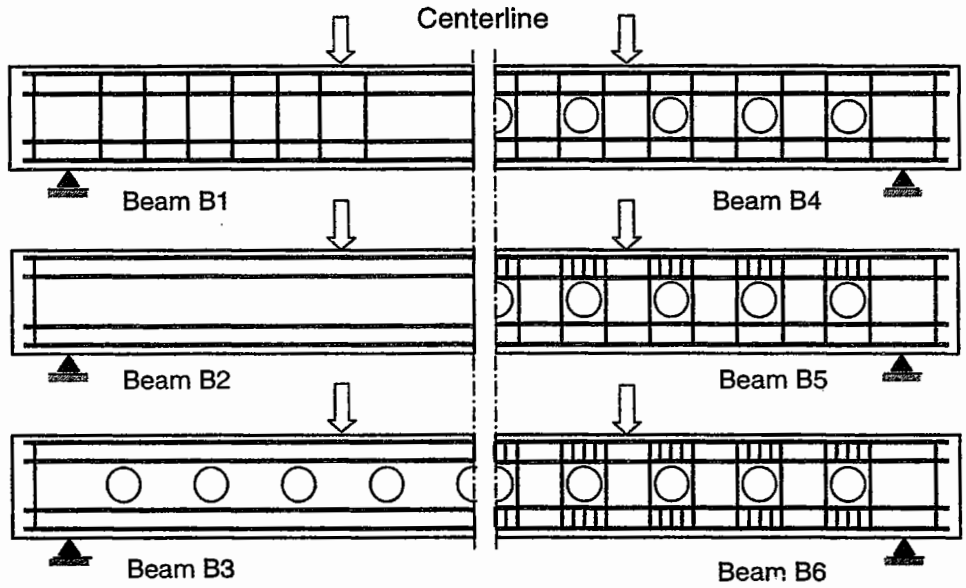

Figure 2.5 Reinforcement schemes for beams with openings (Salam, 1977).

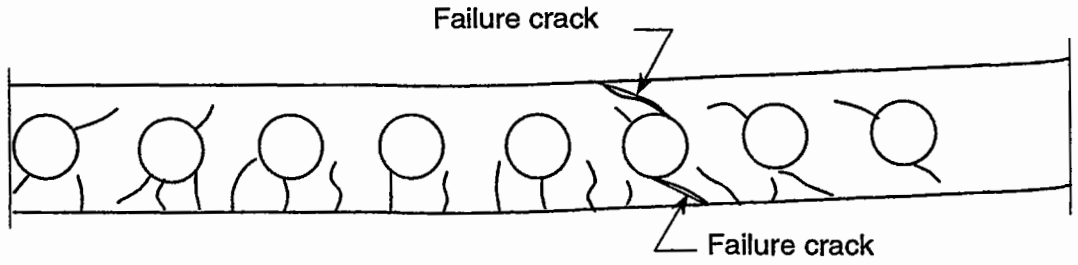

Figure 2.6 Shear failure of Beam B4 at the throat section (Salam, 1977).

2.3.2 TRADITIONAL DESIGN APPROACH

According to the traditional design philosophy, bending moment and shear force are treated separately. A section subject to combined bending and shear, therefore, is designed first for bending. The longitudinal reinforcement thus arrived at is then taken into account in the design of transverse reinforcement for shear because it indirectly contributes to the shearing resistance. The total resistance to shear is considered to be supplied by two components, concrete and transverse reinforcement. The former combines the shear resistance provided by the concrete compression zone, aggregate interlock action, and dowel action of longitudinal bars through an inclined crack. It is generally taken as the strength of a beam without shear reinforcement. When the factored shear force exceeds the resistance provided by the concrete, reinforcement is provided using a 45° truss model to take care of the balance. The following sections give a brief review of the shear design method for slender concrete beams specified in the ACI Code (1995) and explore the applicability of a similar approach to beams containing a small opening.

2.3.2.1 Shear Strength of Beams without Shear Reinforcement

Beams without openings

To estimate the nominal shear (inclined cracking) strength, V_c, of a beam without shear reinforcement, the ACI Code (1995) suggests two alternative methods: the detailed method and the simplified method.

(a) *Detailed method*. The detailed method makes an attempt to include the effect of concrete strength, dowel action of longitudinal bars, and the moment-to-shear ratio at the section on ultimate shear strength. The equation predicting the shear strength of a beam is given as

$$V_c = \frac{1}{6}\left(\sqrt{f'_c} + 100\frac{\rho_w V_u d}{M_u}\right) b_w\, d \le 0.3\sqrt{f'_c}\, b_w d \qquad (2.8)$$

in which V_u = factored shear force; M_u = factored moment; ρ_w = reinforcement ratio = $A_s / (b_w d)$; b_w = web width; and d = effective depth. According to the Code, the value of $V_u d / M_u$ shall not be taken greater than 1.0 except when axial compression is present.

(b) *Simplified method*. Since the above equation is not so simple to use as a design equation, and because of the wide scatter of shear test data, the ACI Code permits use of the following simple equation:

$$V_c = \frac{1}{6}\sqrt{f'_c}\, b_w d \qquad (2.9)$$

In the case of continuous beams, ACI-ASCE Committee 426 (1973) recommends the use of Eq. (2.9) instead of Eq. (2.8).

Although Eq. (2.9) has been found to be conservative, recent studies have shown otherwise when ρ_w is below 0.012. For values of ρ_w smaller than 0.012, the following equation is suggested:

$$V_c = (0.07 + 8.3\rho_w)\sqrt{f'_c}\, b_w d \tag{2.10}$$

Beams with openings

When the beam contains a small opening, Mansur (1998) proposed that the term d in Eq. (2.9) be replaced by the net depth, $(d - d_o)$, irrespective of vertical and horizontal location of the opening. The nominal shear strength of a beam without shear reinforcement, but containing a small opening thus becomes

$$V_c = \frac{1}{6}\sqrt{f'_c}\, b_w (d - d_o) \tag{2.11}$$

Eq. (2.11) is applicable for beams made up of normal-weight concrete. For light-weight concrete beams, an average reduction factor of 0.8 may be assumed, as suggested in the ACI Code (1995).

The applicability of Eq. (2.11) was tested by Mansur (1998) against the results reported by Hanson (1969) and Somes and Corley (1974). The comparison presented in Fig. 2.7 shows that Eq. (2.11) gives conservative prediction of shear strength for the entire range of test data. Although the specimens with openings closer to the supports exhibited considerably higher strength than the prediction of Eq. (2.11), such enhancement in shear strength is generally ignored in design. Therefore, Eq. (2.11) may be used for shear strength prediction of a longitudinally reinforced concrete beam containing a small transverse opening.

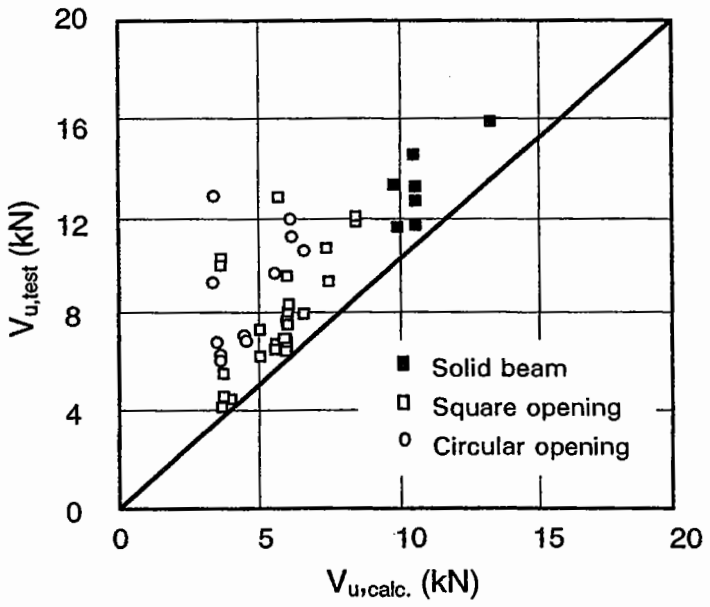

Figure 2.7 Comparison of Eq. (2.11) with test data (Mansur, 1998).

2.3.2.2 Shear Strength of Beams with Shear Reinforcement

Beams without openings

The traditional ACI approach to design for shear strength is to consider the total nominal shear strength, V_n, as the sum of two components as

$$V_n = V_c + V_s \tag{2.12}$$

in which V_c is the shear strength of the beam attributable to the concrete and V_s is the shear strength attributable to the shear reinforcement.

The expression for V_s has been derived using a 45° truss model as shown in Fig. 2.8. It is assumed that all stirrups yield at failure. For stirrups inclined at an angle α with the horizontal, the shear strength attributable to the reinforcement can be derived as

$$V_s = \frac{A_v f_{yv} (\sin\alpha + \cos\alpha) d}{s} \tag{2.13}$$

in which A_v is the area of the shear reinforcement within a distance s, and f_{yv} is the yield strength of the shear reinforcement.

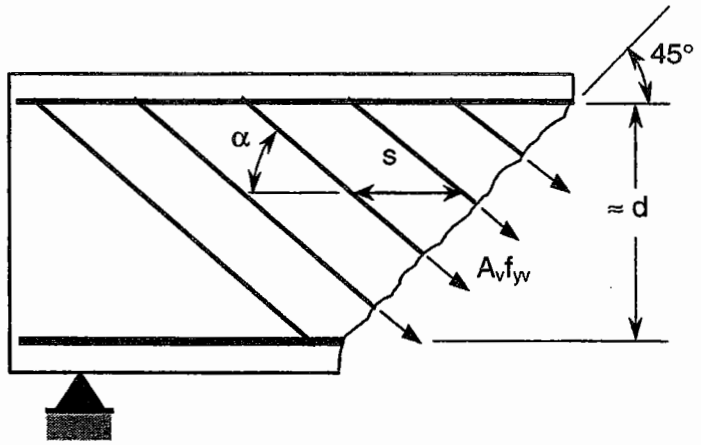

Figure 2.8 Shear strength V_s provided by shear reinforcement.

When vertical stirrups are used, that is, when $\alpha = 90°$, Eq. (2.13) reduces to

$$V_s = \frac{A_v f_{yv} d}{s} \tag{2.14}$$

In the ACI strength design method for shear (1995), it is required that

$$\phi V_n \geq V_u \tag{2.15}$$

where V_u is the factored shear force, and ϕV_n is the design strength in shear. The strength reduction factor ϕ is 0.85 for shear. The nominal shear strength is given by Eq. (2.12).

For vertical stirrups only, the design equation may be obtained from Eqs. (2.12), (2.14), and (2.15) as

$$\frac{A_v}{s} = \left(\frac{\frac{V_u}{\phi} - V_c}{f_{yv} d} \right) \tag{2.16}$$

in which V_c is given by either Eq.(2.9) or Eq. (2.10), whichever is applicable.

Minimum shear reinforcement. In order to avoid a sudden and explosive failure, ACI Code (1995) requires that a minimum amount of shear reinforcement be provided whenever V_u exceeds $0.5\phi V_c$. This amount is given by

$$\left[\frac{A_v}{s} \right]_{min} = \frac{1}{3} \frac{b_w}{f_{yv}} \tag{2.17}$$

Maximum spacing of stirrups. For shear reinforcement to function effectively without any localized failure before the load-carrying mechanism is fully established, some limitations on maximum spacing of stirrups must be followed. Assuming that V_c is given by Eq. (2.9), ACI Code (1995) limits the stirrup spacing as follows:

When $0.5\phi V_c < V_u \leq 3\phi V_c$

$$s_{max} = \frac{d}{4} \leq 600 \text{ mm} \tag{2.18a}$$

When $3\phi V_c < V_u \leq 5\phi V_c$

$$s_{max} = \frac{d}{4} \leq 300 \text{ mm} \tag{2.18b}$$

Maximum shear. In order to ensure yielding of steel reinforcement when the failure strength in shear is reached and, hence, avoid web crushing failure, the upper limit of factored shear is given by

$$[V_u]_{max} = 5\phi V_c = \frac{5}{6} \phi \sqrt{f'_c} b_w d \tag{2.19}$$

Beams with openings

When the beam contains a small opening, a similar approach may be followed, that is, the total shear may be assumed to be resisted partly by the concrete and partly by the shear reinforcement crossing the failure plane as depicted by Eq. (2.12). As discussed in Art. 2.3.1, however, two types of diagonal tension failure are possible for beams containing a small opening. The first type is typical of the

failure commonly observed in solid beams except that the failure plane passes through the center of the opening. In the second type, formation of two independent diagonal cracks, one in each member bridging the two solid beam segments, leads to the failure. These types of failure have been labeled by Mansur (1998) as "*beam-type*" failure and "*frame-type*" failure, respectively (Fig. 2.9), and they require separate treatment for a complete design.

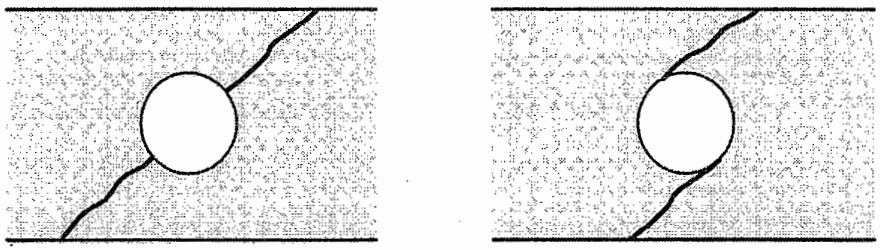

(a) Beam-type failure (b) Frame-type failure

Figure 2.9 Two modes of shear failure at small opening.

Beam-type failure. In designing for this type of failure, a 45° inclined failure plane, similar to a solid beam may be assumed, the plane being traversed through the center of the opening (Fig. 2.10). The component V_c should then be calculated by Eq. (2.11).

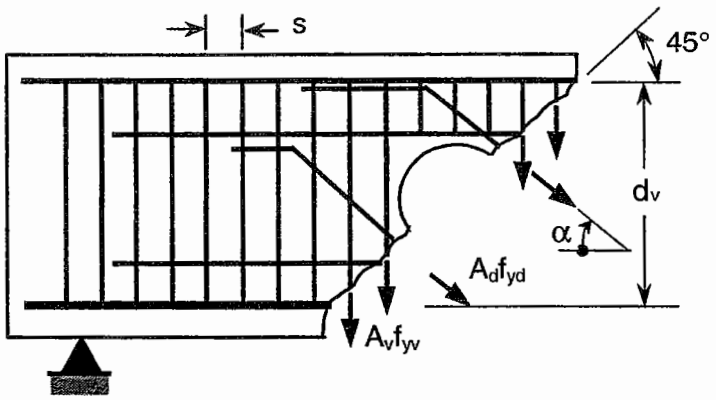

Figure 2.10 Shear strength V_s provided by shear reinforcement at an opening.

For the other component V_s, reference may be made to Fig. 2.9. It may be seen that the stirrups available to resist shear across the failure plane are those by the sides of the opening within a distance $(d_v - d_o)$, where d_v is the distance between the top and bottom longitudinal rebars, and d_o is the depth of opening, as shown. The contribution of diagonal reinforcement, if any, intercepted by the failure plane may also be taken into account in the calculation of shear resistance. Including the contribution of diagonal reinforcement, Eq. (2.14) thus becomes

$$V_s = V_{sv} + V_{sd} = \frac{A_v f_{yv}}{s}(d_v - d_o) + A_d f_{yd} \sin\alpha \qquad (2.20)$$

in which V_{sv} and V_{sd} are the contribution of vertical and diagonal reinforcement, respectively; A_d is the total area of diagonal reinforcement through the failure surface; α is the inclination of diagonal reinforcement; and f_{yd} is the yield strength of diagonal reinforcement.

The total amount of web reinforcement thus calculated should be contained within a distance $(d_v - d_o)/2$ on either side of the opening, and other restrictions as given by Eqs. (2.18) and (2.19) with respect to the usual shear design procedure must be strictly adhered to. In applying these equations, however, V_c should be calculated on the basis of net cross-sectional area through the opening as given by Eq. (2.11) or may be ignored for conservative design.

Frame-type failure. Frame-type failure occurs due to the formation of two independent diagonal cracks, one in each of the chord members above and below the opening, as shown in Fig. 2.9(b). From the type of failure, it appears that each member behaves as an independent entity similar to the members in a framed structure. In design, therefore, the chord members should receive independent treatment, as suggested by Mansur (1998).

In order to comprehend the design method, let us consider the free-body diagram at beam opening of Fig. 2.11. Clearly, the applied moment, M_u, at the center of the opening from the global action is resisted by the usual bending mechanism, that is, by the couple formed by the compressive and tensile stress resultants, N_u, in the members above and below the opening. These stress resultants may be obtained by

$$(N_u)_t = \frac{M_u}{\left(d - \frac{a}{2}\right)} = -(N_u)_b \qquad (2.21)$$

subject to the restrictions given by Eq. (2.7). In this equation, the subscripts t and b denote the top and bottom cross members of the opening.

The applied shear, V_u, is, however, shared by the two members. According to Nasser et al. (1967), the applied shear may be distributed between the two members in proportion to their cross-sectional areas. Thus,

$$(V_u)_t = V_u\left[\frac{A_t}{A_t + A_b}\right] \qquad (2.22a)$$

and

$$(V_u)_b = V_u - (V_u)_t \qquad (2.22b)$$

Knowing the factored shear and axial forces, each member can be independently designed for shear by following the usual procedure for conventional solid beams.

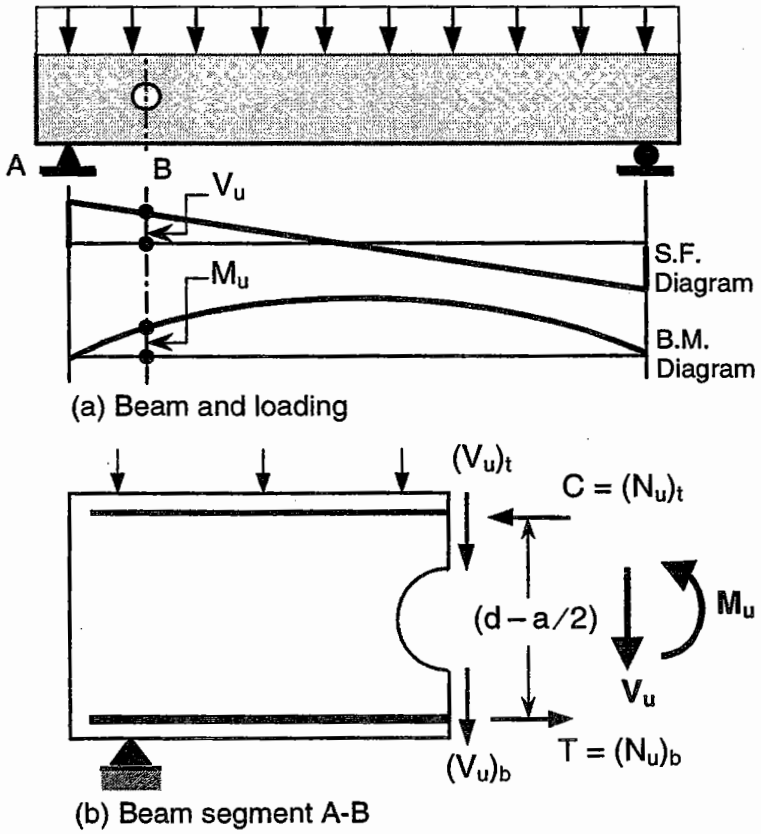

Figure 2.11 Free-body diagram at beam opening.

Maximum shear. It was suggested by Mansur (1998) and recently confirmed by Weng (1998) that the maximum shear that can be applied to the beam to avoid primary crushing failure be limited for the sections above and below the opening as well as the overall section through the opening in accordance with Eq.(2.19). In the latter case, however, the value of V_c to be used in Eq.(2.19) should be calculated on the basis of the net section by Eq.(2.11).

Crack control. The reinforcement designed as above would ensure adequate strength. However, due to sudden reduction in beam cross section, stress concentration occurs at the edge of the opening. Adequate reinforcement with proper detailing should therefore be provided to prevent wide cracking under service load conditions.

To deal with crack control in beams with large openings, Nasser et al. (1967) suggested the use of diagonal bars at each corner of the opening and recommended that a sufficient quantity should be provided to carry twice the amount of external shear. Lorensten (1962) and Barney et al. (1977) suggested the use of full-depth stirrups adjacent to each vertical face of the opening to carry the entire shear but without any magnification. By analyzing test evidence, Mansur et al. (1985) recommended a combination of both diagonal bars and full-depth stirrups. In their proposal, the shear concentration factor η should be taken as 2,

and at least 50% of the shear resistance should be assigned to the diagonal bars. All these recommendations were, however, based on tests conducted on beams with large rectangular openings where failure occurs in a mode completely different from that of beams with small openings.

In the case of small openings, the reinforcement requirement for crack control may not be that large. Since full-depth stirrups are already provided by the sides of the opening to ensure adequate strength, provision of diagonal reinforcement may be considered to restrict the growth of cracks along the failure plane. An amount of diagonal reinforcement that is sufficient to carry the total shear along the 45° failure plane (beam-type failure) has recently been recommended by Mansur (1998). Thus, the total area of diagonal reinforcement, A_d, through the failure surface (Fig. 2.10) is

$$A_d = \frac{V_u}{\phi f_{yd} \sin\alpha} \tag{2.23}$$

in which α is the inclination of diagonal reinforcement and f_{yd} is the yield strength of diagonal reinforcement. This amount should be distributed equally on either side of the opening and be placed normal to the potential failure surface. An equal amount should be placed perpendicular to this reinforcement to avoid confusion during construction and to take care of any possible load reversal.

EXAMPLE PROBLEM 2.2

A simply supported rectangular beam 300 mm wide and 600 mm deep carries a total factored load of 90 kN/m on a span of 6 m. The beam contains a 200 mm-diameter circular opening located at mid-depth of the beam at a distance of 600 mm from the support. Design shear reinforcement for the opening segment of the beam. Assume f'_c = 25 MPa, f_y = 460 MPa, and $f_{yv} = f_{yd}$ = 250 MPa.

SOLUTION

(a) Analysis

At the center of opening,

$$V_u = 216 \text{ kN}, \quad M_u = 146 \text{ kNm}$$

Therefore, Eqs. (2.21) and (2.22) give

$$(V_u)_t = 108 \text{ kN}, \quad (N_u)_b = 108 \text{ kN}$$

(b) Design for bending

Flexural design of the section through the center of opening yields 2T20 (two numbers of 20 mm bars with f_y = 460 MPa) and 1T10 tension rebars. Provide 2T12 bars on the compression side of the beam for anchorage of stirrups.

(c) Shear design for beam-type failure

Assuming 30 mm clear concrete cover and M10 bar (10 mm-diameter bars with f_y = 250 MPa) stirrups,

$$d = 550 \text{ mm}, \; d_v = 504 \text{ mm}$$

Check adequacy of the section

Eq. (2.11) gives

$$\phi V_c = \left(\frac{1}{6}\right) \times 0.85 \sqrt{25} \times 300 \times (550 - 200) 10^{-3} = 74.4 \text{ kN}$$

From Eq. (2.19)

$$[V_u]_{max} = 5\phi V_c = 372 \text{ kN}$$

Since this value is greater than V_u = 216 kN, the section is satisfactory.

Design of full-depth stirrups

V_u = 216 kN > 0.5 ϕ V_c = 37.2 kN but is less than 3 ϕ V_c = 223.2 kN, hence shear reinforcement is required, and s_{max} = 275 mm. Since $\phi V_s = V_u - \phi V_c = 216 - 74.4 =$ 141.6 kN,

$$V_s = 141.6/0.85 = 166.6 \text{ kN}$$

Assuming that the shear resistance of the steel is provided by vertical stirrups only and that two-legged M10 stirrups are used, the required number of stirrups, n, is given by

$$n = \frac{V_s}{A_v f_{yv}} = \left[\frac{166.6}{157 \times 250} \right] 10^3 = 4.24$$

Use of two full-depth stirrups on either side of the opening at a spacing of 100 mm would satisfy the requirements of maximum spacing and positioning of the stirrups, $(d_v - d_o)/2$. Provide nominal diagonal bars for crack control.

(d) Shear design for frame-type failure

Member below the opening (tension member)

For this section, d = 200 – 30 – 10 – 20/2 = 150 mm; therefore, $(V_u)_{max}$ = 159 kN, which is less than V_u = 108 kN. The section is adequate to avoid diagonal compression failure.

Neglecting the contribution of concrete and using two-legged stirrups of M10 bars we have

$$s = \frac{\phi A_v f_{yv} d}{V_u} = \frac{0.85 \times 157 \times 250 \times 150}{108{,}000} = 46 \text{ mm}$$

As V_u is greater than $3\phi V_c \doteq 95.6$ kN, the maximum s is $d/4 = 37.5$ mm. But these values are quite close. Considering the difficulty in achieving proper compaction of concrete and keeping in mind that diagonal bars for crack control would resist part of the applied shear, it is decided to use five short stirrups below the opening in between the full-depth stirrups, which gives a spacing of about 40 mm. Provide two nominal T10 longitudinal bars just below the opening for anchorage of stirrups.

Member above the opening (compression member)

Since the section for this member has dimensions identical to those of the section below, and it is subjected to axial compression, use of the same spacing of stirrups would provide a conservative design and avoid any confusion during construction.

(e) Design for crack control

Diagonal reinforcement is used to achieve crack control under service load condition. Using Eq. (2.23), and assuming f_{yd} = 460 MPa, the required area of diagonal reinforcement is

$$A_d = 216 \times 10^3 / (0.85 \times 460 \times \sin 45^\circ) = 781 \text{ mm}^2$$

Use 4T16 diagonal bars in each direction.

(f) Reinforcement details

The final arrangement of reinforcement in the opening region of the beam is shown in Fig. E2.2.1.

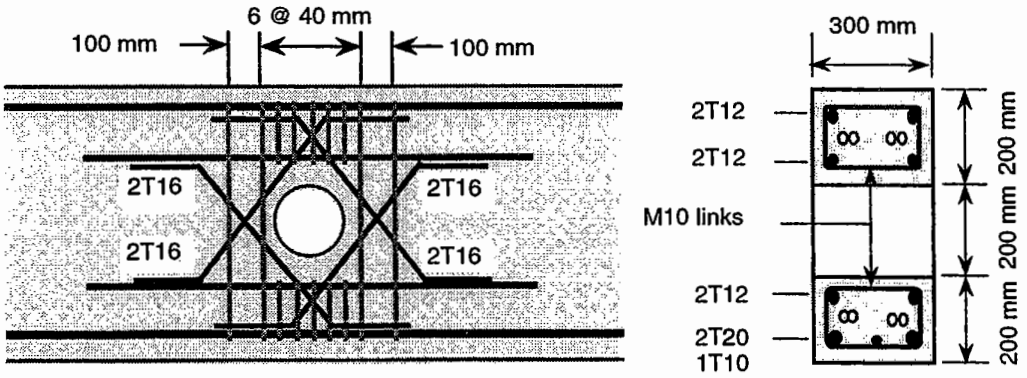

Figure E2.2.1 Reinforcement details of the beam in Example Problem 2.2.

2.3.3 AIJ APPROACH

In the Architectural Institute of Japan (AIJ) Standard for Structural Calculation of Reinforced Concrete Structures (1988), a formula (designated as Hirosawa's formula) has been incorporated to evaluate the shear capacity, V_n, of beams that contain a small opening. Similar to the traditional approach discussed above, this empirical formula considers that the total shear resistance is provided by both concrete and the steel crossing a 45° failure plane passing through the center of opening. The formula given is as follows,

$$V_n = \left[\frac{0.092\ k_u k_p\ (f'_c + 17.7)}{\frac{M}{Vd} + 0.12} \left(1 - \frac{1.61 d_o}{h}\right) + 0.846\ \sqrt{\overline{\rho}_w f_{yv}} \right] b d_v \qquad (2.24)$$

where k_u is a function of the effective depth d to account for the size effects in shear and has a value between 0.72 and 1.0 as shown in Fig. 2.12; $k_p = 0.82\ (100 A_s / bd)^{0.23}$; d_o = diameter of the circular opening or diameter of the circumscribed circle in the case of a square opening which should be taken as less than or equal to $h/3$; h is the overall depth of the beam, and $M/(Vd)$ is taken as less than or equal to 3.

The term $\overline{\rho}_w$ in Eq. (2.24) refers to the ratio of web reinforcement placed within a longitudinal distance $d_v/2$ from the center of the opening as shown in Fig. 2.13, and is defined as

$$\overline{\rho}_w = \frac{A_v(\sin\alpha + \cos\alpha)}{b d_v} \qquad (2.25)$$

in which d_v = the distance between the top and bottom longitudinal bars; A_v = area of web reinforcement (vertical stirrup or diagonal bar); α = angle of inclination of web reinforcement; and f_{yv} = yield strength of web reinforcement.

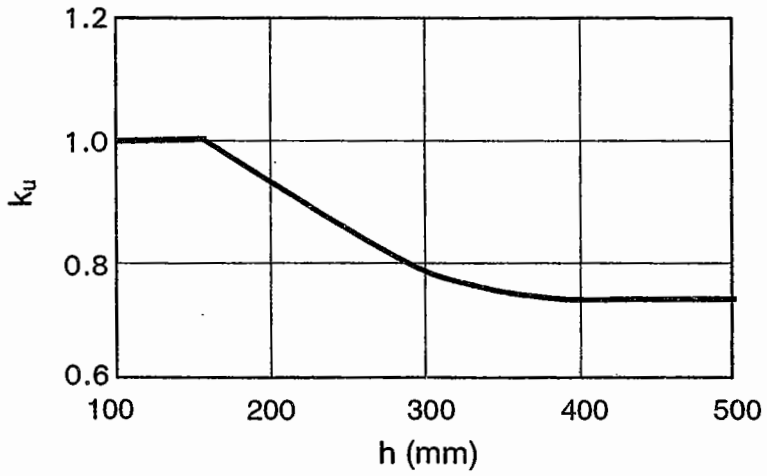

Figure 2.12 Determination of k_u.

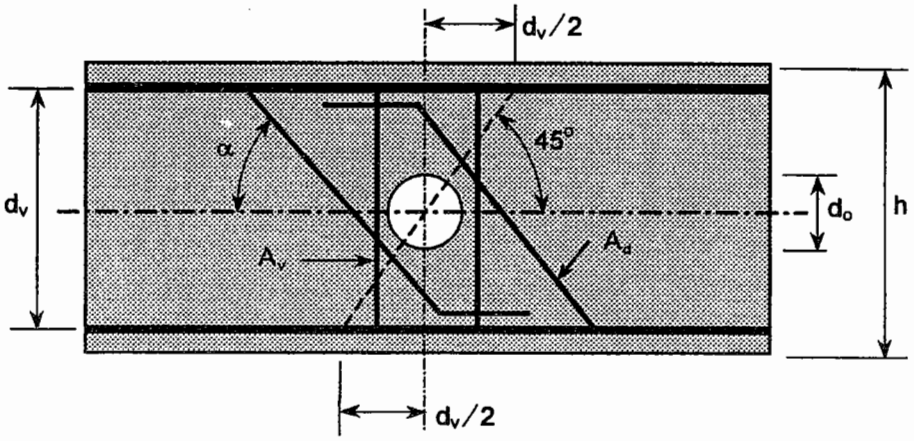

Figure 2.13 Effective web reinforcement for opening.

The first term in Eq. (2.24) gives the contribution of concrete to shear resistance, which is assumed to decrease in proportion to the opening depth. The second term gives the shear resistance due to the web reinforcement. It has been suggested that for normal web reinforcement ratio, the second term be replaced by $(3 + 0.5\ \overline{\rho}_w f_{yv})$.

EXAMPLE PROBLEM 2.3

Check the shear capacity for the opening segment of the beam designed in Example Problem 2.2 using the AIJ approach.

SOLUTION

From the details shown in Fig. E2.2.1,

$$d = 550 \text{ mm}, \ d_v = 504 \text{ mm}, \ A_s = 707 \text{ mm}^2$$

Also, for the given problem,

$$b = 300 \text{ mm}, \ h = 600 \text{ mm}, \ d_o = 200 \text{ mm}$$

$$f'_c = 25 \text{ MPa}, \ M_u = 146 \text{ kNm}, \ V_u = 216 \text{ kNm}$$

Therefore,

$$k_u = 0.72 \text{ (from Fig. 2.12)}$$

$$k_p = 0.82\ [(100 \times 707)/(300 \times 550]^{0.23} = 0.675$$

and the concrete contribution to shear capacity according to Eq. (2.24) may be obtained as

$$V_c = \frac{0.092 \times 0.72 \times 0.675 \times (25 + 17.7)}{\frac{146{,}000}{216 \times 550} + 0.12}\left(1 - 1.61\frac{200}{600}\right) b\, d_v = 0.656\, b\, d_v$$

Considering only the four two-legged stirrups placed adjacent to the opening (see Fig. E2.2.1) resist shear, the web steel ratio $\bar{\rho}_w$ from Eq. (2.25) is

$$\bar{\rho}_w = \frac{157 \times 4}{300 \times 504} = 0.0042$$

The contribution of web reinforcement to shear capacity according to Eq. (2.24) is

$$V_s = 0.846\sqrt{0.0042 \times 250}\, b\, d_v = 0.867\, b\, d_v$$

The ultimate shear capacity of the opening segment is, therefore,

$$V_n = V_c + V_s = 1.518\, b\, d_v = 1.518 \times 300 \times 504 \times 10^{-3} = 230 \text{ kN}$$

This is greater than the factored shear V_u of 216 kN. Hence, the web reinforcement provided is adequate.

2.3.4 PLASTICITY TRUSS METHOD

In a separate development, the phenomenon of shear in reinforced concrete beams can be treated using the theory of plasticity (Nielsen, 1984).

Beams without openings

In general, the shear force, V, acting on a section is given by the change of applied moment over an infinitesimal distance dx, that is:

$$V = \frac{dM}{dx} \tag{2.26}$$

where M is the applied moment on the section. Noting that $M = T(jd)$ where T is the force in the longitudinal tension reinforcement and jd is the lever arm for the resisting moment, expanding Eq. (2.26) gives

$$V = T\,\frac{d(jd)}{dx} + jd\,\frac{dT}{dx} \tag{2.27}$$

The first term on the right-hand side of Eq. (2.27) represents a situation where the force in the tension reinforcement remains constant while the lever arm varies along the length of the beam to provide the necessary moment of resistance. Such structural action is referred to as *arch action* in reinforced concrete beams.

Arch action is predominant in the so-called *D-regions* for which Bernoulli's hypothesis is not valid, that is, where plane sections do not remain plane due to the application of external loads. These regions may be assumed to occur within a distance equal to the beam depth from supports, from points of application of concentrated loads and locations where there is an abrupt change in cross-sectional geometry.

The second term in Eq. (2.27) indicates the case where the force in the tension reinforcement varies along the length of the beam with the lever arm for the moment resistance remaining a constant. This is referred to as *beam* or *truss action* and it occurs predominantly in so-called *B-regions*. These are regions other than *D-regions*, in which Bernoulli's hypothesis is assumed to apply.

It may thus be seen from Eq. (2.27) that the shear force applied on a reinforced concrete beam is, in general, resisted by a combination of arch and truss mechanisms. Fig. 2.14 shows the truss mechanism that develops in a beam.

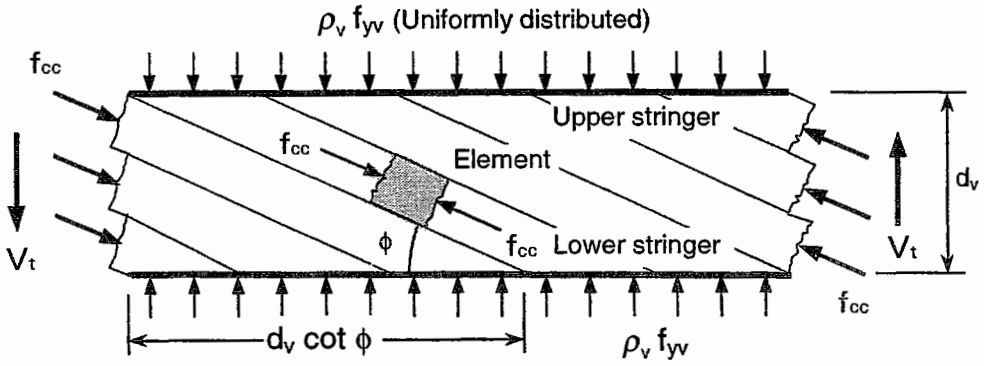

(a) Analogous truss model

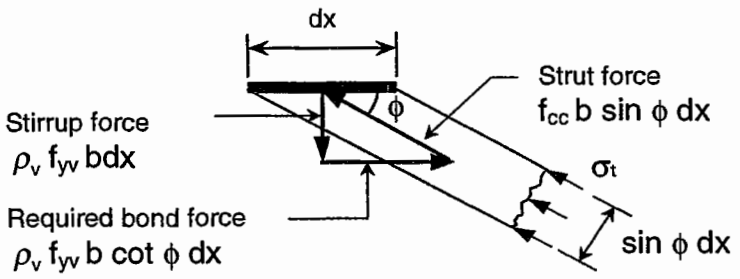

(b) Equilibrium of an infinitesimal stringer element

Figure 2.14 Truss action in solid beams.

Assuming yielding of shear reinforcement, the shear force carried by the truss mechanism, V_t, is given by:

$$V_t = b\, d_v \rho_v f_{yv} \cot\phi \qquad (2.28)$$

where $V_t \leq \frac{1}{2} b d_v \nu f_c'$; b = width of the section; d_v = the distance between the top and bottom longitudinal bars; ρ_v = the shear reinforcement ratio; f_{yv} = the yield strength of the shear reinforcement; ϕ = angle of inclination of the concrete compression strut to the beam axis; $\nu f_c'$ = the effective compressive strength of concrete, in which ν is the effectiveness factor given by

$$\nu = 0.7 - \frac{f_c'}{200} \tag{2.29}$$

The concrete stress in the compression strut of the analogous truss, f_{cc}, is obtained by considering equilibrium of an infinitesimal stringer element as:

$$f_{cc} = \frac{\rho_v f_{yv}}{\sin^2 \phi} = \left(1 + \cot^2 \phi\right) \rho_v f_{yv} \tag{2.30}$$

where f_{cc} is less than or equal to the effective compressive strength of concrete $\nu f_c'$.

If $f_{cc} < \nu f_c'$, the difference between f_{cc} and $\nu f_c'$ would contribute to an arch action as shown in Fig. 2.15. Ignoring the difference in the angle of concrete struts, ϕ in the truss mechanism and θ in the arch mechanism, so that the compressive concrete stress f_a in the strut of the arch mechanism would be $(f_{cc} - \nu f_c')$. The shear force carried by the arch mechanism, V_a, would then be given by:

$$V_a = f_a \tan\theta \left(\frac{bh}{2}\right) = \left(\nu f_c' - f_{cc}\right) \tan\theta \left(\frac{bh}{2}\right) \tag{2.31}$$

where

$$\tan\theta = \sqrt{1 + \left(\frac{a}{h}\right)^2} - \frac{a}{h} \tag{2.32}$$

in which a is the shear span and h is the overall depth of the beam.

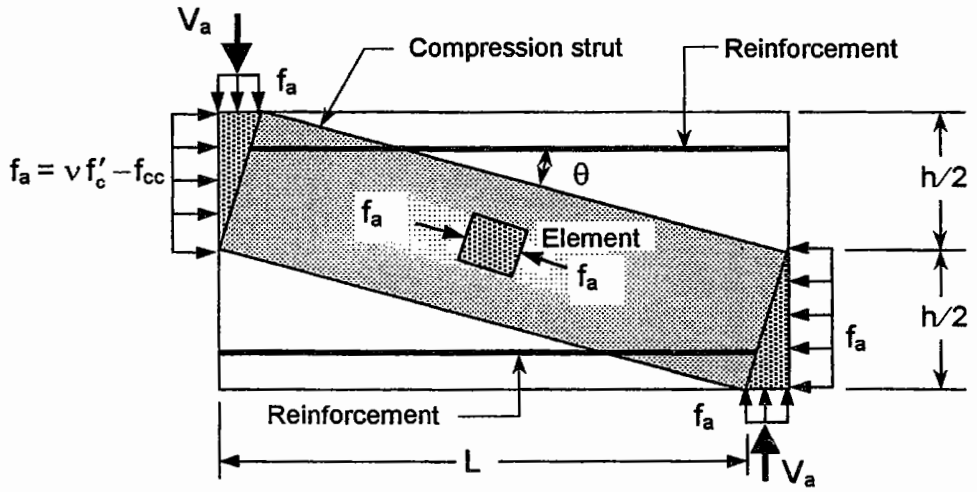

Figure 2.15 Arch action in solid beams (AIJ, 1994).

The nominal shear strength of the beam, V_n, is obtained by adding the contribution of the truss mechanism, V_t [Eq. (2.28)], and shear force carried by the arch mechanism, V_a [Eq. (2.31)], giving the nominal shear strength as

$$V_n = bd_v \rho_v f_{yv} \cot\phi + (1-\beta)\, bh \tan\theta \frac{\nu f_c'}{2} \tag{2.33}$$

in which β is given by

$$\beta = \frac{(1+\cot^2\phi)\rho_v f_{yv}}{\nu f_c'} \tag{2.34}$$

In applying Eq. (2.33), the value of $\cot\phi$ should be less than that given by any of the following equations (AIJ, 1994):

$$\cot\phi = 2 \tag{2.35a}$$

$$\cot\phi = \frac{d_v}{h\tan\theta} \tag{2.35b}$$

$$\cot\phi = \sqrt{\frac{\nu f_c'}{\rho_v f_{yv}} - 1} \tag{2.35c}$$

Eq. (2.35a) gives the allowable maximum value of cot ϕ to ensure development of adequate aggregate interlock action along a diagonal crack (Thurlimann, 1978). Eq. (2.35b) gives the value of ϕ which maximizes V_u in Eq. (2.33), and Eq. (2.35c) is derived from the condition that f_{cc} is less than or equal to $\nu f_c'$ using Eq. (2.30).

From Eqs. (2.28) and (2.35c), the value of V_t can be expressed in terms of the shear reinforcement index ψ as:

$$\bar{v} = \frac{V_t}{bd_v \nu f_c'} = \sqrt{\psi\,(1-\psi)} \le 0.5 \tag{2.36}$$

where $\psi = \rho_v f_{yv}/\nu f_c' \le 1$.

In addition, Eq. (2.35c), with the upper limit given by Eq. (2.35a), may be re-expressed as:

$$\cot\phi = \sqrt{\frac{1}{\psi} - 1} \le 2 \tag{2.37}$$

The variations of $\bar{v}$ and cot ϕ with ψ as depicted by Eqs. (2.36) and (2.37), respectively, are shown in Fig. 2.16.

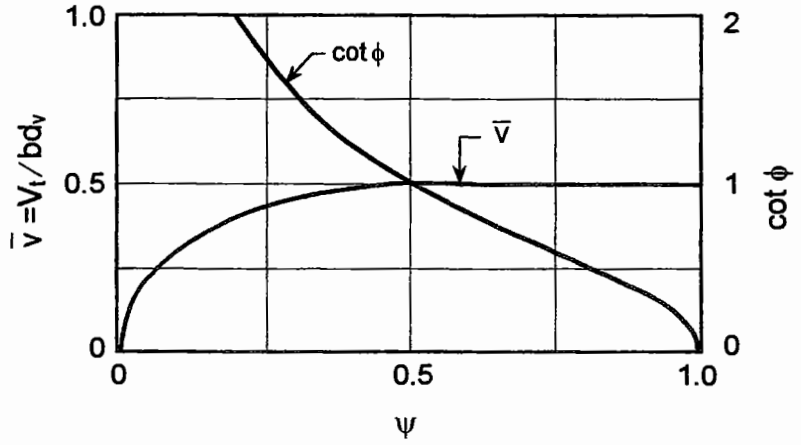

Figure 2.16 Relations of $\bar{v}$ and cot ϕ with ψ.

Beams with openings

In a beam with an opening, however, it is difficult to develop an arch mechanism, and, consequently, the applied shear is transferred by means of a truss mechanism. This is illustrated in Fig. 2.17 for a beam with a circular opening (Ichinose and Yakoo, 1990) where the beam is reinforced transversely by vertical stirrups only.

In Fig. 2.17, the angle of concrete compression strut in the upper and lower chord members of the opening is denoted by ϕ_s; the horizontal arrows show bond stresses and the vertical arrows represent forces acting on the concrete due to the forces in the stirrups. The unshaded portion shows the zone where the diagonal compressive stress field is not formed. The diagonal compressive stress in concrete around the opening becomes larger as the unshaded portion widens or as the opening becomes larger. The effective depth d_{tw} for the truss mechanism is defined as (see Fig. 2.17c)

$$d_{tw} = d_v - \frac{d_o}{\cos\phi_s} - s_v \tan\phi_s \tag{2.38}$$

where d_o is the diameter of the circular opening (or that of a circumscribed circle in the case of a square or rectangular opening), and s_v is the spacing between the two stirrups, one on each side adjacent to the opening.

In Eq. (2.38), the vertical height of the unshaded portion is given by the term ($d_o/\cos\phi_s + s_v \tan\phi_s$). The vertical stirrups should be provided adjacent to the opening within a distance of ($d_{tw}/2 + e$)cot ϕ_s, as shown in Fig. 2.17(a), where e is the eccentricity of the opening measured from the center of the opening to the centroidal axis of the beam.

Assuming yielding of stirrups, the concrete compressive stress in the shaded portion is given by [refer to Eq. (2.30)]

$$f_{cw} = \rho_v f_{yv}\left(1+\cot^2\phi_s\right) \tag{2.39}$$

where ρ_v is the ratio of shear reinforcement placed adjacent to the opening and f_{yv} is yield strength of the stirrups.

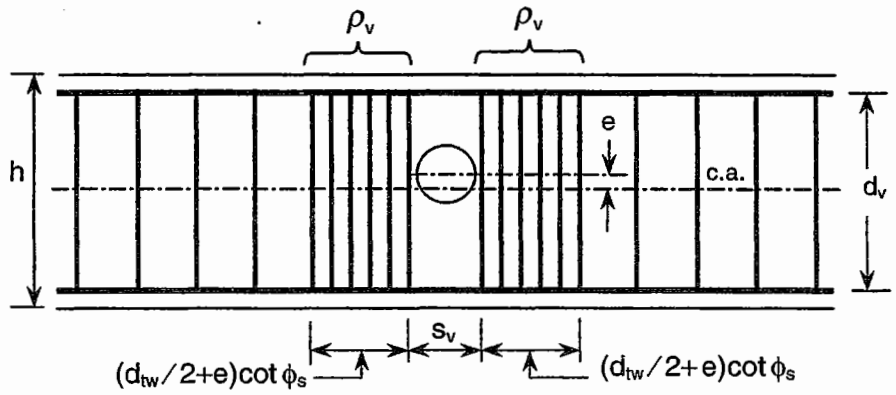

(b) Arrangement of reinforcement (vertical stirrups)

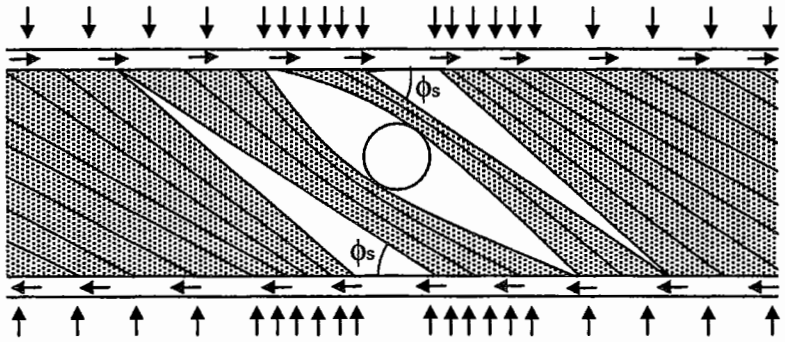

(b) Truss model

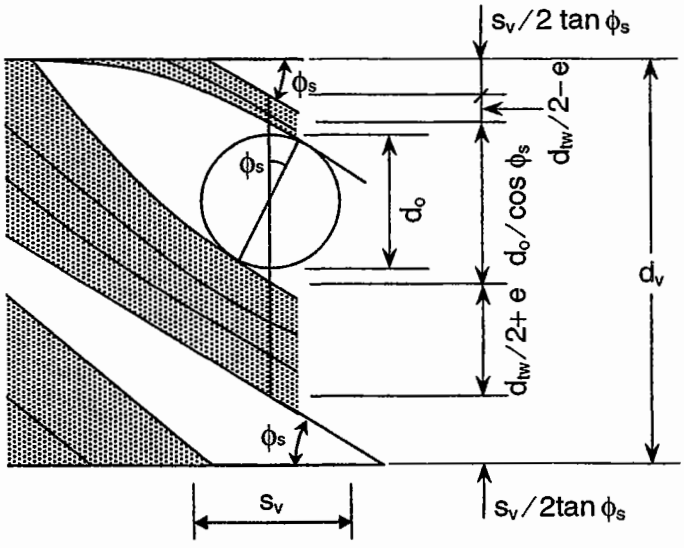

(c) Truss near the opening

Figure 2.17 Truss action in beam with opening.

Equating the value of f_{cw} in Eq. (2.39) to the effective compressive strength of concrete, $\nu f_c'$, gives the value of ϕ_s as:

$$\cot\phi_s = \sqrt{\frac{\nu f_c'}{\rho_v f_{yv}} - 1} \tag{2.40}$$

Unlike solid prismatic beams, the value of cot ϕ_s may be taken to be more than 2.0, in order to ensure the validity of truss action in the vicinity of the opening. Following Eq. (2.28), the shear strength of the beam with an opening is given by:

$$V_n = bd_{tw}\rho_v f_{yv}\cot\phi_s \tag{2.41}$$

From Eqs. (2.40) and (2.41), it can be seen that V_n has an upper limit with respect to $\rho_v f_{yv}$. Conservatively, $\rho_v f_{yv}$ should not be taken to be greater than $(½ - d_o / d_v)\nu f_c'$ for which the maximum value of V_n is obtained (AIJ, 1994; Ichinose and Yokoo, 1990).

Eq. (2.41) has been verified against test data (AIJ, 1994; Ichinose and Yokoo, 1990), as shown in Fig. 2.18. In this figure, $V_{u,test}$ is the observed shear strength of the specimens, V_n is the shear capacity according to Eq. (2.41), and V_f is the shear force that would result in flexural failure of the specimens. It is seen that Eq. (2.41) gives accurate predictions of the shear capacity of beams with openings reinforced by vertical stirrups.

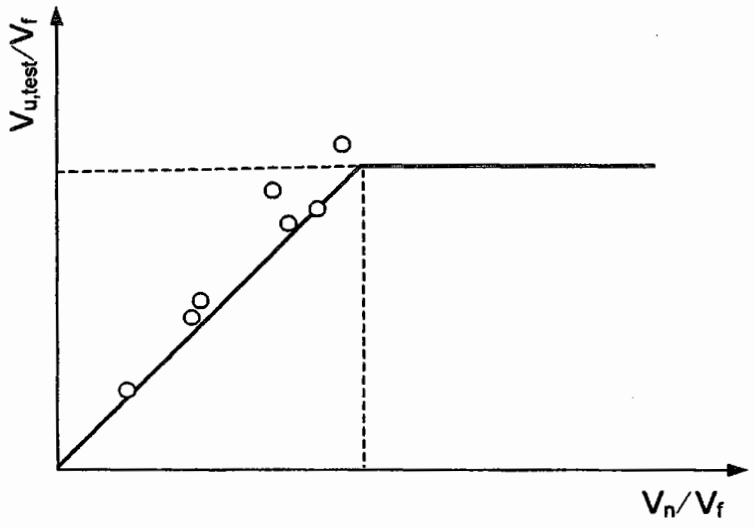

Figure 2.18 Verification of strength equation [Eq. (2.41)] (AIJ, 1994).

The maximum attainable shear strength of beam for different opening depth ratios, d_o / d_v, is shown in Fig. 2.19, for which s_v has been assumed to be equal to $1.2d_o$. As an example, when $d_v = 0.8h$, $d_o = 0.2h$, then $d_o / d_v = 0.2 / 0.8 = 0.25$, and the upper limit of $V_u / b d_v \nu f_c'$ is 0.24.

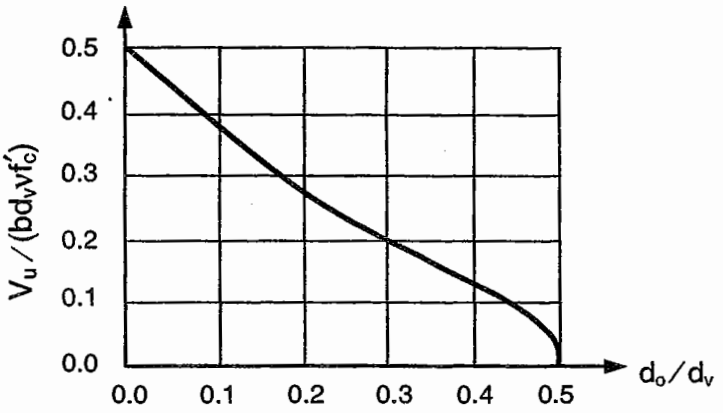

Figure 2.19 Effect of opening size on maximum attainable shear strength.

When diagonal steel reinforcement bars are provided and their development lengths are anchored outside of stirrups adjacent to the opening as shown in Fig. 2.20, where the compressive stress in concrete is relatively low, the contribution of the diagonal bars to the shear capacity is given by:

$$V_{nd} = A_d f_{yd} \sin\theta_d \tag{2.42}$$

where θ_d is the angle of inclination to the axis of the beam, and A_d is the cross-sectional area of the diagonal bars. The value of V_{nd} in Eq. (2.42) can be added to the value of V_n in Eq. (2.41) to give the total shear strength of the beam.

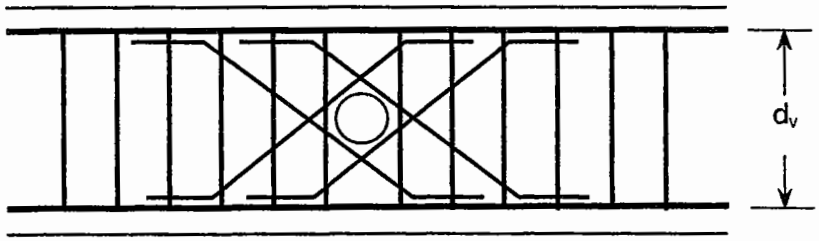

(a) Arrangement of diagonal reinforcement around opening

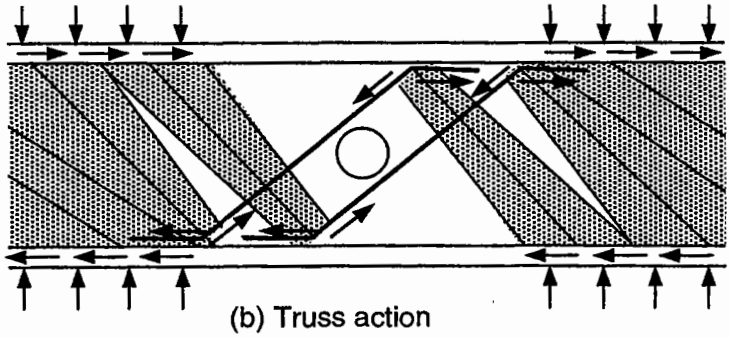

(b) Truss action

Figure 2.20 Beam with small opening reinforced by diagonal bars (AIJ,1994).

EXAMPLE PROBLEM 2.4

Evaluate the shear capacity of the opening segment of the beam designed in Example Problem 2.2 by considering the effect of (a) vertical stirrups only; (b) both vertical stirrups and diagonal bars.

SOLUTION

(a) Consider vertical stirrups only

An iterative procedure is required to evaluate the shear capacity of the opening segment. First, a value of ϕ_s is assumed. The value of d_{tw} is calculated from Eq. (2.38) and $\rho_v f_{yv}$ is obtained and verified to be less than or at most equal to $(½ - d_o/d_v)v f'_c$. From Eq. (2.40), the value of ϕ_s is calculated and compared to the assumed value. If these values are different, assume a new value for ϕ_s and repeat the procedure until the calculated value is approximately equal to the assumed value. Once the correct value of ϕ_s is obtained, the shear capacity can be obtained from Eq. (2.41).

For the problem under consideration, a few trials led to the assumption of $\phi_s = 8°$. Therefore, from Eq. (2.38) and assuming $s_v = 270$ mm,

$$d_{tw} = 504 - 200/\cos 8° - 270 \tan 8° = 264 \text{ mm}$$

Shear reinforcement consisting of four two-legged vertical stirrups is provided adjacent to the opening (see Fig. E2.2.1). Thus, the shear reinforcement ratio is

$$\rho_v = A_{sv}/(bd_{tw} \cot \phi_s/2) = (157 \times 2)/ (300 \times 264 \cot 8°/2) = 0.0011$$

Since f_{yv} = 250 MPa and f'_c = 25 MPa, $\rho_v f_{yv}$ = 0.0011 × 250 = 0.279 MPa, $v = 0.7 - 25/200 = 0.575$, and $v f'_c = 14.38$ MPa. Also, $d_o / d_v = 200 / 504$. Thus, $(½ - d_o/d_v)v f'_c = (½ - 200/504) \times 14.38 = 1.484$ MPa > $\rho_v f_{yv}$. Therefore, from Eq. (2.40),

$$\cot\phi = \sqrt{(14.38/0.2785 - 1)} = 7.116; \quad \phi_s = 8°$$

Hence, the assumed value of ϕ_s is correct and

$$V_n = 300 \times 264 \times 0.2785 \times 7.116 \times 10^{-3} = 157 \text{ kN}$$

This is lower than the factored shear of 216 kN; hence, additional shear reinforcement would be required.

(b) Consider vertical stirrups and diagonal reinforcement

The diagonal reinforcement consists of four M10 bars placed in each direction. Assuming an angle of inclination of 45°, the shear resistance provided by the diagonal bars in one direction from Eq. (2.42) is

$$V_{nd} = 314 \times 250 \sin 45° \times 10^{-3} = 55.5 \text{ kN}$$

The total shear capacity of the beam is (157 + 55.5) or 212.5 kN, almost equal to the factored shear at the opening. Compared to the traditional methods used in Example Problems 2.2 and 2.3, it is seen that the plasticity truss method requires more reinforcement for the opening.

2.4 EFFECT OF TORSION

2.4.1 BEHAVIOR OF BEAMS IN TORSION

The rational theories for torsion in concrete beams may be broadly classified into two categories: (a) "Space-Truss" model and (b) "Skew-Bending" theory. In order to comprehend the bases of these theories, consider qualitatively the behavior of a beam which is subject to a gradually increasing torsional moment, *T*. The beam has a rectangular cross section and contains both longitudinal and transverse rebars, as shown in Fig. 2.21(a).

A small torsional moment, *T*, produces shear stresses in the concrete. Assuming elastic behavior before cracking, the maximum shear stress occurs at midpoints of the deeper faces of the beam. These shear stresses, in turn, produce principal tensile and compressive stresses [Fig. 2.21(b)], which are inclined at 45° to the beam axis. Before cracking, the steel acquires very little stress.

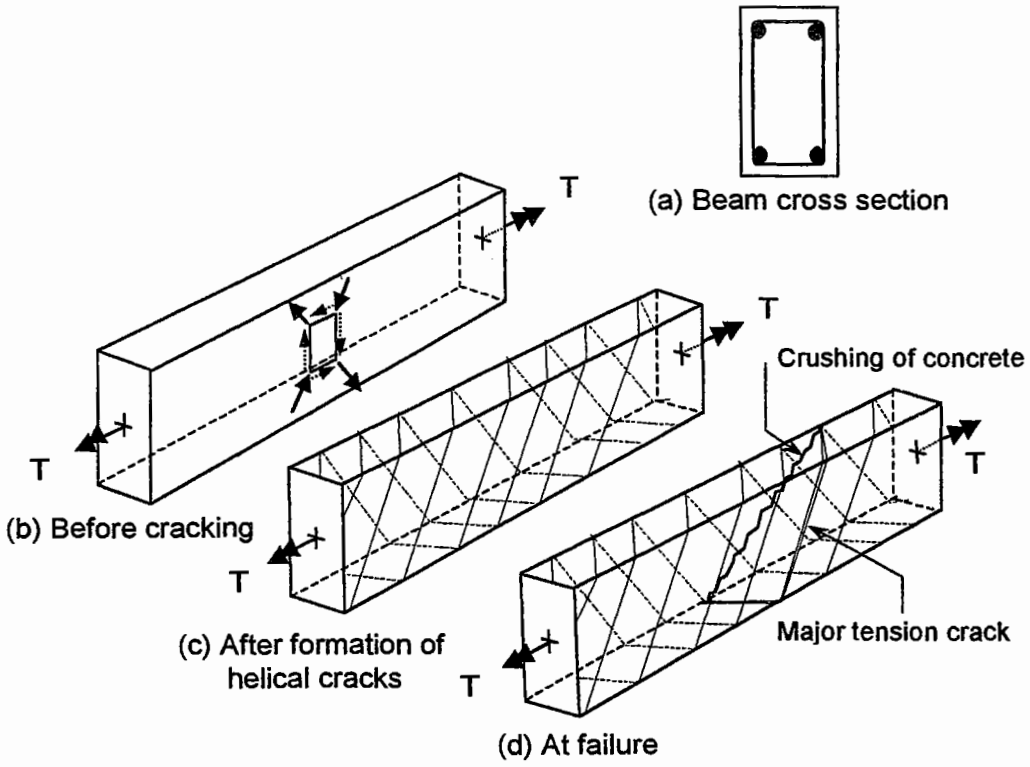

Figure 2.21 Behavior of reinforced concrete beams in pure torsion.

In the case of a plain concrete beam, failure occurs suddenly when the principal tensile stress reaches the tensile strength of the concrete. Observing the failure surface as shown in Fig. 2.22(a), Hsu (1968) has concluded that the failure of a plain concrete beam, in fact, occurs by bending about a skew axis. With the idealization of the failure surface as in Fig. 2.22(b), Hsu has derived the following equation for the ultimate torque of a plain concrete beam, $T_{u,p}$, simply by applying the elastic bending theory and equating the tensile stress to the reduced (due to the existence of perpendicular compression) tensile strength of the concrete:

$$T_{u,p} = 0.85\frac{b^2 h}{3} f_r \tag{2.43}$$

where b = width of the section (shorter dimension); h = overall depth of the section; and f_r = modulus of rupture of the concrete. In Eq. (2.43), the factor 0.85 accounts for the reduction in tensile strength of the concrete due to the presence of perpendicular compression.

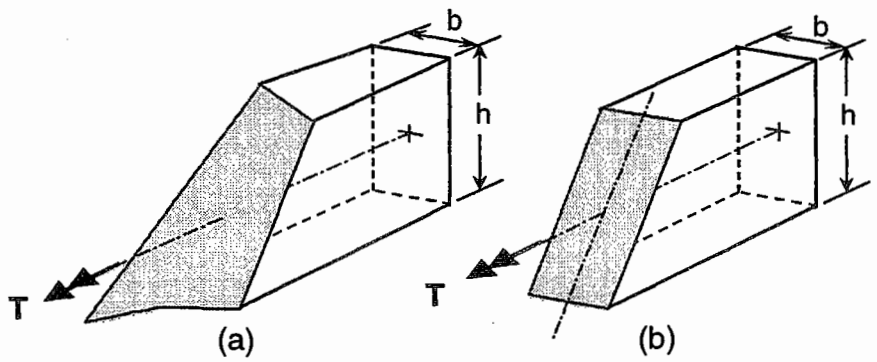

Figure 2.22 Failure surface of a plain concrete beam in torsion (a) Typical failure surface, and (b) Idealized skew-bending surface.

Eq. (2.43) has been found to agree quite well not only with the ultimate torque of a plain concrete beam but also with the torque at which first cracking occurs in a reinforced concrete beam. In the latter case, cracks originate at the center of the deeper faces and propagate toward the shorter faces of the beam at an inclination of approximately 45° to the beam axis. At this stage, the strains in both longitudinal and transverse steel reinforcement increase significantly, that is, a considerable redistribution of the stresses from concrete to steel takes place.

With increasing torsional moment, diagonal cracks of approximately the same inclination also appear on the shorter faces of the beam. These new cracks join with the existing diagonal cracks on the other two faces, thus forming spirals of cracks on the beam surface at a finite spacing as shown in Fig. 2.21(c). After the formation of cracks, torsional shear stresses can no longer be resisted unless a different mechanism is formed to enable stresses to be transferred in a manner essentially different from the Saint-Venant's concept. Such a mechanism may be assumed to consist of a space-truss with longitudinal corner bars acting as stringer,

stirrup legs as chords, and concrete in between the cracks as diagonals. This assumption forms the basis of the familiar "*Space-Truss*" model for torsion in concrete beams.

As the torque, T, is further increased, the beam rotates, which results in some of the diagonal cracks becoming excessively wide on the three faces. The beam finally fails by crushing on the fourth face along a diagonal line joined by the ends of the primary cracks [Fig. 2.21(d)]. It appears that the ultimate failure of the beam is due to bending about a skew axis. This observation has led to the development of the well-known "*Skew-Bending*" theory for torsion, which was originally proposed by Lessig (1959), and later advanced by many other researchers (Collins et al., 1968; Elfgren, 1974; Hsu, 1968; Thurlimann,1979).

The above discussion dealt with the behavior of solid beams in torsion. If a small transverse opening is introduced in the beam web, test results (Hasnat and Akhtaruzzaman, 1987; Mansur and Hasnat, 1979; Mansur and Paramasivam, 1984; Mansur et al., 1982; Salam, 1977) have shown that the beam behavior essentially remains the same. As the opening represents a source of weakness, however, the first diagonal crack originates at the periphery of the opening. A plain concrete beam would obviously fail at this torque. The failure surface remains identical to that of a solid beam except that, in this case, the plane passes through the center of opening, as shown in Fig. 2.23. Using the elastic theory for bending about a skew axis, Mansur and Hasnat (1979) have suggested the following expression for ultimate torque, $T_{u,po}$, of a plain concrete beam with small openings:

$$T_{u,po} = 0.85\frac{b^2 h}{3}\left(1-\frac{d_o}{h}\right)f_r \qquad (2.44)$$

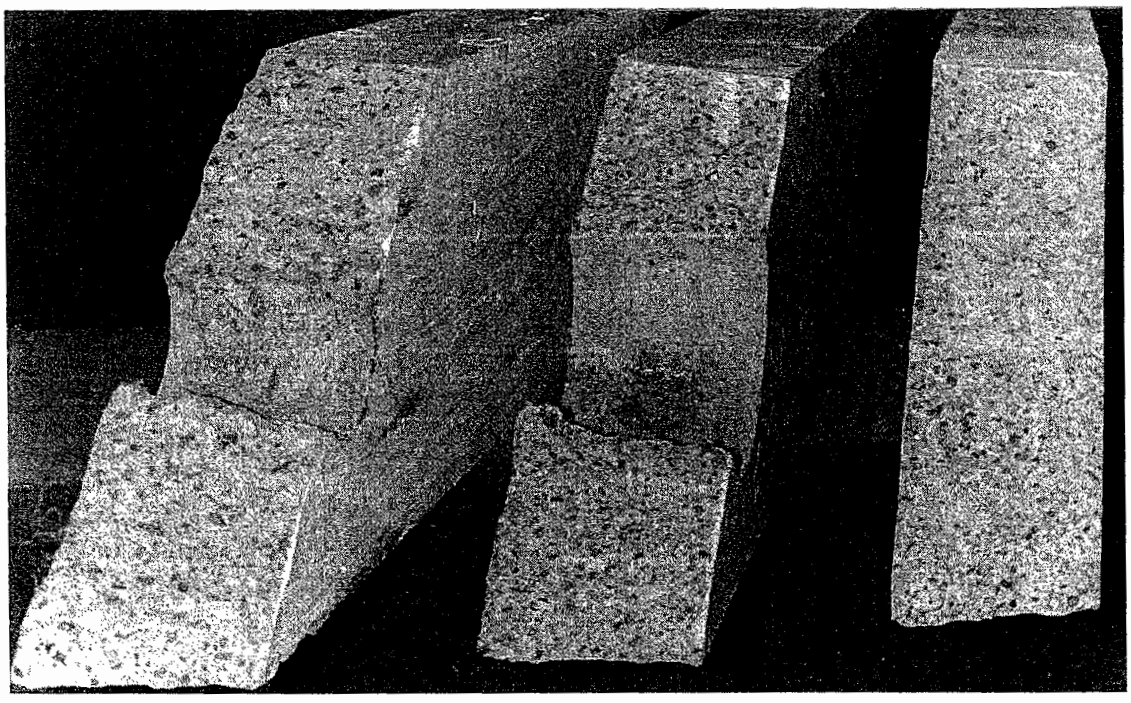

Figure 2.23 Failure surface of a plain concrete beam with circular opening.

When properly reinforced with longitudinal bars and closed stirrups, such a beam will exhibit a well-developed pattern of diagonal cracks close to the ultimate load and eventually fail in a mode that may be idealized as bending about a skew axis. However, in this case, the failure surface always passes through the center of the opening (Mansur and Hasnat, 1979). A typical skew-bending failure of a reinforced concrete beam in torsion is shown in Fig. 2.24.

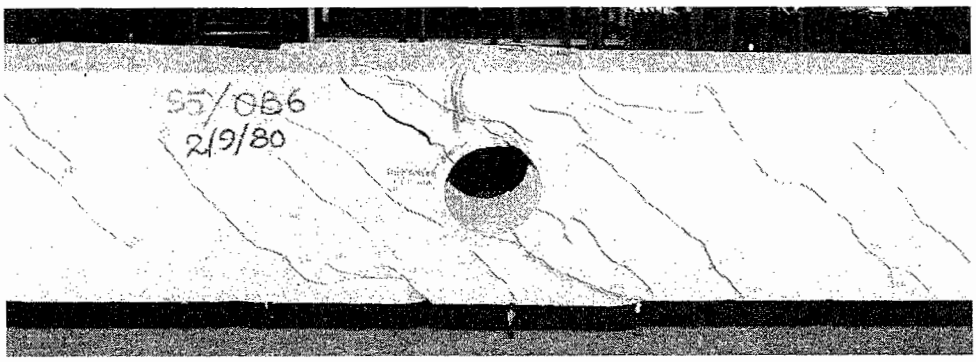

Figure 2.24 Typical skew-bending type of torsional failure of a reinforced concrete beam with opening.

2.4.2 ANALYSIS FOR ULTIMATE STRENGTH

The analysis presented here is based on the well-known *skew-bending theory* for torsion in concrete beams. In the case of a solid beam, the theory considers three basic failure modes classified as Mode 1, Mode 2, and Mode 3, according to the location of concrete compression zone near the top, side, and bottom of the beam, respectively, as shown in Fig. 2.25. Aspect ratio of the beam section, relative proportion of top and bottom longitudinal steel, and the ratio of applied torque to bending moment with or without a combination with transverse shear generally govern the failure modes.

When a relatively small transverse opening is introduced through the beam web, and the beam is subject to predominant torsion, one would expect no changes in the mode of failure. This has been confirmed experimentally by several investigators (Hasnat and Akhtaruzzaman, 1987; Mansur and Hasnat, 1979; Mansur and Paramasivam, 1984; Mansur et al., 1983b). As a result, an analysis similar to that of a prismatic beam is applicable to beams containing a small opening. With this contention, the analysis is based on three failure modes classified as Mode 1, Mode 2, and Mode 3. Since the opening represents the potential source of weakness in a beam, the failure surface is assumed to be traversed through the center of the opening. In developing strength equations for such beams, each failure mode is considered separately, and the following assumptions are made to simplify the problem:

1. The pattern of reinforcement in the vicinity of the opening consists of longitudinal bars above and below the opening, full-depth stirrups close to either side of the opening, and closed stirrups at the throat section (sections

above and below the opening), in addition to the normal top and bottom reinforcement in the solid section.

2. The spacing of stirrups at the solid cross section as well as at the throat section is uniform along the length of the beam.
3. Failure occurs on a warped plane. The boundaries of the warped plane are defined on the three sides of the beam by a spiral crack and on the fourth side by a compression zone that joins the ends of the spiral crack.
4. The crack defining the failure plane on three sides of the beam consists of three straight lines spiraling around the beam at a constant angle.
5. The concrete outside the compression zone is cracked and carries no tension.
6. All reinforcement crossing the failure plane outside the compression zone yields at failure.
7. Any reinforcement in the compression zone and dowel action of reinforcement are ignored.

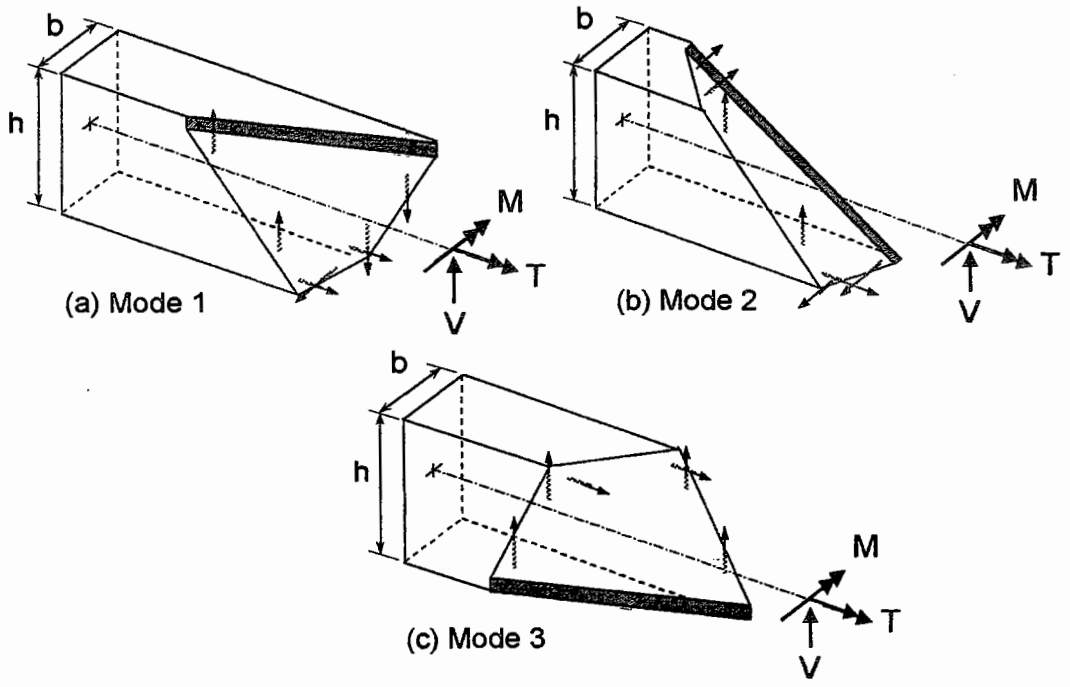

Figure 2.25 Failure surfaces for a solid beam in Modes 1, 2, and 3.

2.4.2.1 Combined Torsion, Bending, and Shear

A structural member is, in general, subjected to torsion, bending, shear, and axial forces, but when the analysis and design of a beam is concerned, the effect of axial load is usually ignored. Combined torsion, bending, and shear, therefore, may be considered as the general loading case for beams, and this loading case is treated first.

Mode 1 failure

The assumed failure surface for Mode 1 is shown in Fig. 2.26 together with the internal forces developed in steel reinforcement. The skewed compression zone at the top makes an angle θ_1 to the normal cross section. It originates from the tip of the tension crack, that traverses through the opening on one of the side faces of the beam. The resultant of the forces developed in the longitudinal bars intercepted by the tension zone is F_s, and the force in the bottom legs of stirrups that cross the failure surface is F_{wh}. Similarly, F_{wv} and F'_{wv} are the forces in the vertical legs of the long and short stirrups, respectively. Let the forces F_s and F_{wh} be located at y_s and y_{wh}, respectively, below the center of compression and x_1 be the width of stirrups.

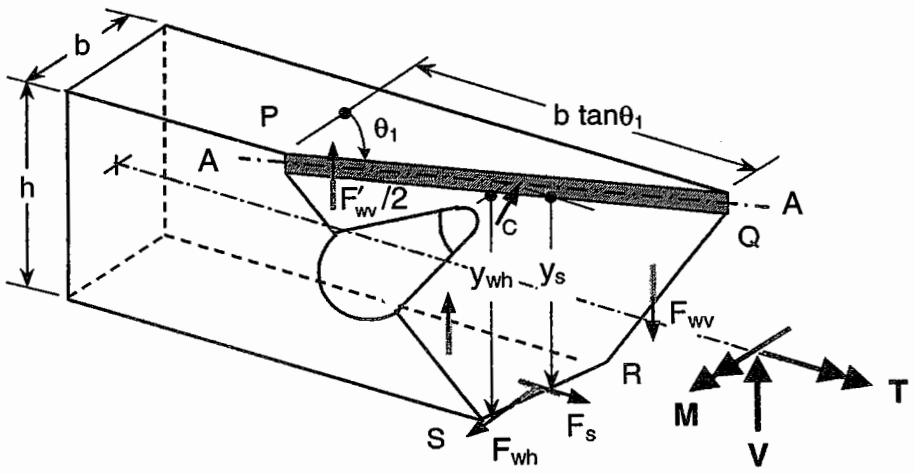

Figure 2.26 Mode 1 failure surface for beams with a small opening.

Take moments about axis A-A, which passes through the center of the compression zone. The moment about A-A of the applied vectors M, T, and V acting at the midsection of the opening (Hasnat and Akhtaruzzaman, 1987) must be equal to the moment of forces in steel reinforcement. The resulting expression may be obtained as follows:

$$T\sin\theta_1 + M\cos\theta_1 + V\left(\frac{b^2 + bh}{2b+4h}\right)\sin\theta_1 = F_s\cos\theta_1\, y_s + F_{wh}\sin\theta_1\, y_{wh} + \frac{1}{2}(F_{wv} + F'_{wv})\left[1 - \frac{b(b+h)}{x_1(b+2h)}\right]x_1\sin\theta_1 \tag{2.45}$$

The three expressions on the right-hand side of Eq. (2.45) represent the contributions of longitudinal steel, the bottom legs of stirrups, and the vertical legs of stirrups, respectively. However, forces in the vertical legs of the stirrups have lever arms about A-A so small that their contributions to the resisting moment for

Mode 1 failure may be neglected. Dropping the third expression on the right-hand side and dividing the resulting equation by $\cos\theta_1$, Eq. (2.45) thus reduces to

$$T\tan\theta_1 + M + V\mu\tan\theta_1 = F_s y_s + F_{wh} y_{wh}\tan\theta_1 \tag{2.46}$$

where

$$\mu = \frac{b^2 + bh}{2b + 4h} \tag{2.47}$$

Fig. 2.27 shows a developed diagram of the line PQRS (Fig. 2.26) of the failure surface, where PQ is the zone of compression and QR, RS, and SP are the cracks on the other three faces. It may be seen that the number of stirrup legs intersected at the bottom of the beam by the crack is approximately ($x_1 \tan\beta_1 / s$), where x_1 is the width of stirrups, s is the stirrup spacing, and β_1 is the inclination of the failure crack for Mode 1. Referring to Fig. 2.27, it can be shown that β_1 is related to θ_1 by:

$$\tan\beta_1 = \frac{b\tan\theta_1}{b + 2h} = \frac{\tan\theta_1}{(1 + 2\alpha)} \tag{2.48}$$

where $\alpha = h/b$, and b and h are the overall width and depth, respectively, of the solid cross section of the beam. If A_w denotes the area of one leg of the stirrups and f_{yw} is its yield strength, then

$$F_{wh} = \frac{A_w f_{yw}}{s}\, x_1 \tan\beta_1 \tag{2.49}$$

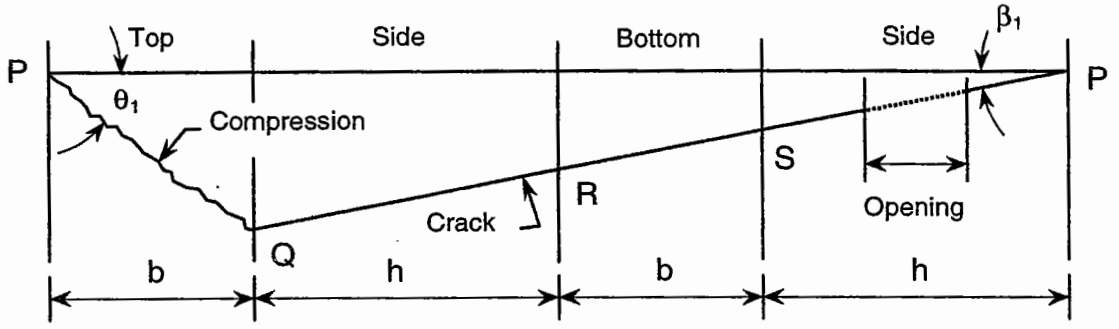

Figure 2.27 Geometry of the boundary of failure surface.

The term $F_s y_s$ in Eq. (2.46) represents approximately the pure positive bending strength of the section M_{o1}. If y_{wh} is taken as approximately equal to y_1, the dimension of the long stirrups parallel to h, then upon substitution of $\tan\theta_1$ from Eq. (2.48) and F_{wh} from Eq. (2.49), Eq. (2.46) becomes

$$(T + V\mu)(1 + 2\alpha)\tan\beta_1 + M = M_{o1} + \frac{A_w f_{yw}}{s} x_1 y_1 (1 + 2\alpha)\tan^2\beta_1 \tag{2.50}$$

The angle β_1 is determined on the basis of minimum value of T. In order to achieve this, Eq. (2.50) is first differentiated with respect to tan β_1. The resulting expression for $dT/d(\tan\beta_1)$, when equated to zero, yields

$$T + V\mu = 2\frac{A_w f_{yw}}{s} x_1 y_1 \tan\beta_1 \tag{2.51}$$

Substitution of Eq. (2.51) into Eq. (2.50) gives

$$\frac{T + V\mu}{2}(1+2\alpha)\tan\beta_1 + M = M_{o1} \tag{2.52}$$

The strength in failure Mode 1, which will be denoted by T_1, is obtained by eliminating tan β_1 from Eqs. (2.51) and (2.52). This leads to the following quadratic equation in T_1

$$T_1 = \frac{2M_{o1}K_1}{\Delta}\left[\sqrt{\frac{1}{K_1} + \frac{1}{(\psi\Delta)^2}} - \frac{1}{\psi\Delta}\right] \tag{2.53}$$

where $\psi = T/M$, $\lambda = M/V$,

$$K_1 = \frac{1}{1+2\alpha}\left[\frac{A_w f_{yw}}{s}\ \frac{x_1 y_1}{M_{o1}}\right] \tag{2.54}$$

and

$$\Delta = 1 + \frac{\mu}{\psi\lambda} \tag{2.55}$$

Mode 2 failure

The failure surface for this mode is illustrated in Fig. 2.28. In this failure mode, the compression zone is located along a lateral side of the beam making an angle θ_2 with the normal cross section. It is assumed that the longitudinal steel is concentrated at the corners and the lever arm of the force in this steel is x_1. The equation of moments about B-B is given by

$$T\sin\theta_2 + V\frac{x_1}{2} = F_s\cos\theta_2\, x_1 + F'_{wv}\sin\theta_2\, x_1 + F_{wh}\left[\frac{b}{h+2b}\right]\sin\theta_2\, y_1 \tag{2.56}$$

Similar to Mode 1 failure, the lever arm of the force F_{wh} about B-B is very small, and, hence, its contribution to the resisting moment may be ignored. Also, the first term on the right-hand side of Eq. (2.56) represents approximately the lateral flexural strength, M_{o2}, of the beam at the opening section. Thus, Eq. (2.56) reduces to

$$\left(T + V\frac{x_1}{2}\right)\tan\theta_2 = M_{o2} + F'_{wv}\tan\theta_2 x_1 \tag{2.57}$$

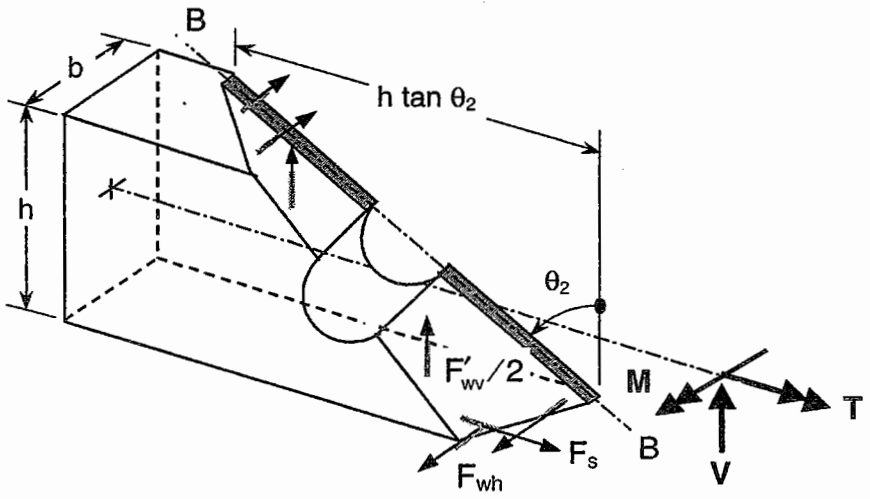

Figure 2.28 Mode 2 failure surface for beams with a small opening.

It may be shown that the inclination, β_2, of the failure crack for Mode 2 is related to the angle θ_2 by:

$$\tan\beta_2 = \frac{h\tan\theta_2}{h+2b} = \frac{\tan\theta_2}{1+2/\alpha} \tag{2.58}$$

and that

$$F'_{wv} = \frac{A_w f_{yw}}{s} y'_1 \tan\beta_2 \tag{2.59}$$

in which y'_1 is the total length of vertical legs of short stirrups at throat section on one face of the beam.

Inserting the values of $\tan\theta_2$ and F'_{wv} from Eqs. (2.58) and (2.59), respectively, into Eq. (2.57), we get

$$\left(T+V\frac{x_1}{2}\right)\left(1+\frac{2}{\alpha}\right)\tan\beta_2 = M_{o2} + \frac{A_w f_{yw}}{s} x_1 y'_1 \left(1+\frac{2}{\alpha}\right)\tan^2\beta_2 \tag{2.60}$$

Minimization of T with respect to $\tan\beta_2$ yields

$$T+V\frac{x_1}{2} = 2\frac{A_w f_{yw}}{s} x_1 y'_1 \tan\beta_2 \tag{2.61}$$

Substitution of Eq. (2.61) into Eq. (2.60) gives

$$\left(T+V\frac{x_1}{2}\right)\left(1+\frac{2}{\alpha}\right)\tan\beta_2 = M_{o2} \tag{2.62}$$

The strength equation for Mode 2 is obtained by eliminating tan β_2 from Eqs. (2.61) and (2.62) as:

$$T_2 = \frac{2\ M_{o1}}{1+\delta}\sqrt{R_2 K_2} \tag{2.63}$$

in which $\delta = x_1 V/2T$; $R_2 = M_{o2}/M_{o1}$, and

$$K_2 = \frac{1}{1+\dfrac{2}{\alpha}}\left[\frac{A_w f_{yw}}{s}\ \frac{x_1\, y_1'}{M_{o1}}\right] \tag{2.64}$$

Mode 3 failure

The analysis for Mode 3 is very similar to that for Mode 1. In this case, the skewed compression zone is at the bottom instead of at the top (see Fig. 2.25). The equations for Mode 1 can be used to derive the equations for Mode 3 by turning the beam upside down and taking $M = -M$, $V = -V$ and $\beta_1 = \beta_3$. Eqs. (2.51) and (2.52) thus, respectively, become

$$T - V\mu = 2\frac{A_w f_{yw}}{s} x_1\, y_1 \tan\beta_3 \tag{2.65}$$

and

$$\frac{T - V\mu}{2}\ (1+2\alpha)\tan\beta_3 - M = M_{o3} \tag{2.66}$$

The term M_{o3} is the pure flexural strength in negative bending. Being denoted by T_3, the strength in Mode 3 is obtained by eliminating tan β_3 from Eqs. (2.65) and (2.66) as:

$$T_3 = \frac{2M_{o1}K_1}{\Delta'}\left[\frac{1}{\psi\Delta'} - \sqrt{\frac{R_3}{K_1} + \frac{1}{(\psi\Delta)^2}}\ \right] \tag{2.67}$$

in which $R_3 = M_{o3}/M_{o1}$ and $\Delta' = \mu/(\psi\lambda) - 1$.

Shear-compression mode of failure

The three modes of failure, namely Mode 1, Mode 2, and Mode 3, as described above, may be termed as flexural type of torsional failure. Although the failure surface is skewed and warped, it has the general characteristics of the failure surface in pure flexure. As a result, the analysis is very similar to that for bending. These modes of failure usually occur when the beam contains adequate stirrups such that the main steel yields and the full flexural strength of the beam is reached when loaded to failure.

In the case of beams containing inadequate stirrups, the concrete compression zone may shear through prior to yielding of the main steel, and this will precipitate failure at a load below the corresponding flexural failure load. This type of failure may be called *shear-compression* mode of failure. A detailed analysis to predict the strength of the beam failing in this mode is rather too complex for practical use and is hardly justified because of the limited test data available.

For beams without an opening, it was found empirically (Collins et al.,1968) that the possibility of a shear type failure could be checked in a single step by introducing an "equivalent shear," V_{eq}, as given by

$$V_{eq} = V_u + \frac{1.6}{b} T_u \tag{2.68}$$

in which V_u and T_u are the factored shear and torsion, respectively, at the section under consideration. The shear compression strength of the beam can then be evaluated by means of the shear strength equation for a section using V_{eq} instead of V_u to account for torsional effects. This procedure has been found to give results well on the conservative side.

A similar equation has been proposed by Hasnat and Akhtaruzzaman (1987) to evaluate the shear compression strength of a beam containing a small opening. It is given as

$$V_{eq} = V_u + \frac{1.2}{b} T_u \tag{2.69}$$

EXAMPLE PROBLEM 2.5

A reinforced concrete beam of rectangular cross section, 400 mm wide by 800 mm overall depth, contains a 320 mm diameter circular opening at mid-depth. The reinforcement details of the beam around the opening region are shown in Fig. E2.5.1. The material properties are: $f'_c = 30$ *MPa;* $f_y = f_{yw} = 460$ *MPa.*

If the ratio of M / T is 2 and the ratio of T / V is 500 mm at the center of opening, calculate the nominal values of T, M, and V at failure.

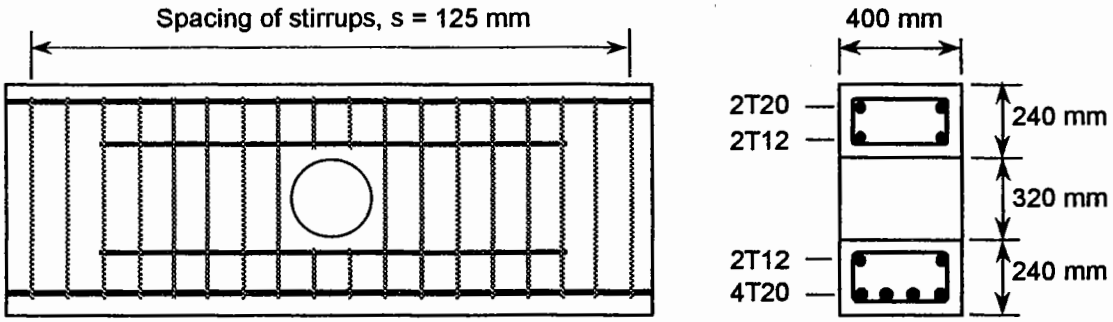

Figure E2.5.1 Reinforcement details of beam.

SOLUTION

(a) Pure flexural strengths, M_{o1}, M_{o2}, and M_{o3}

The calculation of pure flexural strength of the section through the opening in positive, lateral, and negative bending involves four levels of rebars. Following the strain compatibility approach using ACI Code (1995) provisions, these strengths may be obtained as

$$M_{o1} = 490 \text{ kNm}, \quad M_{o2} = 176 \text{ kNm}, \quad \text{and } M_{o3} = 288 \text{ kNm}$$

Therefore,

$$R_2 = 176 / 490 = 0.36, \text{ and } R_3 = 288/490 = 0.59$$

(b) Design data

For the given problem, the following design parameters are obtained.

Sectional details

For the given section

$h = 800$ mm; $b = 400$ mm
$x_1 = 340$ mm; $y_1 = 740$ mm; $y_1' = 180 \times 2 = 360$ mm
$s = 125$ mm; $A_w = 78.5$ mm^2; $f_{yw} = 460$ MPa.

Therefore,

$$\alpha = h/b = 800/400 = 2 \text{ and } \mu = 120 \text{ mm [Eq. (2.47)]}$$

Loading details

$\psi = T/M = 0.5$, $e = T/V = 500$ mm
$\lambda = M/V = e/\psi = 500/0.5 = 1000$ mm

(c) Strength in Mode 1

Substituting the relevant values in Eqs. (2.54) and (2.55), we obtain, respectively,

$$K_1 = 0.03, \text{ and } \Delta = 1.24$$

With $\psi\Delta = 0.6$, Eq. (2.53) yields

$$T_1 = 103 \text{ kNm}$$

(d) Strength in Mode 2

From Eq. (2.64), we obtain

$$K_2 = 0.036$$

Also

$$\delta = x_1 V/(2T) = x_1/(2e) = 340/(2 \times 500) = 0.34, \text{ and } R_2 = 0.36$$

Thus Eq. (2.63) gives

$$T_2 = 83 \text{ kNm}$$

(e) Strength in Mode 3

$$K_1 = 0.03, \text{ and } R_3 = 0.59$$
$$\Delta' = \mu/(\psi\lambda) - 1 = 120/(0.5 \times 1000) - 1 = -0.76$$

Therefore,

$$\psi\Delta' = -0.38$$

With these values, Eq. (2.67) gives

$$T_3 = 301 \text{ kNm}$$

(f) Strength in shear compression

Following the ACI Code approach, the nominal shear resistance provided by the concrete is obtained from Eq. (2.10) as

$$V_c = 159 \text{ kN}$$

Assuming a 45° inclined diagonal crack through the center of the opening, the failure plane intercepts only four full-depth stirrups. Therefore, the nominal shear resistance provided by stirrups is taken, according to Eq. (2.20), as

$$V_s = 4 \times 157 \times 460 \times 10^{-3} = 289 \text{ kN}$$

Hence,

$$V_n = 159 + 289 = 448 \text{ kN}$$

Equating this value with V_{eq} in Eq. (2.69), we have

$$448 = T/e + 1.2\ T/b = T/0.5 + 1.2\ T/0.4 = 5T$$

Therefore, the nominal torsional strength in shear compression mode is

$$T_{sc} = 448/5 = 90 \text{ kNm}$$

(g) Ultimate strength

Since $T_2 < T_{sc} < T_1 < T_3$, the beam will fail in Mode 2 at a nominal torsional strength of

$$T_n = 83 \text{ kNm}$$

Hence,

$$M_n = T_n/\psi = 83/\ 0.5 = 166 \text{ kNm}$$

$$V_n = T_n/e = 83/\ 0.5 = 166 \text{ kN}$$

2.4.2.2 Combined Torsion and Bending

The strength equations under combined torsion and bending for different failure modes can be obtained easily from Eqs. (2.53), (2.63), and (2.67) by eliminating the effect of shear, which reduces the terms $\Delta = 1$, $\Delta' = -1$, and $\delta = 0$. Obviously, there is no possibility of a shear-compression mode of failure. The equations to predict the torsional strength for the three flexural-type failure modes are obtained as

$$T_1 = 2M_{o1}K_1\left[\sqrt{\frac{1}{K_1}+\frac{1}{\psi^2}}-\frac{1}{\psi}\right] \tag{2.70}$$

$$T_2 = 2M_{o1}\sqrt{R_2 K_2} \tag{2.71}$$

$$T_3 = 2M_{o1}K_1\left[\sqrt{\frac{R_3}{K_1}+\frac{1}{\psi^2}}+\frac{1}{\psi}\right] \tag{2.72}$$

The least of T_1, T_2, and T_3 gives the torsional strength and the mode of failure.

EXAMPLE PROBLEM 2.6

For the beam in Example Problem 2.5, find the nominal ultimate strength of the beam if V = 0.

SOLUTION

Substituting the design data from Example Problem 2.5 into Eqs. (2.70), (2.71), and (2.72) for combined torsion and bending, we obtain

$$\begin{aligned} T_1 &= 2 \times 490 \times 0.03 \times \{[\,1/0.03 + 1/(0.5)^2]^{1/2} - 1/0.5\} \\ &= 121 \text{ kNm} \end{aligned}$$

$$\begin{aligned} T_2 &= 2 \times 490 \times (0.36 \times 0.036)^{1/2} \\ &= 112 \text{ kNm} \end{aligned}$$

$$\begin{aligned} T_3 &= 2 \times 490 \times 0.03 \times \{[\,0.59/0.03 + 1/(0.5)^2]^{1/2} + 1/0.5\} \\ &= 202 \text{ kNm} \end{aligned}$$

Thus $T_n = 112$ kNm and $M_n = 224$ kNm.

2.4.2.3 Pure Torsion

The effect of bending moment can be eliminated by putting $\psi = \infty$ in Eqs. (2.70)-(2.72), thus obtaining the case of pure torsion. The corresponding strength equations for Mode 1, Mode 2, and Mode 3 failures may be obtained as follows:

$$T_{o1} = 2M_{o1}\sqrt{K_1} \tag{2.73}$$

$$T_{o2} = 2M_{o1}\sqrt{R_2 K_2} \tag{2.74}$$

$$T_{o3} = 2M_{o1}K_1\sqrt{R_3 K_1} \tag{2.75}$$

EXAMPLE PROBLEM 2.7

Find the pure torsional strength of the beam in Example Problem 2.5.

SOLUTION

Substituting the relevant values from Example Problem 2.5 into Eqs. (2.73)-(2.75), we obtain

$$T_{o1} = 2 \times 490 \times 0.03^{1/2} = 170 \text{ kNm}$$

$$T_{o2} = 2 \times 490 \times (0.36 \times 0.036)^{1/2} = 112 \text{ kNm}$$

$$T_{o3} = 2 \times 490 \times (0.59 \times 0.03)^{1/2} = 130 \text{ kNm}$$

Thus, $T_n = 112$ kNm.

2.5 DESIGN FOR TORSION

In the preceding presentation of the skew-bending theory for torsion in concrete beams containing a small opening, the failure surface for a particular mode has been considered to pass through the center of the opening and encroach the solid part of the beam. Observed in many torsion tests (Hasnat and Akhtaruzzaman, 1987; Mansur and Hasnat, 1979; Mansur and Paramasivam, 1984; Mansur et al., 1982), these failure modes are basically identical to those of a beam without an opening, and, hence, may be termed as "*beam-type*" failure. A careful examination of the equations derived reveals that only the reinforcement in the solid section outside the opening participates in carrying the external load. When sufficient rebars are used to prevent failure to occur in these modes, then there is a possibility that the failure may precipitate in the members above and below the opening. This type of failure is shown in Fig. 2.29. It is similar to the "*frame-type*" shear failure of a beam with small openings shown in Fig. 2.9 and will be referred to as "*frame-type*" failure. In this type of failure, the entire applied actions are

resisted, independent of the solid part of the beam, by the members framing the opening, and, hence, require a separate treatment in design.

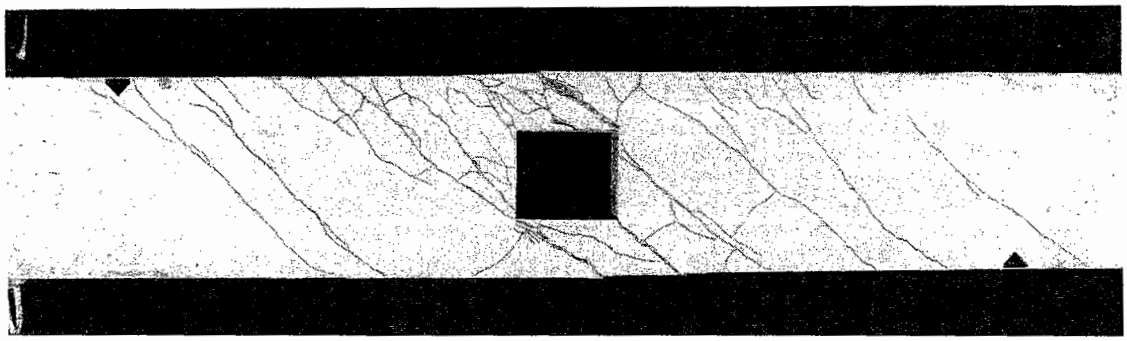

Figure 2.29 Frame-type failure of a beam with a small opening under torsion.

2.5.1 DESIGN FOR BEAM-TYPE FAILURE

The modes of failure considered in the skew-bending theory as discussed in Art. 2.4 are all considered as beam-type failure. These failure modes form the bases of the torsional design provision in the Australian Code, AS 1480 (1974), in which inclusion of the effect of torsion has essentially been reduced to usual flexural and shear design procedures. According to the code, the cross section is first proportioned on the basis of Mode 1 failure. Checks are then made and, if necessary, modifications are introduced to ensure that the beam will not fail in Modes 2 or 3, or the shear-compression mode. Steel percentages are also limited to guard against a primary crushing failure. Since the strength equations for different modes of failure remain basically similar when a small opening is introduced, and they are found to agree very well with reported test data (Hasnat and Akhtaruzzaman, 1987; Mansur and Hasnat, 1979; Mansur and Paramasivam, 1984; Mansur et al., 1982), the same approach with minor modifications for the inclusion of opening may be used for designing such beams (Mansur, "In press"). The design steps involved to account for the various possible modes of failure under predominant torsion are described in sequence as follows.

Mode 1 failure

Equations similar to those given in the Australian Code AS 1480 (1974) can be obtained directly from Eqs. (2.51) and (2.52). According to the Code, the value of $\tan \beta_1$ is chosen as

$$\tan \beta_1 = \frac{2}{\sqrt{1+2\alpha}} \tag{2.76}$$

Substitution of this value into Eqs. (2.51) and (2.52) gives

$$(T + V\mu)\sqrt{1+2\alpha} = 4\frac{A_w f_{yw}}{s} x_1 y_1 \tag{2.77}$$

$$(T + V\mu)\sqrt{1+2\alpha} + M = M_{o1} \tag{2.78}$$

In a design situation, the factored bending moment, torsional moment, and the shear force at the center of the opening are known. Thus, $M = M_u$, $T = T_u$, and $V = V_u$. Designating the first term of Eq. (2.78) as $M_{eq(1)}$, the equivalent moment due to torsion and shear in Mode 1 failure, that is,

$$M_{eq(1)} = (T_u + V_u\mu)\sqrt{1+2\alpha} \tag{2.79}$$

the required strength in positive bending becomes

$$M_{o1} = M_{eq(1)} + M_u \tag{2.80}$$

The designer chooses a value of α (= h/b) if the sectional dimensions are not given or known in advance, evaluates $M_{eq(1)}$, and then finds the value of M_{o1}. The section and the longitudinal reinforcement must be designed for this moment using the normal flexural design procedure.

The transverse reinforcement is obtained from Eq. (2.77). Introducing a capacity reduction factor, ϕ, the following equation is obtained

$$\frac{A_w}{s} = \frac{1}{\phi}\left[\frac{M_{eq(1)}}{4\, x_1\, y_1\, f_{yw}}\right] \tag{2.81}$$

in which the capacity reduction factor $\phi = 0.85$.

Mode 2 failure

In the Australian Code (1974), the design equations were derived by assuming that tan β_2 is given by the following equation:

$$\tan\beta_2 = \frac{2}{\sqrt{1+\dfrac{2}{\alpha}}} \tag{2.82}$$

Substitution of Eq. (2.82) for tan β_2 in Eq. (2.62) yields

$$M_{o2} = M_{eq(2)} \tag{2.83}$$

in which $M_{eq(2)}$, the equivalent moment due to shear and torsion for Mode 2 failure, is given by

$$M_{eq(2)} = \left(T_u + V_u\frac{x_1}{2}\right)\sqrt{1+\frac{2}{\alpha}} \tag{2.84}$$

AS 1480-1974 suggests that if $M_u < 0.5 M_{eq(2)}$, the cross section of the beam and the area of longitudinal reinforcement should be such that the beam can withstand an equivalent bending moment, $M_{eq(2)}$, as given above in lateral bending. Also, the area of web steel should not be less than that given by

$$\frac{A_w}{s} = \frac{1}{\phi}\left[\frac{M_{eq(2)}}{4 x_1 y_1 f_{yw}}\right] \tag{2.85}$$

Mode 3 failure

Taking tan β_3 = tan β_1, which is given by Eq. (2.76), upon substitution, Eq. (2.66) then reduces to

$$M_{o3} = M_{eq(3)} - M_u \tag{2.86}$$

in which

$$M_{eq(3)} = (T_u - V_u \mu)\sqrt{1+2\alpha} \tag{2.87}$$

is the equivalent moment due to torsion and shear in Mode 3 failure.

Thus, if the numerical value of M_u is greater than $M_{eq(3)}$, there is no possibility of a Mode 3 failure. Physically it means that any tensile stress at the top of the beam induced by $M_{eq(3)}$ is canceled by the compression due to M_u. No top steel is, therefore, required. However, nominal steel comprising at least one bar at each of the top two corners must be provided for anchorage of stirrups.

If $M_u < M_{eq(3)}$, there will be residual tension at the top of the beam, and top steel should be introduced according to the usual flexural theory to withstand a negative bending (that is, one of opposite sign to M_u) of magnitude $(M_{eq(3)} - M_u)$.

Shear-compression mode of failure

Similar to the Australian Code (1974) approach, Eq. (2.69) may be used to preclude a shear-compression mode of failure of a beam containing a small opening. Thus, the equivalent shear for this mode is calculated as

$$V_{eq(sc)} = V_u + \frac{1.2}{b} T_u \tag{2.88}$$

The transverse reinforcement is then designed to resist this equivalent shear on the basis of the normal shear design provisions by assuming that the failure plane passes through the center of opening. If the steel area, A_w, thus determined is greater than that already found during the previous design steps, the larger quantity should be adopted.

Primary compression failure

The design for the three flexural modes of failure, that is, Mode 1, Mode 2, and Mode 3, are carried out on the basis of the normal procedure for flexural design,

which involves a limitation on the area of longitudinal steel for ductility reasons. It is considered that this limitation will ensure that the beam is under-reinforced with regard to the longitudinal steel.

In the case of a solid beam under torsion, the Australian Code suggests that the primary compression failure by crushing of concrete diagonals may be avoided by ensuring that

$$V_{eq(sc)} \leq [V_u]_{max} = \phi\, 0.83 \sqrt{f'_c}\, b\, d \tag{2.89}$$

where the quantities are expressed in SI units. This equation is identical to Eq. (2.19) given in the ACI Code (1995).

For beams with small openings, an equation similar to Eq. (2.11) has been suggested (Mansur, "In press") by considering the area of concrete removed by the opening as

$$V_{eq(sc)} \leq [V_u]_{max} = \phi\, 0.83 \sqrt{f'_c}\, b\,(d - d_o) \tag{2.90}$$

2.5.2 DESIGN FOR FRAME-TYPE FAILURE

This type of failure occurs when the members above and below the opening are not adequately reinforced for the actions being transmitted through them. In the case of combined bending and shear, it has been shown in Art. 2.3.2 that the applied shear may be assumed to be shared by the chord members in proportion to their cross-sectional areas. Similarly, the applied torque, that produces lateral shear stresses in the chord members, may be assumed to be resisted by the couple formed by the resultant of these stresses, as shown in Fig. 2.30.

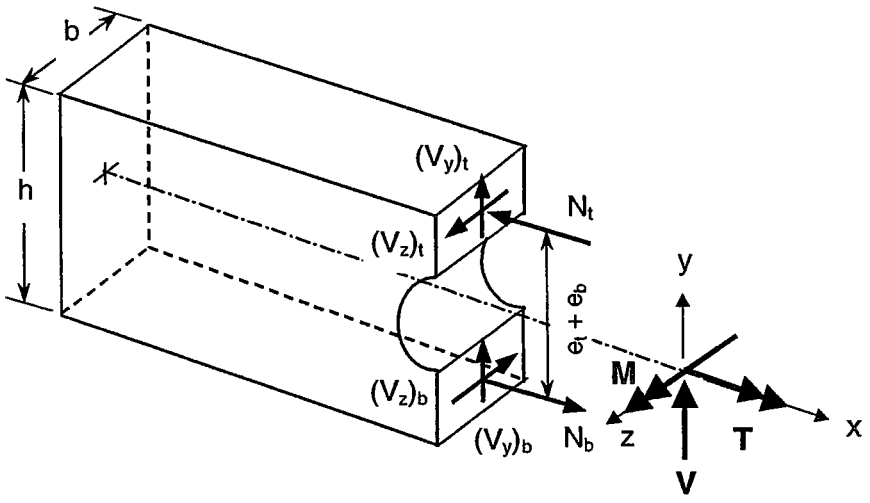

Figure 2.30 Idealized free-body diagram at opening of a beam under combined loading.

The above assumption may be justified from the work of Mansur et al. (1983b). They have assumed that for a beam containing an opening, the applied torque is resisted by torsion in each member and by the couple formed by the lateral shear and shown analytically that the torsional component becomes smaller as the length of opening is decreased and eventually becomes negligible in comparison to the latter component (couple formed by the lateral shear) when the opening reduces to square (or circular) in size. Thus, referring to Fig. 2.30, the lateral shear, V_z, may be assumed to be given by

$$(V_z)_t = (V_z)_b = \frac{T_u}{e_t + e_b} \tag{2.91}$$

With the usual mechanism for applied bending moment, the problem of combined torsion, bending, and shear for frame-type failure thus reduces to designing each chord member at the opening for shear in two directions, as shown in Fig. 2.30.

2.5.3 CONSIDERATIONS FOR DETAILING

In the case of a solid beam under predominant torsion, the usual detailing requirement is that closed links with the ends sufficiently anchored inside the concrete core must be used and that at least one longitudinal bar be placed at each corner of the stirrup. Also, to prevent spalling of concrete cover due to bending of the longitudinal rebars in between stirrup supports (Michell and Collins, 1976), spacing of stirrups should be restricted by the following requirements:

$$s \leq \frac{x_1 + y_1}{4} \tag{2.92}$$

$$\text{or} \quad s \leq 300 \text{ mm}$$

whichever is less. The same detailing requirements for stirrups should apply to beams containing a small opening for the section both through and beyond the opening.

Here, design for the beam-type failure will fix the top and bottom longitudinal reinforcement for the overall section, and the requirements of stirrups for the solid section outside the opening. Design for frame-type failure will give the amount of vertical and horizontal legs of stirrups in each chord member for vertical and lateral shear, respectively. The larger amount should be adopted in the form of closed stirrups subject to the spacing limit of Eq. (2.92). Also, nominal longitudinal bars must be used at the top and bottom of the opening for anchorage of these short stirrups. In order to contain the growth of cracks, nominal diagonal bars should also be added next to the edges of the opening normal to the direction of potential cracking due to applied loading with sufficient length for the development of yield strength. These bars should be arranged in such a way as to avoid any confusion and possible construction error.

EXAMPLE PROBLEM 2.8

A 300 mm diameter opening is to be provided through a reinforced concrete beam of rectangular cross section, 400 mm wide and 800 mm deep. The beam is subject to combined torsion, bending, and shear. The opening is located at mid-depth of the beam, and the moments and shear at the section through the center of the opening due to factored loads are T_u = 120 kNm, M_u = 250 kNm, and V_u = 100 kN. Design the reinforcement for the opening region of the beam. Use f'_c = 30 MPa, f_y = f_{yv} = f_{yw} = 460 MPa.

SOLUTION

1. DESIGN FOR BEAM-TYPE FAILURE

(a) Check adequacy of the section

From Eq. (2.88), the equivalent shear,

$$V_{eq(sc)} = 100 + 1.2\frac{120}{0.4} = 460 \text{ kN}$$

Assuming T25 longitudinal bars, T10 bars for stirrups, and 25 mm clear concrete cover,

$$d = 800 - (25 + 10 + 12.5) = 752.5 \text{ mm}$$

Therefore, Eq. (2.90) gives

$$[V_u]_{max} = 0.85 \times 0.83 \times \sqrt{30} \times 400 \times (752.5 - 300)\ 10^{-3} = 699 \text{ kN}$$

Since $[V_u]_{max} > V_{eq(sc)}$, the cross section is adequate.

(b) Design of main longitudinal steel

For the given cross section, α = 2, and Eq. (2.47) gives μ = 120 mm. Eqs. (2.79) and (2.80) thus give

$$M_{o1} = (120 + 100 \times 0.12)\sqrt{(1 + 2 \times 2)} + 250 = 545 \text{ kNm}$$

The longitudinal tensile reinforcement should therefore be proportioned to provide a nominal resistance of $M_n = M_{o1}$ = 545 kNm. Using a capacity reduction factor, ϕ = 0.9 for bending, Eq. (2.5) becomes

$$0.59\, q_s^2 - q_s + \frac{545 \times 10^6}{0.9 \times 400 \times 752.2^2 \times 30} = 0$$

or

$$0.59\, q_s^2 - q_s + 0.089 = 0$$

which yields $q_s = 0.095$. Therefore,

$$A_s = \frac{b d f_c'}{f_y} q_s = \frac{400 \times 752.5 \times 30}{460} \times 0.095 = 1865 \text{ mm}^2$$

Use 4T25, which gives $\rho = 0.0066$. This reinforcement ratio has been found to be less than 0.75 times the balanced ratio. Hence, ductility of the section is ensured.

(c) Design of longitudinal top steel

The equivalent moment due to shear and torsion for Mode 3 failure is given by Eq. (2.87) as

$$M_{eq(3)} = (120 - 100 \times 0.12)\sqrt{(1 + 2 \times 2)} = 241 \text{ kNm}$$

Since $M_u = 250$ kNm > $M_{eq(3)}$, there is no possibility of a Mode 3 failure. Therefore, use nominal top steel, say, 2T12 bars.

(d) Check for Mode 2 failure

The equivalent lateral bending moment due to shear and torsion for Mode 2 failure is given by Eq. (2.83). As $x_1 = 340$ mm,

$$M_{eq(2)} = \left(120 + 100 \times \frac{0.34}{2}\right)\sqrt{\left(1 + \frac{2}{2}\right)} = 194 \text{ kNm}$$

Thus, $M_u = 250$ kNm > 0.5 $M_{eq(2)}$. Hence, there is no danger of a Mode 2 failure for the section.

(e) Design of stirrups

For torsion

Assuming that T10 bars are used for stirrups with a clear concrete cover of 25 mm,

$$x_1 = 400 - 2 \times 25 - 10 = 340 \text{ mm}$$
$$y_1 = 800 - 2 \times 25 - 10 = 740 \text{ mm}$$

Also,

$$M_{eq(1)} = 545 - 250 = 295 \text{ kNm}$$

Eq. (2.85) therefore gives

$$\frac{A_w}{s} = \frac{1}{0.85}\left[\frac{295 \times 10^6}{4 \times 340 \times 740 \times 460}\right] = 0.75 \text{ mm}^2/\text{mm}$$

For shear

Using the simplified method of the ACI Code, the shear resistance of the concrete for a beam with a small opening is given by Eq. (2.11). Thus,

$$V_c = \frac{1}{6} \times \sqrt{30} \times 400 \ (752.5 - 300) \times 10^{-3} = 165 \text{ kN}$$

Since $V_{eq(sc)} = 535$ kN > V_c, shear reinforcement is required. Using Eq.(2.16) and noting that for two-legged stirrups, $A_v = 2\ A_w$, we have

$$\frac{A_w}{s} = \frac{1}{0.85} \left[\frac{535 - 0.85 \times 165}{2 \times 752.5 \times 460} \right] \times 10^3 = 0.67 \text{ mm}^2/\text{mm}$$

This is smaller than that required for torsion. Hence, spacing of two-legged T10 stirrups required is

$$s = A_w/0.75 = 78.5/0.75 = 104 \text{ mm, say, } 100 \text{ mm.}$$

It should be noted here that this spacing applies only to the solid sections adjacent to the opening.

2. DESIGN OF CHORD MEMBERS FOR FRAME-TYPE FAILURE

(a) Design of bottom chord

Vertical shear

Since the members above and below the opening have identical cross section, the factored shear of 100 kN at the center of the opening will be shared equally by the two members. Therefore, V_u = 50 kN for the bottom chord. Also, d = 202.5 mm. Therefore,

$$[V_u]_{max} = \frac{5}{6} \times 0.85 \times \sqrt{30} \times 400 \times 202.5 \times 10^{-3} = 314 \text{ kN}$$

Since $V_u < [V_u]_{max}$, the section is adequate.

This member is subject to axial tension due to global bending. Neglecting the contribution of concrete, and using two-legged stirrups of T10 bars, we have

$$\frac{A_v}{s} = \frac{50{,}000}{0.85 \times 460 \times 202.5} = 0.63 \text{ mm}^2/\text{mm}$$

This is larger than $[A_v/s]_{min} = 0.29$ by Eq. (2.16). Hence,

$$s = 157/0.63 = 249 \text{ mm}$$

As this spacing is larger than $d/2 = 101$ mm, use $s = 100$ mm for the vertical legs.

Lateral shear

The lateral shear is given by Eq. (2.91) as

$$V_u = 120/0.55 = 218 \text{ kN}$$

With $b = 250$ mm, and $d = 400 - (25 + 10 + 12.5) = 352.5$ mm,

$$[V_u]_{max} = 342 \text{ kN and } V_c = 68 \text{ kN}$$

Thus, $3\phi V_c = 205$ kN $< V_u < [V_u]_{max}$. Hence,

$$\frac{A_v}{s} = \frac{218{,}000}{0.85 \times 460 \times 352.5} = 1.58 \text{ mm}^2/\text{mm}$$

and

$$s = 157/1.58 = 99.4 \text{ mm} > d/4 = 88 \text{ mm}$$

Hence, use $s \approx 88$ mm for the horizontal legs. This, together with the spacing requirement for vertical legs, will be satisfied if three closed stirrups are provided in between the two full-depth stirrups by the side of the opening.

(b) Design of top chord

Top chord is subject to axial compression due to bending. Since it has the same dimensions as those of the bottom chord, and as the magnitudes of both transverse and lateral shear are the same, the use of same stirrups for the top chord will be on the conservative side.

3. Detailing of reinforcement

The detailed arrangement of reinforcement for the opening region is shown in Fig. E2.8.1.

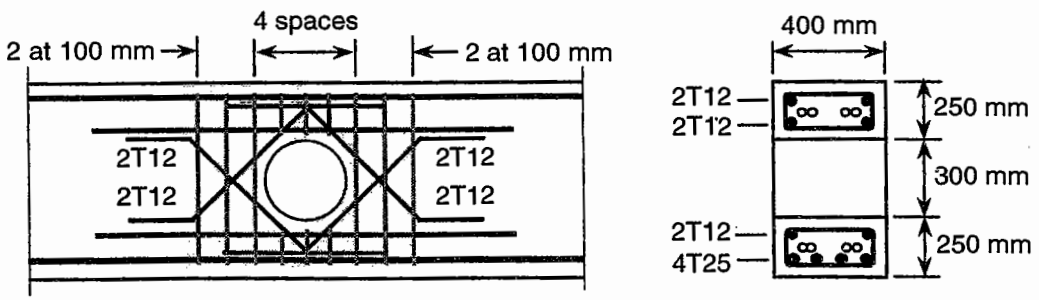

Figure E2.8.1 Reinforcement details.

It may be seen in Fig. E2.8.1 that nominal longitudinal bars are provided on the top and bottom faces of the bottom and top chords, respectively, for anchorage of short stirrups. Also, nominal diagonal bars are added for crack control.

2.6 EFFECT OF CREATING OPENINGS IN EXISTING BEAMS

It is obvious from the preceding discussion that transverse openings provided through beams to accommodate utility ducts and pipes for better utilization of the otherwise dead space above the beam soffit are a potential source of weakness in a beam. When the service systems are preplanned and the sizes and locations of openings required to achieve the necessary layout of pipes and ducts are decided upon well in advance, adequate strength and serviceability may be ensured during the design stage by following the methods described in the preceding sections.

However, this is not always the case. There are at least two circumstances that necessitate drilling of holes in an existing structure. The first is in a newly constructed building. While laying the service ducts, the M&E contractor frequently comes up with the request to drill an opening for the sake of simplifying the arrangement of pipes not carefully considered during the design stage. When such a request comes, the structural designer finds it difficult to make a decision. Of course, from the owner's viewpoint, creating an opening may represent some financial savings, but the structural engineer would have to take the risk of jeopardizing the safety and serviceability of the structure.

The second circumstance arises in an old building. Here, the openings are created by removing concrete cores for structural assessment of the building. However, in such a case, the holes are generally filled in by nonshrink grout. If the structure is to remain, then the question is whether such a repair is adequate to restore the original level of safety and serviceability of the structure. A recent study conducted at the National University of Singapore (Weng, 1998) made an attempt to answer some of these frequently asked questions related to drilling of holes in an existing beam.

In the study, a total of nine prototype T-beams simulating the conditions that exist in the negative moment region of a continuous beam were tested. All beams were 2.9 m long and contained a central stub to represent the continuous support. The cross section consisted of a 400-mm-deep and 200-mm-wide web and a 100-mm-thick and 700-mm-wide flange. To allow for the clearance needed to install the coring machine, the openings in all the beams were located in the web at a distance of 50 mm from the flange. For symmetry, one identical opening was created on each side of the central stub, and all beams contained the same amount and arrangement of reinforcement as can be seen in Fig. 2.31.

The beam designated S in Table 2.1 did not contain any opening. It served as a reference to assess the performance of the beams with openings. The remaining beams with openings were divided into three distinct groups according to the test parameters: size of openings, location of openings, and method of repair or strengthening. They were designated basically by two letters, D and X. The subscript to D represents the diameter of openings in centimeters and that to X stands for opening location with 1 representing the nearest and 4 being the furthest from the face of the central stub. At these locations, each opening intercepted one of the stirrups on its way. To simulate the condition of coring the opening, these

stirrups were cut during fabrication of the reinforcement cage. But instead of physically coring the opening, they were preformed at the time of casting.

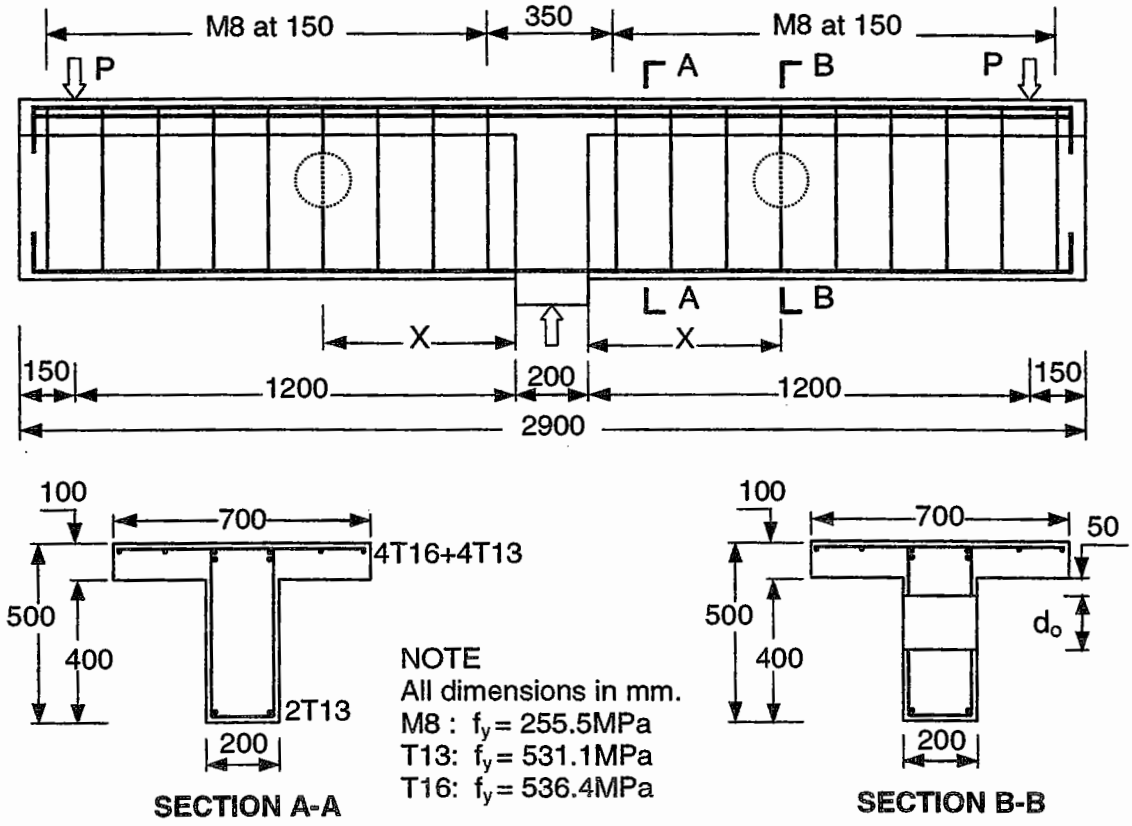

Figure 2.31 Reinforcement details of beams (Weng, 1998).

Table 2.1 Details of test program (Weng, 1998).

Beam	Diameter of openings, d_o (mm)	Location of openings, X (mm)	Cylinder compressive strength, f'_c (MPa)
S	NA	NA	30.8
$D_{10}X_4$	100	525	29.7
$D_{15}X_4$*	150		29.7
$D_{20}X_4$	200		48.8
$D_{15}X_1$	150	125	50.6
$D_{15}X_2$		275	50.6
$D_{15}X_3$		400	38.0
$D_{15}X_4$*		525	29.7
$D_{15}X_4$-G	150	525	37.9
$D_{15}X_4$-F			37.1

* Same beam.

Beams $D_{15}X_4$-G and $D_{15}X_4$-F were identical to beam $D_{15}X_4$ except for subsequent repair and strengthening. While the beam $D_{15}X_4$-G was repaired by filling the openings with nonshrink construction grout to simulate the field condition of removing a concrete core to find the in situ concrete strength, beam $D_{15}X_4$-F was strengthened by externally bonded carbon fiber reinforced polymer (FRP) plates in an attempt to restore the original response.

In the following sections, the test data generated for the nine beams is discussed from the viewpoints of the two fundamental design requirements – strength and serviceability. In the case of serviceability, only cracking and deflection (stiffness) aspects of the beams with openings in relation to the one without an opening are presented. The effectiveness of the two repair methods is also discussed.

2.6.1 CRACKING AND CRACK WIDTHS

The cracking loads and the maximum crack widths at the assumed service load are summarized in Table 2.2. The cracking patterns of some of the typical beams after failure and the load versus maximum crack width curves for the beams are presented in Fig. 2.32 and Fig. 2.33, respectively.

It was reported (Weng, 1998) that beam $D_{15}X_1$, which contained an opening nearest to the center stub (see Table 2.1), exhibited a cracking pattern remarkably similar to that of the solid beam S. The major diagonal crack, which led to the failure of all the nonrepaired beams, always passed through the center of the opening. Beam $D_{15}X_4$-G, the openings of which were filled with nonshrink grout, behaved in a similar manner except that failure crack bypassed the center of the opening, as can be seen in Fig. 2.32, due to inadequate interfacial bond between the parent and in-filled concrete. In contrast, beam $D_{15}X_4$-F, which was strengthened by FRP plates, had almost the same behavior as the solid beam except that it had less number of narrower web cracks.

Table 2.2. Cracking and service load behavior.

Beam	Cracking load(kN)		At service load*	
	Flexural crack (kN)	Shear crack (kN)	Maximum crack width (mm)	Maximum deflection (mm)
S	80	200	0.27	4.83
$D_{10}X_4$	75	155	>1.00	5.55
$D_{15}X_4$	85	134	>1.00	5.57
$D_{20}X_4$	85	98	>1.00	8.56
$D_{15}X_1$	94	120	0.47	5.65
$D_{15}X_2$	82	128	0.67	5.41
$D_{15}X_3$	85	130	0.97	6.04
$D_{15}X_4$-G	95	195	0.98	4.91
$D_{15}X_4$-F	95	215	0.25	3.57

*Service load of the solid beam S = ultimate load/1.7 = 268.6kN.

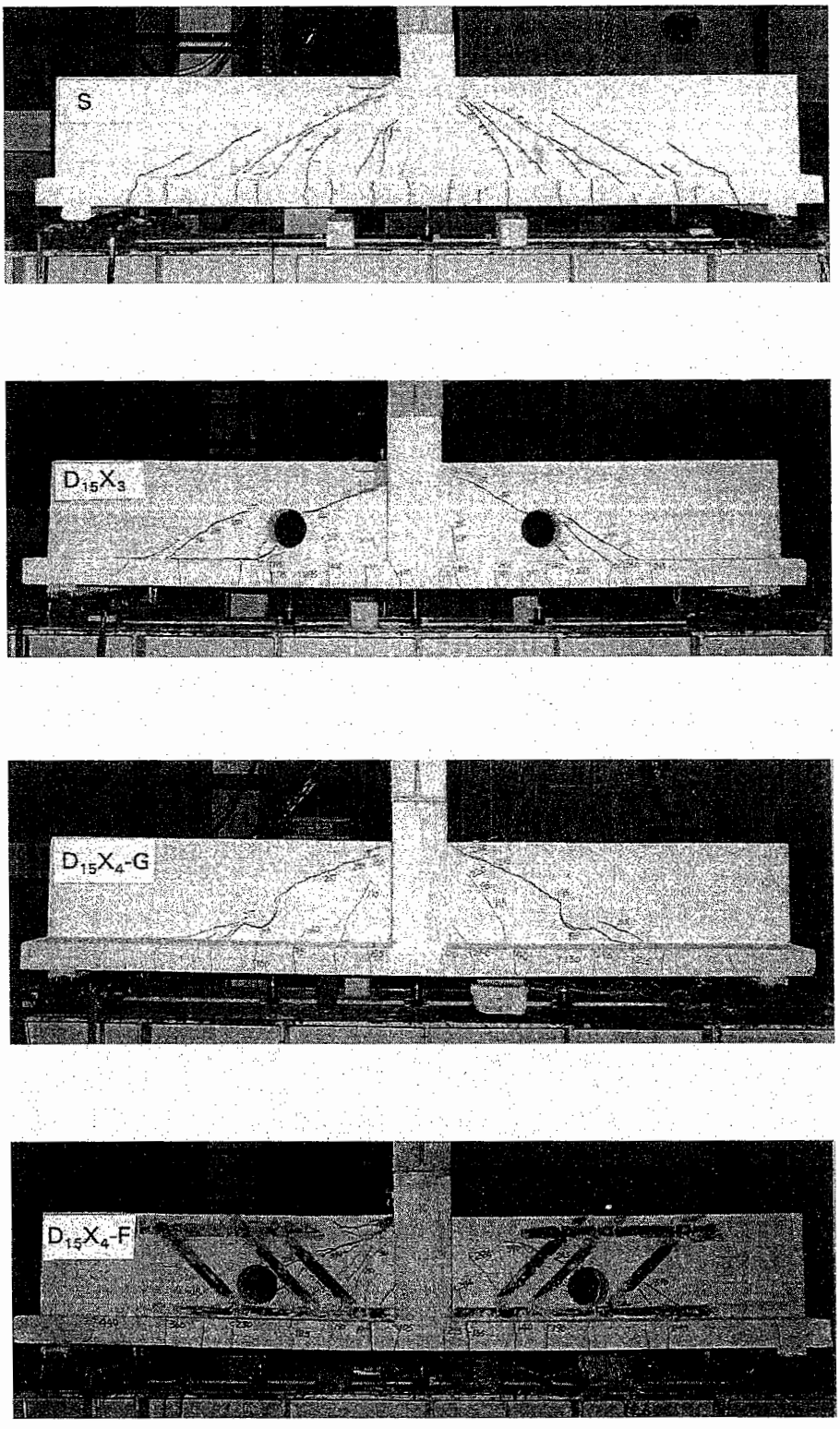

Figure 2.32 Cracking patterns of some typical beams (Weng, 1998).

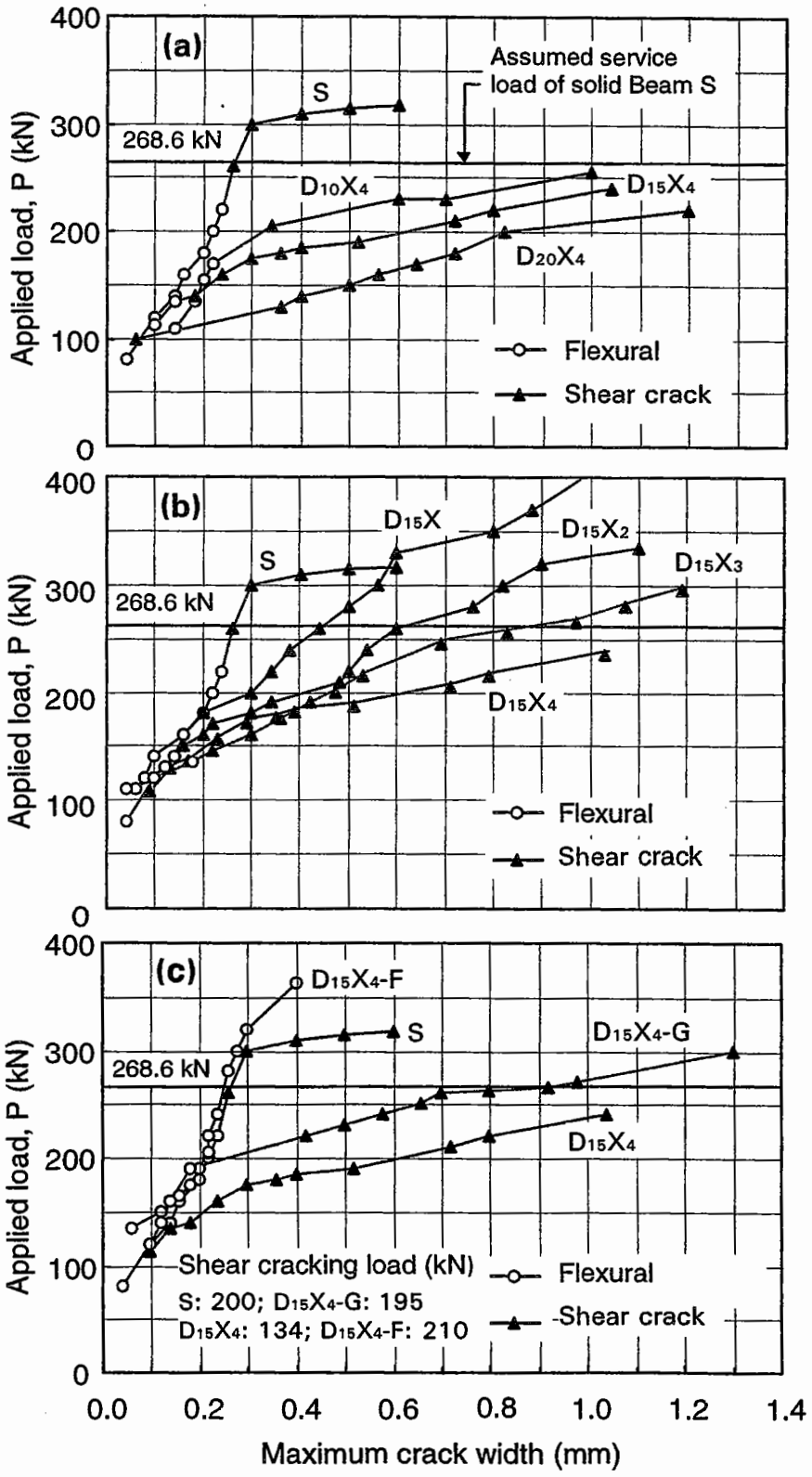

Figure 2.33 Load vs. maximum crack width curves (a) effect of opening size; (b) effect of opening location; (c) effect of repair and strengthening.

The loads at which first vertical (flexural) and diagonal (shear) cracks occurred are summarized in Table 2.2. It may be seen that shear cracking was always preceded by flexural cracking, and that the load at which first flexural crack occurred remained relatively unaffected by the presence of an opening. But the shear cracks in the beams with openings appeared much earlier than in the solid beam. The diagonal cracking load decreases with an increase in the size of opening, but remains within a narrow range when the same opening is placed at different locations. For beams $D_{15}X_4$-G and $D_{15}X_4$-F, the first shear crack appeared almost at the same load as the solid beam, thus indicating the effectiveness of the repair methods as far as the first diagonal cracking was concerned.

Figs. 2.33(a) and (b) show the load versus maximum crack width curves for beams with different sizes and locations of openings, respectively. It may be seen that an increase in the size of opening increases the maximum crack width at all load levels. Similarly, an increase in the distance of opening from the center stub, which simulates a continuous support, leads consistently to larger crack widths.

In order to evaluate the effect of creating an opening on the serviceability limit state of cracking, the solid beam S is taken as the reference. For this beam, the service load of 268.6 kN is calculated by dividing the experimental ultimate load by a factor of 1.7. At this load, the solid beam exhibited a maximum crack width of 0.27 mm, which is less than the maximum width generally allowed for indoor condition. However, as shown in Table 2.2, the maximum crack width at the same load level in all the remaining beams well exceeded this permissible value. This serves as a warning that openings, when created in an existing beam, might seriously affect the serviceability limit state of cracking, irrespective of their size and location.

Fig. 2.33(c) shows the load versus maximum crack width curves for beams S, $D_{15}X_4$, $D_{15}X_4$-G, and $D_{15}X_4$-F. It indicates that the beam strengthened with FRP plates has crack control characteristics even better than the solid beam. As for the beam with grout-filled openings, maximum crack width was comparable to that in the solid beam prior to shear cracking. However, after the first shear crack occurred, the diagonal crack grew rapidly, as in the case of beam $D_{15}X_4$. Although grout filling resulted in some improvement over the corresponding beam $D_{15}X_4$ without a grout in-fill, the performance with regard to cracking was far beyond the target performance of the solid beam S.

2.6.2 STIFFNESS AND DEFLECTION

In the study by Weng (1998), the concrete strength varied from about 29.7 to 50.6 Mpa, as indicated in Table 2.1. This large variation in the grade of concrete affected the strength and stiffness of the beams. In order to make a meaningful assessment of the performance of a beam with openings in relation to the reference solid beam, some adjustments to the ultimate strength and the load-deflection response for the variation in concrete strength are made. The adjusted curves are presented in Fig. 2.34.

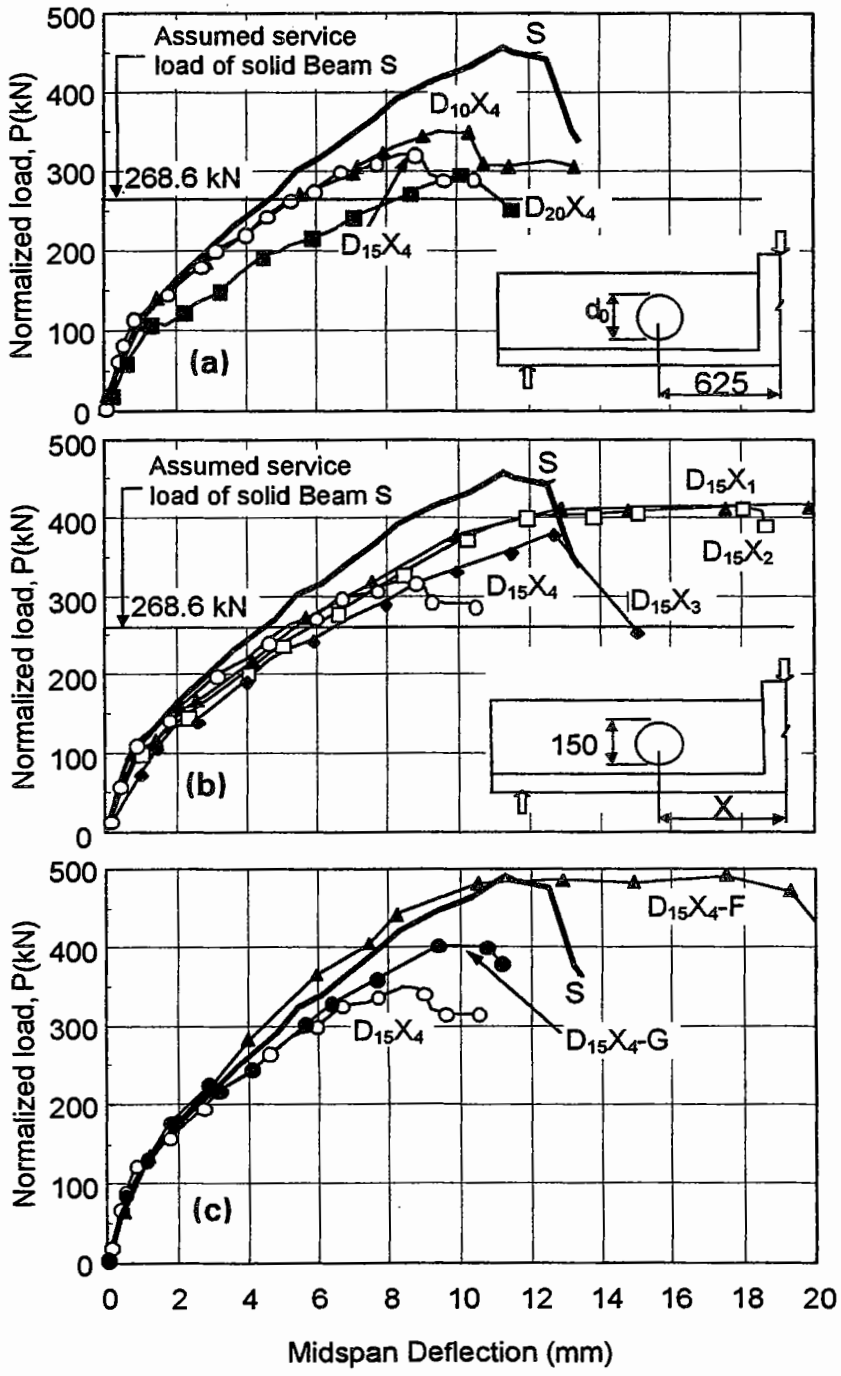

Figure 2.34 Load vs. midspan deflection curves (a) effect of opening size; (b) effect of opening location; (c) effect of repair and strengthening.

It may be seen in Fig. 2.34(a) that the post-cracking stiffness of a beam is reduced substantially when an opening is created and that an increase in the size of opening decreases the beam stiffness. However, the effect of opening location

is not quite obvious as can be noted in Fig. 2.34(b). At the calculated service load for the reference beam S, the maximum deflections recorded in Table 2.2 indicate that the provision of an opening, irrespective of its size or location, produced larger deflections, which may affect the serviceability of the beam.

The effects of repair and strengthening may be observed in Fig. 2.34(c). It may be seen that repair by grout filling improves the stiffness when compared to that of the corresponding beam $D_{15}X_4$ without an in-fill, but the improvement is still a long way behind the target response of the solid beam. However, strengthening by externally bonded FRP plates as used in beam $D_{15}X_4$-F can completely eliminate the weakness introduced in the beam by creating the opening.

2.6.3 ULTIMATE STRENGTH

The ratio of ultimate shear strength of beams with openings to that of the reference beam, normalized for the differences in concrete strength, are plotted against the size and location of openings in Figs. 2.35(a) and (b), respectively. It may be seen that the strength of a beam decreases either with an increase in the size of opening or with an increase in the distance X from the center stub. Even for the beam $D_{15}X_1$ in which the opening was located close to the support so as to bypass the potential failure plane, the strength is reduced by about 11% as compared to the solid beam. This might be due to the fact that one of the stirrups was intercepted by the opening and made it ineffective to carry any significant applied shear.

The ratios of normalized ultimate shear strength of beams $D_{15}X_4$, $D_{15}X_4$-G, and $D_{15}X_4$-F to that of the solid beam S are shown in Fig. 2.35(c). Similar to the effects on cracking and deflection, filling the opening by nonshrink grout (beam $D_{15}X_4$-G) restores part of the strength, but it is still about 20% lower than the original strength, that is, the strength of the solid beam. Some form of strengthening, like the use of FRP plates as employed here for beam $D_{15}X_4$-F or any other suitable means, is necessary to restore the strength of the beam to the original level.

2.6.4 REMARKS

The results of the nine prototype T-beams described in Art. 2.6 clearly indicate that an opening, when created near the support region of an existing beam, where shear is predominant, may seriously impair the safety and serviceability of the structure. Also, filling an opening by nonshrink grout, as usually done for openings created by removing concrete cores for the determination of in situ concrete strength of an old building, is not adequate to restore the original strength and stiffness. Limiting the size of opening or drilling the opening without cutting any stirrups may, however, minimize the risk. In any case, the designer must carefully analyze and assess the situation. No opening should be created in an existing beam unless larger-than-usual factor of safety is incorporated in the original design or suitable measures to strengthen the beam are undertaken, such as the use of externally bonded FRP plates.

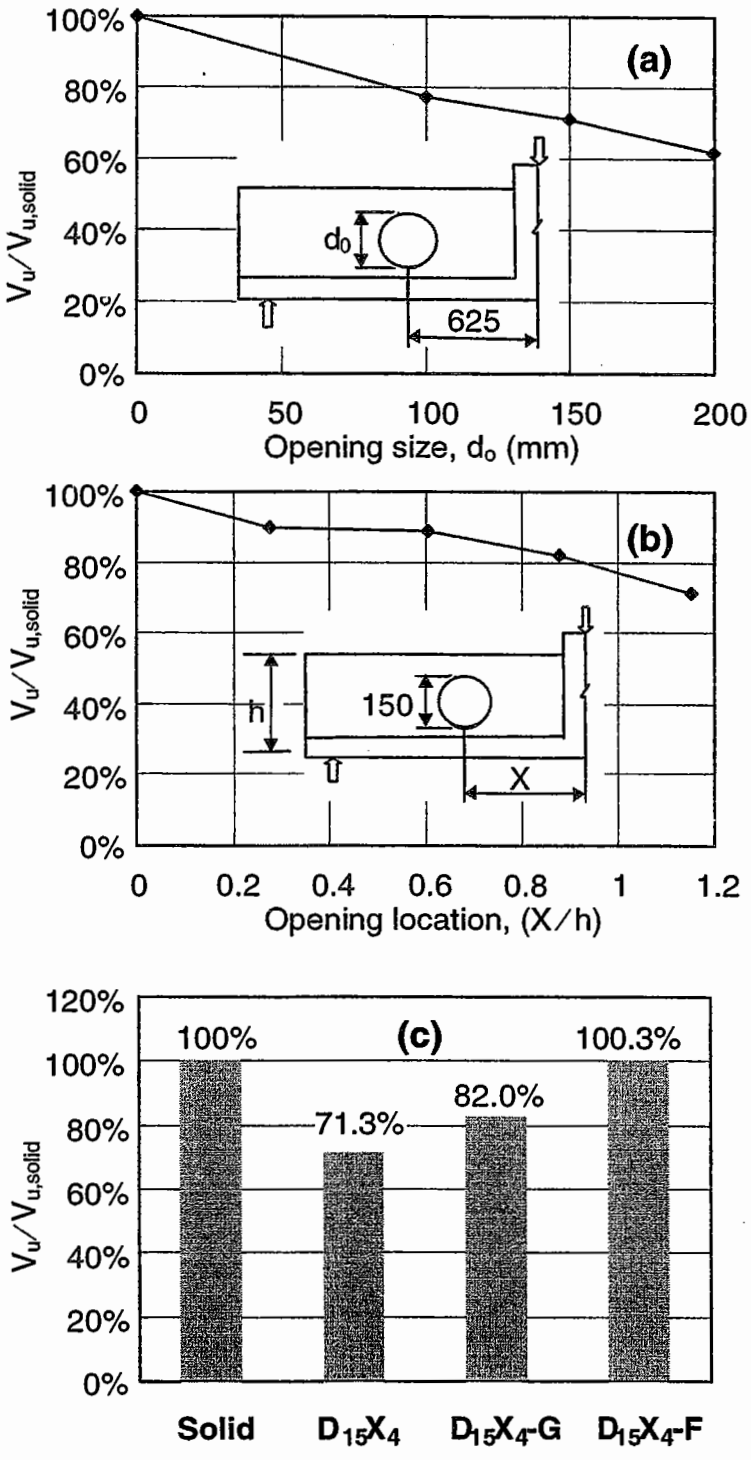

Figure 2.35 Ultimate shear strength ratio (a) effect of opening size; (b) effect of opening location; (c) effect of repair and strengthening.

3
Beams with Large Rectangular Openings

3.1 GENERAL INTRODUCTION

The introduction of a large opening in a reinforced concrete beam would normally reduce its load-carrying capacity considerably. However, it is possible to reinforce such a beam, restoring its strength to that of a similar solid beam. This can be illustrated by comparing the behavior under pure bending of a solid beam with that of a similar beam containing a web opening, as shown in Fig. 3.1.

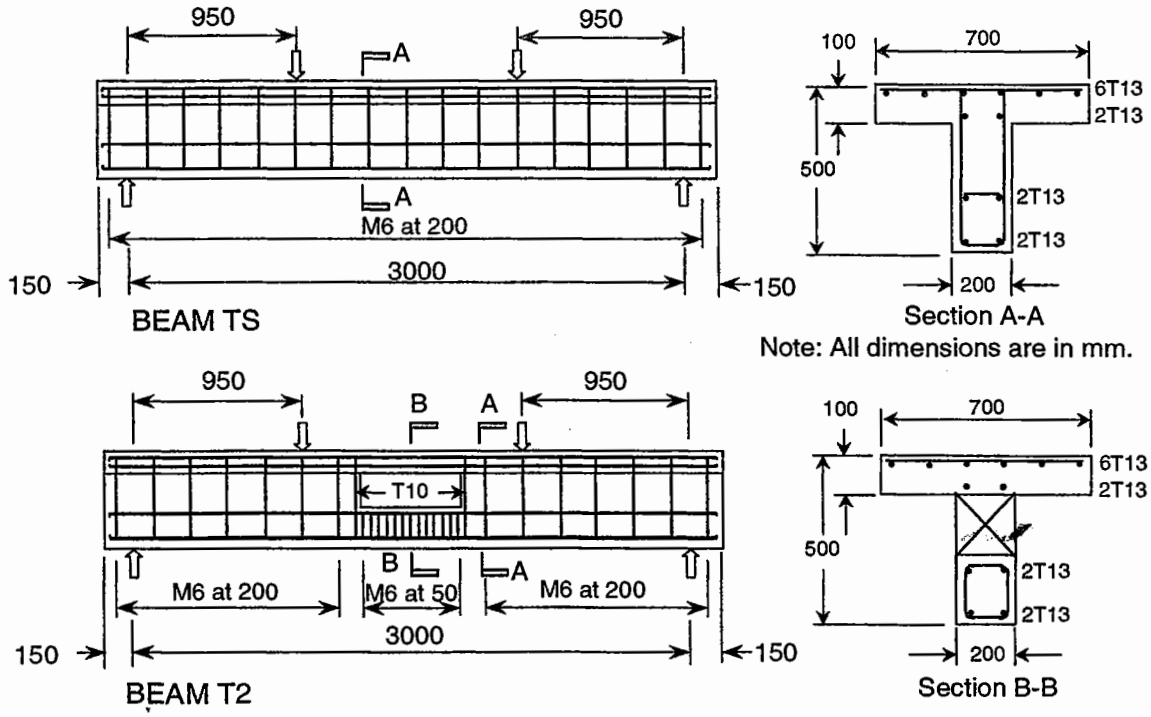

Figure 3.1(a) Reinforcement details of beams TS and T2.

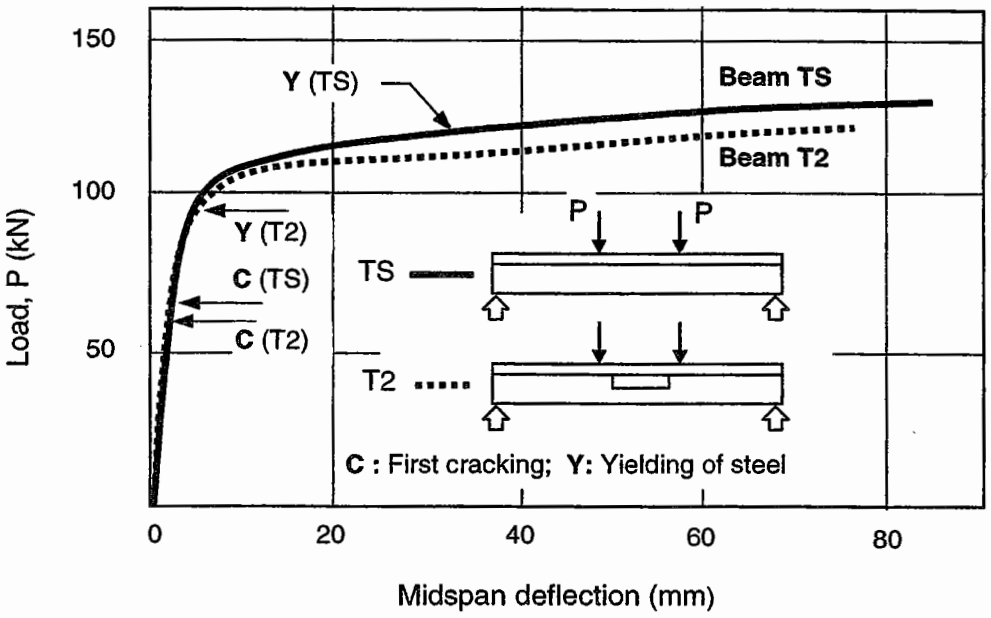

Figure 3.1(b) Load vs. deflection curves for beams TS and T2.

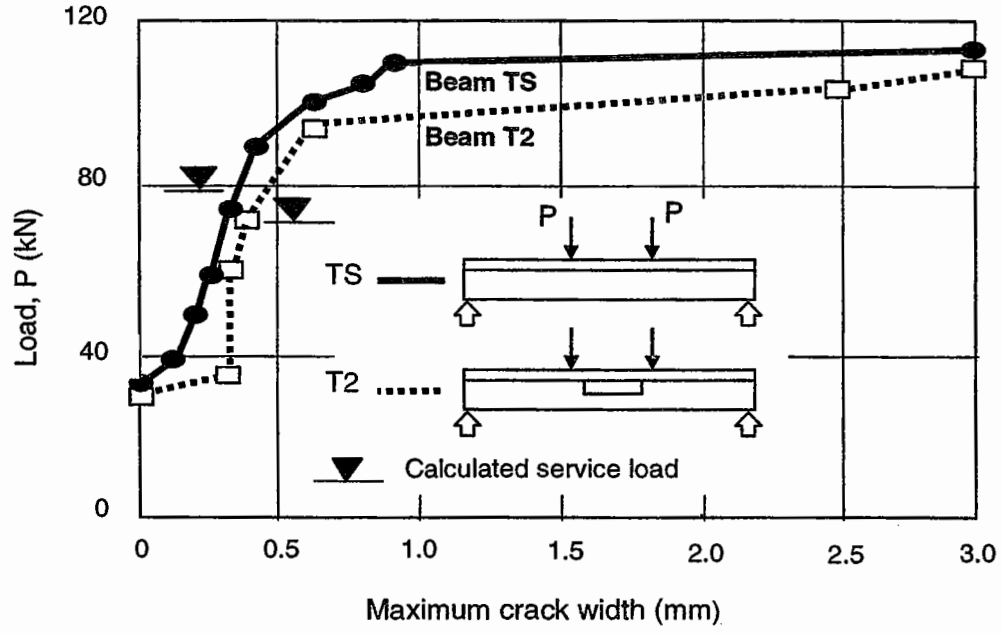

Figure 3.1(c) Load vs. maximum crack width curves for beams TS and T2.

The two T-beams, designated as TS and T2, had identical dimensions and material properties, except for the region where an opening had been provided in beam T2. Both beams were under-reinforced in flexure with the same amount of steel reinforcement and cast from the same batch of concrete. Reinforcement details for these beams are shown in Fig. 3.1(a). In beam T2 additional full-depth vertical stirrups were provided close to the opening to account for stress concentration and to control the crack width under service load conditions. The beams were tested to failure in flexure under two symmetrical point loads as shown in Fig. 3.1(a).

Fig. 3.1(b) compares the load versus midspan deflection curves obtained for the two beams. Both beams exhibited similar behavior up to when cracks first began to appear. The cracking load and the beam stiffness were slightly higher in the solid beam TS than in the beam with an opening, T2. However, the longitudinal reinforcement in the beam T2 yielded at a much earlier stage, which led to a large increase in deflections. Nevertheless, both beams attained comparable ultimate flexural strength.

The growth in crack width with increasing load is shown in Fig. 3.1(c). Both beams showed similar trends. That is, crack widths kept increasing steadily upon first cracking, and this continued up to the load when yielding of longitudinal steel occurred. Thereafter, crack widths increased quite rapidly. The growth of crack widths in the solid beam trails that in the beam with an opening. It may be observed from Fig. 3.2 that both beams developed almost identical flexural crack pattern, except for slightly more cracks in the beam containing an opening than in the solid beam. This was due to the closer spacing of stirrups provided in the lower chord member of beam T2.

As in the case of small openings, the flexural strength of a beam depends on the area of concrete in compression that is available above the opening to provide the moment of resistance. The analysis described in Art. 2.2 is therefore applicable to beams with large openings under pure bending. However, noting that the chord members above and below the opening behave as compression strut and tension tie, respectively, it is essential that the slenderness effect in the compression strut be accounted for. As the length of the opening and, hence, the length of the compressive strut becomes longer, premature instability failure of the beam may occur. According to the ACI Code (1995), for compression members in a non-sway frame, the effects of slenderness may, in general, be neglected when

$$\frac{k\ell_u}{r} < 22 \tag{3.1}$$

in which k is the effective length factor which may be taken as 1, ℓ_u is the unsupported length of the compression chord, and r is the radius of gyration which may be taken as

$$r = 0.3\, d_c \tag{3.2}$$

where d_c can be taken as the depth of the compression chord.

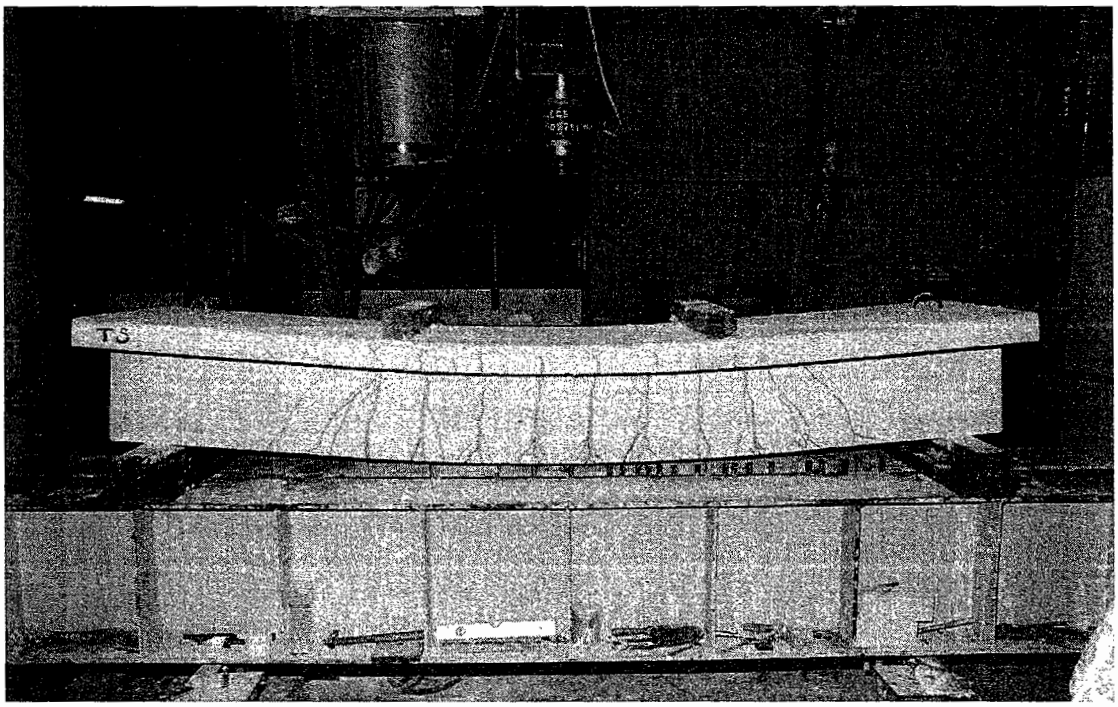

(a) Beam TS

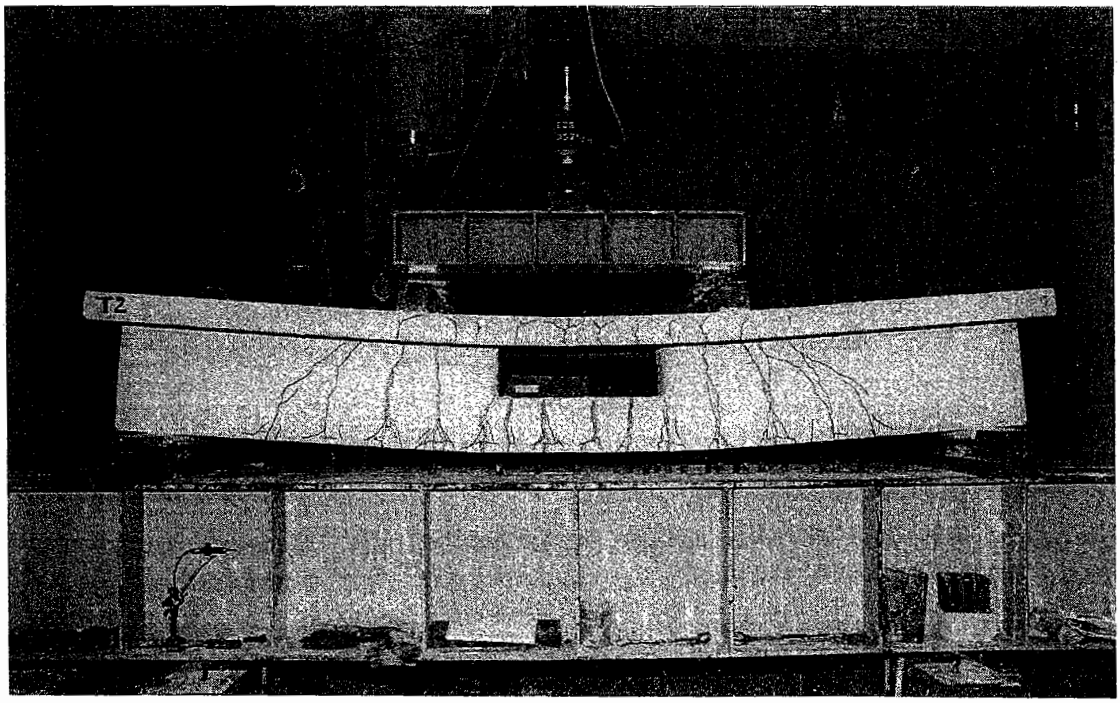

(b) Beam T2

Figure 3.2 Cracking patterns of beams TS and T2 after failure.

EXAMPLE PROBLEM 3.1

A rectangular opening measuring $\ell_o \times d_o$, is to be provided at the midspan section of a slender beam where the shear force is small. The center of the opening is located at an eccentricity e from the centroidal axis of the beam. The beam is rectangular in cross section with an overall depth of h. Determine the domain of (ℓ_o/h, e/h, d_o/h) within which the effect of slenderness may be neglected for the compression chord.

SOLUTION

Referring to Fig. E3.1.1(a), the depth of compression chord member is

$$d_c = \frac{h}{2} - \frac{d_o}{2} + e$$

Assuming $k = 1$, $\ell_u = \ell_o$, Eq. (3.2) and the inequality condition, Eq. (3.1), give

$$\ell_o < 22r = 3.3(h - d_o + e)$$

or

$$\frac{\ell_o}{h} < 3.3\left(1 - \frac{d_o}{h} + 2\frac{e}{h}\right) \qquad \text{(E3.1.1)}$$

Also, from Fig. E3.1.1(a), it is seen that the depth of the tension chord is given by ($h/2 - d_o/2 - e$). For the tension chord to exist, therefore,

$$\frac{h}{2} - \frac{d_o}{2} - e > 0$$

The above equation may be written in the following form:

$$\frac{d_o}{h} < 1 - 2\frac{e}{h} \qquad \text{(E3.1.2)}$$

The inequalities represented by Eqs. (E3.1.1) and (E3.1.2) may be plotted in a graphical form to obtain the required domain of (ℓ_o/h, d_o/h, e/h) within which the slenderness effect in the compression chord may be neglected. This is presented in Fig. E3.1.1(b).

In practice, Eq. (E3.1.2) would be more restrictive, due to the requirement of a minimum physical dimension for the tension chord member to contain the reinforcement. The effect of this on the domain is shown in Fig. E3.1.1(b).

Assuming that the eccentricity of the opening is zero (that is, $e = 0$), the length of the opening ℓ_o would be limited to 0.825 to 1.65 times the beam depth for the case where the depth of the opening is between half to three-quarter times the depth of the beam.

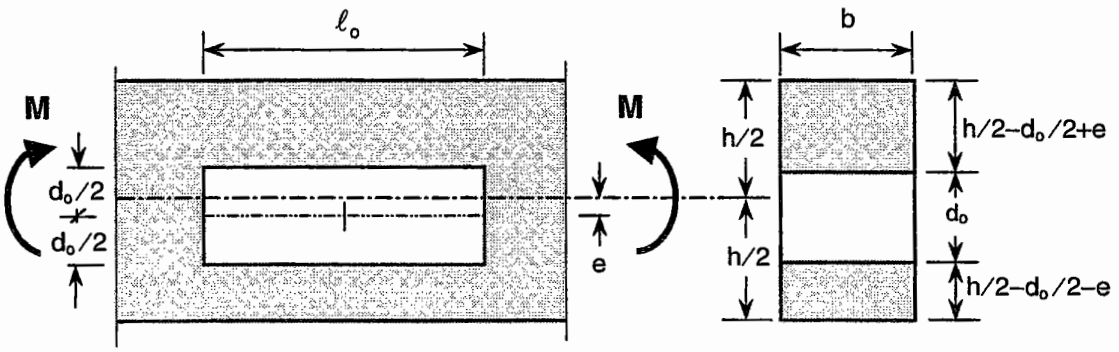

(a) Beam under pure bending

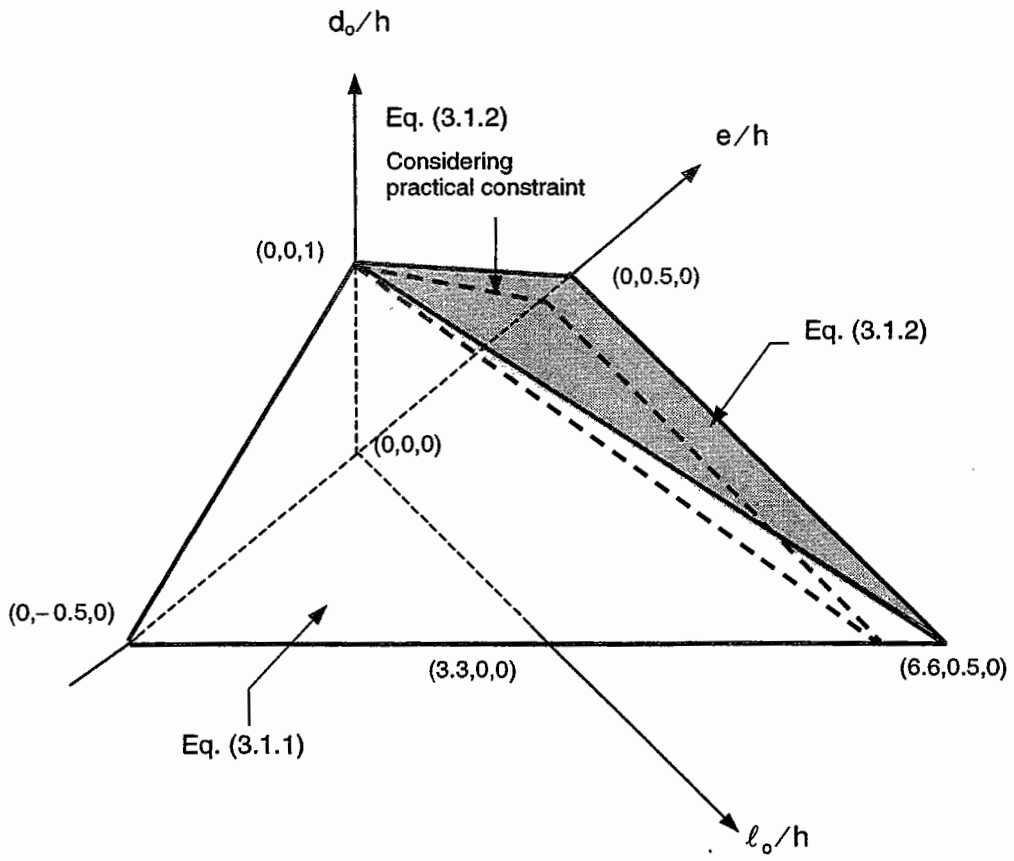

(b) Domain of (ℓ_o, d_o, e) for which slenderness effect in compression chord can be ignored

Figure E3.1.1 Slenderness effect in compression chord.

3.2 BEAM BEHAVIOR UNDER BENDING AND SHEAR

In practice, beams are usually subject to combined bending and shear. Fig. 3.3 shows a simply-supported, reinforced concrete beam with an opening, subject to a concentrated load at a distance x from the support on the same side of the opening. The free-body diagram at the beam opening can be represented as in Fig. 3.3(b), and the free-body diagrams of the chord members above and below the opening as in Fig. 3.3(c). It is observed that the unknown action effects at the center of the opening are the axial forces (N_t and N_b), the bending moments (M_t and M_b), and the shear forces (V_t and V_b) in the chord members. There are three equilibrium equations relating these six unknowns. These are:

$$M_t + M_b + Nz = M_m \tag{3.3}$$

$$N_t + N_b = 0 \tag{3.4}$$

$$V_t + V_b = V_m \tag{3.5}$$

in which M_m and V_m are the applied moment and shear force, respectively, at the center of the opening. Thus, the beam is statically indeterminate to the third degree.

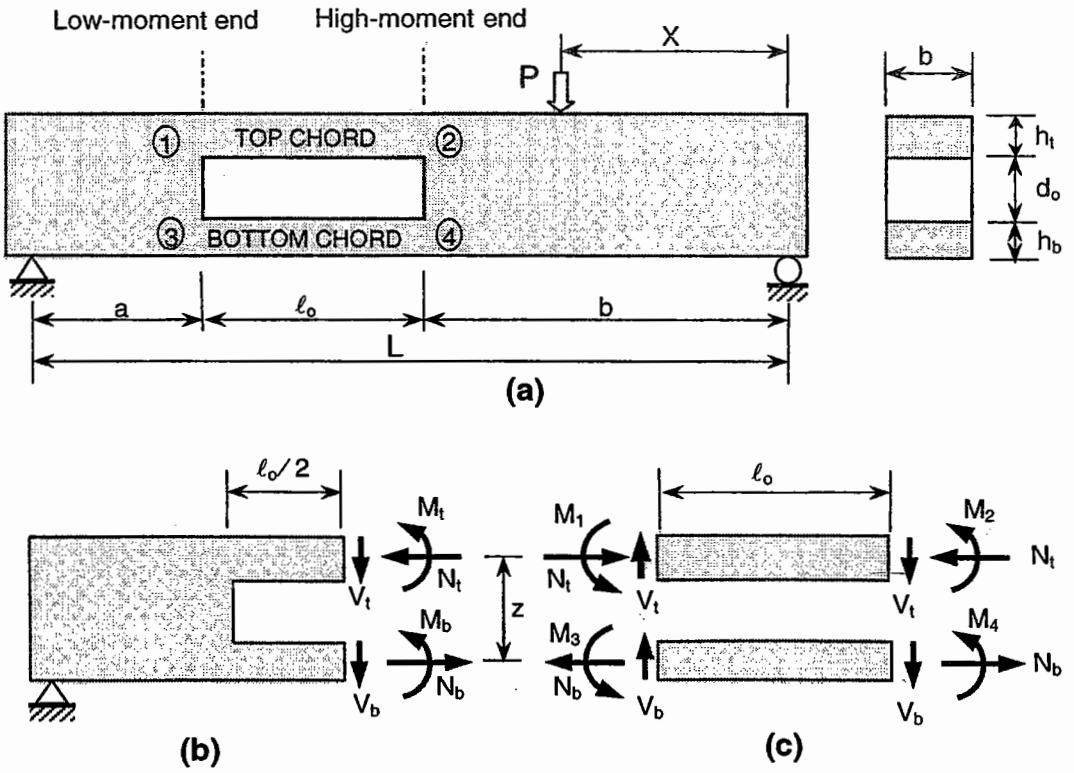

Figure. 3.3 Beam with an opening under bending and shear. (a) The beam; (b) Free-body diagram at opening; (c) Free-body diagram of the chords.

Tests conducted on such beams have indicated that the chord members behave like a Vierendeel panel, with points of contraflexure occurring approximately at midpoints of the chord members. Fig. 3.3(c) shows that the high-moment ends of the chord members are subject to positive moments (that is, sagging moments) while the low-moment ends are subject to negative moments (that is, hogging moments). It is seen that, in general, both longitudinal reinforcement and shear reinforcement would be required in each chord member. If the opening is not reinforced (Siao and Yap, 1990), the compression chord would split diagonally with crushing of the concrete at the high-moment end, as shown in Fig. 3.4. The failure is brittle and undesirable.

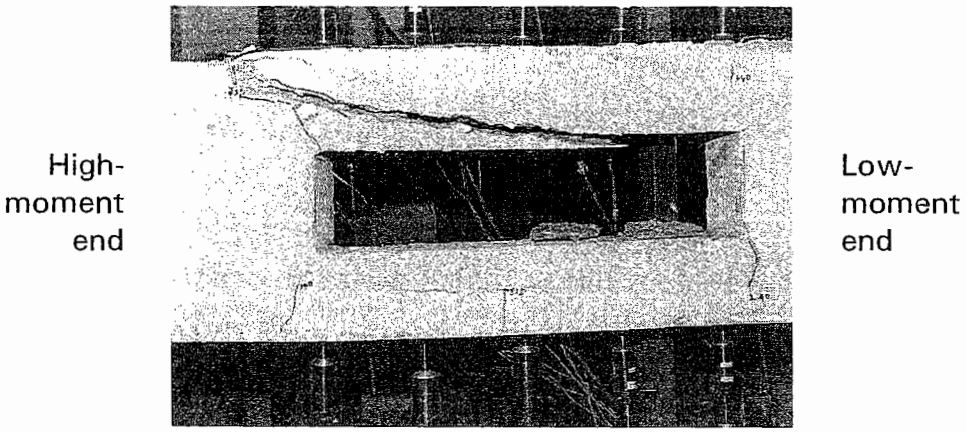

Figure 3.4. Typical failure pattern at unreinforced opening (Siao and Yap, 1990).

When the opening is reinforced with both shear and longitudinal reinforcement, as given in Fig. 3.5(a), a different crack pattern is observed, as shown in Fig. 3.5(b). In this case, the cracks first appeared either in the top or bottom chord member at the high-moment end of the opening [see Fig. 3.3(a)]. These cracks initiated at the bottom faces of the chord members. As the load was increased, cracks also appeared from the top faces of the chord members at the low-moment end of the opening. More cracks appeared with increasing load. The order of appearance of these cracks was from the ends to the center of the opening. The solid section of the beams cracked only at later stages of loading.

At each corner of the opening, the cracks in the chord members progressively converged to a common point, where crushing of the concrete occurred at collapse. It can be seen in Fig. 3.5(b) that the bottom chord was severely cracked at failure. The middle half of the top chord, which was subject to axial compression, remained virtually uncracked even at collapse.

At failure, crushing of the concrete was observed on the top and bottom faces of the chord members at the high- and low-moment ends of the opening, respectively. The extent of crushing in the top chord member was more severe since it was under a compressive force. The collapse of the beam occurred due to the formation of a mechanism with four plastic hinges, with one at each corner of the opening.

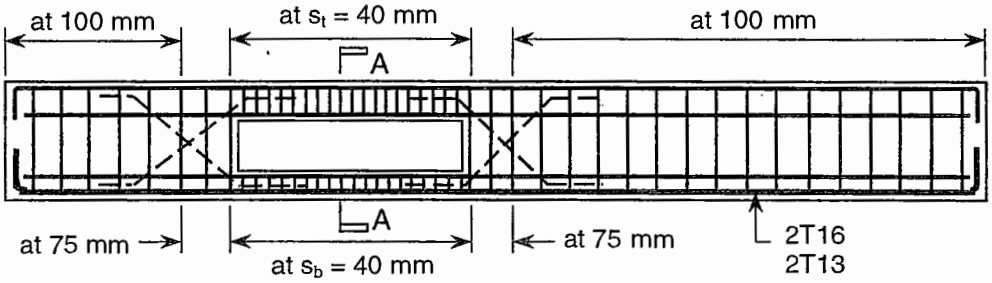

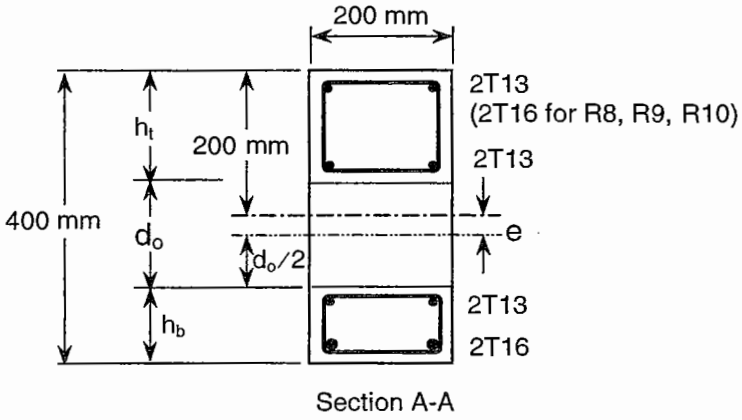

(a) Longitudinal and shear reinforcement

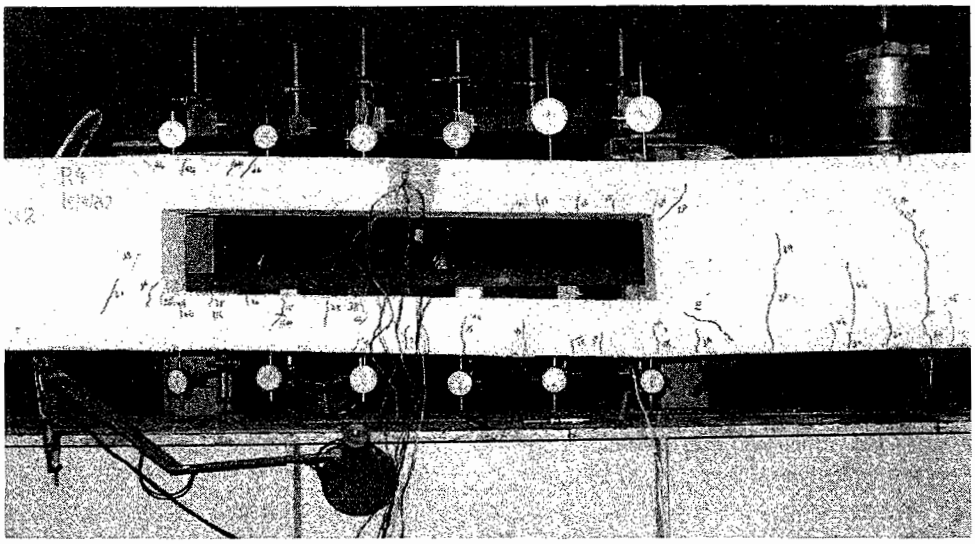

(b) Typical crack pattern

Figure 3.5 Beams with reinforced opening (Tan, 1982).

In general, the ultimate strength of a beam decreases with increasing length or depth of opening or with increasing moment-to-shear ratio at the center of the opening, but increases with increasing opening eccentricity (see Art. 3.3.1.1).

Structural design of beams with openings entails the check for ultimate strength and serviceability with respect to cracking and deflection. In the subsequent sections, available approaches for the analysis of beams with openings at collapse are presented, following which design methods for ultimate strength are described. Crack control is ensured through proper steel detailing at the comers of openings. In general, deflections have to be calculated and compared to allowable values. The calculation of deflections is dealt with briefly in this chapter and in more detail in Chapter 5.

3.3 ANALYSIS AT COLLAPSE

Three approaches are available for the analysis of beams with large openings at collapse. The first is based on the principles of *limit analysis*, which assumes that the collapse of a beam occurs when a sufficient number of plastic hinges is formed to transform the beam into a mechanism. The second approach uses an analogous truss for force transfer and is referred to as the *plasticity truss* method. The third approach is based on the *strut-and-tie* method. These three approaches are described in detail in the following sections.

3.3.1 LIMIT ANALYSIS

The method based on limit analysis yields a closed-form solution for the collapse load, as described below for a simply-supported beam subject to a point load, P, at a solid section distant, x, from its right support (refer to Fig. 3.3). The analysis of ultimate strength for such a beam is based on the following assumptions:

1. The opening is rectangular in shape. The members above and below the opening are prismatic, that is, the chord members have uniform cross section and reinforcement throughout the length.
2. Different sections of the chord have sufficient ductility in combined bending, shear, and axial deformations. This can be achieved by using under-reinforced sections and proper detailing of reinforcement.
3. The chord members are adequately designed for shear. Also, a sufficient quantity of reinforcement is provided at the comers of the opening to prevent premature failure due to stress concentration.
4. The dimensions of the top, that is, the compression chord member are such that the slendemess effect can be ignored.
5. The top and bottom chords are assumed to frame into the rigid abutments on either side of the opening. Failure occurs by the formation of a mechanism with four hinges in the chord members, one at each corner of the opening, as shown in Fig. 3.6.

According to the method, collapse of a structure will occur if it is possible to find a distribution of internal actions such that the conditions of equilibrium, yield, and a mechanism are satisfied simultaneously.

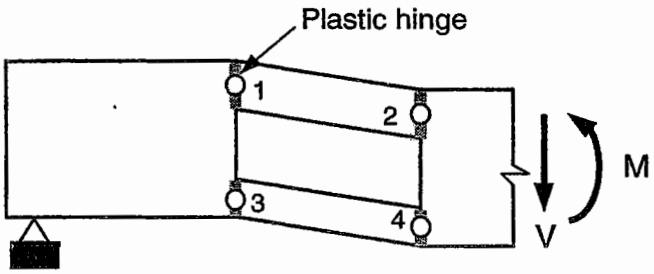

Figure 3.6 Collapse mechanism at opening.

Yield Conditions

As shown in Figs. 3.3(b) and (c), the chord members are subject to a combination of bending moment, *M*, shear force, *V*, and axial force, *N*. Therefore, an interaction curve (to be used as yield surface) among these stress resultants is required for the analysis. It is assumed that the chord members are adequately designed for shear, and the interaction diagram between bending moment and axial force be adopted as the required yield surface. Thus, the top and bottom chord members can be considered as eccentrically loaded compression and tension members, respectively. The interaction diagram can then be obtained by the method of equilibrium and strain compatibility. Fig. 3.7 shows a typical interaction diagram.

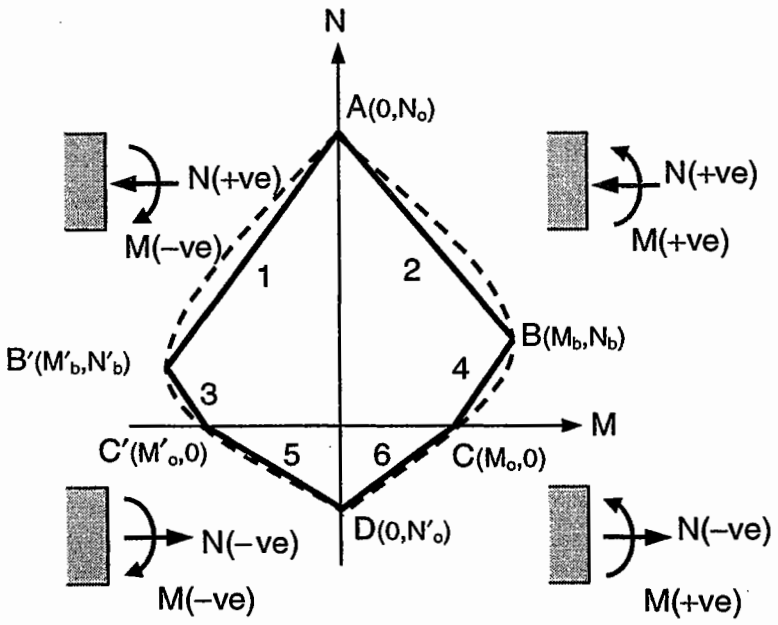

Figure 3.7 Piecewise linear approximation of yield surface.

In order to simplify the analysis, the interaction curve may be approximated by the piecewise linear surface ABCDC′B′A, as shown by the dotted lines. It consists of six planes, AB′, AB, B′C′, BC, C′D, and CD. The yield criterion required for the present analysis can, therefore, be expressed in matrix form as

$$[F]^T \begin{Bmatrix} m \\ n \end{Bmatrix} \leq \{C\} \tag{3.6}$$

in which $m = M/M_o$ and $n = N/N_o$, and the matrices $[F]$ and $\{C\}$ are given, respectively, by

$$[F] = \begin{bmatrix} \dfrac{(N_o - N'_b)M_o}{M'_b N_o} & \dfrac{(N_o - N_b)M_o}{M_b N_o} & \dfrac{M_o}{M'_o} & 1 & \dfrac{M_o}{M'_o} & 1 \\ 1 & 1 & \dfrac{(M_o - M_b)N_o}{M'_o N'_b} & \dfrac{(M_o - M_b)N_o}{M_o N_b} & \dfrac{N_o}{N'_o} & \dfrac{N_o}{N'_o} \end{bmatrix} \tag{3.7}$$

and

$$\{C\}^T = \langle 1 \quad 1 \quad 1 \quad 1 \quad 1 \quad 1 \rangle \tag{3.8}$$

in which M_o, M'_o = ultimate moment of resistance of the section in positive and negative bending, respectively; N_o, N'_o = ultimate strength of the section in axial compression and axial tension, respectively; M_b, M'_b = moments at balanced failure under positive and negative bending, respectively; N_b, N'_b = axial compressive loads at balanced failure corresponding to M_b and M'_b, respectively; and the superscript T denotes transpose.

Collapse Modes

It is assumed that the solid sections of the beam are rigid, and collapse occurs by the formation of a mechanism with four plastic hinges, one at each end of the top and bottom chords, as shown in Fig. 3.6. Hinges in the top chord member are denoted by 1 and 2 and in the bottom chord member by 3 and 4.

When the beam is subject to a positive bending moment, the axial stress resultant in the top chord member is a compressive force. As no shear force is applied along the beam axis, the axial stress resultant in the bottom chord member would be a tensile force equal in magnitude to the thrust in the top chord member. Consequently, the portion of the yield surface above the M-axis (Fig. 3.7) will be applicable to the top chord member and that below the same axis will be applicable to the bottom chord member.

In general, the chord members are not identically reinforced. Therefore, each member will have different yield surface. If they are unsymmetrically reinforced, the respective yield surface will also be unsymmetrical, that is, $M_b \neq M'_b$, $N_b \neq N'_b$, and $M_o \neq M'_o$ (Fig. 3.7). Thus, there are four possible combinations of the yield planes AB′, B′C′, AB, and BC on which hinges at locations 1 and 2 may

form. Designated by **Case 1**, **Case 2(a)**, **Case 2(b)**, and **Case 3**, these combinations are clearly shown in Fig. 3.8. In all cases, hinges at 3 and 4 form at points on C′D and CD, respectively. It should be noted that if the top chord is symmetrically reinforced, only Cases 1 and 3 need to be considered.

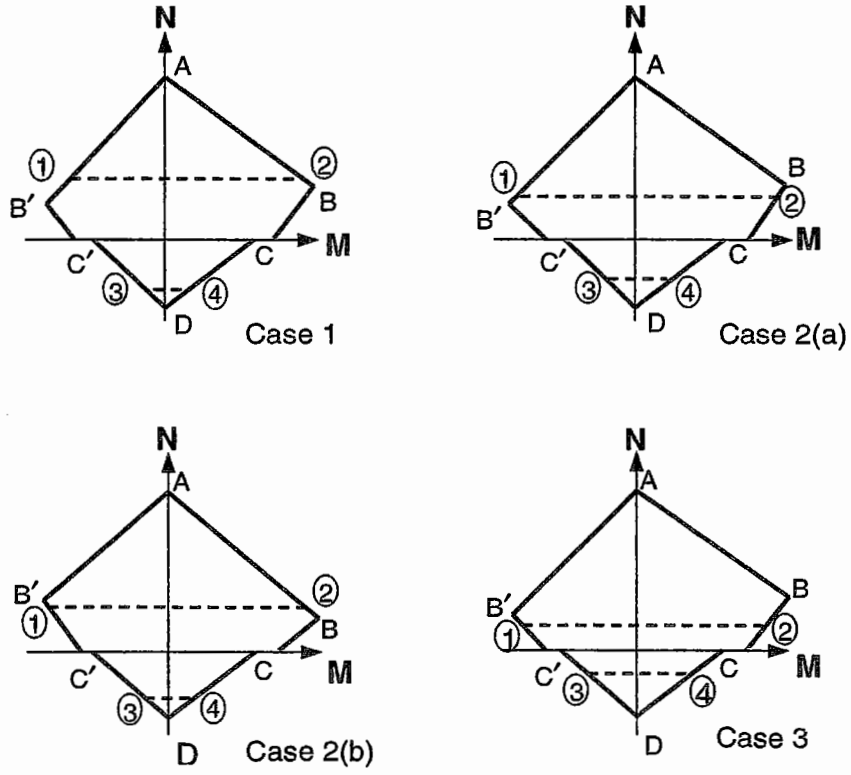

Figure 3.8 Possible combinations of yield planes for hinge formation.

Plastic Flow Rule

The yield criterion represented by Eq. (3.8) is in linearized form. Therefore, the generalized strain (rotation, ϕ, and axial deformation, δ) rates $\dot{\phi}$ and $\dot{\delta}$ corresponding to M and N, respectively, are given by the flow rule as

$$\begin{Bmatrix} \dot{\phi} \\ \dfrac{N_o \dot{\delta}}{M_o} \end{Bmatrix} = [F]\{\lambda\} \tag{3.9}$$

in which $\{\lambda\}$ = vector of plastic multipliers. It may be noted that during yielding only one of the six possible yield planes as shown in Fig. 3.7 will be active at each hinge. Thus, only one of the six components of $\{\lambda\}$ will be non-zero. In other words, when plane i is active, λ_j for $j = 1, 2, \ldots 6$ can be non-zero only when $i = j$.

Let the planes AB′, AB, B′C′, BC, C′D, and CD in Fig. 3.7 be denoted by 1, 2, 3, 4, 5, and 6, respectively. Then the yield planes active at hinges 1, 2, 3, and 4

(Fig. 3.6) will be *i*, *j*, 5, and 6, respectively, where the values of *i* and *j* for various cases are given in Table 3.1.

Table 3.1 Values of *i* and *j* for different cases.

Case	*i*	*j*
1	1	2
2(a)	1	4
2(b)	3	2
3	3	4

3.3.1.1 Solution for Ultimate Strength

The original shape of the beam with a rectangular opening is shown in Fig. 3.9 with the chord members represented by their centroidal axes. The dotted lines in this figure represent the deformed shape of the beam at collapse, which has been exaggerated for clarity. Let the rotation and axial deformation at hinge *i* ($i = 1, 2, 3, 4$) be ϕ_i and δ_i, respectively. The compatibility conditions in terms of velocities represented by a dot can then be written as

$$\dot{\phi}_1 = \dot{\phi}_3 \tag{3.10}$$

$$\dot{\phi}_2 = \dot{\phi}_4 \tag{3.11}$$

$$\dot{\delta}_1 + \dot{\delta}_2 = (\dot{\phi}_1 + \dot{\phi}_2)\, z + \dot{\delta}_3 + \dot{\delta}_4 \tag{3.12}$$

in which z = distance between the plastic centroids of the top and bottom chord members.

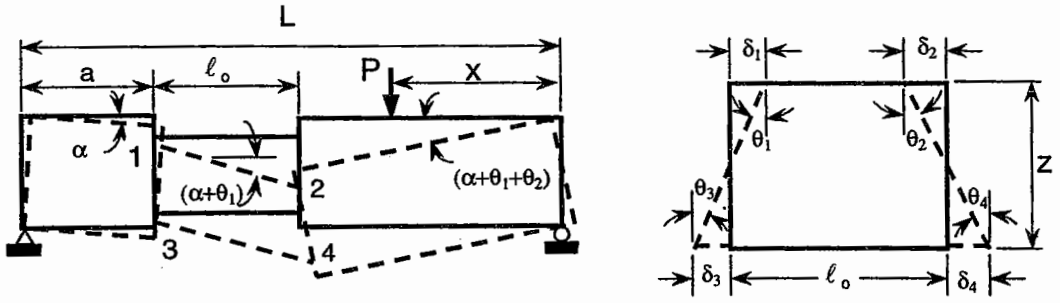

(a) Deformed shape

(b) Rotation and axial deformation at hinges

Figure 3.9 Beam deformation at collapse.

Eqs. (3.10) - (3.12), by virtue of Eq. (3.9), reduce, respectively, to

$$F_{1i}\lambda_i = F_{15}\lambda_5 \tag{3.13a}$$

$$F_{1j}\lambda_j = F_{16}\lambda_6 \tag{3.13b}$$

$$\gamma_t\left(F_{2i}\lambda_i + F_{2j}\lambda_j\right) = \left(F_{1i}\lambda_i + F_{1j}\lambda_j\right) + \gamma_b\left(F_{25}\lambda_5 + F_{26}\lambda_6\right) \tag{3.13c}$$

in which $\gamma = M_o/(N_o z)$; and the subscripts t and b refer to the top and bottom chords, respectively. Eqs. (3.13) can be simplified to the form

$$\phi_i\lambda_i + \psi_j\lambda_j = 0 \tag{3.14}$$

in which

$$\phi_i = \gamma_t F_{2i} - \left(1 + \gamma_b \frac{F_{25}}{F_{15}}\right)F_{1i} \tag{3.15a}$$

$$\psi_j = \gamma_t F_{2j} - \left(1 + \gamma_b \frac{F_{26}}{F_{16}}\right)F_{1j} \tag{3.15b}$$

The collapse load is first obtained by the upper bound approach using the virtual work equation which states that, for any system, the rate of work, W_e, done by the external loads must be equal to the rate of internal energy dissipation, W_i. For the structural system shown in Fig. 3.9,

$$W_i = \{C\}^T\{\lambda\} = \lambda_i + \lambda_j + \lambda_5 + \lambda_6 \tag{3.16}$$

The moments M_L and M_H at the low- and high-moment ends, respectively, of the opening [Fig. 3.3(a)] are given by

$$M_L = Px\frac{a}{L} \tag{3.17a}$$

$$M_H = Px\frac{(a+\ell_o)}{L} \tag{3.17b}$$

in which L = beam span and ℓ_o = length of opening. Thus,

$$W_e = Px\left[\frac{a}{L}\dot{\theta}_1 + \frac{(a+\ell_o)}{L}\dot{\theta}_2\right] \tag{3.18}$$

The virtual work equation, $W_e = W_i$, therefore, becomes

$$Px\left[\frac{a}{L}\dot{\theta}_1 + \frac{(a+\ell_o)}{L}\dot{\theta}_2\right] = \lambda_i + \lambda_j + \lambda_5 + \lambda_6 \tag{3.19}$$

Substituting Eq. (3.9) and Eqs. (3.13a and 3.13b) into Eq. (3.19) leads to

$$\frac{Px}{L}\left[aF_{1i}\lambda_i + (a+\ell_o)F_{ij}\lambda_j\right] = \lambda_i + \lambda_j + \frac{F_{1j}}{F_{15}}\lambda_i + \frac{F_{1j}}{F_{16}}\lambda_j \tag{3.20}$$

Introducing Eq. (3.14) into Eq. (3.20), the final expression for the collapse load, P_u, is obtained as

$$P_u = \frac{\phi_i B_j - \psi_j A_i}{\frac{x}{L}\left[(a+\ell_o)\phi_i F_{1j} - a\psi_j F_{1i}\right]} \tag{3.21}$$

in which $A_i = 1 + F_{1i}/F_{15}$ and $B_j = 1 + F_{1j}/F_{16}$, and i and j are the assumed values, according to Table 3.1. The correct collapse load is given by the smallest value of P_u as predicted by Eq. (3.21) for all possible combinations of i and j. It should be noted that the values of F_{ij} correspond to the top chord member when j = 1, 2, 3, and 4 and to the bottom chord member when j = 5 and 6.

The solution thus obtained gives the exact collapse load since the conditions of statical admissibility and safety are already satisfied. Virtual work equation ensures equilibrium and the assumption of uniform strength for the top and bottom chords ensures safety. Thus, a lower bound solution is not required to prove. [A lower bound approach to obtain Eq. (3.21) is given by Tan (1982).]

When the chord members are provided with adequate reinforcement, the beam may fail at a solid section beyond the opening. Therefore, the collapse load, P_u, as obtained from the foregoing analyses, must not be greater than the strength of the solid section. Otherwise, the later case will govern.

Table 3.2 Details of beams with openings tested by Tan (1982).

Beam	P_{ud} kN	ℓ_o mm	h_t mm	d_o mm	h_b mm	e mm	$a+\ell_o/2$ mm	Stirrup spacing		Corner reinforcement	
								s_t mm	s_b mm	Closed sti rup	Diagonal bars
R1	204	400	110	180	110	0	1000	40	40	1T13	-
R2	162	600	110	180	110	0	1000	40	40	1T10	-
R3	132	800	110	180	110	0	1000	40	40	1T10	-
R4	107	1000	110	180	110	0	1000	40	40	1T16	2T10
R5	89	1200	110	180	110	0	1000	40	40	1T16	2T10
R6	164	800	130	140	130	0	1000	50	50	1T10	-
R7	92	800	90	220	90	0	1000	30	30	1T10	-
R8	138	800	120	180	100	10	1000	45	35	2M6	4M6
R9	144	800	130	180	90	20	1000	50	30	1M 6	2T10
R10	137	800	110	180	110	0	800	40	40	1M6	2T10
R11	131	800	110	180	110	0	1000	40	40	1T10	-
R12	127	800	110	180	110	0	1200	40	40	1M6	4M4

NOTE: Clear concrete cover is 15mm; distance of loading point from right support x is 1000 mm; P_{ud} = design ultimate load.

Fig. 3.10 shows the predicted collapse loads of the beams tested by Tan (1982) with reinforcement shown in Fig. 3.5(a) and Table 3.2. Beams R1, R2, R3, R6, R7, and R11 had vertical stirrups only as corner reinforcement for the opening. The other beams were provided with both vertical stirrups and diagonal bars as corner reinforcement.

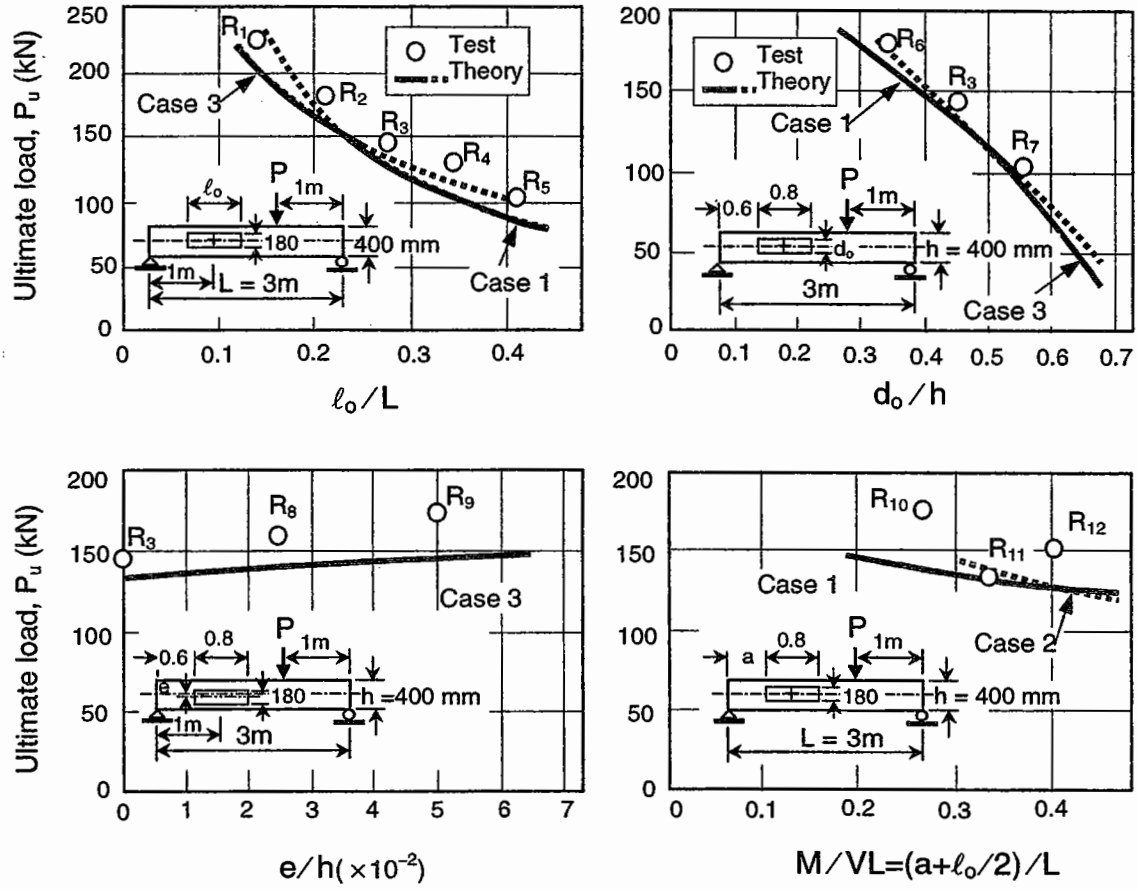

Figure 3.10 Predicted ultimate strength compared with test results.

The experimental ultimate loads of the test beams are presented in Table 3.3 along with a comparison of the corresponding design values. In all cases, the experimental ultimate loads exceeded the design values. Hence, the effects of slenderness on beam strength are not evident for the range of slendemess ratios employed for the top compression chord member. The experimental to design ultimate load ratio varies from 1.01 to 1.27, with an average of 1.14. This ratio varied from 1.01 to 1.12 for beams with vertical corner reinforcement only, whereas it varied from 1.12 to 1.27 for beams with both vertical and diagonal corner reinforcement. This may be attributed to the contribution of diagonal reinforcement, which protruded into the chord members, to the strength of the chord members at their ends.

Table 3.3 Comparison of theory with test results of Tan (1982).

Beam	Concrete cylinder strength, f'_c (MPa)	Collapse load (kN)		$\frac{P_{u,test}}{P_{u,design}}$ [a]	Type of corner reinforcement[b]
		Test, $P_{u,test}$	Design, $P_{u,design}$		
R1	30.4	223.9	204.9	1.09	S
R2	30.4	182.5	162.9	1.12	S
R3	33.5	144.1	134.5	1.07	S
R4	33.5	133.4	108.7	1.23	SD
R5	29.8	104.1	89.3	1.17	SD
R6	29.8	180.0	164.3	1.10	S
R7	35.1	102.9	98.6	1.04	S
R8	35.1	159.3	142.0	1.12	SD
R9	34.8	174.0	148.6	1.17	SD
R10	34.8	177.4	144.8	1.23	SD
R11	28.8	133.5	131.8	1.01	S
R12	28.8	154.3	126.9	1.22	SD
R13	28.7	112.0	88.3	1.27	SD
R14	28.7	76.0	71.2	1.07	S

[a]Average = 1.14; standard deviation = 0.08.
[b]S = full-depth closed stirrups close to one side of the opening.
SD = both stirrups and diagonal reinforcement.

EXAMPLE PROBLEM 3.2

A rectangular reinforced concrete beam containing two transverse openings and subject to a point load is shown in Fig. E3.2.1. The center of each opening is located at an equal distance from the nearer support, with the point load being applied at the location shown. The chord members above and below each opening are symmetrically reinforced. In addition, the top chord members, as well as the bottom chord members, have identical cross-sectional dimensions and material properties. If the chord members are adequately designed for shear, show that for the beam to collapse by simultaneous failure at both openings,

$$\frac{\ell_{o1}}{\ell_{o2}} = \frac{a_1}{a_2}$$

The failure at each opening is due to the formation of a mechanism with four hinges in the chord members, one at each comer of the opening.

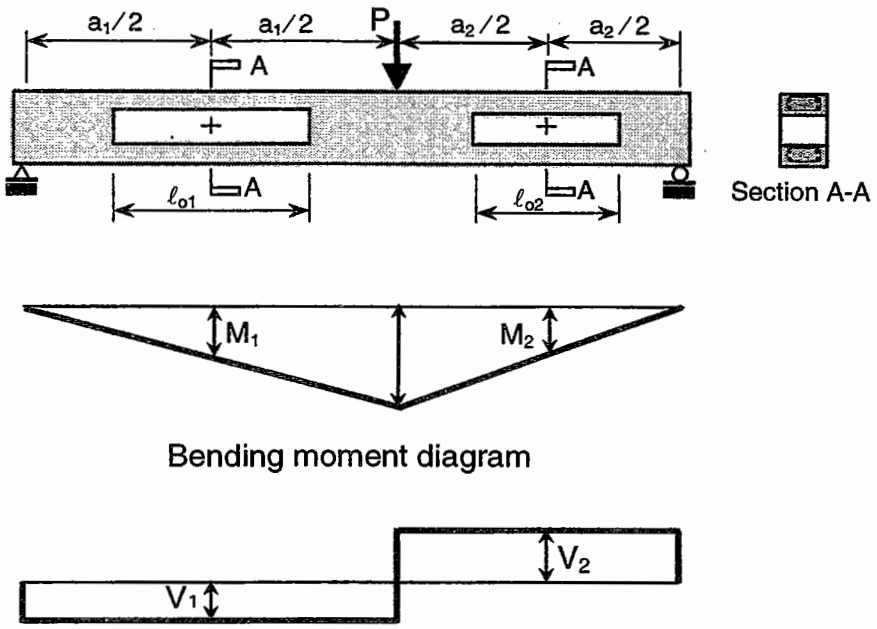

Figure E3.2.1 Beam with two transverse openings.

SOLUTION

For bending moment and shear force, see Fig. E3.2.1.

At center of opening 1,

$$M_1 = Pa_1a_2 / [2(a_1 + a_2)] \; ; \; V_1 = Pa_2/(a_1 + a_2) \qquad \text{(E3.2.1a)}$$

At center of opening 2,

$$M_2 = Pa_1a_2/[2(a_1 + a_2)] = M_1 \; ; \; V_2 = Pa_1/(a_1 + a_2) \qquad \text{(E3.2.1b)}$$

Since the top chord and the bottom chord members have identical cross-sectional dimensions and material properties, the distance z between the plastic centroids of the top and bottom chords is the same for both the openings.

As the chord members are symmetrically reinforced, contraflexure points occur at midpoints; hence, the axial force in each chord member (compression in top chords and tension in bottom chords) is

$$N^* = M_1/z = M_2/z = Pa_1a_2 / [2z(a_1 + a_2)] \qquad \text{(E3.2.2)}$$

The bending moments corresponding to N^* are determined from interaction diagrams, which are symmetrical about the N-axis, as shown in Fig. E3.2.2.

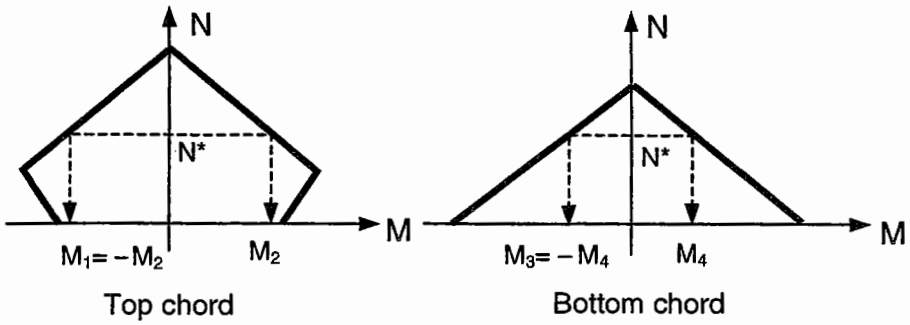

Figure E3.2.2 M-N interaction diagrams.

From the free-body diagrams of the chord members (Fig. E3.2.3), the shear forces acting on the chord members are determined as follows.

At opening 1,

$$V_{t1} = (M_2 - M_1)/\ell_{o1} = 2M_2/\ell_{o1}\ ; \quad V_{b1} = (M_4 - M_3)/\ell_{o1} = 2M_4/\ell_{o1} \qquad \text{(E3.2.3)}$$

At opening 2,

$$V_{t2} = (M_2 - M_1)/\ell_{o2} = 2M_2/\ell_{o2}\ ; \quad V_{b2} = (M_4 - M_3)/\ell_{o2} = 2M_4/\ell_{o2} \qquad \text{(E3.2.4)}$$

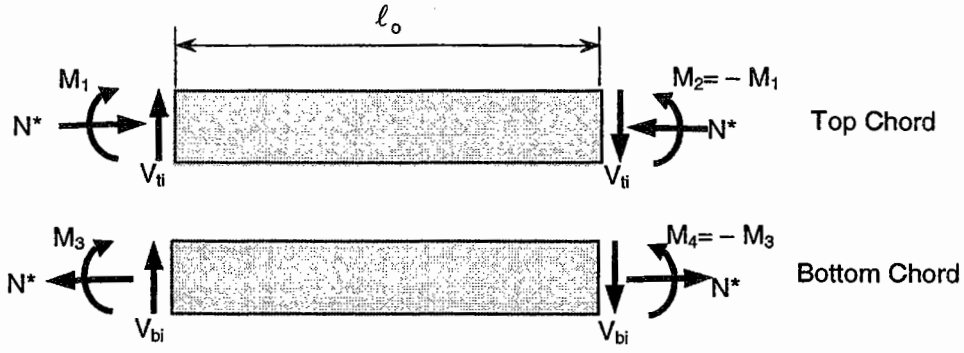

Figure E3.2.3 Free-body diagram of chord members.

Since $V_1 = V_{t1} + V_{b1}$ and $V_2 = V_{t2} + V_{b2}$, then from Eqs. (E3.2.1), (E3.2.3), and (E3.2.4),

$$Pa_2/(a_1 + a_2) = 2M_2/\ell_{o1} + 2M_4/\ell_{o1} \qquad \text{(E3.2.5)}$$

$$Pa_1/(a_1 + a_2) = 2M_2/\ell_{o2} + 2M_4/\ell_{o2} \qquad \text{(E3.2.6)}$$

Dividing Eq. (E3.2.6) by Eq. (E3.2.5),

$$a_1/a_2 = \ell_{o1}/\ell_{o2} \qquad \text{(E3.2.7)}$$

3.3.1.2 Shear Force Carried by Chord Members

Fig. 3.3(c) shows the free-body diagrams of the chord members. Equilibrium of moments for each chord at the low-moment end yields

$$\frac{V_t}{V_b} = \frac{M_{ot}(m_2 - m_1)}{M_{ob}(m_4 - m_3)} \tag{3.22}$$

in which $m_1 = M_1/M_{ot}$, $m_2 = M_2/M_{ot}$, $m_3 = M_3/M_{ob}$, and $m_4 = M_4/M_{ob}$, and the subscripts 1, 2, 3, and 4 refer to the hinge locations 1, 2, 3, and 4, respectively. Equilibrium of forces in the horizontal direction gives

$$n_t = \nu n_b \tag{3.23}$$

in which $n_t = N/N_{ot}$, $n_b = N/N_{ob}$, and $\nu = N_{ob}/N_{ot}$.

The yield conditions at hinges 1, 2, 3, and 4 are given, respectively, by

$$F_{1i}m_1 + F_{2i}n_t = 1 \tag{3.24a}$$

$$F_{1j}m_2 + F_{2j}n_t = 1 \tag{3.24b}$$

$$F_{15}m_3 + F_{25}n_b = 1 \tag{3.24c}$$

$$F_{16}m_4 + F_{26}n_b = 1 \tag{3.24d}$$

From the first and second pairs of Eqs. (3.24), the following equations are obtained:

$$m_2 - m_1 = \frac{1}{F_{1i}F_{1j}}\left[(F_{1i} - F_{1j}) - (F_{1i}F_{2j} - F_{1j}F_{2i})n_t\right] \tag{3.25a}$$

$$m_4 - m_3 = \frac{1}{F_{15}F_{16}}\left[(F_{15} - F_{16}) - (F_{15}F_{26} - F_{16}F_{25})\nu n_t\right] \tag{3.25b}$$

These equations, together with Eq. (3.22), yield

$$\frac{V_t}{V_b} = \frac{M_{ot}}{M_{ob}} \cdot \frac{F_{15}F_{16}}{F_{1i}F_{1j}} \cdot \frac{(F_{1i} - F_{1j}) - (F_{1i}F_{2j} - F_{1j}F_{2i})n_t}{(F_{15} - F_{16}) - (F_{15}F_{26} - F_{16}F_{25})\nu n_t} \tag{3.26}$$

In order to obtain the ratio of shear forces carried by the chord members, the value of n_t is expressed in terms of the geometry and cross-sectional properties of the beam by equating the external moment to the resisting moment at the high-moment end of the opening. That is,

$$\frac{P_u x(a + \ell_o)}{L} = M_{ot}m_2 + M_{ob}m_4 + N_{ot}n_t z \tag{3.27}$$

Replacing m_2 and m_4 by Eqs. (3.24b) and (3.24d), we get

$$n_t = \frac{\dfrac{P_u x (a+\ell_o)}{L} - \left(\dfrac{M_{ot}}{F_{1j}} + \dfrac{M_{ob}}{F_{16}}\right)}{N_{ot} z \left(\dfrac{F_{2j}}{F_{1j}} M_{ot} + \nu \dfrac{F_{26}}{F_{16}} M_{ob}\right)} \tag{3.28}$$

Thus, knowing the collapse load P_u and the corresponding combination of i and j, as in Table 3.1, n_t can be obtained from Eq. (3.28) and then the ratio V_t / V_b from Eq. (3.26). Since $V_t + V_b = V = P_u x/L$, the values of V_t/V and V_b/V at collapse can be found easily. Fig. 3.11 shows the distribution of shear force between the chord members for the beam shown in Fig. 3.5, calculated by assuming f'_c = 30 MPa.

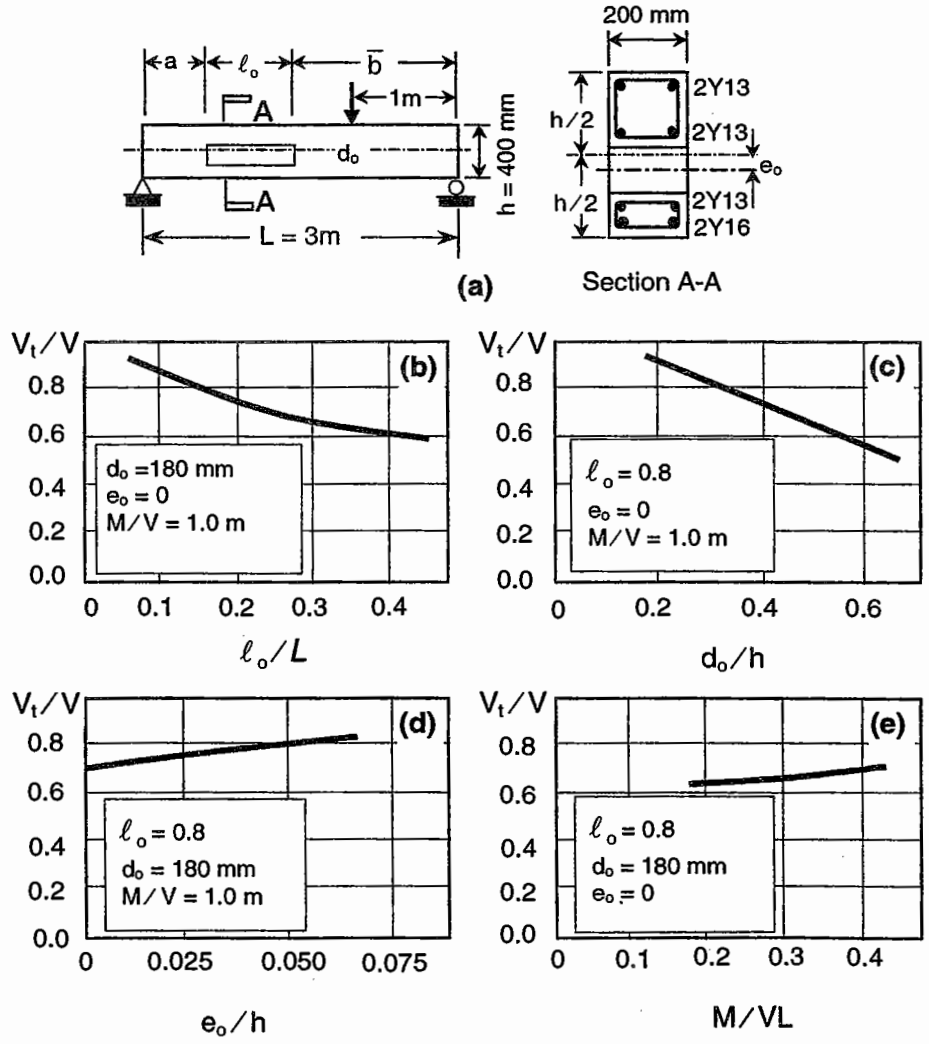

Figure 3.11 Distribution of shear between chord members. (a) Assumed beam details; (b) Effect of opening length; (c) Effect of opening depth; (d) Effect of opening eccentricity; (e) Effect of opening location.

EXAMPLE PROBLEM 3.3

A reinforced concrete rectangular beam contains a transverse opening and is subject to a point load, as shown in Fig. E3.3.1(a). The chord members above and below the opening are symmetrically reinforced. The interaction diagram between bending moment M and axial force N for the top and bottom chords are shown above and below the M-axis, respectively, in Fig. E3.3.1(b). If the beam fails at a load of 145 kN by the formation of a mechanism with four hinges in the chord members, one at each corner of the opening, calculate the amount of shear carried by each chord member at collapse.

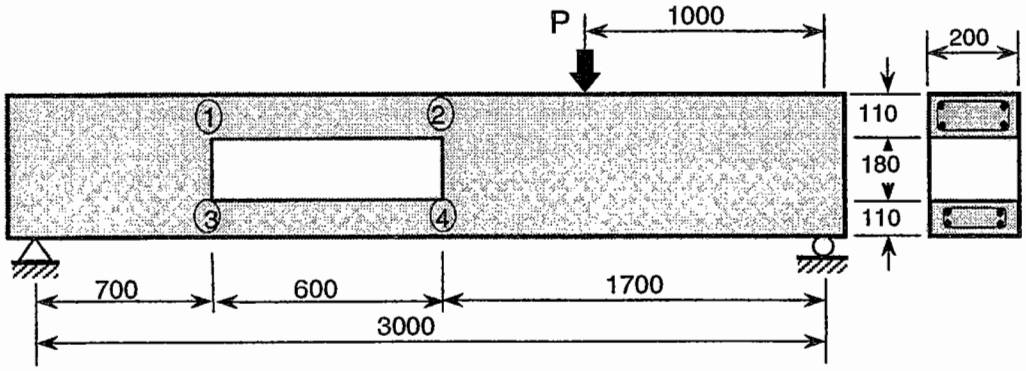

(a) Beam details

NOTE: All dimensions are in mm

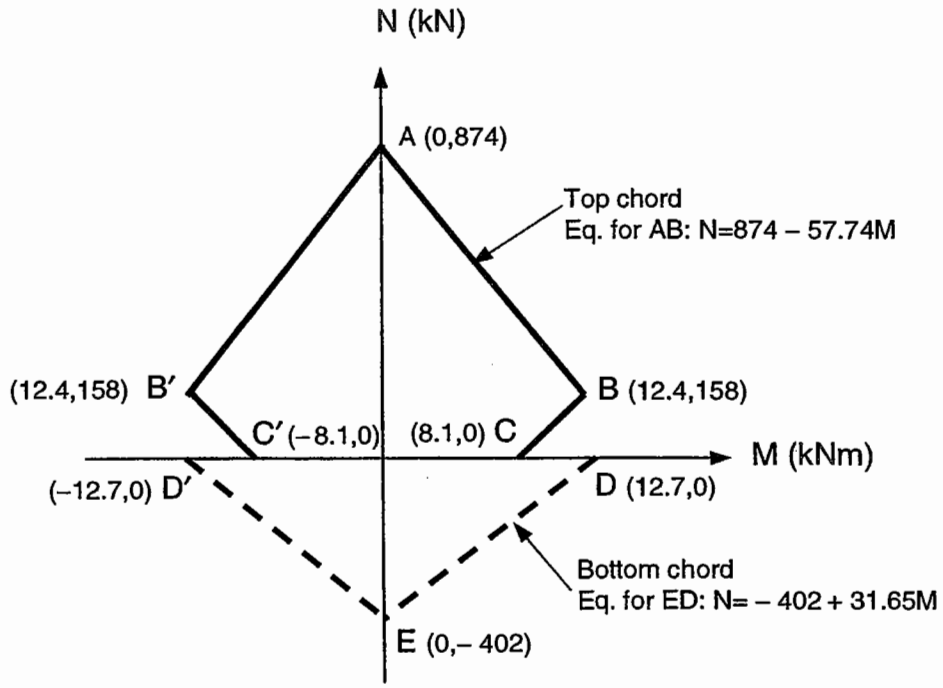

(b) Interaction diagram

Figure E3.3.1 Example Problem 3.3.

SOLUTION

Since the chord members are symmetrically reinforced, contraflexure points occur at midspan. At the center of the opening,

$$M = N_t z \text{ or, as } M = P_u/3 \text{ and } z = 400 - 110 = 290 \text{ mm},$$

$$P_u/3 = N_t \times 0.29$$

thus giving

$$N_t = 145/(3 \times 0.29) = 167 \text{ kN} > 158 \text{ kN}.$$

Therefore, the yield planes corresponding to hinges 1, 2, 3, and 4 are AB', AB, D'E, and DE, respectively. Moments at hinges are

$$|M_1| = |M_2| = (874 - 167)/57.74 = 12.25 \text{ kNm}$$

$$|M_3| = |M_4| = (402 + 167)/31.65 = 17.97 \text{ kNm}$$

Hence, the shear forces carried by the top and bottom chords, respectively, are

$$V_t = 2|M_1|/\ell_o = 2 \times 12.25/0.6 = 40.8 \text{ kN}$$

$$V_b = 2|M_3|/\ell_o = 2 \times 17.97/0.6 = 59.9 \text{ kN}$$

Check that $V_t + V_b = 40.8 + 59.9 = 100.7 \text{ kN} \approx P_u = 96.7$ kN.

3.3.2 PLASTICITY TRUSS MODEL

As discussed in Art. 2.3.3, shear is resisted by a beam by a combination of arch and truss mechanisms. In the case of a beam with an opening, it is difficult to develop an arch mechanism and, in general, load is transferred by truss action. Fig. 3.12(b) shows the truss action by which the load is transferred through the depth of a beam with an opening, reinforced as shown in Fig. 3.12(a). A truss mechanism exists in each chord member, which is reinforced both longitudinally and transversely. As in the case of a small opening (see Art. 2.3.4), a certain portion of the concrete is ineffective for load transfer.

Fig. 3.12 shows the case where the top and bottom chord members are of equal depth and in which the distance between the top and bottom longitudinal reinforcement is d_{vs}. It has been recommended by the Architectural Institute of Japan (AIJ, 1994) that vertical stirrups be provided uniformly throughout the chord members and for a distance equal to $d_{vs} \cot \phi_s$ on each side of the opening, where ϕ_s is the angle of inclination of the compression concrete struts in each chord member. The longitudinal reinforcement adjacent to the opening should be extended beyond the above vertical stirrups and provided with anchorage hooks bent inside of the beam.

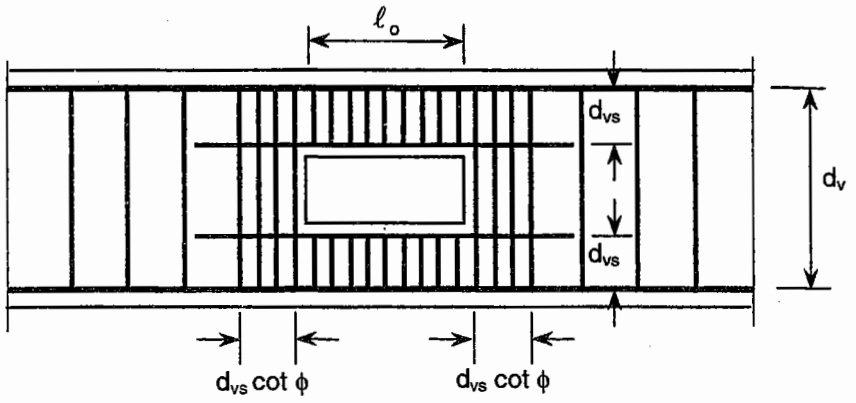

(a) Arrangement of reinforcement

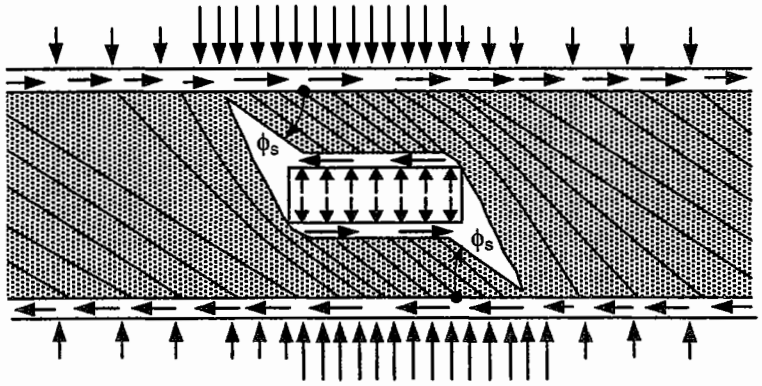

(b) Truss action

Figure 3.12. Truss action in beam with reinforced rectangular opening.

Assuming the yielding of the vertical stirrups and with reference to Eq. (2.28), the shear force carried by each truss mechanism in the chord members is $bd_{vs}\rho_v f_{yv}\cot\phi_s$, where b = width of section, ρ_v = shear reinforcement ratio of stirrups, and f_{yv} = yield strength of stirrups. Thus, the shear capacity of the beam can be obtained as

$$V_u = 2bd_{vs}\rho_v f_{yv}\cot\phi_s \tag{3.29}$$

where

$$\cot\phi_s = \sqrt{\frac{\nu f_c'}{\rho_v f_{yv}} - 1} \leq 2 \tag{3.30}$$

and

$$\rho_v f_{yv} \leq \nu f_c' \tag{3.31}$$

in which f_c' = cylinder compressive strength of concrete, and ν = effectiveness factor for the compressive strength of concrete as given by Eq. (2.29). The lower limit for

cot ϕ_s as indicated in Eq. (3.30) is to ensure aggregate interlocking in cracks and to prevent excessive crack widths.

The required force in the longitudinal reinforcement near the opening in each chord member is given by

$$T_{sn} = A_{sn} f_y = \frac{V_u \ell_o}{2\, d_{vs}} \tag{3.32}$$

and that in the longitudinal reinforcement away from the opening is

$$T_{sf} = A_{sf} f_y = \frac{V_u \left(\ell_o + d_{vs} \cot\phi_s\right)}{2 d_{vs}} \tag{3.33}$$

in which A_{sn} and A_{sf} are the area of longitudinal reinforcement in each chord member near and away, respectively, from the opening.

Where diagonal reinforcement is provided, as shown in Fig. 3.13, the shear resistance provided is given by

$$V_d = A_d f_{yd} \sin\theta_d \tag{3.34}$$

where A_d, f_{yd}, and θ_d are the area, yield strength, and angle of inclination, respectively, to the beam axis of the diagonal bars.

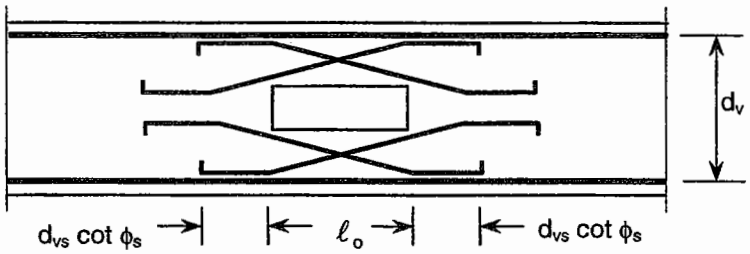

(a) Arrangement of diagonal reinforcement

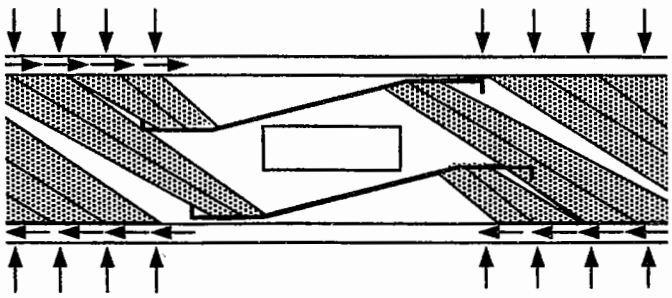

(b) Truss action

Figure 3.13 Truss action in beam with rectangular opening reinforced with diagonal bars (Architectural Institute of Japan, 1994).

3.3.3 STRUT-AND-TIE MODEL

As discussed in Art. 2.3.4, a structure may be divided into B- and D-regions. The B-regions refer to regions where the Bernoulli hypothesis of plane strain distribution is assumed to be valid and the flexural theory can be applied with great accuracy. The D-regions are those where the strain distribution is significantly nonlinear, for example, near concentrated loads, corners, bends, openings, and other discontinuities. In order that it can be applied to every part of the structure, the truss analogy may be generalized in the form of a strut-and-tie model. The strut-and-tie model condenses all stresses in compression and tension members and joins them by nodes. The tension and compression members, including their nodes, are designed with regard to safety and serviceability using uniform design criteria, thus providing a consistent design approach (Schlaich et al., 1987).

Fig. 3.14(a) shows the subdivision of a beam with an opening into B- and D-regions and the corresponding moment and shear force diagrams. The boundary forces (moments M and shear forces V) of the B-regions are applied as loads to the D-regions and vice-versa. The B_1-region is represented by a standard truss, with the compression strut forces C_1 and C_2 and tension tie force T_1 given by

$$C_1 = \frac{M_1}{z} - \frac{V_1}{2}\cot\theta \tag{3.35}$$

$$C_2 = \frac{V_1}{\sin\theta} \tag{3.36}$$

$$T_1 = \frac{M_1}{z} + \frac{V_1}{2}\cot\theta \tag{3.37}$$

where M_1 and V_1 are the moment and shear force, respectively, at the section between the B_1- and D_2-regions; z is the lever arm determined from the assumption of plane strain in the cross section at the middle of the opening using standard methods as given in Art. 2.2; and θ is the angle of inclination of the diagonal compression strut which may be taken to be between 30 and 60°.

A strut-and-tie model for the vicinity of the opening is shown in Fig. 3.14(c). For simplicity, the model of the B_2-region is extended somewhat into the D_2- and D_3-regions, leaving for modeling only the D_2'- and D_3'-regions, as shown in Fig. 3.14(b). If the opening is near the bottom of the beam, the B_3-region can be designed for a constant tensile force

$$T_2 = \frac{M_2}{z} \tag{3.38}$$

where M_2 is the moment at the center of the opening.

Thus, the B_2-region has to carry an axial compressive force $C = T_2$, which is eccentric with respect to its axis, plus a differential moment $\Delta M = M - M_2$ and the total shear V. Under the combined action of these forces, the B_2-region shows a transition from the column type B-region on its left end (with stress resultant C_3) to the truss type B-region at the other end (with stress resultants C_4, C_5, and T_3).

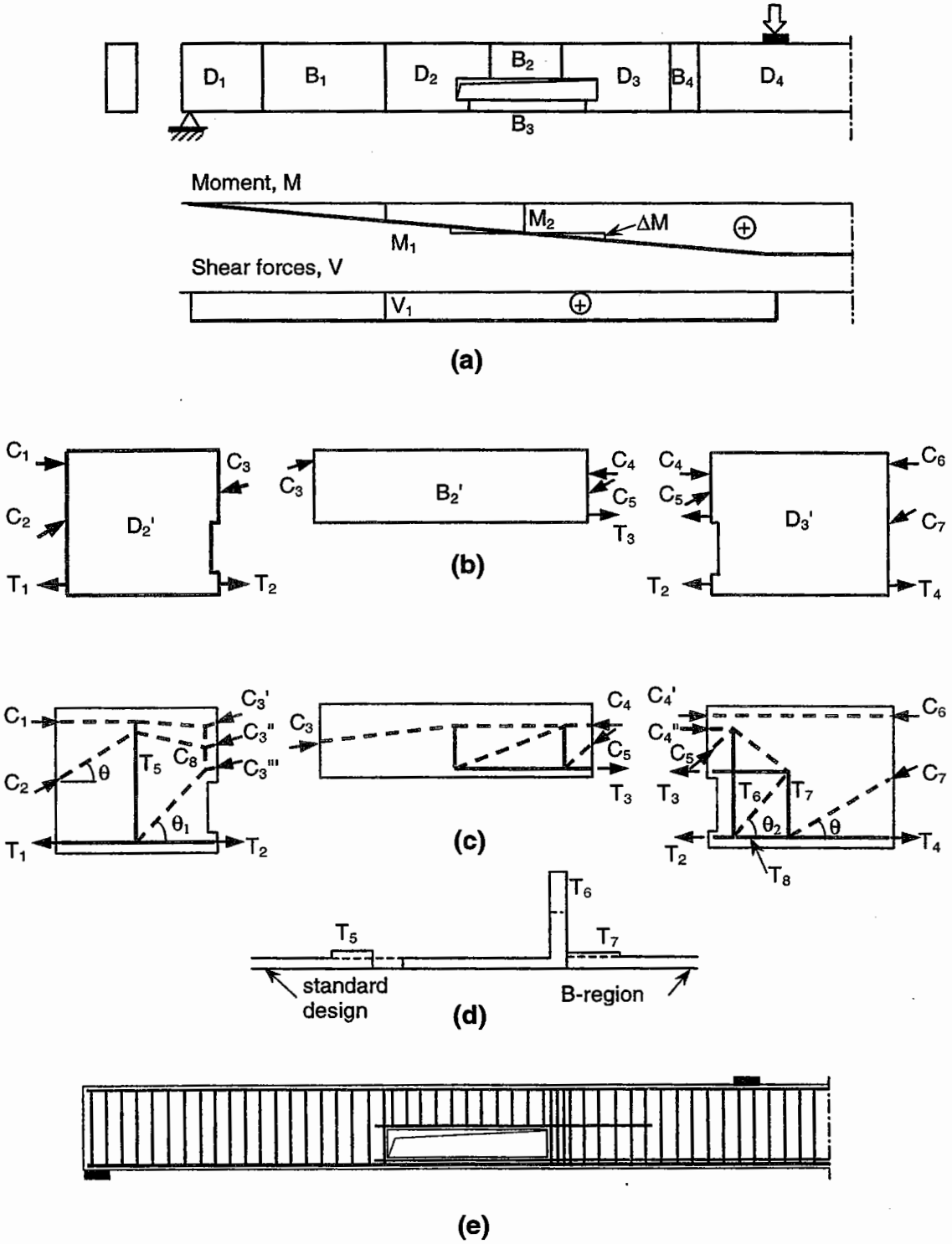

Figure 3.14 Strut-and-tie model. (a) B- and D-regions; (b) reduced D-regions at opening ends; (c) D_2- and D_3-regions; (d) forces for stirrup design; (e) reinforcement layout (Schlaich et al., 1987).

With known boundary conditions from B_1-, B_2-, and B_3-regions, the model for the D_2-region can be developed as shown in Fig. 3.14(c). In order to establish the load paths from C_1, C_2, and T_1 on one side of the D_2'-region to C_3 and T_2 on the other side, one may consider C_3 as the resultant of three forces C_3', C_3'' and C_3'''. These forces balance the horizontal components of C_1 and C_2, and the tie forces T_1 and T_2, that is, $C_{3h}' = C_1$; $C_{3h}'' = C_{2h}$; and $C_{3h}''' = T_2 - T_1$.

The vertical equilibrium in the D_2'-region is established by a vertical tension tie T_5 and by a vertical compressive strut C_8. Their forces depend on the choice of their position. Since they represent transverse stresses and tend to fill the available space inside the D_2-region, the resultant tension T_5 may be taken as at the middle of the D_2'-region and the resultant compression C_8 at the right end of D_2'. Then,

$$T_5 = (T_2 - T_1)\tan\theta_1 \tag{3.39}$$

The D_3'-region at the other end of the opening may be treated in a similar way. The transverse tension forces are

$$T_7 = V = P_u = (T_4 - T_8)\tan\theta \tag{3.40}$$

$$T_6 = (T_8 - T_2)\tan\theta_2 = (T_4 - T_2 - V\cot\theta)\tan\theta_2 \tag{3.41}$$

The tie force T_5, T_6 and T_7 may be interpreted as the transverse tension necessary to anchor the differential forces (T_2 – T_1), (T_8 – T_2), and (T_4 – T_8), respectively, of the tension chord of the beam. Fig. 3.14(d) shows the relative magnitude of these forces, and it is noted that they generally exceed the normal shear force for a similar beam without the opening. Knowing these forces, transverse shear reinforcement can be provided uniformly and centered at their locations. Similarly, the required longitudinal reinforcement at the opening can be obtained from the values of T_2 and T_3. Fig. 3.14(e) shows the required reinforcement layout for the beam with the opening.

When the opening is near the top of the beam such as a T-beam, a strut-and-tie system in the bottom can be considered, as shown in Fig. 3.15.

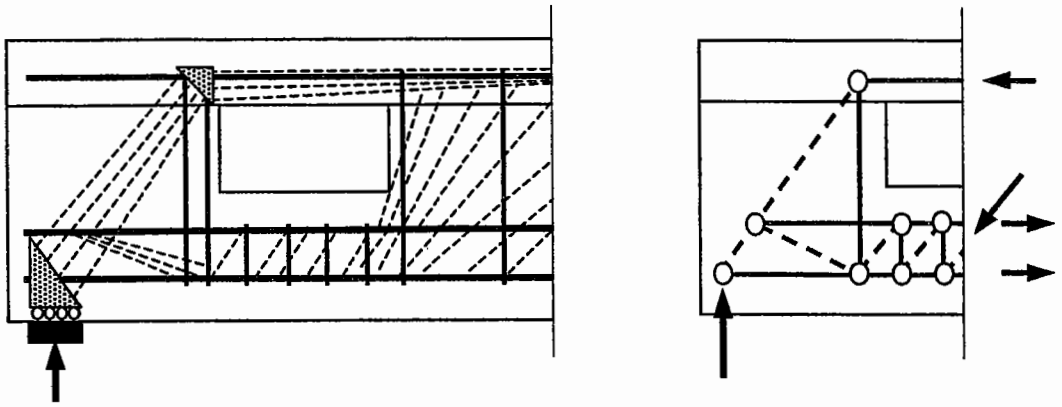

Figure 3.15 Strut-and-tie model for T-beam with opening near the top (Cook and Mitchell, 1988).

3.4 DESIGN FOR ULTIMATE STRENGTH

It has been noted in Art. 3.2 that the unknown actions at an opening are the axial forces (N_t and N_b), the bending moments (M_t and M_b), and the shear forces (V_t and V_b) in the chord members (see Fig. 3.3). There are three equilibrium equations [Eqs. (3.3) - (3.5)] relating these six unknowns. Thus, if three additional equations can be found, it would be possible to solve for the unknown actions. The additional equations can be obtained by assuming contraflexure points to occur at the midpoint of the chord members and by assuming an appropriate distribution of shear forces between the chord members, which lead to:

$$M_t = 0 \tag{3.42a}$$

$$M_b = 0 \tag{3.42b}$$

$$V_b = k_v V_t \tag{3.42c}$$

in which k_v is a known value. The beam then becomes statically determinate and the critical sections at the ends of the chord members that are subject to combined bending shear and axial force can be designed in the standard manner following the provisions of any current building codes.

There are, however, three schools of thought regarding the distribution of applied shear between the chord members at an opening. The first, as proposed by Lorensten (1962), assumes that the compression chord carries the total shear and the tension chord merely acts as a link carrying no shear. This is probably true in the case of a beam containing an opening near the bottom. The second proposal (Nasser et al., 1967 and Reagan and Warwaruk, 1967), distributes the total shear between the chord members in proportion to their cross-sectional areas. And the third, suggested by Barney et al. (1977), distributes the shear force in proportion to the flexural stiffnesses of the chord members. Accordingly,

$$k_v = 0 \qquad \text{(Lorensten)} \tag{3.43a}$$

$$k_v = A_b / A_t \qquad \text{(Nasser et al.)} \tag{3.43b}$$

$$k_v = I_b / I_t \qquad \text{(Barney et al.)} \tag{3.43c}$$

Although for design purpose the distribution of shear forces can be simply assumed as above, a more rational approach which may be extended to the case of continuous beams is desirable from an economical point of view. Such an approach may be based on any of the analytical methods described in Art. 3.3.

3.4.1 PLASTIC HINGE METHOD

The limit analysis approach described in Art. 3.3.1 assumes a failure mechanism consisting of four hinges in the chord members, one at each corner of the opening. In the approach, the conditions of equilibrium, yield, and a mechanism were satisfied simultaneously. Based on the exact solution for the collapse load thus

obtained and recasting it in a graphical form (Mansur et al., 1985), a method suitable for the direct design of beams with large openings for ultimate strength can be formulated. The steps involved in the method are as follows.

1. Calculate the bending moment, M_u, and the shear force, V_u, at the center of the opening due to design ultimate load.

2. Assume a suitable amount and arrangement of reinforcement in the chord members.

3. Determine the axial force, N_u, in the chord members due to the ultimate load as follows:

   The critical sections are at the ends of the chord members. Forces and moments acting at these sections are shown in Fig. 3.3(c). It is to be noted that the shear forces are acting in the positive direction and sagging bending moment is taken as positive. As there is no external force acting on the chord members, the magnitude of shear remains constant along the opening length. At plastic collapse,

$$(V_u)_t = [(M_u)_{t,2} - (M_u)_{t,1}]/\ell_e \tag{3.44}$$

$$(V_u)_b = [(M_u)_{b,4} - (M_u)_{b,3}]/\ell_e \tag{3.45}$$

   where V_u = ultimate shear force; M_u = ultimate bending moment; and ℓ_e = effective length of a chord; the subscripts t and b stand for the top and bottom chords, and 1, 2 and 3, 4 denote the ends of the top and bottom chords, respectively, where plastic hinges form at collapse (see Fig. 3.6).

   The secondary moments $(M_s)_t$ and $(M_s)_b$, respectively, at the center of the opening are given by

$$(M_s)_t = [(M_u)_{t,1} + (M_u)_{t,2}]/2 \tag{3.46}$$

$$(M_s)_b = [(M_u)_{b,3} + (M_u)_{b,4}]/2 \tag{3.47}$$

   The applied moment, M_u, at the center of the opening is resisted by the couple formed by the axial forces, N_u, in the chord members and the secondary moments $(M_s)_t$ and $(M_s)_b$. Hence,

$$M_u = N_u z + (M_s)_t + (M_s)_b \tag{3.48}$$

   where z = distance between the plastic centroids of the two chord members.

   Inserting Eqs. (3.46) and (3.47) into Eq. (3.48) yields

$$N_u \frac{z}{h} = \left\{ M_u - \frac{1}{2}\left[(M_u)_{t,1} + (M_u)_{t,2} + (M_u)_{b,3} + (M_u)_{b,4} \right] / h \right\} \tag{3.49}$$

where h = overall depth of the beam. Introducing

$$M^* = M_u - \frac{1}{2}\left[(M_u)_{t,1} + (M_u)_{t,2} + (M_u)_{b,3} + (M_u)_{b,4} \right] \tag{3.50}$$

and

$$\frac{z}{h} = \tan\theta \tag{3.51}$$

the following relationship may be obtained

$$\theta = \tan^{-1}\left(\frac{z}{h}\right) = \tan^{-1}\left(\frac{M^*}{N_u h}\right) \tag{3.52}$$

Since the collapse of the beam occurs by the formation of four hinges in the chord members, the values of M_u at locations 1, 2, 3, and 4 must lie on the respective interaction surfaces. The corresponding value of N_u that must satisfy Eq. (3.49) can be obtained by graphical construction, as illustrated in Fig. 3.16.

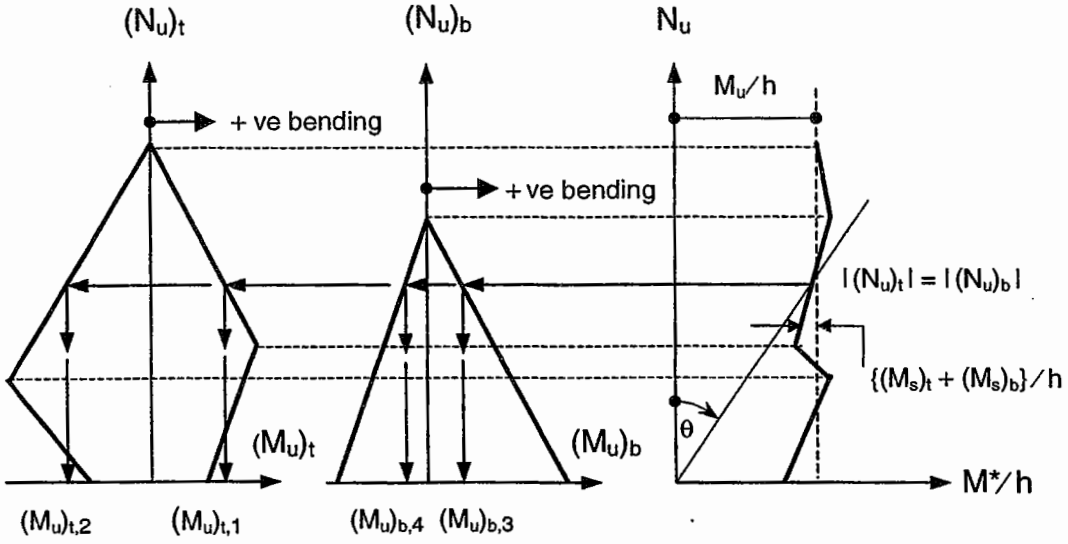

(a) Interaction diagram for top (compression) chord (b) Interaction diagram for bottom (tension) chord (c) Graph of N_u versus M^*/h [$\theta = \tan^{-1}(z/h)$]

Figure 3.16 Determination of N_u.

In Fig. 3.16, the applicable portions of the interaction curve (approximated by straight lines) for the top (compression) and bottom (tension) chords are first drawn so that they appear above the M-axis [Figs. 3.16(a) and (b)]. It should be noted here that the chord members bend in double curvature. As a result, bending moments at two ends of each chord have opposite senses. The values of M_u at 1, 2, 3, and 4 that correspond to any value of N_u can be obtained from these diagrams, and, hence, the graph of N_u versus M'/h. The point of intersection of this graph with the straight line represented by Eq. (3.52) gives the desired value of N_u [Fig. 3.16(c)].

If the top and bottom chords are each symmetrically reinforced, then the corresponding interaction diagrams are symmetrical about the N-axis and, therefore, contraflexure points occur at midpoint of the chord members. Eq. (3.48) then reduces to:

$$M_u = N_u z \tag{3.53}$$

In practice, approximately equal amounts of top and bottom reinforcement for each chord member are provided. In such cases, the values of $\frac{1}{2}[(M_u)_{t,1} + (M_u)_{t,2}]$ and $\frac{1}{2}[(M_u)_{b,3} + (M_u)_{b,4}]$ are found to be very small when compared to M. Hence, N can be obtained directly from Eq. (3.53) without any significant error.

4. Obtain the values of $(M_u)_t$ at 1 and 2 and $(M_u)_b$ at 3 and 4 that correspond to the value of N_u as determined above. If any of these values are not obtainable, the longitudinal reinforcement in the respective chord member must be increased and Step 3 repeated.

5. The values of $(V_u)_t$ and $(V_u)_b$ can then be calculated from Eqs. (3.44) and (3.45), respectively. If $(V_u)_t + (V_u)_b < V_u$, then the section is not satisfactory, and more longitudinal reinforcement has to be provided. If $(V_u)_t + (V_u)_b > V_u$, a smaller amount of reinforcement could be used. The process is repeated until $(V_u)_t + (V_u)_b \approx V_u$. Once $(V_u)_t$ and $(V_u)_b$ are determined, the beam becomes statically determinate and can be designed, following the provisions of any suitable building code.

It follows from the above discussion that the design of a beam with rectangular openings is primarily concerned with the design of chord members. Three types of graphs as shown in Figs. 3.16(a), (b), and (c) are required for this purpose. Two simplified versions of the above method (Mansur, 1988) are presented, as follows.

3.4.1.1 Simplified Method 1

In most situations, the quantity and arrangement of main reinforcement, A_s, for a beam with known dimensions and loading would have been determined first from flexural design of the solid section. If the beam is subject to a sagging bending moment as shown in Fig. 3.17, the main reinforcement, A_s, will be at the bottom, and the top reinforcement would be lighter than the bottom reinforcement.

Due to the introduction of an opening, additional reinforcement must be provided in the chord members so as to retain the original strength of the beam. This additional reinforcement may be conveniently arranged in a symmetrical manner for the top (compression) chord member, as shown in Fig. 3.17(d). For the bottom (tension) chord member, which had already been provided with a relatively large amount of reinforcement near the bottom face, it is difficult to reinforce in a symmetrical manner because of the danger of steel congestion and over-reinforcement. Hence, it is most likely that the bottom chord will be unsymmetrically reinforced.

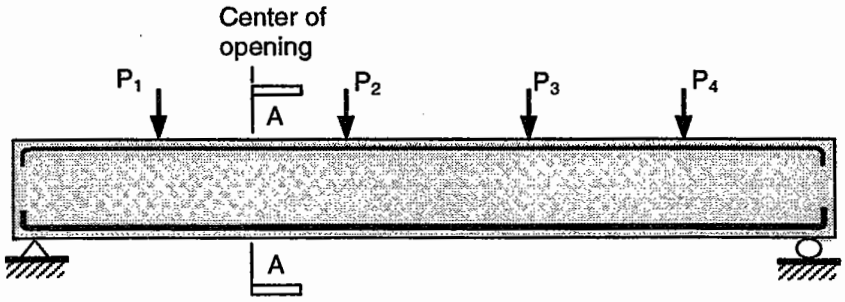

(a) Solid beam

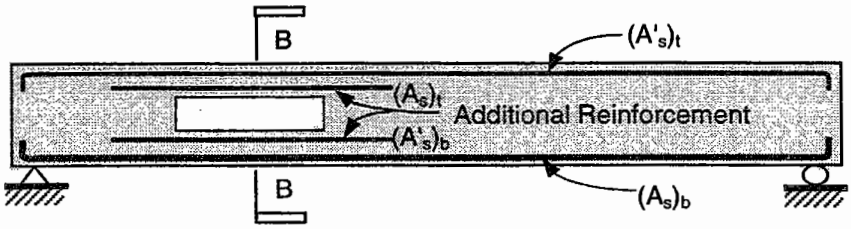

(b) Beam after introducing the opening

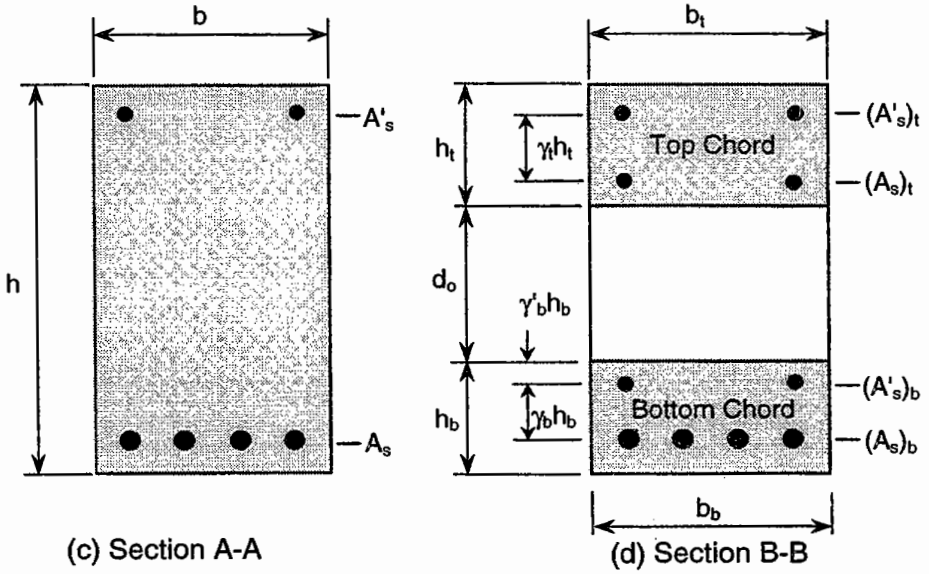

(c) Section A-A

(d) Section B-B

Figure 3.17 Beam before and after introduction of opening.

With the assumption that the top chord is symmetrically reinforced, the interaction diagrams for positive and negative bending will be numerically the same. Hence, Eqs. (3.44) and (3.46) reduce, respectively, to

$$(V_u)_t = 2(M_u)_{t,2}/\ell_o \tag{3.54}$$

and

$$(M_s)_t = 0 \tag{3.55}$$

The nondimensional interaction charts for the top (compression) chord may be obtained by the method of equilibrium and strain compatibility. A typical linearized chart, corresponding to the case where the distance between the centroids of the two layers of reinforcement, as indicated in Fig. 3.17(d), γ_t equals 0.5, is presented in Fig. 3.18.

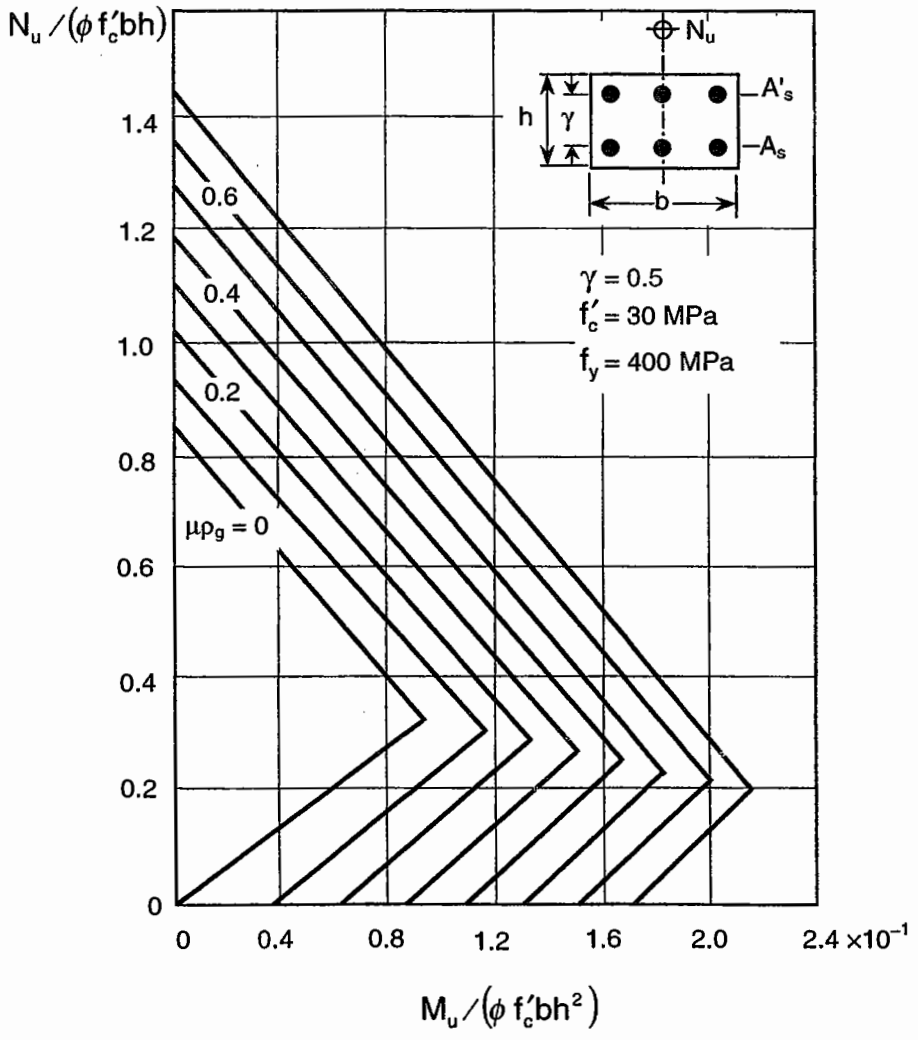

Figure 3.18 Interaction for compression chord.

The chart has been developed using the stress-strain relationship for steel and the compressive stress block for concrete as recommended in the ACI Code (1995), and it is valid for $f_c' < 30$ MPa and $f_y = 400$ MPa. The curves in this chart are labeled with values of $\mu\rho_g$, where $\mu = f_y / 0.85 f_c'$ and $\rho_g = 2A_s / bh$, and b and h are the overall depth of the chord member, and they are expressed in terms of nominal strengths with a capacity reduction factor ϕ of 0.9.

The interaction charts for the bottom (tension) chord may be obtained in a similar manner. Fig. 3.19 shows a chart for a typical value of γ_b and for equal concrete cover for the top and bottom reinforcement. For unequal concrete covers, similar charts may be plotted by varying the position of top reinforcement as defined by γ_b', keeping γ_b at a fixed value. In Fig. 3.19, each linearized curve with a particular $\mu\rho_g$ is subdivided into three curves labeled with different values of α, where $\alpha = A_s' / A_s + A_s'$, $\rho_g = (A_s + A_s') / bh$, and A_s' = area of reinforcement for negative bending, and they are expressed in terms of ultimate axial load and moment also using a capacity reduction factor, ϕ, of 0.9.

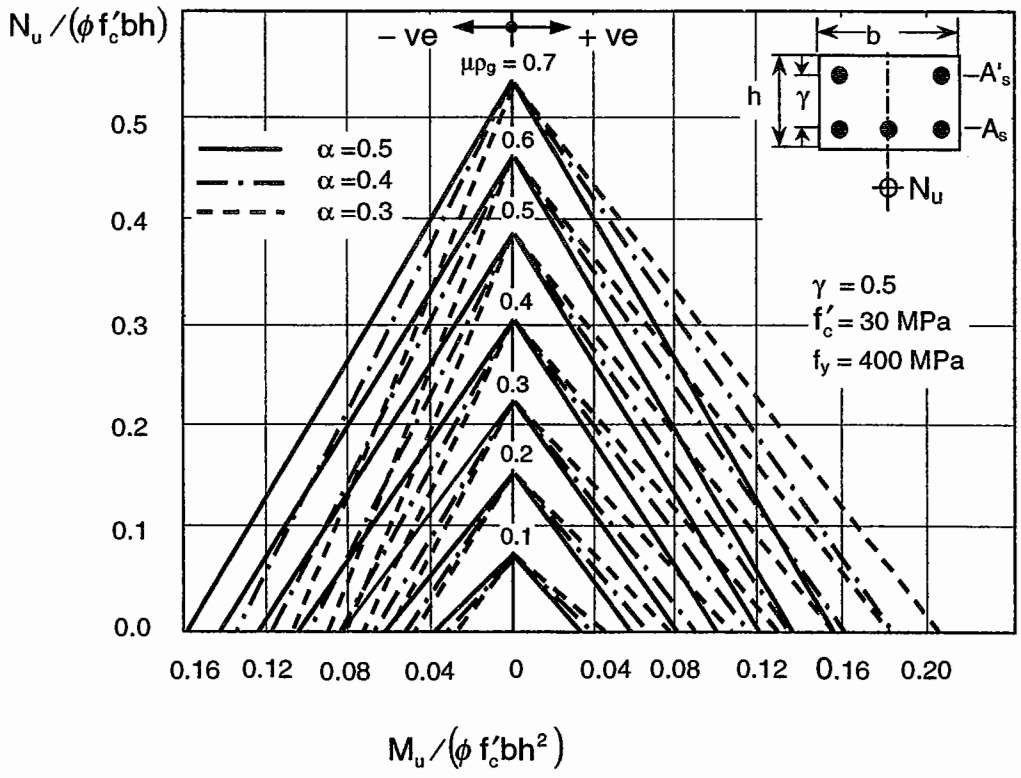

Figure 3.19 Interaction chart for tension chord.

As the term within the square brackets of Eq. (3.50) is usually a small quantity when compared with M_u, it is rather difficult to maintain an accurate construction of the N_u versus M^*/h graph shown in Fig. 3.16(c). Provided the interaction diagrams are linearized, an analytical approach may be used instead.

For known interaction diagrams in positive and negative bending, the value of N_u that satisfies Eq. (3.49) may be readily derived as

$$(N_u)_b = \frac{2M_m - (M'_o)_b - (M_o)_b}{2z - [(M'_o)_b + (M_o)_b]/(N_o)_b} \tag{3.56}$$

where N_o = axial load capacity in direct tension and M_o and M'_o = pure bending moment capacities in positive and negative bending, respectively.

The corresponding positive and negative bending moments at the two ends of the bottom chord member are given, respectively, by

$$(M_u)_b = [(N_o)_b - (N_u)_b](M_o)_b/(N_o)_b = (M_u)_{b,3,or\,4} \tag{3.57}$$

$$(M'_u)_b = [(N_u)_b - (N_o)_b](M'_o)_b/(N_o)_b = (M_u)_{b,3,or\,4} \tag{3.58}$$

The sense of the bending moments at 3 and 4 can be determined easily by inspection of the deformed shape of the chord member.

The design steps involved in this simplified method can be summarized as follows:

1. Assuming that the beam is prismatic, determine the main flexural reinforcement, A_s. Take this as the bottom reinforcement, $(A_s)_b$, of the lower chord member.

2. Calculate the moment, M_m, and shear force, V_m, at the center of the opening due to design ultimate load.

3. Assuming a value of α less than or equal to 0.5, depending on the ease of steel placement, establish γ_b and $\mu(\rho_t)_b$. Select the appropriate chart in Fig. 3.19 and calculate $(N_u)_b$ from Eq. (3.56), in which for equal concrete cover to the top and bottom reinforcement bars in each chord member,

$$z = \frac{(h_t + h_b)}{2} + d_o + (0.5 - \alpha)\gamma_b h_b \tag{3.59}$$

The values of bending moments at the two ends, $(M_u)_{b,3}$ and $(M_u)_{b,4}$, at collapse are then given either by Eq. (3.57) or (3.58), depending on their sense.

4. Calculate the shear force in the chord members $(V_u)_b$ and $(V_u)_t$ from as follows:

$$(V_u)_b = [(M)_{b,4} - (M)_{b,3}]/\ell_o \tag{3.60}$$

$$(V_u)_t = V_m - (V_u)_b \tag{3.61}$$

5. Calculate the axial force and the end moment in the top chord member as follows:

$$(N_u)_t = -(N_u)_b \tag{3.62}$$

$$(M_u)_{t,2} = \frac{(V_u)_t \ell_o}{2} = -(M_u)_{t,1} \tag{3.63}$$

6. Determine reinforcement for the top chord member from Fig. 3.18 using the values of $(N_u)_t$ and $(M_u)_{t,2}$.

3.4.1.2 Simplified Method 2

If the bottom chord is also assumed to be symmetrically reinforced, the number of design charts may be minimized, leading to a considerable simplification of the overall design process. In this case, the moment-tension interaction diagram would be numerically the same for positive and negative bending, as represented by the solid lines in Fig. 3.19, and the contraflexure point would occur at midspan. Therefore, Eqs. (3.60) and (3.56), respectively, reduce to

$$(V_u)_b = 2(M_u)_{b,4} / \ell_o \tag{3.64}$$

$$(N_u)_b = \frac{M_m}{z} \tag{3.65}$$

Eq. (3.65) gives the magnitude of axial force in the chord members directly irrespective of the amount of reinforcement. However, to proceed with the design, it is necessary either to assume a certain quantity of reinforcement or to assign a fraction of the total shear to be carried by the bottom chord. The latter approach is suggested because it offers greater flexibility.

When assigning the shear force, it should be kept in mind that the shear carrying capacity of a chord member depends on the moment capacities of the critical end sections. These in turn depend on the amount of longitudinal reinforcement and whether the depth is sufficient to provide effective shear reinforcement. Thus, if the opening is provided in a T-beam just below the flange, and the flange thickness is inadequate for the placement of stirrups, the entire shear should be assigned to the bottom chord. Similarly, situations may arise where the opening is near the bottom of the beam and the bottom chord member is very shallow compared to the top chord. In such a case, the top chord member should be designed to carry the total shear force. For equal size of the chord members, however, assignment of less than half of the external shear to the bottom (tension) chord member leads to a more economical design.

Once a suitable shear force is assigned to the bottom chord, $(M_u)_{b,4}$ can be calculated from Eq. (3.64) and the required reinforcement read from the appropriate chart in Fig. 3.19. The design of the top chord member follows the same way as in Simplified Method 1.

EXAMPLE PROBLEM 3.4

A simply-supported reinforced concrete beam, 300 mm wide and 600 mm deep, contains a rectangular opening and is subjected to a series of point loads as shown in Fig. E3.4.1. Design the beam if the design ultimate load P_u is 52.8 kN. The material properties are f'_c = 30 MPa, f_{yv} = 250 MPa, and f_y = 400 MPa.

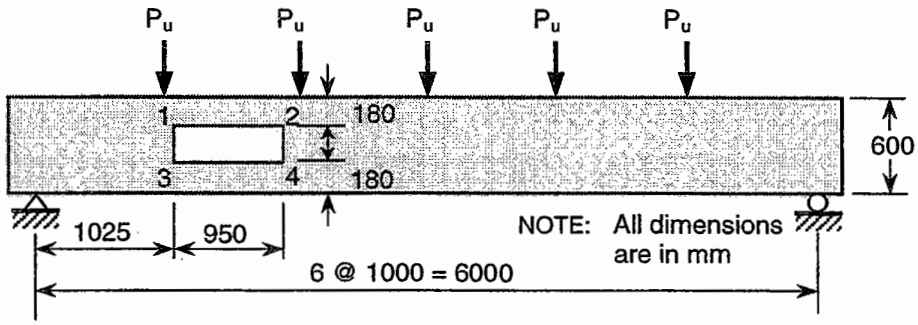

Figure E 3.4.1 Example 3.4.

SOLUTION

Simplified Method 1

(a) Design of midspan section of the beam

$$M_u = 52.8 \times 2.5 \times 3 - 52.8 \times 2 \times 1.5 = 237.6 \text{ kNm}$$

Effective depth,

$$d = 600 - (25 + 10 + 10) = 555 \text{ mm}$$

Therefore, $M_u/(\phi b d^2) = 237.6 \times 10^6/(0.9 \times 300 \times 555^2) = 2.86$ MPa

From flexural design chart (Nilson, 1997),

$$A_s/bd = 0.0073 > \rho_{min}$$

Therefore, $A_s = 1215 \text{ mm}^2$; Use 4T20 bars.

(b) Design of bottom (tension) chord member

$$M_u = 52.8 \times 2.5 \times 1.5 - 52.8 \times 0.5 = 171.6 \text{ kNm}$$

$$V_u = 79.2 \text{ kN}$$

Since curtailment of reinforcement required for the beam is not possible before reaching the throat section, the same reinforcement is continued throughout the

length of the bottom chord. Therefore, $(A_s)_b$ is provided by 4T20 bars. Using 2T20 bars at the top

$$\alpha = 0.33 \text{ and } \mu\,(\rho_g)_b = 0.55$$

Assuming a 25 mm clear concrete cover for the top and bottom reinforcement and M10 stirrups,

$$\gamma_b = 0.5 \text{ and } \ell_u = 950 + 2 \times 25 = 1000 \text{ mm}$$

By linear interpolation from Fig. 3.19

$$(N_o)_b = 688.5 \text{ kN} ; (M'_o)_b = -26.24 \text{ kNm} ; (M_o)_b = 48.15 \text{ kNm}$$

Also, from the above and from Eq. (3.59),

$$M_u = 171.6 \text{ kNm} ; z = 435 \text{ mm}$$

It may be noted that the ends 3 and 4 are subject to negative and positive moments, respectively. Therefore, from Eqs. (3.56), (3.57), and (3.58),

$$(N_u)_b = 383.4 \text{ kN} ; (M_u)_{b,3} = -11.63 \text{ kNm} ; (M_u)_{b,4} = 21.34 \text{ kNm}$$

Eq. (3.60) thus gives

$$(V_u)_b = 33.0 \text{ kN} < V_u = 79.2 \text{ kN}$$

From Eqs. (2.8) and (2.15), the required shear reinforcement is given by

$$A_v f_y d_t / s = (V_u)_b/\phi - \sqrt{f'_c}\, b_t d_t / 6$$
$$= 33.0/0.85 - \sqrt{30} \times 300 \times 135 \times 10^{-3}/6 = 1.852 \text{ kN}$$

Assuming $f_{yv} = 250$ MPa,

$$A_v / s = 1.852 \times 10^6/(250 \times 135) = 55 \text{ mm}^2/\text{m}$$

This is less than

$$(A_v/s)_{min} = 0.33\, b_t / f_y = 0.33 \times 300 \times 10^3/250 = 400 \text{ mm}^2/\text{m}.$$

Therefore, use two-legged M6 stirrups at 100 mm spacing [$(A_v/s)_{provided} = 566 \text{ mm}^2/\text{m}$].

(c) Design of top (compression) chord

$$(N_u)_t = 383.4 \text{ kN (compression)} ; (V_u)_t = V_u - (V_u)_b = 46.2 \text{ kN}$$

Therefore, from Eq. (3.63)

$$(M_u)_{t,2} = 23.1 \text{ kNm} \quad \text{[from Eq. (3.63), replacing } \ell_o \text{ by } \ell_u\text{]}$$

Referring to Eqs. (3.1) and (3.2),

$$k\ell_u / r = 1 \times 1000/(0.3 \times 180) = 18.5 < 22$$

Hence, the compression chord may be designed as a short column.

$$(N_u)_t/(\phi f'_c\, b_t h_t) = 0.338 \quad (\phi = 0.7); \quad (M_u)_t/(\phi f'_c\, b_t h_t^2) = 0.113$$

From design chart of Fig. 3.18,

$$\mu(\rho_g)_t = 0.11$$

Therefore, $(A_s + A_s')_t = 0.11 \times (0.85 \times 30/400) \times 300 \times 180 = 379 \text{ mm}^2$

Use 4T12 bars.

The required shear reinforcement is given by

$$A_v f_y d_b / s = 46.2/0.85 - \sqrt{30} \times 300 \times 135 \times 10^{-3}/6 = 17.38 \text{ kN}$$

Assuming $f_y = 250$ MPa,

$$A_v/s = 17.38 \times 10^6/(250 \times 135) = 515 \text{ mm}^2/\text{m}$$
$$> (A_v/s)_{min} = 0.33\, b_t/f_y = 0.33 \times 300 \times 10^3/250 = 400 \text{ mm}^2/\text{m}$$

Use M6 two-legged stirrups at 100 mm spacing [$(A_v/s)_{provided} = 566 \text{ mm}^2/\text{m}$].

The required reinforcement to resist the applied load is shown in Fig. E3.4.2. Further reinforcement would be required for crack control at the corners of the opening (see Art. 3.5). Design for the rest of the beam follows the usual procedure for prismatic beams and is completed with a check on deflection.

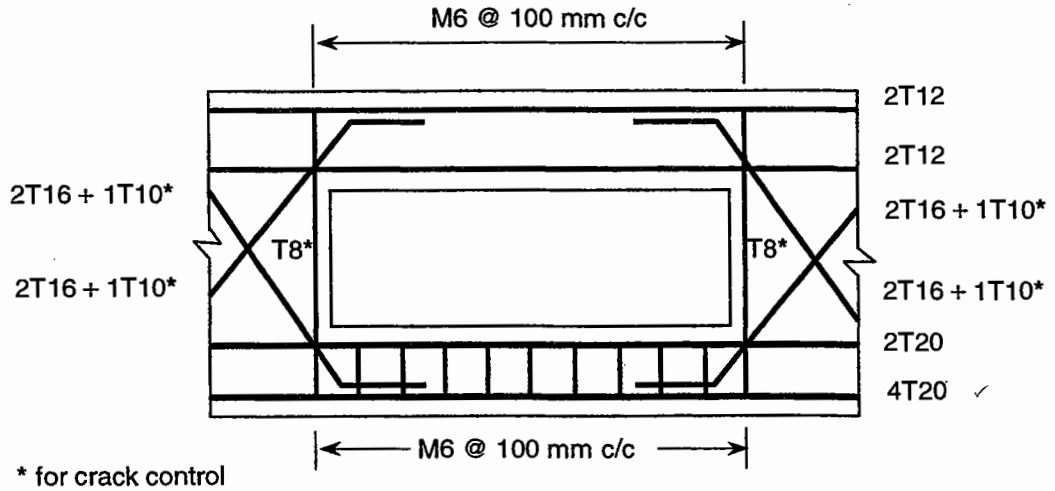

Figure E3.4.2 Reinforcement details at opening.

Simplified Method 2

(a) Design of bottom chord member

The axial load in the chord members is directly given by Eq. (3.65).

$$(N_u)_b = 171.6/(0.6 - 0.18) = 408.6 \text{ kN}$$

Therefore, $(N_u)_b/(f'_c\, b_b\, h_b) = 0.252$

Assuming 40% of the applied shear force is carried by the bottom chord member,

$$(V_u)_b = 0.4 \times 79.2 = 31.7 \text{ kN}$$

Eq. (3.64) then gives

$$(M_u)_b/(\phi f'_c\, b_b\, h_b^2) = (V_u)_b\, \ell_o/(2\phi f'_c\, b_b\, h_b^2) = 0.0543$$

From the design chart of Fig. 3.19 in which only the solid lines are applicable,

$$\alpha = 0.33 \quad \text{and} \quad \mu(\rho_g)_b = 0.565$$

$$2A_s = 0.565 \times (0.85 \times 30/400) \times 300 \times 180 = 1945 \text{ mm}^2$$

Use 6T20 bars, arranged symmetrically about the horizontal axis. Since the solid section adjacent to the opening requires 4T20 bars at the bottom, the same reinforcement is continued through the opening. The top reinforcement in the bottom chord member thus consists of 3T20 bars. The required shear reinforcement in the chord member is the same as given by Simplified Method 1.

(b) Design of top (compression) chord member

$$(N_u)_t = 408.6 \text{ kN} \; ; \; (V_u)_t = V_u - (V_u)_b = 47.5 \text{ kN};$$

Therefore, $(M_u)_{t,2} = 23.75$ kNm [from Eq. (3.63)]

$$(N_u)_t/(\phi f'_c\, b_t\, h_t) = 0.356 \;\; (\phi = 0.7); \;\; (M_u)_t/(\phi f'_c\, b_t\, h_t^2) = 0.116$$

The design chart of Fig. 3.18 gives

$$\mu(\rho_g)_t = 0.15$$

Therefore, $2A_s = 0.15 \times (0.85 \times 30/400) \times 300 \times 180 = 516 \text{ mm}^2$

Use 2T12 and 1T10 on each face. The required shear reinforcement would be similar to that obtained by Method 1. It can be seen that Method 2 is much simpler and gives a conservative design.

3.4.2 PLASTICITY TRUSS METHOD

Based on the plasticity truss model described in Art. 3.3.2, a procedure for the direct design of reinforcement around a large opening can be formulated as follows.

STEP 1: Calculate the value of v from

$$v = \frac{V_m}{2b\,d_{vs}\,\nu\,f_c'} \tag{3.66}$$

where b is the width of chord members; d_{vs} is the average distance between the top and bottom longitudinal reinforcement in the chord members; f_c' is the concrete cylinder compressive strength; ν is effectiveness factor as given by Eq. (2.29); and

$$V_m = V_u - A_d f_{yd} \sin\theta_d \tag{3.67}$$

where A_d, f_{yd}, and θ_d are the area, yield strength, and angle of inclination, respectively, to the beam axis of the diagonal bars.

STEP 2: From Fig. 2.16, determine the value of ψ such that $½ \le \cot\phi_s \le 2$ or from Eq. (3.30), $0.2 \le \psi \le 0.8$. Normally, the lower limit of ψ will apply. Calculate ρ_v from $\rho_v = \psi(\nu f_c')/f_{yv}$. Check that

$$\rho_v = \frac{A_v}{bs} \ge (\rho_v)_{min} \tag{3.68}$$

where A_v, f_{yv}, and s are the area, yield strength, and spacing, respectively, of the stirrups. These stirrups should be provided uniformly throughout the chord and for a distance equal to $d_{vs}\cot\phi_s$ on each side of the opening [see Fig. 3.12(a)].

STEP 3: Calculate the required longitudinal reinforcement near the opening [see Fig. 3.12(a)] from Eq. (3.32) as

$$A_{sn} = \frac{V_u \ell_o}{2 f_y d_{vs}} \tag{3.69}$$

where ℓ_o is the length of opening, and f_y is the yield strength of longitudinal reinforcement.These reinforcing bars must be extended beyond the vertical stirrups and be provided with anchorage hooks bending toward the inside of the beam.

STEP 4: Calculate the required longitudinal reinforcement away from the opening [see Fig. 3.12(a)] from Eq. (3.33) as

$$A_{sf} = \frac{V_u(\ell_o + d_{vs}\cot\phi_s)}{2 f_y d_{vs}} \tag{3.70}$$

EXAMPLE PROBLEM 3.5

Design the reinforcement for the opening region of the beam described in Example Problem 3.4 using the plasticity truss method. Use f'_c = 30 MPa and f_y = 460 MPa.

SOLUTION

(a) Calculate v.

From Example 3.4, the shear force at the opening is V_u = 79.2 kN. Assuming vertical stirrups only, Eqs. (3.66) and (3.67) give

$$v = 79.2 \times 10^3/(2 \times 300 \times 90 \times 0.55 \times 30) = 0.089$$

(b) Determine the required shear reinforcement.

From Fig. 2.16(a),

$$\psi = 0.008$$

from which, assuming f_{yv} = 250 MPa,

$$\rho_v = 0.008 \text{ x } 0.55 \text{ x } 30/250 \approx 0.000528$$
$$< \rho_{v,min} = (A_v/bs)_{min} = 1/(3f_y) = 1/(3 \times 250) \approx 0.00133$$

Therefore, $A_v/s = 0.00133 \times 300 \times 10^3 = 400 \text{ mm}^2/\text{m}$

Use M6 double-legged stirrups at 100 mm spacing [$(A_v/s)_{provided}$ = 566 mm^2/m].

(c) Determine the required longitudinal reinforcement.

From Eqs. (3.69) and (3.70),

$$A_{sn} = 79.2 \times 10^3 \times 950/(2 \times 460 \times 90) = 909 \text{ mm}^2$$

Use 3T20 (943 mm^2) bars near the opening in each chord member.

$$A_{sf} = 79.2 \times 10^3 \times (950 + 2 \times 90)/(2 \times 460 \times 90) = 1080 \text{ mm}^2$$

Use 4T20 (1256 mm^2) bars away from opening in each chord member.

The final reinforcement detail at the opening is shown in Fig. E3.5.1. It is seen that compared to the plastic hinge methods used in Example Problem 3.4, the plasticity truss method requires more shear reinforcement as well as longitudinal reinforcement in the chord members. This is because the truss method neglects the direct contribution of concrete to the shear resistance of the chord members. (Also see Example Problem 2.4.)

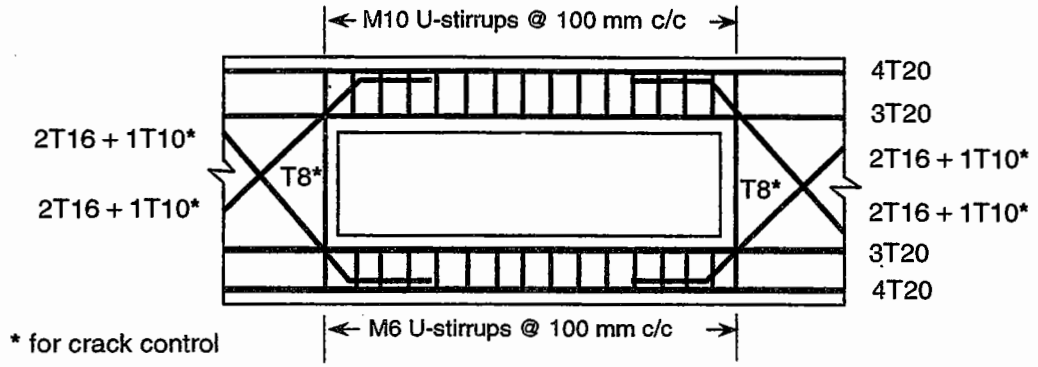

Figure E3.5.1 Required reinforcement according to plasticity truss method.

3.4.3 STRUT-AND-TIE METHOD

The first step in this method is to visualize the flow of forces from the applied loads to the supports. This is accomplished by a truss model consisting of concrete compressive struts and reinforcement tension ties. Several different models may be available, but the one that depicts the conditions under elastic behavior probably resembles the actual situation closely. Once the model is obtained, the forces in the struts and ties can be calculated from statics. The required area of tension tie reinforcement is then chosen.

EXAMPLE PROBLEM 3.6

Design the reinforcement for the opening in the beam described in Example Problem 3.4 using the strut-and-tie method. Use $f_y = 460$ *MPa.*

SOLUTION

(a) Postulate the strut-and-tie model.

A strut-and-tie model for the beam in Example Problem 3.4 is shown in Fig. E3.6.1. Here, the compressive struts are shown in dotted lines while tension ties are shown in solid lines.

(b) Calculate member forces.

The forces in the truss members are determined from statics and their magnitudes are as indicated in Fig. E3.6.1(a) and (d). The top chord member takes a shear force of 72.1 kN or about 91% of the total shear force at the opening. Note that the stirrup force at the high-moment end of the opening is as high as 259.4 kN, or 3.3 times the applied shear force of 79.2 kN.

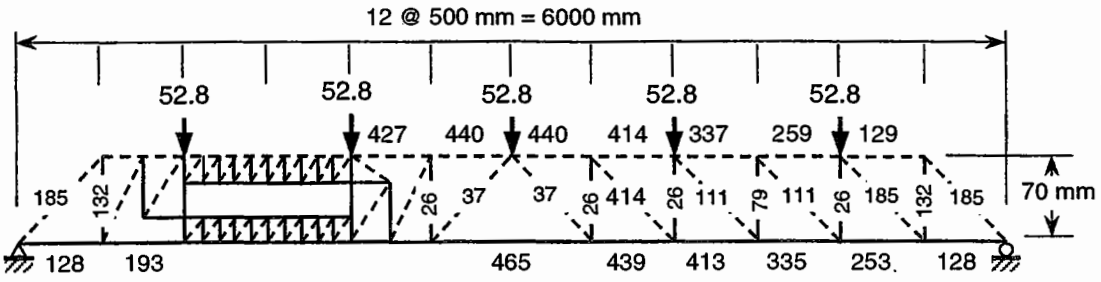

(a) Strut-and-tie model (Forces in kN)

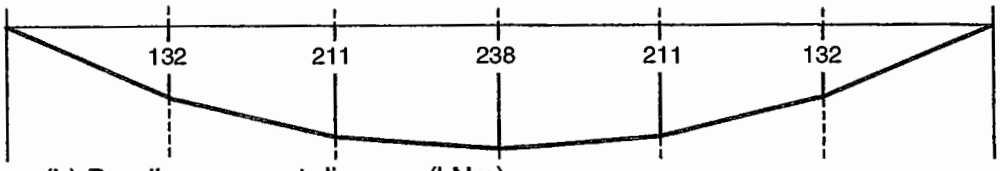

(b) Bending moment diagram (kNm)

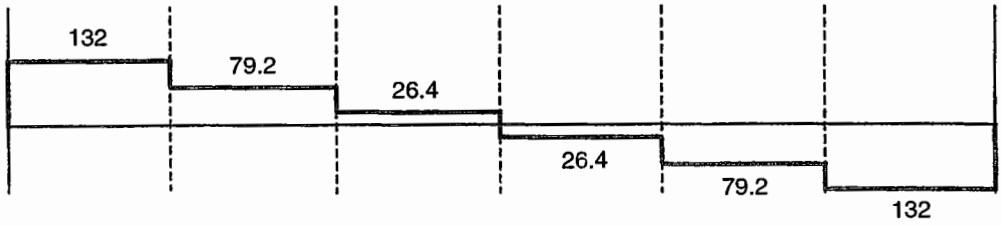

(c) Shear force diagram (kN)

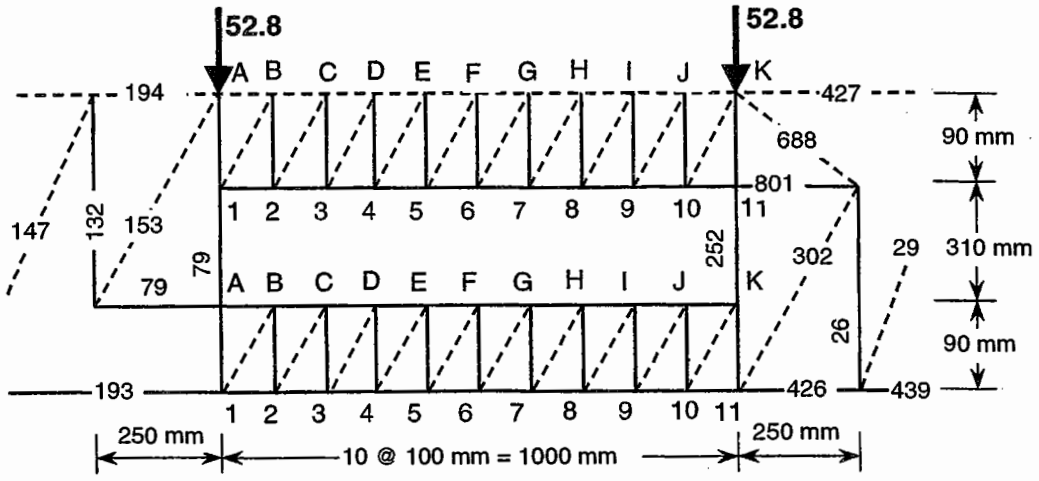

(d) Opening segment (Forces in kN)

Figure E3.6.1 Strut-and-tie model for beam with opening.

Table E3.6.1 Forces in the truss members for the top chord of the opening segment (kN).

Upper stringer		Lower stringer		Vertical members		Diagonal members	
Member	Force	Member	Force	Member	Force	Member	Force
A-B	273	1-2	80	A-1	79	B-1	107
B-C	353	2-3	160	B-2	79	C-2	107
C-D	433	3-4	240	C-3	79	D-3	107
D-E	513	4-5	320	D-4	79	E-4	107
E-F	593	5-6	400	E-5	79	F-5	107
F-G	673	6-7	481	F-6	79	G-6	107
G-H	753	7-8	561	G-7	79	H-7	107
H-I	833	8-9	641	H-8	79	I-8	107
I-J	913	9-10	721	I-9	79	J-9	107
J-K	993	10-11	801	J-10	79	K-10	107
				K-11	252		

Table E3.6.2 Forces in the truss members for the bottom chord of the opening segment (kN).

Upper stringer		Lower stringer		Vertical members		Diagonal members	
Member	Force	Member	Force	Member	Force	Member	Force
A-B	79	1-2	201	A-1	7	B-1	11
B-C	71	2-3	209	B-2	7	C-2	11
C-D	63	3-4	217	C-3	7	D-3	11
D-E	55	4-5	224	D-4	7	E-4	11
E-F	47	5-6	232	E-5	7	F-5	11
F-G	39	6-7	240	F-6	7	G-6	11
G-H	31	7-8	248	G-7	7	H-7	11
H-I	24	8-9	256	H-8	7	I-8	11
I-J	16	9-10	264	I-9	7	J-9	11
J-K	8	10-11	272	J-10	7	K-10	11
				K-11	259		

(c) Determine reinforcement area.

Longitudinal reinforcement

Top chord member: Maximum compressive force is 993.6 kN. Referring to the prismatic section on the right of the beam under the same moment and shear force, the concrete may be assumed to take 336.5 kN, with the remaining force of (933.6 – 336.5) = 597.1 kN to be resisted by compressive steel reinforcement. Thus, with f_y = 460 MPa, the required area of top steel required is

$$597.1 \times 10^3/460 = 1298 \text{ mm}^2$$

Therefore, provide 4T20 bars (1256 mm^2) at the top of the top chord member.

Maximum tensile force is 801.0 kN. Hence, the required area of bottom steel is

$$801.0 \times 10^3/460 = 1741 \text{ mm}^2$$

Therefore, provide 4T25 bars (1964 mm^2) at the bottom of the top chord member.

Bottom chord member: For the top reinforcement, the maximum tensile force is 78.6 kN. Therefore, the required area is

$$78.6 \times 10^3/460 = 171 \text{ mm}^2$$

Therefore, provide 2T12 bars (226 mm^2) at the top of the bottom chord.

For the bottom reinforcement, the maximum tensile force is 271.5 kN. Hence, the required area is

$$271.5 \times 10^3/460 = 590 \text{ mm}^2$$

Therefore, provide 2T20 bars (628 mm^2) at the bottom of the bottom chord.

Transverse reinforcement

Top chord member: Assuming f_y = 460 MPa, the area of shear reinforcement required is

$$A_v/s = (72.1 \times 10^3/460) \times 1000/100 = 1567 \text{ mm}^2/\text{m}$$

Therefore, provide T8 double-legged stirrups at 65 mm spacing (1554 mm^2/m).

Bottom chord member: Assuming f_y = 250 N/mm^2, the area of shear reinforcement required is

$$A_v/s = (7.1 \times 10^3/250) \times 1000/100 = 284 \text{ mm}^2/\text{m}$$

Therefore, provide M6 double-legged stirrups at 65 mm spacing (877 mm^2/m).

Sides of opening: Area of shear reinforcement required at the low-moment end of the opening is

$$79.2 \times 10^3/460 = 172 \text{ mm}^2$$

Therefore, provide two T8 double-legged, full-depth stirrups (202 mm^2) to the left of the opening. For the high-moment end, the required area is

$$259.4 \times 10^3/460 = 564 \text{ mm}^2$$

Therefore, provide four T10 double-legged, full-depth stirrups (628 mm^2) to the right side of the opening.

The reinforcement details near the opening are as shown in Fig. E3.6.2.

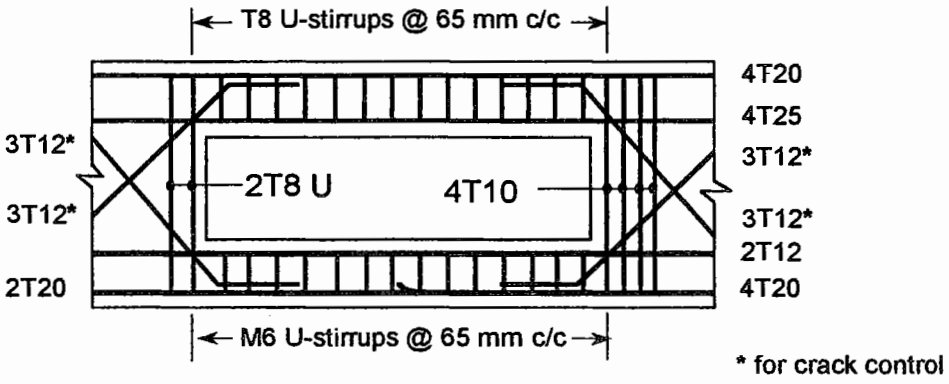

Figure E3.6.2 Required reinforcement according to strut-and-tie method.

3.5 CRACK CONTROL

Under load, wide cracks are observed near the end of the chord members at the corner of the opening in beams [see Fig. 3.5(b)]. Fig. 3.20 shows the measured maximum crack width with increasing applied load for a series of beams tested by Tan (1982) with reinforcement details given in Fig. 3.5 and Table 3.2. Two types of corner reinforcement were provided, one with vertical stirrups only and the other with a combination of vertical stirrups and diagonal bars.

The results of beams R1 to R3 in Fig. 3.20(a) show that for the same type of corner reinforcement (that is, vertical stirrups only), the maximum crack width at a particular load level is wider for beams with longer openings. With the addition of diagonal bars as in beam R4, however, the maximum crack width became smaller than that in R3 at all stages of loading, except near the ultimate load, despite beam R4 having a longer opening length. The smaller crack width in beam R4 was contributed partly by the diagonal bars and by the larger amount of corner reinforcement (see Table 3.2). A careful analysis of test data reveals that the provision of diagonal bars was mainly responsible for smaller crack widths in the beam designated as R4.

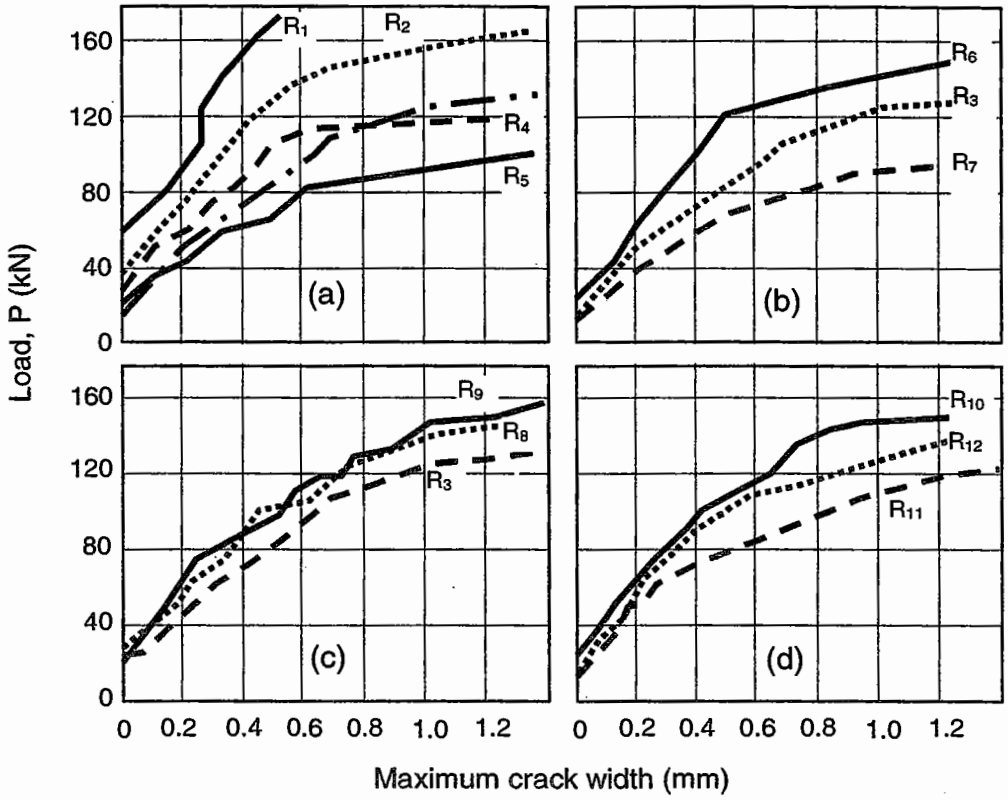

Figure 3.20 Load versus maximum crack width curves for beams tested by Tan (1982).

Fig. 3.20(b) shows that the maximum crack width increases as the opening depth is increased. In addition, it increases with an increase in the moment-shear ratio at the center of the opening (equivalent to position of opening along the beam length) for the same type of corner reinforcement, as indicated by the beams R10 and R12 in Fig. 3.20(d). However, poor crack control provided by vertical stirrups as corner reinforcement becomes evident from the result of beam R11. The variation in maximum crack widths with small opening eccentricities as in beams R8 and R9 is insignificant, as indicated by Fig. 3.20(c). Nevertheless, the advantages of using diagonal bars to control crack width are also clear from this figure.

Maximum crack width is one of the major serviceability requirements of concrete structures. According to the ACI Code (1995), the allowable maximum crack widths at service for the exterior and interior exposure conditions are 0.3 and 0.4 mm, respectively. Table 3.4 shows the maximum crack width at the service loads, taken as the design ultimate loads divided by a load factor of 1.7. The serviceability criterion of maximum crack width for interior exposure conditions is satisfied by all beams irrespective of the type of corner reinforcement, except for beams R3 and R11. However, this criterion is violated in most of the cases for exterior exposure conditions.

Table 3.4 Maximum crack width under service load.

Beam	Concrete cylinder strength f'_c (MPa)	Test ultimate load P_{ue} (kN)	Calculated service load * (kN)	Maximum crack width at service load (mm)	Corner reinforce-ment +
R1	30.4	223.9	120.0	0.26	□
R2	30.4	182.5	95.3	0.29	□
R3	33.5	144.1	77.6	0.43	□
R4	33.5	133.4	62.9	0.23	×
R5	29.8	104.1	52.4	0.23	×
R6	29.8	180.0	96.5	0.37	□
R7	35.1	102.9	54.1	0.33	□
R8	35.1	159.3	81.2	0.35	×
R9	34.8	174.0	84.6	0.39	×
R10	34.8	177.4	80.6	0.31	×
R11	28.8	133.5	77.1	0.45	□
R12	28.8	154.3	74.7	0.31	×

* Calculated service load = design ultimate load/1.7.
+ □ = full-depth vertical stirrups only; × = stirrups and diagonal bars.

Since the widest cracks always occurred at the corner of the opening due to the effect of stress concentration, the shear concentration factor, defined as the ratio of the design shear force to the factored shear at the opening, for each beam should be taken into account when considering the serviceability criterion of maximum crack width. Fig. 3.21 shows the maximum crack width at service load plotted against the shear concentration factor. The chain lines drawn through the critical test data denote the greatest value of maximum crack width that can be expected for a particular type of corner reinforcement, regardless of the opening size and its location. The maximum crack width decreases with an increase in the shear concentration factor. The chain lines also indicate that the shear concentration factor for the two types of corner reinforcement shall be at least 1.96 (for diagonal bars and vertical stirrups) and 2.48 (for vertical stirrups only) to satisfy the serviceability requirement of maximum crack width for exterior exposure conditions. Thus a shear concentration factor of 2, as recommended by Nasser et al. (1967) appears to be satisfactory regardless of the size and location of the opening only when a combination of diagonal bars and vertical stirrups is used as corner reinforcement.

Fig. 3.21 also shows that, for the same shear concentration factor, the maximum crack width is smaller for beams with diagonal reinforcement than for the beams with vertical stirrups only. Therefore, the maximum crack widths also depend on the proportion of the diagonal reinforcement used. Beams R8 and R9, with a shear concentration factor of about 1.5 and with 41% and 71%, respectively, of the shear resistance was provided by the diagonal bars (see Table 3.5), recorded the largest maximum crack width at service load (see Fig. 3.21). Hence, a shear concentration factor of 2 with 50 – 75% of the shear resistance contributed by diagonal bars may be considered as satisfactory in

controlling crack width. This will also relieve reinforcement congestion at the corners of the opening as compared to using diagonal bars or vertical stirrups alone.

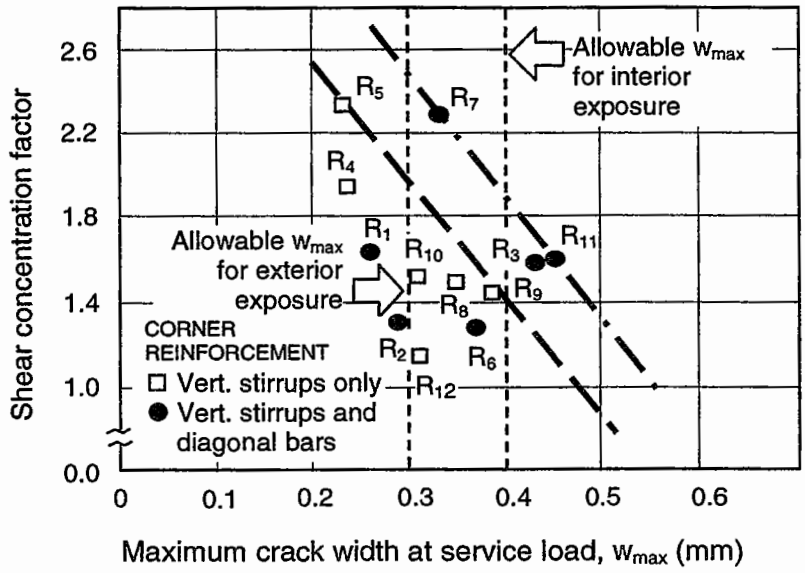

Figure 3.21 Effect of shear concentration factor on maximum crack width under service load.

Table 3.5 Shear concentration factor for beams tested by Tan (1982).

Beam	Shear resistance provided by		Total shear resistance		Design shear	Shear concentration factor
	Closed stirrups $V_{Rv} = A_v f_{yv}$ (kN)	Diagonal bars $V_{Rd} = A_d f_{vd} \sin\alpha$ (kN)	V_R (kN)	$\frac{V_{Rd}}{V_R}$	$P_{un} X/L$ (kN)	$\frac{V_R}{V}$
R1	111.5	-	111.5	-	68.0	1.64
R2	70.2	-	70.2	-	54.0	1.30
R3	70.2	-	70.2	-	44.0	1.60
R4	20.1	49.6	69.7	0.71	35.7	1.96
R5	20.1	49.6	69.7	0.71	29.8	2.34
R6	70.2	-	70.2	-	54.7	1.28
R7	70.2	-	70.2	-	30.7	2.30
R8	40.2	28.4	68.6	0.41	46.0	1.49
R9	20.1	49.6	69.7	0.71	48.0	1.45
R10	20.1	49.6	69.7	0.71	45.7	1.53
R11	70.2	-	70.2	-	43.7	1.60
R12	20.1	28.4	48.5	0.59	42.3	1.15

EXAMPLE PROBLEM 3.7

Design the corner reinforcement for the opening of the beam described in Example Problem 3.4 . Also, check whether the corner reinforcement provided according to the plasticity truss method (Example Problem 3.5) and the strut-and-tie method (Example Problem 3.6) satisfy the requirement for crack control.

SOLUTION

(a) Plastic hinge method (Fig. E3.4.2)

The factored shear at the opening is

$$V_u/\phi = 79.2/0.85 = 93.2 \text{ kN}$$

Seventy-five percent of this shear may be resisted by diagonal bars with a shear concentration factor of 2.

Assuming bars to be inclined at 45° and f_y = 460 MPa, the required area of diagonal bars is

$$A_d = (2 \times 0.75 \times 93.2 \times 10^3) / (460 \times \sin 45^\circ) = 430 \text{ mm}^2$$

Therefore, use two T16 and one T10 diagonal bars (481 mm^2) at each corner.

The remaining part of the shear should be resisted by stirrups with area

$$A_v = (2 \times 0.25 \times 93.2 \times 10^3) / 460 = 101 \text{ mm}^2$$

Therefore, use one T8 double-legged stirrup (101 mm^2) at each end.

(b) Plasticity truss method (Fig. E3.5.1)

The same requirement as for the plastic hinge method should be provided.

(c) Strut-and-tie method (Fig. E3.6.2)

The factored shear at the opening is V_u/ϕ = 93.2 kN and the design shear assuming a shear concentration factor of 2 is 2 × 93.2 or 186.4 kN. At the low-moment end, the shear resistance provided by two T8 double-legged stirrups is 92.9 kN or about 50% of the design shear. Therefore, provide additional diagonal bars at 45° to resist the remaining shear. The required area is

$$A_d = (186.4 - 92.9) \times 10^3 / (460 \times \sin 45^\circ) = 288 \text{ mm}^2$$

Therefore, use three T12 bars (339 mm^2) at each corner of the opening.

3.6 CALCULATION OF DEFLECTIONS

For beams with an opening, the maximum deflection usually occurs at the high-moment end of the opening, as observed in the beams tested by Tan (see Fig. 3.5 and Table 3.2). Fig. 3.22 shows that, in general, the slope of the load-deflection curve of the beam decreases with increasing load until it becomes horizontal at ultimate load.

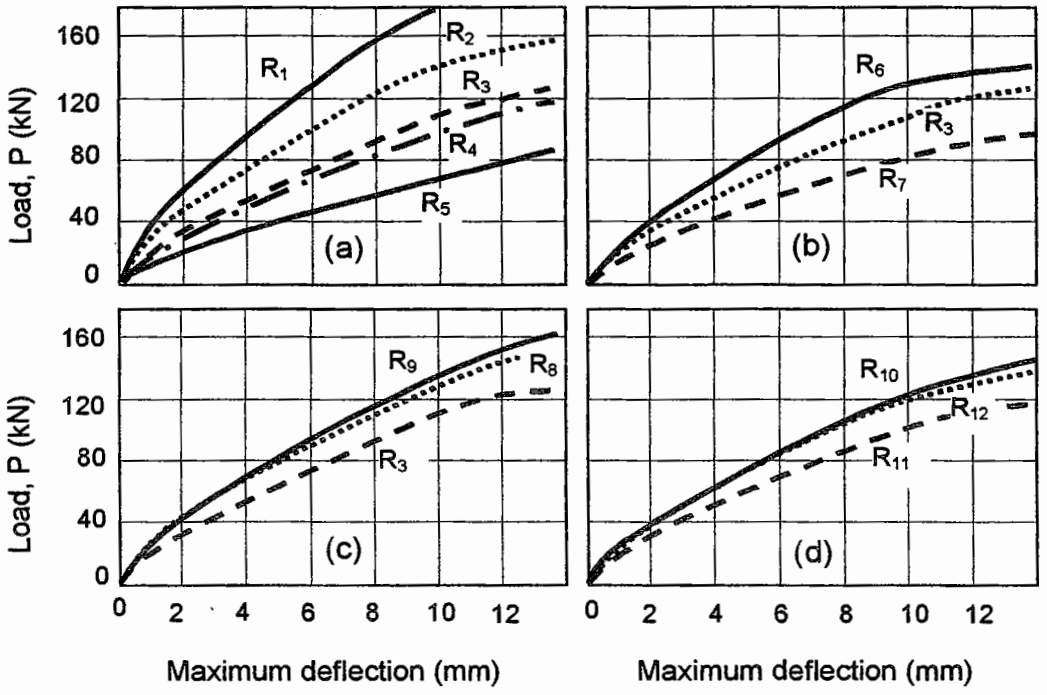

Figure 3.22 Load versus deflection curves for beams tested by Tan (1982).

At any particular load, the deflection is larger for beams with longer openings, as is evident from Fig. 3.22(a). Deflection also increases with increasing opening depth, as can be seen from Fig. 3.22(b). The results of beams R8 and R9 in Fig. 3.22(c) indicate that the effect of eccentricity on beam deflection is insignificant. Fig. 3.22(d) shows that for the same type of corner reinforcement (R10 and R12), deflection increases with an increasing moment-to-shear ratio at the center of the opening. The use of diagonal bars in beams R3 and R11 resulted in better deflection control, however. All beams were found to satisfy the serviceability requirement of maximum deflection of (span / 360) or 8.3 mm, according to the ACI Code (1995). Barney et al. (1977) made the same observation regarding service load deflections and concluded that the influence of openings on deflection is minor in properly detailed beams.

It is difficult to set limiting span-effective depth ratios for beams with openings which would satisfy the serviceability limit state of deflection. Therefore, deflections of beams with large openings should be calculated and checked against

allowable values. A simple method to estimate the midspan deflection of simply-supported beams with openings is as follows (Barney et al., 1977).

Consider the model of the beam with an opening as shown in Fig. 3.23, in which the chord members are idealized as struts framing into rigid abutments on each side of the opening. The length, ℓ_e, of the struts is conservatively taken as the distance between vertical stirrups on each side of the opening. To reflect the Vierendeel truss action observed in the tests (see Art. 3.2), hinges (points of contraflexure) are assumed at the mid-length of each strut. The moments of inertia for the top compressive and bottom tensile struts are denoted as I_t and I_b, respectively.

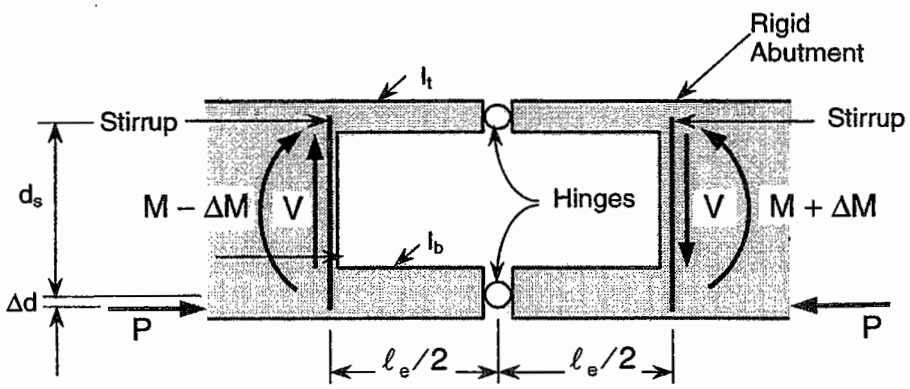

Figure 3.23 Idealized model for the estimation of deflection at opening (Barney et al., 1977).

Applying the moment-area principles, the relative displacement of the hinge with respect to one end of the opening under the action of shear force V is

$$\bar{\delta} = \frac{V\left(\frac{\ell_e}{2}\right)^3}{3E_c(I_t + I_b)} \tag{3.71}$$

where E_c is the modulus of elasticity of concrete. Under service load conditions, the value of I_t may be based on gross concrete section while the value of I_b can be conservatively based on a fully cracked section. Thus, the relative displacement of one end of the opening with respect to the other end is

$$\delta_v = 2\bar{\delta} = \frac{V\ell_e^3}{12E_c(I_t + I_b)} \tag{3.72}$$

The midspan deflection of the beam can be calculated as

$$\delta = \delta_w + (\delta_v)_{opening1} + (\delta_v)_{opening2} + \cdots\cdots \tag{3.73}$$

where δ_w is the midspan deflection in the absence of openings.

A more rigorous method to calculate deflections that entails an elastic analysis is also available. In the method, the beam is treated as a structural member with several segments constituting the portions with solid beam sections and those with sections traversed by the opening. An equivalent stiffness is adopted for the latter segments and the beam can be analyzed using methods such as the Direct Stiffness Method to obtain the maximum beam deflection under the assumed service load. Further treatment of the method is given in Chapter 5.

EXAMPLE PROBLEM 3.8

Calculate the midspan deflection of the beam described in Example Problem 3.4 under service load condition.

SOLUTION

The service load is

$$P_s = P_u / 1.7 = 52.8 / 1.7 = 31.1 \text{ kN}$$

and the corresponding shear force is

$$V = 1.5\, P_s = 46.6 \text{ kN}$$

The effective length of chord members for deflection calculation is taken as

$$\ell_e = (950 + 50) = 1000 \text{ mm}$$

Based on gross section properties, the moment of inertia of the chord members is each equal to $300 \times 180^3 / 12$ or 146×10^6 mm^4. For the estimation of deflection, conservatively assume

$$I_t = 146 \times 10^6 \text{ mm}^4; \quad I_b = 0.1 \times 146 \times 10^6 \text{ mm}^4 \approx 15 \times 10^6 \text{ mm}^4$$

Also, the modulus of elasticity of concrete is

$$E_c = 4730 \sqrt{f'_c} = 4730 \sqrt{30} = 26 \times 10^3 \text{ MPa}$$

Hence, from Eq. (3.72), the deflection due to shear force at the opening is

$$\delta_v = V\ell_e^{\,3} / [12\, E_c (I_t + I_b)] = 46.6 \times 10^{12} / [12 \times 26 \times (146 + 15) \times 10^9] = 0.94 \text{ mm}$$

For the load arrangement as shown in Fig. E3.4.1, the midspan deflection, δ_w, of the beam with a span L is $11PL^3/144E_cI$, where I can be conservatively estimated as the moment of inertia of the beam at a section through the opening. That is,

$$I = 2 \times [300 \times 180^3 / 12 + 300 \times 180 \times 210^2] = 5054 \times 10^6 \text{ mm}^4$$

As the span is 6 m, therefore,

$$\delta_w = 11 \times 31.1 \times 10^3 \times (6000)^3 / [144 \times 26 \times 5054 \times 10^9]$$
$$= 3.91 \text{ mm}$$

Hence, the total midspan deflection is calculated as

$$\delta = \delta_v + \delta_w = 0.93 + 3.91 = 4.84 \text{ mm} < L/360 = 16.7 \text{ mm}$$

3.7 MULTIPLE OPENINGS AND DESIGN OF POSTS

When multiple openings are placed close to each other in a beam, the element between two adjacent openings is known as a post. Proper design and detailing for the post should be provided. Tests carried out at the laboratory of Portland Cement Association (ACI-ASCE, 1973) have indicated that closely spaced multiple openings can be placed in a beam if each opening has adequate side reinforcement. Specimens with multiple circular and oval holes failed in the chord members when the width of the post was equal to or greater than 3/8 the depth of the web. Fig. 3.24 shows an inverted T-beam with multiple rectangular openings separated by adequately reinforced posts after it has been tested to failure.

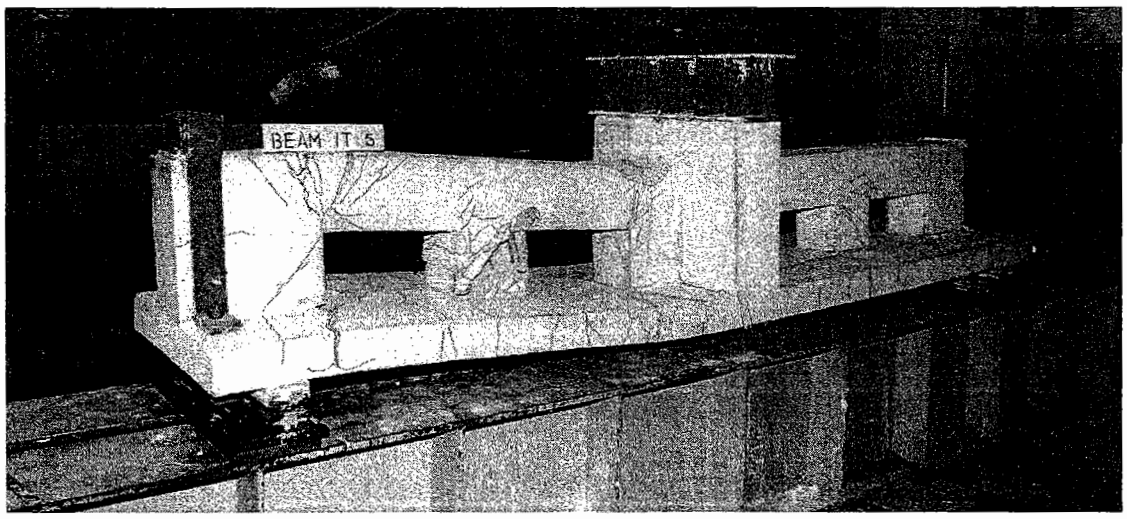

Figure 3.24 Failure of a beam with multiple rectangular openings separated by adequately reinforced post.

To ensure that the posts behave rigidly, Barney et al. (1977) recommended that adjacent openings should be separated by posts having overall width-to-height ratios of at least 2.0 where the width of the posts is the distance between adjacent stirrups. It was also suggested that the nominal design shear stress for the posts be limited to $0.17\sqrt{f'_c}$ (MPa).

When two openings are placed close to each other, it is evident from the free-body diagram shown in Fig. 3.25 that a horizontal shear, V_p, compression force, N_p, and bending moment, M_p, act on the post between the openings. Assuming that points of contraflexure occur at the mid-length of the chord members in each opening, equilibrium of forces gives

$$V_p = T_2 - T_1 \tag{3.74}$$

$$N_p = V_{b1} - V_{b2} \tag{3.75}$$

$$M_p = (T_2 - T_1)\left(d_o + \frac{d_b}{2}\right) - V_{b1}\left(\frac{\ell_{o1} + w_p}{2}\right) - V_{b2}\left(\frac{\ell_{o2} + w_p}{2}\right) \tag{3.76}$$

where w_p = width of post, taken as the distance between vertical stirrups in the post adjacent to the sides of the two openings; T = tensile force acting on the bottom chord member of opening; V_b = vertical shear force acting on the bottom chord member of opening; e = eccentricity of opening; d_b = depth of bottom chord member; ℓ_o = length of opening, taken as the distance between the vertical stirrups adjacent to the two sides of the opening; d_o = depth of opening; and subscripts 1 and 2 refer to the openings to the left and right of the post, respectively. Knowing the values of V_p, N_p, and M_p, the required reinforcement can be obtained by designing the post as a short, braced column.

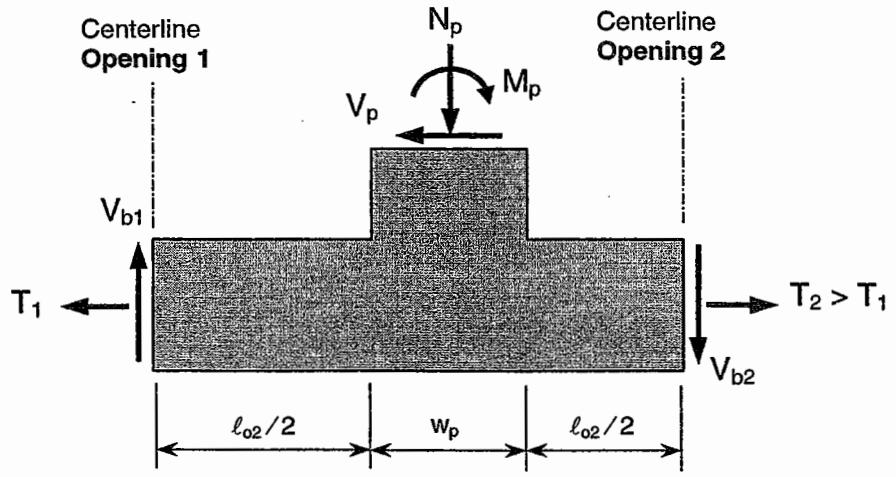

Figure 3.25 Forces acting on post between adjacent openings.

EXAMPLE PROBLEM 3.9

Determine the forces and moment acting on the post in the beam loaded as shown. The ultimate load is P_u = 52.8 kN and the concrete strength is f'_c = 35 MPa. Each opening measures 400 mm in length and 240 mm in depth, with the chord members having equal depth. Assume the bottom chord members to carry 40% of the total shear at each opening.

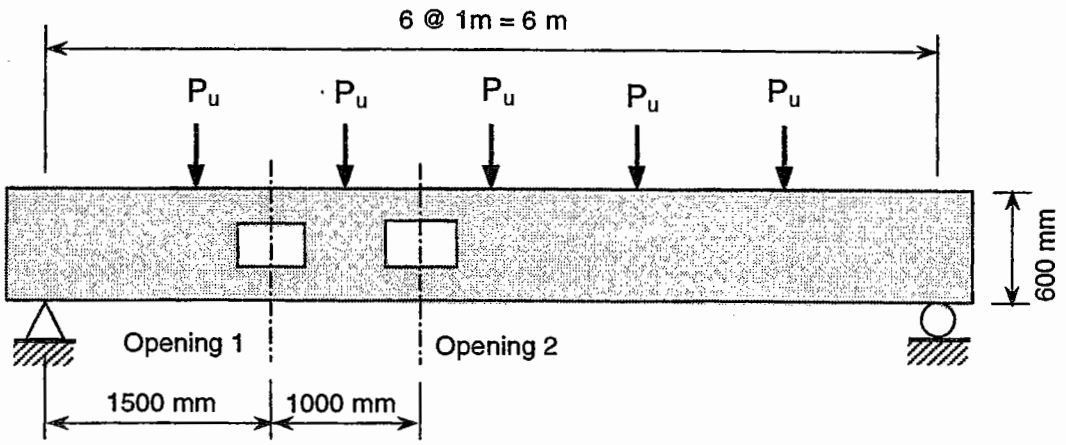

Figure E3.9.1 Design of post.

SOLUTION

The applied moments and shear forces due to P_u at centerlines of the openings 1 and 2 are first determined. From Fig. E3.9.1, these are

$$M_1 = ½ (132 + 211.2) = 171.6 \text{ kNm}$$

$$M_2 = ½ (211.2 + 237.6) = 224.4 \text{ kNm}$$

$$V_1 = 79.2 \text{ kN}$$

$$V_2 = 26.4 \text{ kN}$$

Assuming points of contraflexure at mid-lengths of chord members, the axial forces are

$$T_1 = M_1/[d_o + ½(d_t + d_b)] = 171.6 \times 10^3/420 = 409 \text{ kN}$$

$$T_2 = M_2/[d_o + ½(d_t + d_b)] = 224.4 \times 10^3/420 = 534 \text{ kN}$$

The shear forces acting on the bottom chord members are

$$V_{b1} = 0.4V_1 = 0.4 \times 79.2 = 31.7 \text{ kN}$$

$$V_{b2} = 0.4V_2 = 0.4 \times 26.4 = 10.6 \text{ kN}$$

Assuming a cover to the stirrups adjacent to opening to be 45 mm, then width of post, w_p, is $(600 - 2 \times 45) = 510$ mm $> 2d_o = 480$ mm. From Eqs. (3.74) to (3.76),

$$V_p = T_2 - T_1 = 534 - 409 = 125 \text{ kN}$$

$$N_p = V_{b1} - V_{b2} = 31.7 - 10.6 = 21.1 \text{ kN}$$

$$M_p = (T_2 - T_1)(d_o + d_b/2) - \tfrac{1}{2} V_{b1} (\ell_{o1} + w_p) - \tfrac{1}{2} V_{b2} (\ell_{o2} + w_p)$$

$$= [125 \times 330 - \tfrac{1}{2} \times 31.7 \times 1000 - \tfrac{1}{2} \times 10.6 \times 1000] \times 10^{-3}$$

$$= 20.1 \text{ kNm}$$

The shear stress on the post is $V_p / \phi\, b\, d_p$ or $125 \times 10^3 / (0.85 \times 300 \times 555) = 0.883$ MPa, which is less than $0.17\sqrt{35}$ or 1.01 MPa and, therefore, satisfactory. The post can be designed as a column to resist an axial load of 21.1 kN and bending moment of 20.1 kNm.

4

Torsion in Beams with Rectangular Openings

4.1 GENERAL INTRODUCTION

The effects of torsion in beams containing a small opening have been treated in detail in Chapter 2. It has been shown that torsional failure of such a beam is basically a bending failure, but unlike pure bending, where the compression zone forms parallel to the normal cross section, the presence of torsion causes the compression zone to become inclined or skewed. Based on skew-bending type of torsional failure, strength equations have been derived in Art. 2.4.2 for beams containing a small opening (circular or square) and are subject to a combined action of torsion, bending, and shear. A careful study of these equations reveals that, for a fixed depth, an increase in the length of opening has no effect on ultimate strength of the beam. This is in direct conflict with experimental observations. Tests conducted in pure torsion (Daniel and McMullen, 1977; Mansur et al., 1983a) and in combined torsion, bending, and shear (Mansur and Tan, 1989) have shown that an increase in opening length results in a substantial reduction in the strength of a concrete beam. Such a reduction in beam strength with increasing length of opening may be attributed to the change in the mechanism of failure from skew-bending type to the one that closely resembles the failure of a grid frame (Alwis and Mansur, 1987).

Figure 4.1 shows the typical failure of a beam that contains a large rectangular opening and is subject to a predominant torsional moment. It may be clearly seen in this figure that the opening corners suffered severe distress at failure. On the front face, crushing of the concrete in a diagonal direction may be noted at two diagonally opposite corners of the opening. Diagonal crushing of the concrete also occurred at the remaining two corners, but on the rear vertical face of the beam. It seems that the final failure of the beam was due to the formation of four hinges, one at each corner of the opening where most of the deformations were concentrated. Since the mode of failure is no longer of the skew-bending type, a different approach needs to be sought for the analysis and design of beams with large rectangular openings.

Figure 4.1 Typical mode of failure of a beam with large rectangular opening under predominant torsion.

While dealing with torsion in beams with small openings in Chapter 2, the most complex case of combined torsion, bending, and shear was considered first. The problem was then reduced to the case of combined torsion and bending by dropping the effect of shear and to the case of pure torsion by dropping the effects of bending moment and transverse shear. In discussing the effect of torsion in beams with large rectangular openings, the simplest case of pure torsion will be considered first. This will then be followed by treatment of the problems of increasing complexity, that is, combined torsion and bending, and combined torsion, bending, and shear.

4.2 PURE TORSION

The problem of pure torsion in beams containing a large rectangular opening was treated both analytically (1983b) and experimentally (1983a) by Mansur et al. Although the study has little significance from the viewpoint of structural design as beams with openings are rarely subject to predominant torsion in practice, the study provided some useful information that eventually led to the development of a simple design procedure for such beams under combined loading (Mansur, 1983). It therefore seems relevant to discuss the important experimental observations and the resulting analytical method proposed by Mansur et al. (1983b) for predicting the ultimate strength of a beam with large openings under pure torsion.

4.2.1 BEHAVIOR OF BEAMS IN PURE TORSION

When a beam contains a large rectangular opening, a suitable reinforcement scheme consists of additional longitudinal reinforcement close to the top and

bottom edges of the opening, full-depth stirrups next to the vertical edges, and closed links in both top and bottom chord members at the opening. Otherwise, in pure torsion, premature failure would occur at first cracking of the beam (McMullen and Daniel, 1975).

A series of reinforced concrete beams, detailed in the above manner, was tested in pure torsion by Mansur et al. (1983a). In this study, the amount and arrangement of reinforcement were kept constant for all the beams, but the length, depth, and eccentricity of openings were varied. Some major observations made in this study are highlighted below.

4.2.1.1 Cracking behavior and mode of failure

Figure 4.2 shows the cracking patterns of the beams tested in pure torsion. It may be seen that these patterns are remarkably similar for all the beams. Cracks, inclined at approximately 45° to the beam axis, first appeared at corners of the opening. The torque at which cracking occurs decreases with an increase in either the length or depth of opening. The eccentricity of opening, however, has no effects on cracking torque.

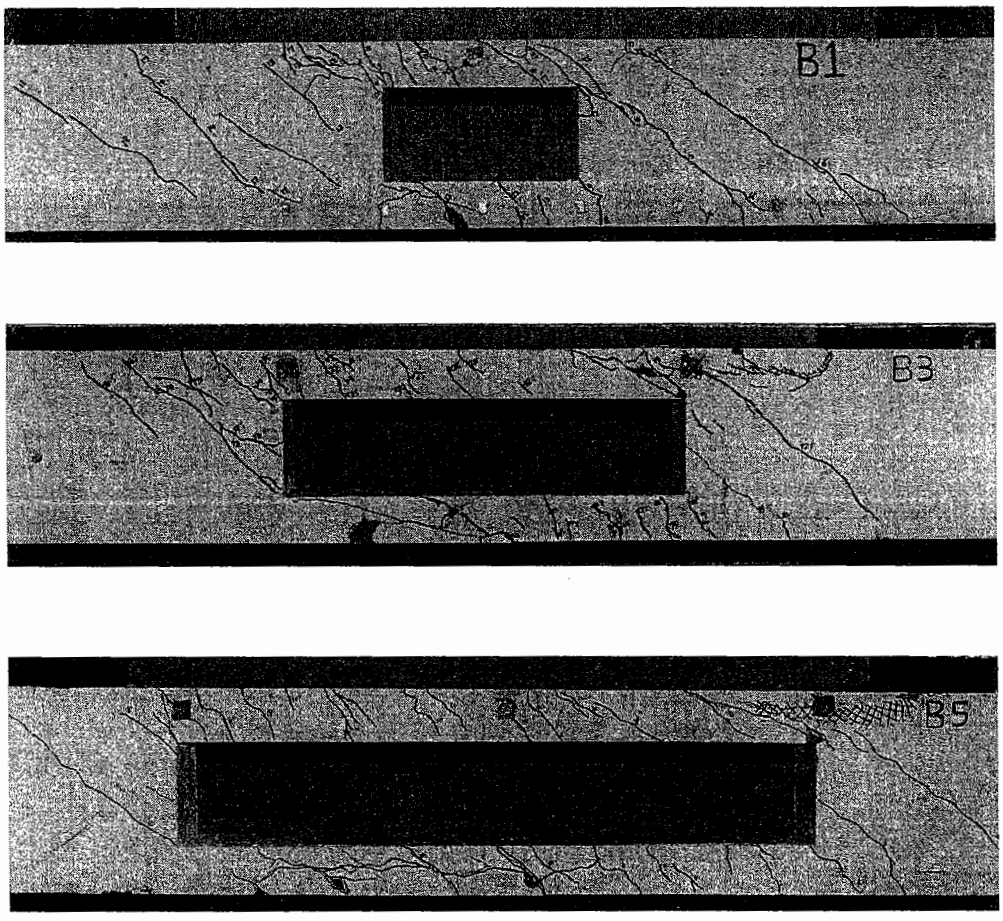

Figure 4.2 Typical cracking patterns of beams in pure torsion after failure (Mansur et al., 1983a).

As the applied torque was increased, the existing cracks at opening corners propagated diagonally towards the solid section of the beam, and more cracks appeared on the vertical and outer horizontal faces of the chord members. Few diagonal cracks also appeared in the solid section outside the opening zone. The cracks on the inside horizontal faces of the chord members occurred at later stages of loading. At failure, the chord members, particularly at the corners, were severely cracked.

A careful study of the beams after failure revealed that crushing of the concrete occurred at all four corners of the opening, two on each of the two vertical faces of the beam, except for the beam with the shortest opening in the series. This beam exhibited a skew-bending type of failure with crushing of the concrete on the bottom face of the beam (not visible in Fig. 4.2). In beams with relatively longer openings, the crushing zones included a part of the solid section and, like a typical solid beam in pure torsion, they were joined by tension cracks, which spiraled around the remaining three beam faces. Thus, it appears that the two ends of each chord member behave like an isolated beam section where skew-bending failure takes place with associated localized deformations similar to a plastic hinge. The development of these four hinges in the chord members leads to the formation of a mechanism, and the beam fails.

4.2.1.2 Contraflexure points

When a beam containing an opening is subject to pure torque at its solid ends, the beam twists and, as a result, lateral bending takes place in each member above and below the opening. Fig. 4.3 shows the lateral deflection measured in the bottom chords for two beams at three different loading stages (Mansur et al., 1983a). This figure clearly shows that the chord members bend in double curvature with contraflexure point occurring essentially at midspan.

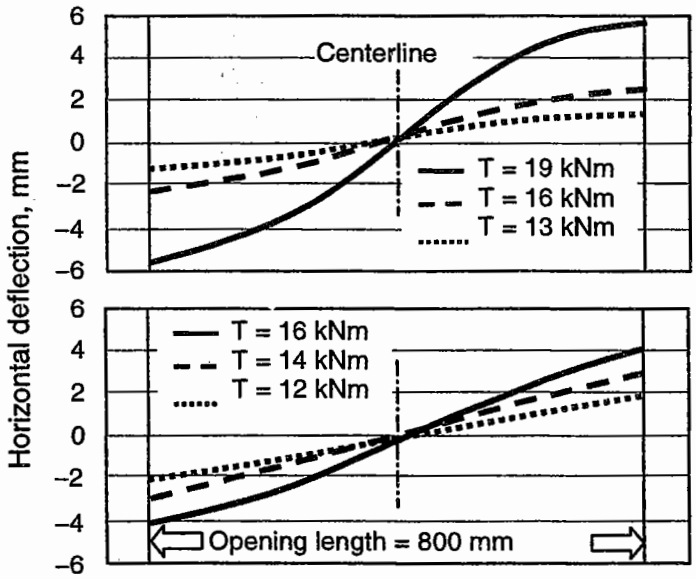

Figure 4.3 Deflected shape of the bottom chord in lateral bending due to torsion applied at solid ends at different loading stages (Mansur et al., 1983a).

The above observation, together with the identification of the mode of failure by the formation of four hinges, one at each corner of the opening, has led to the development of an analytical procedure (Mansur et al., 1983b) to predict the torsional strength of a beam containing a large rectangular opening.

4.2.2 OUTLINE OF ANALYSIS

A reinforced concrete beam with a transverse opening is shown in Fig. 4.4. The beam is subject to pure torsion at its solid ends. The analysis for ultimate torsional strength of such a beam is based on the following assumptions:

1. The opening is rectangular in shape. The members above and below the opening are prismatic, that is, the members have uniform cross section and reinforcement throughout the length.
2. When subject to pure torque, the beam twists and, as a result, the members above and below the opening bend in double curvature. Consistent with experimental observation (Mansur et al., 1983a), the points of contraflexure are assumed to be at midspan of these members. Moments and forces acting in the chord members (chords) can then be calculated from equilibrium requirements, as shown in Fig. 4.5.

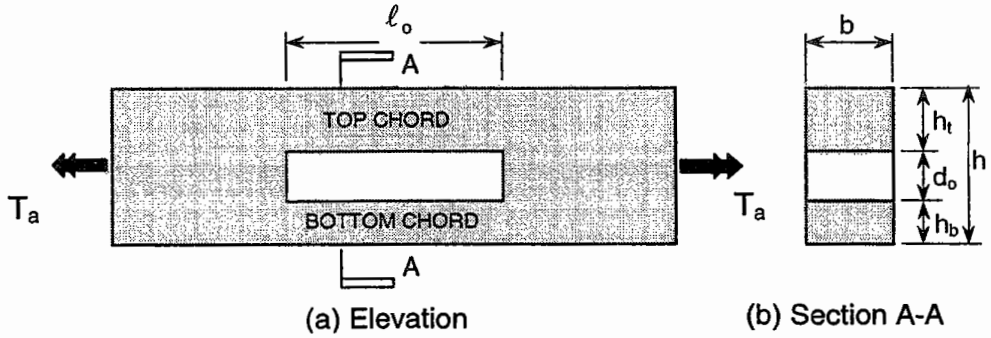

Figure 4.4 Beam with a rectangular opening subject to pure torsion.

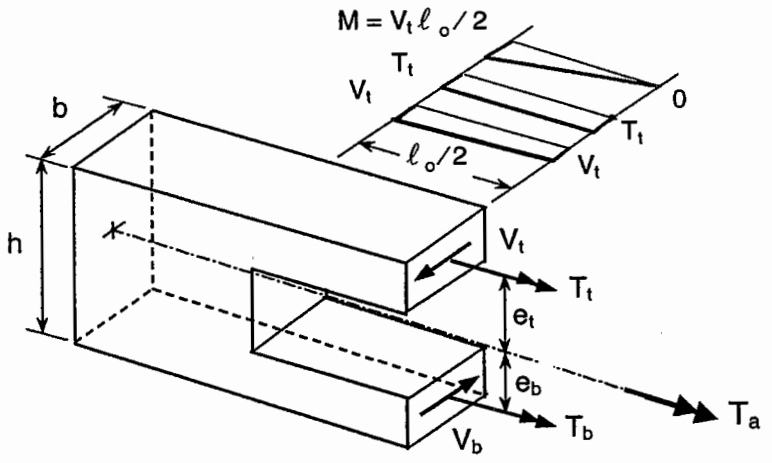

Figure 4.5 Free-body diagram at beam opening.

3. Different sections of the chord members have sufficient ductility in torsion, bending, and shear. This can be ensured by using under-reinforced sections so that steel reaches the yield strain before crushing of the concrete.
4. Failure occurs by the formation of a mechanism with four hinges, two in each member above and below the opening, as shown in Fig. 4.6. This type of failure has been substantiated by experiments (Mansur et al., 1983a).

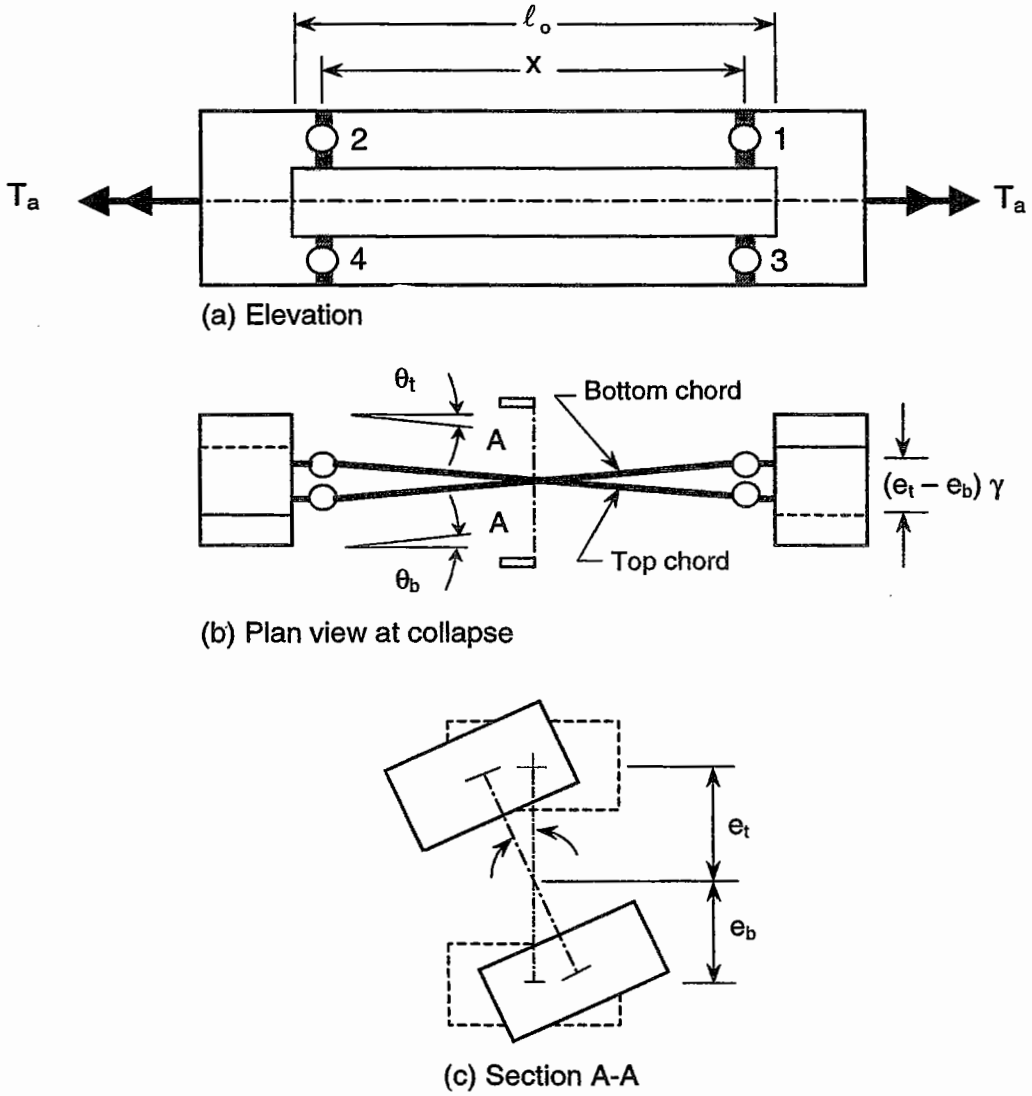

Figure 4.6 Assumed failure mechanism.

The method is based on "*collapse load*" analysis. According to this method, collapse of a structure will occur if it is possible to find a distribution of internal actions such that the conditions of equilibrium, yield, and a mechanism are satisfied simultaneously. If only the equilibrium and yield conditions are satisfied throughout

the structure, then the solution is either the exact or a lower bound to the collapse load. The upper bound solution is found if, for an assumed mechanism, the internal energy absorbed at the plastic hinges are equated to the energy input by the loads, or, in other words, the equilibrium conditions are satisfied. Both approaches are used to obtain a bound solution.

Yield condition

For the purpose of analysis, an interaction surface (to be used as yield surface) is required for reinforced concrete sections in combined torsion, bending, and shear. The yield conditions adopted by Mansur et al. (1983b) are the interaction equations developed by Thurlimann (1979) that are diagramatically shown in Fig. 4.7.

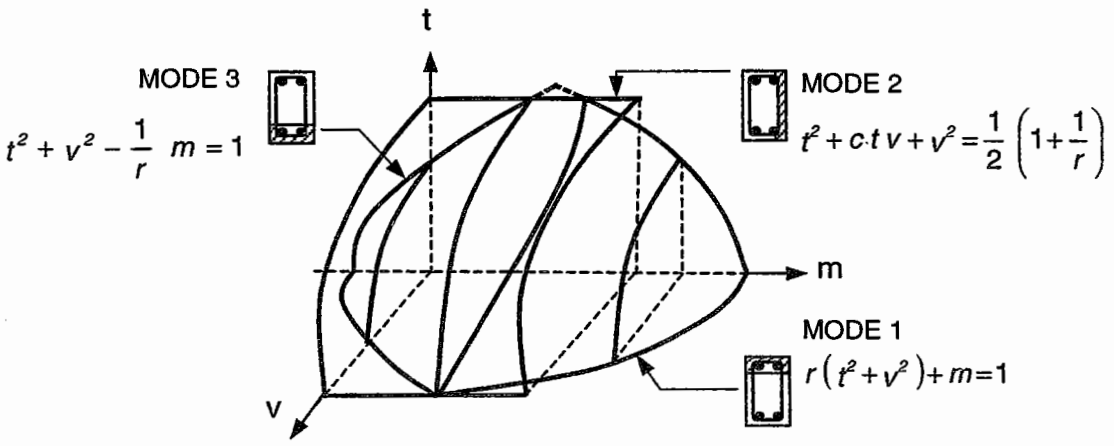

Figure 4.7 Yield surfaces for different modes of sectional failure.

Three equations are required to describe the behavior at yield of a reinforced concrete section under combined loading. These equations may be expressed in non-dimensional form as

$$r\left(t^2+v^2\right)+m=1 \qquad \text{(Mode 1)} \qquad (4.1)$$

$$t^2+ctv+v^2=\frac{1}{2}\left(1+\frac{1}{r}\right) \qquad \text{(Mode 2)} \qquad (4.2)$$

$$t^2+v^2-\frac{1}{r}m=1 \qquad \text{(Mode 3)} \qquad (4.3)$$

in which $r = F_{yu} / F_{y\ell}$; $t = T/T_o$; $m = M/M_o$; $v = V/V_o$; and $c = 2\sqrt{2d_v / u}$ where u = length of perimeter connecting the corner longitudinal bars in a cross section; d_v = distance between the longitudinal tension and compression bars; $F_{y\ell}$, F_{yu} = yield forces of longitudinal tension and compression bars, respectively; T = torsional moment; M = bending moment; V = shear force; and

$$T_o = 2A_o\sqrt{\frac{4F_{yu}S_y}{us}} \tag{4.4}$$

$$M_o = 2F_{yt}d_v \tag{4.5}$$

$$V_o = 2\sqrt{\frac{2F_{yu}S_y d_v}{s}} \tag{4.6}$$

are the plastic capacities of a section in pure torsion, bending, and shear, respectively, in which A_o = area enclosed by u, S_y = yield force of a stirrup, and s = spacing of stirrups.

Eqs. (4.1) and (4.3) correspond to the formation of a compression zone at the top and bottom faces of the beam, respectively. Eq. (4.2) corresponds to the case where the compression zone forms on one of the vertical faces of the beam. These three modes of hinge formation at a section under combined loading are denoted as Mode 1, Mode 3, and Mode 2, respectively. The yield surfaces represented by Eqs. (4.1) - (4.3) are shown in Fig. 4.7.

Plastic flow rule

In plastic analysis, if a kinematically admissible velocity field can be found for a continuum, then the plastic flow that occurs will be governed by the plastic flow rule. The rule states that the plastic strain increment vector at a hinge is normal to the yield surface at the particular stress point (Prager, 1959) and may be expressed in general form as:

$$\dot{q}_i = \lambda\frac{\partial f}{\partial Q_i}, \quad i = 1, 2, \ldots\ldots n \tag{4.7}$$

in which λ = a positive scalar; Q_i = the ith generalized load; $\dot{q}_i$ = the velocity of the ith displacement ; and f = the plastic potential or the yield function as defined by

$$f(Q_1, \ldots\ldots Q_n) = 1 \tag{4.8}$$

In this analysis, the plastic potential is represented by Eqs. (4.1) - (4.3).

4.2.3 ANALYSIS FOR ULTIMATE TORQUE

4.2.3.1 Upper Bound Solution

The upper bound to the collapse load is obtained if, for an assumed mechanism (collapse mode), the work done by the external forces on the beam is equal to the work dissipated at the plastic hinges. In the present case, the external load is the torque applied at the solid ends of the beam.

It is assumed that collapse occurs by the formation of four plastic hinges, two in each chord member at a distance x apart, as shown in Fig. 4.6(a). From

geometry of the deformed shape of the beam, as shown in Figs. 4.6 (b) and (c), the following relationships can be derived:

$$\theta_t = \frac{2e_t}{x}\gamma_t \tag{4.9}$$

$$\theta_b = \frac{2e_b}{x}\gamma_b \tag{4.10}$$

$$\delta = 0 \tag{4.11}$$

in which θ = rotational displacement due to bending moment; γ = rotational displacement due to torsional moment; δ = shear displacement; e = distance of the centroid of a chord member from longitudinal axis of the beam; and the subscripts b and t refer to the bottom and top chord members, respectively.

These geometric relationships can be expressed as velocity fields which satisfy compatibility and therefore are kinematically admissible. The velocity field simply relates the various displacements in terms of velocities represented by a dot, that is,

$$\dot{\theta}_t = \frac{2\,e_t}{x}\dot{\gamma}_t \tag{4.12}$$

$$\dot{\theta}_b = \frac{2\,e_b}{x}\dot{\gamma}_b \tag{4.13}$$

$$\dot{\delta}_b = \dot{\delta}_t = 0 \tag{4.14}$$

The plastic flow rule [Eq. (4.7)] must be applied to the hinges in both chord members. The flow rule corresponding to the hinge mode, Mode 1 [Eq. (4.1)] can be written for the top and bottom chords , respectively, as

$$\dot{\gamma}_t = \frac{\lambda_t}{T_{ot}}\,2r\,t_t;\quad \dot{\theta}_t = \frac{\lambda_t}{M_{ot}};\quad \dot{\delta}_t = \frac{\lambda_t}{V_{ot}}2r\,v_t \tag{4.15}$$

and

$$\dot{\gamma}_b = \frac{\lambda_b}{T_{ob}}2r\,t_b;\quad \dot{\theta}_b = \frac{\lambda_b}{M_{ob}};\quad \dot{\delta}_b = \frac{\lambda_b}{V_{ob}}2r\,v_b \tag{4.16}$$

Using Eqs. (4.12) - (4.16) and Eq. (4.1) for each of the chord members, the following expressions can be derived:

$$t_t = \frac{T_{ot}}{4\,r_t\,M_{ot}}\frac{x}{e_t} \tag{4.17}$$

$$m_t = 1 - r_t\,t_t^2 \tag{4.18}$$

$$t_b = \frac{T_{ob}}{4 r_b M_{ob}} \frac{x}{e_b} \tag{4.19}$$

$$m_b = 1 - r_b t_b^2 \tag{4.20}$$

$$v = v_t = v_b = 0 \tag{4.21}$$

The torsional strength is found by using the virtual work equation as given by

$$T_a \gamma = (T_t + T_b)\gamma + M_t \theta_t + M_b \theta_b \tag{4.22}$$

in which T_a = applied torque. Eqs. (4.9), (4.10), (4.17) - (4.20), and (4.22) give the following expression for the applied torque, t_a:

$$t_a = \left(\frac{T_{ot}}{8 r_t M_{ot}} \frac{x}{e_t} + 2 \frac{M_{ot}}{T_{ot}} \frac{e_t}{x} \right) + \frac{T_{ob}}{T_{ot}} \left(\frac{T_{ob}}{8 r_b M_{ob}} \frac{x}{e_b} + 2 \frac{M_{ob}}{T_{ob}} \frac{e_b}{x} \right) \tag{4.23}$$

in which $t_a = T_a / T_{ot}$.

The lowest value of the upper bound solution for the applied torque, t_a, is desired. Differentiating t_a in Eq. (4.23) with respect to x, and equating the resulting expression to zero, we get

$$x = \ell_c = \sqrt{\frac{16 \, (M_{ot} \, e_t + M_{ot} \, e_b)}{\dfrac{T_{ot}^2}{e_t \, r_t \, M_{ot}} + \dfrac{T_{ob}^2}{e_b \, r_b \, M_{ob}}}} \tag{4.24}$$

in which ℓ_c is defined as the critical opening length.

For small openings, the opening length, ℓ_o, may be less than ℓ_c. It implies that the two hinges will merge into a single one. This is, however, not possible because the mechanism considered assumes that the hinges form in the chord members. Therefore, in such cases, x is taken as equal to ℓ_o, that is,

$$x = \ell_o \qquad \text{if} \qquad \ell_o < \ell_c \tag{4.25}$$

Substitution of the value of x from Eq. (4.24) with the constraint represented by Eq. (4.25) into Eq. (4.23) gives the best upper bound solution for the nominal torsional strength of a beam.

Beams with identical chord members

The preceding solution is based on the plastic potential function corresponding to Mode 1 hinge formation. It can be readily shown that the plastic potential functions based on Modes 2 and 3 result in incompatible loads and displacement vectors. Either λ becomes negative or the load becomes negative. Therefore, these functions are not considered in this analysis.

In the particular case of beams having identical members above and below the opening, the above analysis may be greatly simplified. For beams with such chord members, subscript b = subscript t. Therefore, by dropping the subscripts b and t, the expression for nominal torsional strength, t_n [Eq. (4.23)], reduces to

$$t_n = \frac{T_o}{4rM_o}\frac{x}{e} + \frac{4M_o}{T_o}\frac{e}{x} \tag{4.26}$$

Similarly, Eqs. (4.24) and (4.25) simplify into

$$x = \ell_{ci} = 4e\sqrt{r}\,\frac{M_o}{T_o} \le \ell_o \tag{4.27}$$

in which ℓ_{ci} = critical length of opening when the chord members are identical.

When $\ell_o \ge \ell_{ci}$, Eqs. (4.26) and (4.27) yield

$$t_n = \frac{2}{\sqrt{r}} \tag{4.28}$$

When $\ell_o < \ell_{ci}$, $x = \ell_o$ [Eq. (4.25)]. Therefore, Eq. (4.26) reduces to

$$t_n = \frac{T_o}{4rM_o}\frac{\ell_o}{e} + \frac{4M_o}{T_o}\frac{e}{\ell_o} \tag{4.29}$$

Thus, for beams with identical chord members, Eq. (4.28) shows that the nominal torsional strength remains a constant for $\ell_o \ge \ell_{ci}$. When the chord members have symmetrical longitudinal reinforcement as well, $r = 1$, and Eq. (4.28) then reduces to

$$t_n = 2 \tag{4.30}$$

which implies that $T_n = 2T_o$. Therefore, the torsional capacity of a beam is equal to the sum of pure torsional strengths of the chord members.

4.2.3.2 Lower Bound Solution

In accordance with the lower bound theorem of limit analysis, if for a given load a distribution of moment, torque, and a shear force can be determined that is in equilibrium with the load and which nowhere violates the yield condition, then this load is equal to or less than the true collapse load. The following analysis is based on this approach.

When a beam with a transverse opening is subject to pure torque, the applied torque is resisted by torsion in the chord members and by the couple formed by the transverse shear forces in the members above and below the opening. Due to symmetry, only one-half of the total length of opening needs to be

considered. Forces acting on the beam are shown in Fig. 4.5. It can be seen that the critical sections are at the edges of the opening; therefore, collapse of the beam is likely to occur by the formation of plastic hinges at these sections. The collapse mode assumed in the analysis thus consists of four hinges as shown in Fig. 4.6(a), with $x = \ell_o$.

By considering moments and forces as positive when acting in the directions shown in Fig. 4.5, the overall equilibrium equations for the beam can be written in the following form:

$$T_a = T_t + T_b + V_t e_t + V_b e_b \tag{4.31}$$

$$V_b = V_t \tag{4.32}$$

Introducing $t_b = T_b / T_{ot}$, $t_t = T_t / T_{ot}$, $v_t = V_t / V_{ot}$, $v_b = V_b / V_{ot}$, $\tau = T_{ob} / T_{ot}$, $\omega = V_{ob} / V_{ot}$, $\alpha_t = e_t V_{ot} / T_{ot}$, and $\alpha_b = e_b V_{ob} / T_{ot}$, the above equations may be expressed in non-dimensional form as:

$$t_a = t_t + \tau t_b + \alpha_t v_t + \alpha_b v_b \tag{4.33}$$

$$v_t = \omega v_b \tag{4.34}$$

The internal forces and moments at hinges 1 and 3 (Fig. 4.6) can be expressed in terms of those at the points of contraflexure from equilibrium as

$$t_1 = t_t; \quad m_1 = \beta v_t; \quad v_1 = v_t \tag{4.35}$$

ands

$$t_3 = t_b; \quad m_3 = \frac{\beta \omega v_b}{\mu}; \quad v_3 = v_b \tag{4.36}$$

respectively, in which $\mu = M_{ob} / M_{ot}$; $\beta = (0.5\ V_{ot} \ell_o) / M_{ot}$; and the subscripts 1 and 3 refer to the hinges at 1 and 3, respectively.

The yield conditions, that is, Eqs.(4.1) - (4.3), should be applied to the hinges at 1 and 3. As the cross-sectional dimensions of chord members are different, two sets of yield conditions are required, one for each hinge. Using Eqs. (4.35) and (4.36), the yield conditions for hinge 1 in the top chord are

$$r_t\left(t_t^2 + v_t^2\right) + \beta v_t = 1 \qquad \text{(Mode 1)} \tag{4.37}$$

$$t_t^2 + c_t t_t v_t + v_t^2 = \frac{1}{2}\left(1 + \frac{1}{r_t}\right) \qquad \text{(Mode 2)} \tag{4.38}$$

$$t_t^2 + v_t^2 - \beta \frac{v_t}{r_t} = 1 \qquad \text{(Mode 3)} \tag{4.39}$$

and those for hinge 3 in the bottom chord are

$$r_b\left(t_b^2+v_b^2\right)+\frac{\beta\omega v_b}{\mu}=1 \qquad \text{(Mode 1)} \qquad (4.40)$$

$$t_b^2+c_b t_b v_b+v_b^2=\frac{1}{2}\left(1+\frac{1}{r_b}\right) \qquad \text{(Mode 2)} \qquad (4.41)$$

$$t_b^2+v_b^2-\frac{\beta\omega v_b}{\mu r_b}=1 \qquad \text{(Mode 3)} \qquad (4.42)$$

Thus, there are four independent equations: two equilibrium equations [Eqs. (4.33) and (4.34)] and two yield conditions, one for hinge 1 [one of the Eqs. (4.37) - (4.39)] and one for hinge 3 [one of the Eqs. (4.40) - (4.42)] to solve for five unknowns, t_a, t_t, t_b, v_t, and v_b. Another equation is required to obtain the solution. This equation is provided by the lower bound theorem of limit analysis in which the applied torque is maximized with respect to an independent variable. In this analysis, t_t is chosen as the required variable.

The hinges in the top and bottom chord members may form in any one of the three possible modes. Thus, t_a must be maximized for the following combinations of hinge modes in the top and bottom chord members: 1-1, 1-2, 1-3, 2-1, 2-2, 2-3, 3-1, 3-2, 3-3. For example, Eqs. (4.33) and (4.34) can be combined with Eqs. (4.37) and (4.41) to form an expression for t_a in terms of t_t. The maximum value of t_a is then found from this expression in the usual manner. This maximum value of t_a corresponds to hinge Modes 1 and 3 in the top and bottom chords, respectively. There are, thus, nine possible expressions of t_a for the nine different combinations of the mode of hinge formation. Each of these expressions is maximized for t_a with respect to t_t. That combination which gives the lowest value of the maximized applied torque, t_a, will be the required solution, provided that none of the yield conditions are violated along the length of the beam. It should be remembered that the bending and torsional moments and the shear forces in the chords must always be positive.

Beams with identical chord members

If the chord members are identical, the preceding solution can be greatly simplified similar to the upper bound analysis. Because of symmetry about two axes, it is necessary to consider only one-quarter of the beam, that is, only one hinge. Thus, $\tau = \mu = \omega = 1$. Dropping the subscripts t and b, the equilibrium equations, Eqs. (4.31) and (4.32), reduce to

$$t_a = 2t + \alpha v \qquad (4.43)$$

and

$$m = \beta v \qquad (4.44)$$

respectively, in which $\alpha = \alpha_t + \alpha_b/\omega$, the yield conditions being represented by Eqs. (4.1) - (4.3). Thus, there are three independent equations, two equilibrium equations and one yield condition, to solve for four unknowns, t_a, t, m, and v.

Substituting the values of v and m from Eqs. (4.33) and (4.44) into Eq. (4.1), we obtain

$$t_a = 2t - \frac{\alpha\beta}{2r} + \frac{\alpha}{r}\sqrt{\beta^2 + 4r - 4r^2t^2} \tag{4.45}$$

The applied torque, t_a, is maximum when $dt_a/dt = 0$, and d^2t_a/dt^2 is negative and non-zero. Applying these conditions, t_a is maximum when

$$t = \frac{1}{r}\sqrt{\frac{\beta^2 + 4r}{\alpha^2 + 4}} \tag{4.46}$$

The values of t, m, and v must always be positive. This is ensured when

$$t < \frac{1}{\sqrt{r}} \tag{4.47}$$

Eq. (4.47) is obtained by substituting $m \geq 0$ and $v \geq 0$ into Eq. (4.1).

Solution for Hinge Mode 1

Substituting the value of t from Eq. (4.46) into Eq. (4.45), we obtain the following expression for the nominal torsional strength of a beam with a rectangular opening for Mode 1 hinge formation:

$$t_n = \frac{-\alpha\beta}{2r} + \frac{1}{2}r\sqrt{(\beta^2 + 4r)(\alpha^2 + 4)} \tag{4.48}$$

Putting the values of α and β into Eq. (4.46), it can be readily shown that for $\ell_o < \ell_c$, in which ℓ_c is given by Eq. (4.24), Eq. (4.47) is always satisfied. For $\ell_o \geq \ell_c$, $t = 1/\sqrt{r}$, and Eq. (4.45) reduces to

$$t_n = \frac{2}{\sqrt{r}} \tag{4.49}$$

It can be seen that Eq. (4.49) takes the same form as Eq. (4.28), which is derived from the upper bound approach. Thus, Eq. (4.28) or Eq. (4.49) gives the unique solution when $\ell_o > \ell_c$ and the hinges form in Mode 1.

Solution for Hinge Mode 3

The solution corresponding to hinge Mode 3 can be obtained in a similar manner. Using Eqs. (4.2), (4.43), and (4.44) we get

$$t_a = 2t + \frac{\alpha\beta}{2r} + \frac{\alpha}{2r}\sqrt{\beta^2 + 4r^2 - 4r^2t^2} \tag{4.50}$$

and t_a is maximum when

$$t = \frac{1}{r}\sqrt{\frac{\beta^2 - 4r^2}{\alpha^2 + 4}} \tag{4.51}$$

Since t, m, and v must be positive, it can be shown from Eq. (4.2) that $t < 1$. Thus, from Eqs. (4.50) and (4.51), we get

$$t_n = \frac{\alpha\beta}{2r} + \frac{1}{2r}\sqrt{(\beta^2 + 4r^2)(\alpha^2 + 4)} \le 2 + \frac{\alpha\beta}{r} \tag{4.52}$$

Solution for Hinge Mode 2

Similarly, the ultimate torsional strength corresponding to Mode 2 hinge formation can be obtained as

$$t_n = \sqrt{\frac{\frac{1}{2}\left(1 + \frac{1}{r}\right)\left(\alpha^2 - 2c\alpha + 4\right)}{1 - \frac{1}{4}c^2}} \le \sqrt{2\left(1 + \frac{1}{r}\right)} \tag{4.53}$$

The minimum value of t_n as given by Eqs. (4.48) [or Eq. (4.49)], (4.52), and (4.53) will be the required solution, provided that all the yield conditions are satisfied along the length of both chord members.

The value of T_n as found from the foregoing upper and lower bound analyses must not be greater than the strength of the solid section of the beam, T_{os}, otherwise failure will occur at the solid ends. In calculating T_{os}, all three possible modes of hinge formation must be checked for the solid section. The smallest value will obviously govern. Thus, if $T_n > T_{os}$, then the ultimate torque of the beam will be T_{os}.

4.2.3.3 Torsion Carried by Chord Members

The equilibrium equation, Eq. (4.31), shows that the applied torque is resisted partly by torsion in each chord and partly by the couple formed by the resultants of lateral shear stresses in the chords. It has been shown in the analysis that for opening length greater than or equal to a critical length, ℓ_c, as defined by Eq. (4.24), the entire applied torque is resisted by torsion in the chord members alone. Therefore, in light of the above theory, it may be of interest to evaluate what proportion of the applied torque is resisted by the couple formed by the lateral shear in the chords as the length of opening is decreased. This has particular relevance to the design of beams with small openings under predominant torsional moment. For this purpose, the details of the beams with 200 mm-deep, symmetrically (with respect to the depth) placed opening, as tested by Mansur et al. (1983a) have been selected. The details of these beams are presented in Fig. 4.8.

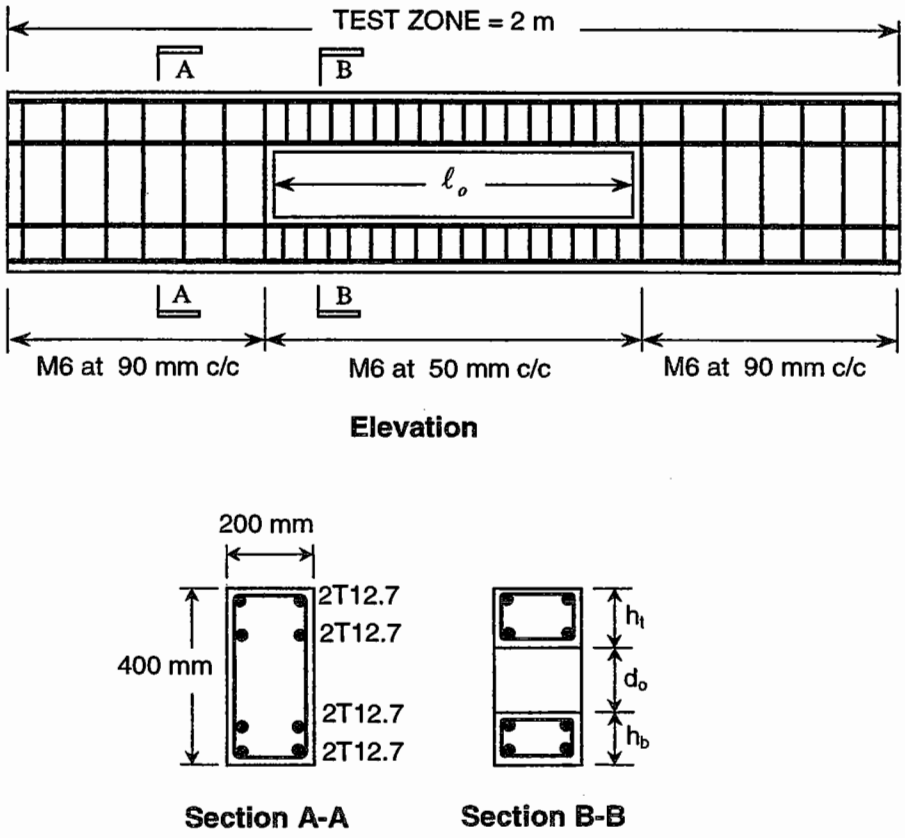

Figure 4.8 Details of beams tested by Mansur et al. (1983a).

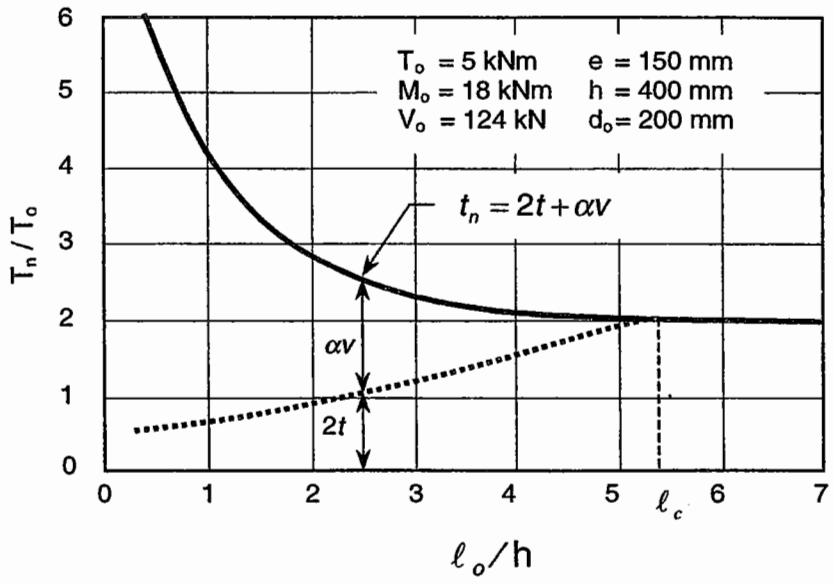

Figure 4.9 Resistance to applied torque provided by torsion and shear in the chord members.

The proportion of the applied torque resisted by torsion in the chord members is plotted against the ratio of opening length to beam depth in Fig. 4.9. It may be seen that as the opening length is decreased, the torsional component (as shown dotted) decreases, but the resistance of the beam increases. This means that the couple formed by the lateral shear provides the major part of the total resistance. In this particular case, this amounts to about 90% of the applied torque when the opening reduces to a square one. This observation justifies the simplification made in Art. 2.5 for beams with small openings.

4.2.4 EXPERIMENTAL VERIFICATION

The predictions of the method described above are compared with the test data of ten beams tested by Mansur et al. (1983a) and fourteen beams tested by Daniel and McMullen (1977). In the study by Mansur et al. (1983a), the overall beam dimensions and the amount and arrangement of reinforcement were kept constant for all the beams, while the length, depth, and eccentricity (with respect to the centroidal axis of the beam) were systematically varied. The beams tested by Daniel and McMullen (1977) were provided with openings in the vertical direction. However, if self-weight of the beam is ignored, orientation of opening has no influence on its torsional capacity.

It has been shown that the lower bound analysis gives a conservative estimate of the torsional strength for all the beams. For the 24 available test results, the average ratio of test to calculated torsional capacities is 1.22 and the standard deviation is 0.11. The upper bound approach also predicts lower strengths than the test values except for the beams containing openings of shorter length. In this case, the average ratio of test to calculated ultimate torques is 1.08, with a standard deviation of 0.13. The main sources of this conservative error may be attributed to the selected yield criteria, which are by themselves lower bound, and observed strain hardening of rebars.

It may be interesting to study the effects of length, depth, and eccentricity of openings on the torsional capacity of a beam. For this purpose, the cross-sectional and material details of the beams tested by Mansur et al. (1983a) are selected. These details are presented in Fig. 4.8.

4.2.4.1 Effect of Opening Length

The effect of varying the length of opening on the ultimate torsional strength of beams as predicted by the analytical method is shown in Fig. 4.10. It may be seen that the torsional capacity of a beam decreases with an increase in the length of opening, but only up to a certain critical length, ℓ_c, as given by Eq. (4.24). For opening length, ℓ_o, greater than ℓ_c, both lower and upper bound approaches predict the same torsional strength for beams with a concentric opening. It has been shown earlier that this value is the sum of individual torsional capacities of the two chord members, which are obviously independent of ℓ_o.

Test results of beams reported (Mansur et al.,1983a) with opening length as the parameter are also plotted in Fig. 4.10. It may be seen that the test data follow the theoretical trend, that is, torsional strength decreases as the length of opening

is increased. However, for the opening depth used in these beams, the critical length is beyond the practical limit.

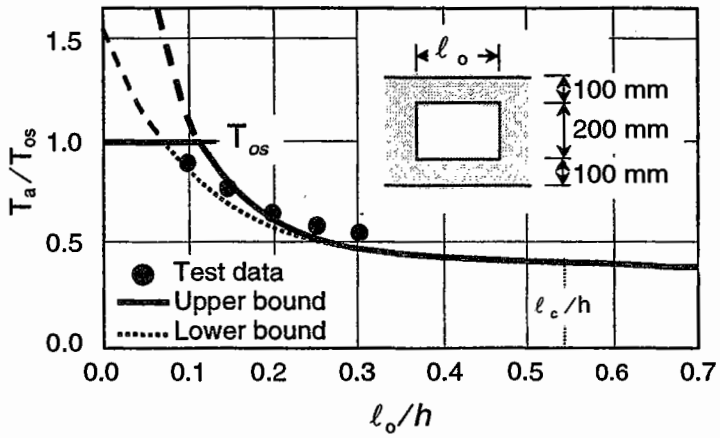

Figure 4.10 Effect of opening length on ultimate torque (Mansur et al., 1983b).

4.2.4.2 Effect of Opening Depth

Figure 4.11 shows the effect of opening depth on torsional strength of a beam. It can be seen that the strength of the solid section controls if the depth of opening is very small. As the depth of opening is increased, torsional capacity decreases. For small depths of opening, both the upper and lower bound analyses predict almost the same torsional capacities. The difference between the two approaches increases as the depth of opening is increased. Considering a practical limit for the depth of opening as 60% of the overall beam depth, the upper bound prediction is only 10% higher than that given by the lower bound approach for the beam section shown in the inset of Fig. 4.11.

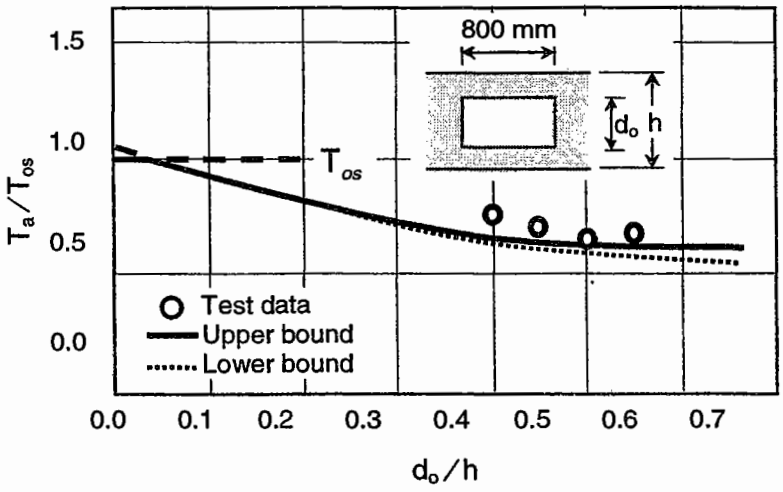

Figure 4.11 Effect of opening depth on ultimate torque.

The results of the tests conducted by Mansur et al. (1983a) on beams with concentric openings but with different depths are also shown in Fig. 4.11. It may be seen that the agreement between theory and experiment is good.

4.2.4.3 Effect of Opening Eccentricity

The effect of varying the eccentricity of openings is shown in Fig. 4.12 for the cross section of the beam shown in Fig. 4.8. It is interesting to note that the torsional capacity of a beam remains nearly a constant for various eccentricities. This observation may be useful for practical purposes because it provides flexibility in placing the opening with respect to the depth. It can be seen in Fig. 4.12 that the trend of the test results reported by Mansur et al.(1983a) is in close agreement with theoretical predictions.

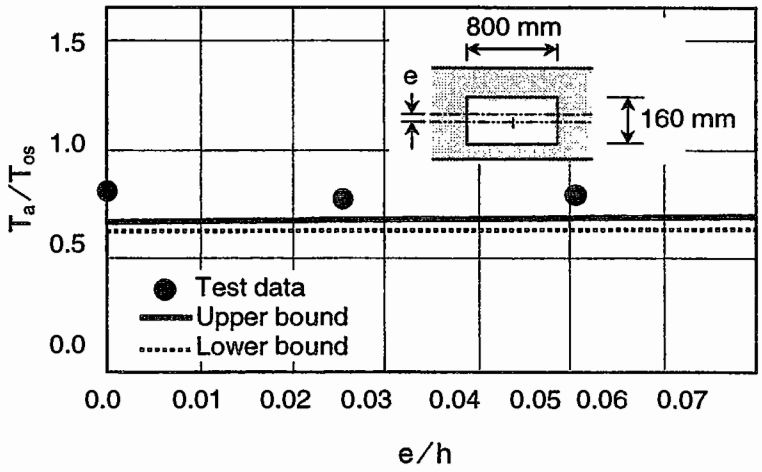

Figure 4.12 Effect of opening eccentricity on ultimate torque.

4.2.5 SIMPLIFIED DESIGN METHOD

4.2.5.1 Background

In designing for torsion in reinforced concrete indeterminate structures, it is helpful to distinguish between two different situations, which were originally recognized by Collins and Lampert (1973) and later redefined by Hsu and Hwang (1977) as:

1. "The torsional moment cannot be reduced by redistribution of internal forces," and
2. "The torsional moment can be reduced by redistribution of internal forces after cracking."

In case of the former, the entire torsional moment must be considered in design. The calculation of torsional moment for the latter category is, however, not so straightforward. As a result, research efforts have been directed towards the

development of a limit design method by utilizing the moment redistribution after cracking. The majority of the research work in this area had been conducted on spandrel beams. These beams, in a monolithic building frame, are subject to the second category of torsion as defined above. In order to obtain an economical design, Collins and Lampert (1973) proposed that the spandrel beam be designed for zero torsion but should be provided with a nominal amount of web reinforcement for torsional ductility and crack control.

Hsu and Hwang (1977) also proposed a method that is similar to the proposal by Collins and Lampert (1973), but the following empirical formula is suggested to establish the amount of minimum torsional web reinforcement:

$$A_{t,\,min} = \frac{1.7\, s\, A_c}{f_{yv}\, p_c} \tag{4.54}$$

in which $A_{t,min}$ = area (one leg) of minimum closed stirrups for torsion in mm^2; A_c = area enclosed by the perimeter of the section following the shape of the stirrups in mm^2; p_c = perimeter of the section following the shape of the stirrups in mm; s = spacing of stirrups in mm; and f_{yv} = yield strength of stirrups in MPa.

In their study, Mansur and Rangan (1978) observed that web reinforcement alone is inadequate to provide the necessary torsional ductility. An equal volume of longitudinal steel must also be added to that required for bending. Later, Hsu and Hwang (1979) agreed to their findings. This minimum longitudinal steel for torsion is given by:

$$A_\ell = \frac{2(x_1 + y_1)}{s}\frac{f_{yv}}{f_{y\ell}} A_{t,min} \tag{4.55}$$

in which A_ℓ = area of total longitudinal steel to resist torsion; x_1 and y_1 = shorter and longer center to center dimensions of a closed rectangular stirrup, respectively; and $f_{y\ell}$ = yield strength of longitudinal reinforcement.

A different approach has been put forward by Hsu and Burton (1974). They have recommended that the spandrel beam be designed for an ultimate torsional moment of $0.33\sqrt{f'_c}\, x^2 y/3$ Nmm at the critical sections, in which f'_c is the concrete cylinder strength in MPa, and x and y are the overall shorter and longer dimensions, respectively, of a rectangular cross section in mm. Based on their test results, Mansur and Rangan (1978) found that the method was satisfactory for the design of spandrel beams.

4.2.5.2 The Method

A beam containing a large opening may be considered as a frame instead of an isolated structural element. The frame consists of the members above and below the opening (chord members) that are fixed to the rigid solid ends of the beam.

First, consider the case of pure torsion. Choosing a three-dimensional co-ordinate system x - y - z, the possible stress resultants that can develop at midspan of the chord members when the beam is subject to pure torque at its solid ends are shown in Fig. 4.13. Forces and moments acting in the respective directions are

indicated by the subscripts x, y, and z. Moments $(M_y)_t$ and $(M_y)_b$ arise from lateral bending of the chords as the beam twists. However, it was noted by Mansur et al. (1983a) that, under pure torsion, contraflexure points occur at midspan of the chord members. Hence, $(M_y)_t = (M_y)_b = 0$ at midspan of the chords.

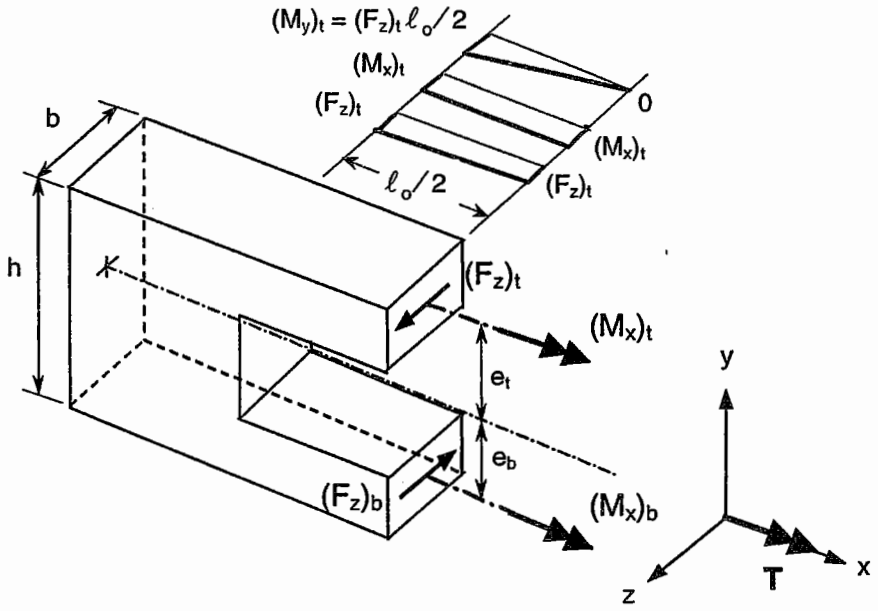

Figure 4.13 Beam with a large opening under pure torsion.

The equilibrium equations for the beam can then be written as

$$(F_z)_t + (F_z)_b = 0 \tag{4.56}$$

$$T = (M_x)_t + (M_x)_b + (F_z)_t e_t + (F_z)_b e_b \tag{4.57}$$

Thus, there are two equilibrium equations to solve for four unknowns, $(M_x)_t$, $(M_x)_b$, $(F_z)_t$, and $(F_z)_b$. Therefore, the beam is statically indeterminate by two degrees. It can, however, be shown that any assumed value, including zero, for the torsional moment $(M_x)_t$ and $(M_x)_b$ satisfies the equilibrium requirements similar to the case of spandrel beams. Hence, the chord members are subject to the second category of torsion as defined by Hsu and Hwang (1977) and, therefore, the findings with respect to spandrel beams should be applicable to beams with a large rectangular opening under pure torsion.

As discussed in the preceding section, two alternatives are possible. First, torsional moments $(M_x)_t$ and $(M_x)_b$ may be assumed as zero, but a minimum amount of torsional web and longitudinal steel in accordance with Eqs. (4.54) and (4.55), respectively, need to be provided for necessary ductility and crack control. In the alternative proposal, the nominal torsional moments in the top and bottom chords may be taken as

$$(T_n)_t = (M_x)_t = 0.33\sqrt{f'_c}\,\frac{x_t^2\, y_t}{3} \tag{4.58}$$

$$(T_n)_b = (M_x)_b = 0.33\sqrt{f'_c}\,\frac{x_b^2\, y_b}{3} \tag{4.59}$$

where the subscripts *b* and *t* refer to the bottom and top chords, respectively.

The former proposal of assuming zero torsion in the chords has been recommended by Mansur (1983) because it leads to a conservative design and results in a relatively simple design procedure.

Once the values of $(M_x)_t$ and $(M_x)_b$ are known, the beam becomes statically determinate. The bending moment and shear force distribution in the chord members can then be easily calculated. As shown in Fig. 4.13, the critical sections in the chord members are at the edges of the opening. The lateral shear force at these sections is obtained from Eq. (4. 57) as

$$V_u = (F_z)_t = (F_z)_b = \frac{T_u}{e_t + e_b} \tag{4.60}$$

and the bending moment is given by

$$M_u = (M_y)_t = (M_y)_b = V_u\,\frac{\ell_o}{2} \tag{4.61}$$

Knowing the values of bending moment and shear force, these sections can be proportioned for shear and moment by any of the current building codes. However, as the torsional moment in the chord members is assumed to be zero, a minimum amount of longitudinal and transverse reinforcement according to Eqs. (4.54) and (4.55), respectively, should be added to those required for bending and shear.

4.3 TORSION COMBINED WITH BENDING

A review of literature reveals that no method of ultimate strength analysis is available for the case of combined bending and torsion in beams containing a large opening. However, a simple design procedure was suggested by Mansur (1983) for such a case. The design procedure for pure torsion as described above has, in fact, been reduced from what was proposed by Mansur to deal with the problem of combined torsion and bending by eliminating the effect of torsion.

In Chapter 3, it was shown that when a beam with a large opening is subject to pure bending, the resisting moment is furnished by the couple formed by the tensile and compressive stress resultants in the bottom and top chords, respectively, as shown in Fig. 3.3 [see Eq. (3.53)]. These forces, when superimposed with those developed in a beam subject to pure torsion (Fig. 4.13),

give the case of combined torsion and bending. The resulting internal forces are shown in Fig. 4.14.

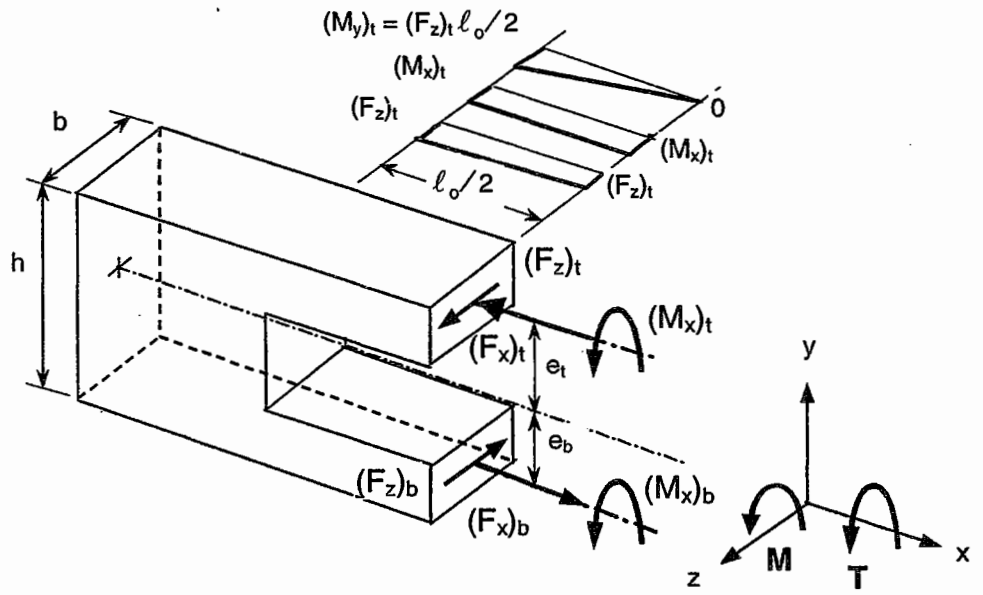

Figure 4.14 Free-body diagram at beam opening subject to combined torsion and bending.

Assuming that the beam is subject to a sagging bending moment and that the opening segment of the beam is free from external loading, the compressive stress resultant in the top chord is

$$(N_u)_t = (F_x)_t = \frac{M_u}{(e_t + e_b)} \tag{4.62}$$

The stress resultant in the bottom chord, N_b, will be numerically equal to N_t but is in tension. Combining the effect of torsion, Eqs. (4.60) and (4.61), the critical sections at the ends of the chord members are thus subject to a combination of axial force, lateral bending (about y-axis), and lateral shear forces (in z-direction). Provided that the sections are adequately designed for shear, the critical sections may be considered as uniaxially loaded tension or compression members and, hence, can be designed by any of the current building codes. The design of such a beam is presented in Example Problem 4.1.

EXAMPLE PROBLEM 4.1

A reinforced concrete beam of rectangular cross section contains a rectangular opening, located symmetrically with respect to the beam depth as shown in Fig. E4.1.1. The following information is given:

(a) Geometry

$h = 400$ mm; $b = 200$ mm;

$d_o = 180$ mm; $\ell_o = 800$ mm; $e_b + e_t = 290$ mm

(b) Factored moments at center of opening

$T_u = 16$ kNm; $M_u = 14.7$ kNm

(c) Material properties

$f_y = 460$ MPa; $f_{yv} = 350$ MPa; $f'_c = 30$ MPa

Design the opening segment of the beam.

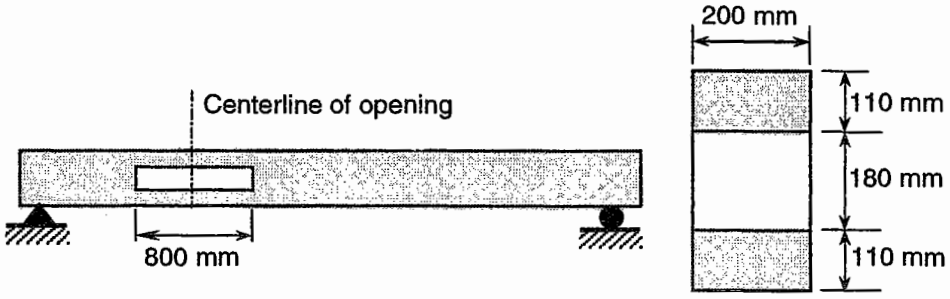

Figure E4.1.1 Details of beam in Example Problem 4.1

SOLUTION

1. DESIGN OF TOP CHORD MEMBER (COMPRESSION + BENDING)

(a) Calculate moments and forces

From Fig. 4.14 and Eqs. (4.60) to (4.63) assuming $(M_x)_b = T_b = 0$ and $(M_x)_t = T_t = 0$,

$$(V_u)_t = T_u/(e_b + e_t) = 55.2 \text{ kN}$$

$$(M_u)_t = (V_u)_t (\ell_o/2) = 22.1 \text{ kNm}$$

$$(P_u)_t = (N_u)_t = M_u/(e_b + e_t) = 50.7 \text{ kN}$$

(b) Determine magnified moment for slenderness effect

According to Section 10.12.3 of ACI Code (1995), for a non-sway frame,

$$\delta = \frac{C_m}{1 - \dfrac{P_u}{\phi P_c}} \geq 1$$

in which $C_m = 1$, $\phi = 0.75$, $P_u = (P_u)_t = 50.7$ kN and

$$P_c = \frac{\pi^2 EI}{(k\ell_u)^2}$$

where

$$EI = \frac{0.4\,E_c I_g}{(1+\beta_d)}$$

Assume β_d = 0 for conservative design and substituting the relevant values, we obtain

$$EI = 0.4\times 4730\sqrt{30}\,\frac{200\times 100^2}{12} = 233\times 10^9\ \text{Nmm}^2$$

Since k = 1 and ℓ_u = 800 m, we get

$$P_c = \frac{\pi^2(233\times 10^9)}{(1\times 800)^2\times 10^3} = 3550\,\text{kN}$$

Hence,

$$\delta = \frac{1}{1-50.5/(0.75\times 3550)} = 1.02$$

Therefore, the magnified moment is

$$\delta(M_u)_t = 1.02\times 22.1 = 22.59\,\text{kNm}$$

(c) Check flexural capacity

Try 4-13 mm diameter bars (4T13) arranged as shown in the inset of Fig. E4.1.2. In order to check its flexural capacity, interaction diagrams are plotted in Fig. E4.1.2 for the assumed amount and arrangement of reinforcement. In plotting these curves, the area of minimum longitudinal steel required for torsion according to Eq. (4.55) was deducted equally from the area of the bars shown.

Assuming 15 mm clear concrete cover and 6 mm diameter stirrups, x_1 = 74 mm; y_1= 164 mm. Therefore,

$$\frac{A_{t,min}}{s} = \frac{1.7\times 74\times 164}{350\times 2(74+164)} = 0.124\,\text{mm}^2/\text{mm}$$

Hence,

$$A_\ell = 2(74+164)(350/460)0.124 = 45\,\text{mm}^2$$

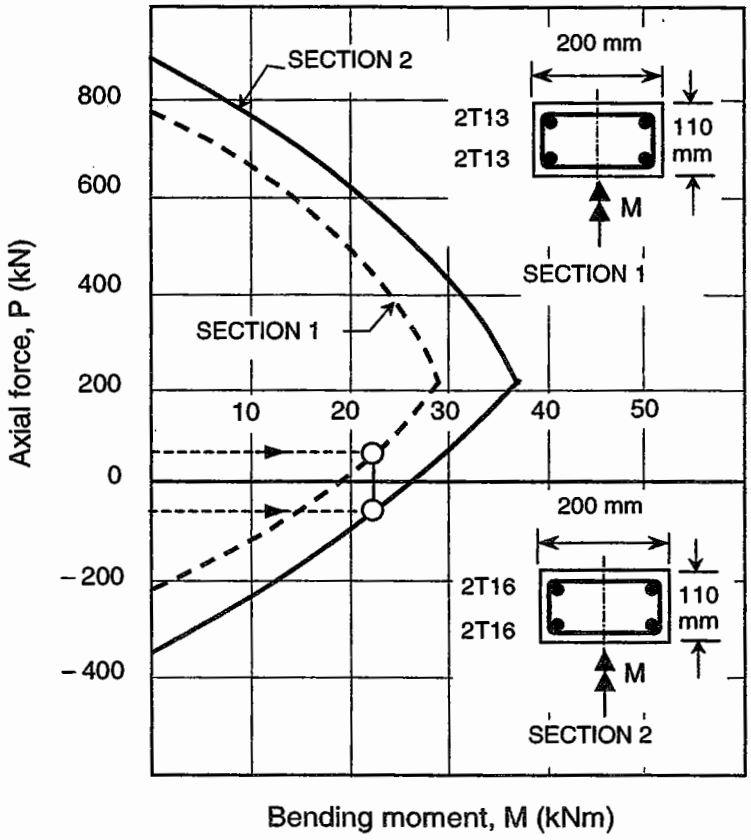

Figure E4.1.2 Interaction diagram.

Thus, an area of $45 / 4 = 11.2$ mm^2 has been deducted from each bar in the calculation of bending-axial load interaction diagram.
From Fig. E4.1.2,

$$[\delta (M_u)_t]_{allowable} = 22.58 \text{ kNm for } (N_u)_t = 50.7 \text{ kN}$$

Hence the assumed reinforcement is satisfactory.

2. DESIGN OF BOTTOM CHORD MEMBER (TENSION + BENDING)

In this case

$$(N_u)_b = 50.7 \text{ kN (tension); and } (M_u)_b = 22.1 \text{ kNm.}$$

It can be seen in Fig. E4.1.2 that the assumed reinforcement comprising 4T16 bars as shown is satisfactory. Similar to the top chord member, the area of longitudinal reinforcement required for torsion was deducted from each bar in the computation of the interaction curve.

3. DESIGN FOR SHEAR

(a) Bottom chord

$$(V_u)_b = 55.2 \text{ kN}$$

According to Clause 11.3.2.3 of ACI Code (1995)

$$V_c = 0.17\left[1-0.29\frac{(N_u)_b}{A_g}\right]\sqrt{f'_c}\,bd$$

$$= 0.17\left[1-0.29\left(\frac{55.2\times10^3}{200\times110}\right)\right]\sqrt{30}\times110\times171\times10^{-2}$$

$$= 4.77 \text{ kN} < (V_u)_b$$

Hence, shear reinforcement is required.

$$\frac{A_v}{s} = \frac{(V_u)_b - V_c}{f_{yv}\,d} = \frac{(55.2-4.77)10^3}{350\times171} = 0.846 \text{ mm}^2/\text{mm}$$

Add to this the minimum torsional web reinforcement of 0.124 mm^2/mm according to Eq. (4.54). Thus, the total web reinforcement is

$$\left[\frac{A_s}{s}\right]_{total} = 0.124\times2+0.846 = 1.1 \text{ mm}^2/\text{mm}$$

Using 6 mm diameter closed stirrups,

$$s = \frac{2\times28.3}{1.1} = 51.5 \text{ mm, say } 50 \text{ mm}$$

(b) Top chord

The same spacing of stirrups as used in the bottom chord will be conservative for the top chord as it is subject to axial compression.

4. CORNER REINFORCEMENT

Assuming that the stirrups in the solid section adjacent to each side of the opening will resist the entire torque, the required diameter of stirrups, d_v, is given by (Mansur, 1983)

$$d_v = \sqrt{\frac{4}{\pi}\left[\frac{T_a}{f_{yv}(x_1+y_1)}\right]}$$

For 10 mm diameter stirrups, x_1 = 168 mm; y_1 = 368 mm. Therefore, from the above equation, torsional resistance provided by one 10 mm diameter closed stirrup is:

$$T_{stirrup} = \left(\frac{\pi \times 10^2}{4} \right) \times 454\,(168 + 368) 10^{-6} = 19.1\,\text{kNm}$$

Since this is larger than the applied torque, the design is satisfactory.

4.4 COMBINED TORSION, BENDING, AND SHEAR

Similar to the case of combined torsion and bending, a design procedure for combined torsion, bending, and shear may be suggested by combining the design for bending and shear with that of pure torsion, as follows.

The case of combined bending and shear has been fully treated in Chapter 3. By assuming contraflexure points at midspan of the chord members, it has been shown that the applied bending moment may be considered to be resisted by the couple formed by the axial stress resultants in the top and bottom chords. Also, the applied shear at the center of the opening may be distributed between the two chords in proportion to their flexural stiffnesses. Superimposing this with pure torsion, we obtain the case of combined torsion, bending, and shear as shown in Fig. 4.15.

By virtue of the above simplifications, the stress resultants generated at the center of the chord members, as shown in Fig. 4.15, are uniquely defined by statical considerations alone. These values are given by

$$(F_z)_t = -(F_z)_b = \frac{T_u}{(e_t + e_b)} \tag{4.61}$$

$$(F_x)_t = -(F_x)_b = \frac{M_u}{(e_t + e_b)} \tag{4.62}$$

$$(F_y)_t = \frac{V_a I_t}{I_b + I_t} \tag{4.63}$$

$$(F_y)_b = \frac{V_a I_b}{I_b + I_t} \tag{4.64}$$

As can be seen in Fig. 4.15, the critical sections are at the ends of the opening and each of these sections is subject to a combination of axial force, biaxial bending, and shear forces in two directions. Provided that the sections are adequately designed for shear, the critical sections may be considered as biaxially loaded tension or compression members and, hence, can be designed using the provisions of any of the current building codes.

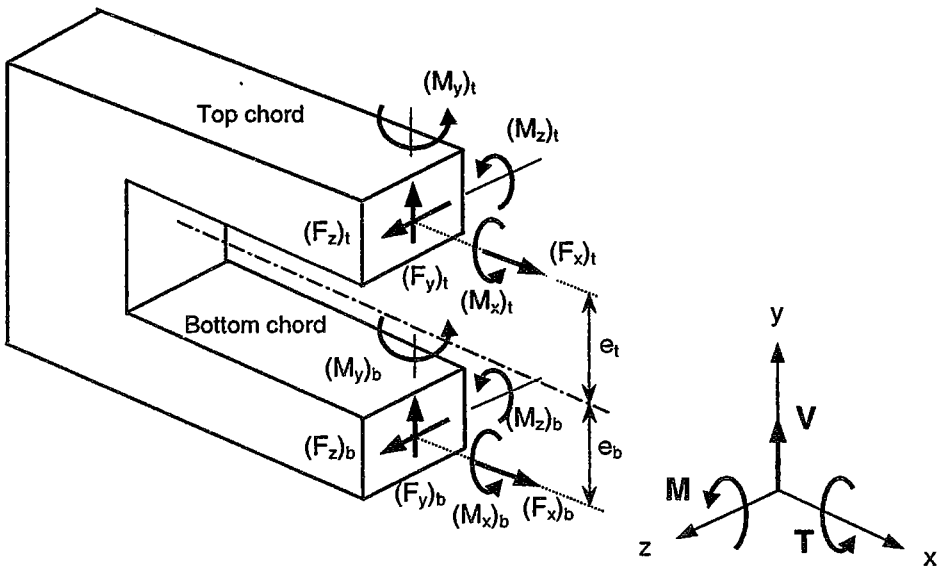

Figure 4.15 Stress resultants at the centers of chord members due to combined torsion, bending, and shear.

5 Continuous Beams

5.1 GENERAL INTRODUCTION

Prior to designing a structure, it is necessary to obtain a set of internal forces and moments throughout the structure, which is in equilibrium with the design loads for the required loading combinations. For this purpose, the method of linear elastic analysis based on gross concrete section is generally employed.

In the case of reinforced concrete structures, the linear elastic method normally gives a realistic set of moments and forces under service loads because, at this stage of loading, both the steel and concrete may be considered as linearly elastic materials with a reasonable degree of accuracy. But at higher loads, concrete behaves in a non-linear fashion. As a result, there will be a considerable redistribution of internal forces and moments from that obtained by a linear elastic analysis at load levels higher than the working loads. Even then, the elastic method has been widely used for the analysis of a structure at ultimate loads, and a design based on the resulting moments and forces has been found to be satisfactory. The effects of non-linear behavior of the constituent materials are recognized by the codes of practices by allowing an arbitrary redistribution of internal forces and moments up to a maximum of 30%, provided certain restrictions on ductility and strength are satisfied. If the designer wishes, he can take advantage of such redistribution, but it is not mandatory.

When a beam contains a transverse opening, it is desirable to carry out a similar elastic analysis in order to be consistent with the analysis of the rest of the structure. However, it is obvious that the provision of openings reduces the overall stiffness of the beam. In a statically determinate system, this will be directly translated into a larger deflection. However, in an indeterminate system, the reduction in stiffness will not only magnify the deflection but also will affect the distribution of bending moment and shear forces in the structure. For small openings, test results on simply supported beams (Prentzas, 1968; Salam, 1977; Salam and Harrop, 1979; Mansur et al.,"In press") have shown that the deflection is affected only marginally which, in serviceability design, can be accounted for by introducing a multiplying factor to the deflection of a corresponding solid beam. But

similar tests involving large openings (Mansur et al., 1985; Mansur et al., 1991a; Nasser et al., 1967; Ragan and Warwaruk, 1967, Tan et al., 1996; Warwaruk, 1974) have shown significant influence of openings on deflection. Therefore, an assessment of the effects of reduced stiffness due to the provision of a large opening is necessary to obtain a realistic picture of the structural response.

In this chapter, the elastic analysis of reinforced concrete continuous beams that contain a large rectangular opening in the web is introduced. While compiling this chapter, an extensive search of available literature reveals only one method to deal with this kind of analysis problem (Mansur et al.,1992). This method treats the beam as a structural member comprising several segments and introduces an equivalent stiffness for the segment traversed by the opening. The beam is then analyzed by the Direct Stiffness Method, which is compatible with most of the existing computer software for structural analysis.

5.2 ELASTIC ANALYSIS

The typical deflected shape of a beam containing a large rectangular opening is shown in Fig. 5.1. Fig. 5.2 shows a reproduction of the deflected configuration of a typical beam as determined experimentally by Mansur et al. (1991a). It may be clearly seen that the beam deflects both in flexural and shear mode responses. The flexural response is due to composite bending of the beam as a whole (global response) as shown by dotted lines in Fig. 5.2(b). The resulting deflection due to flexural action is plotted in Fig. 5.2(c). The shear response is a sort of frame racking action (Vierendeel response) as isolated in Fig. 5.2(d), and it results in bending of the chord members above and below the opening in double curvature.

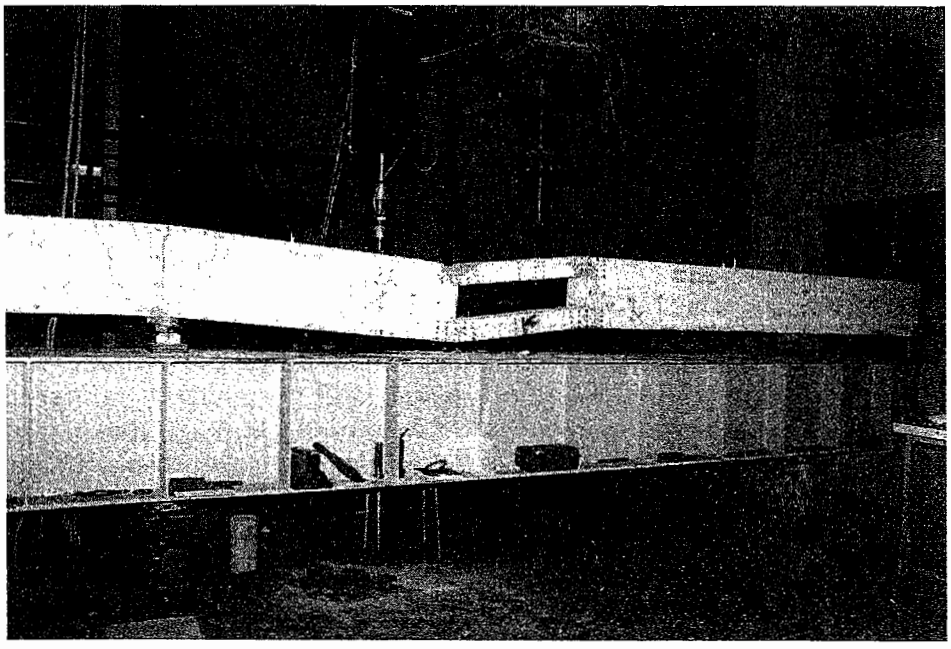

Figure 5.1 Typical deflected shape of a beam with a large opening.

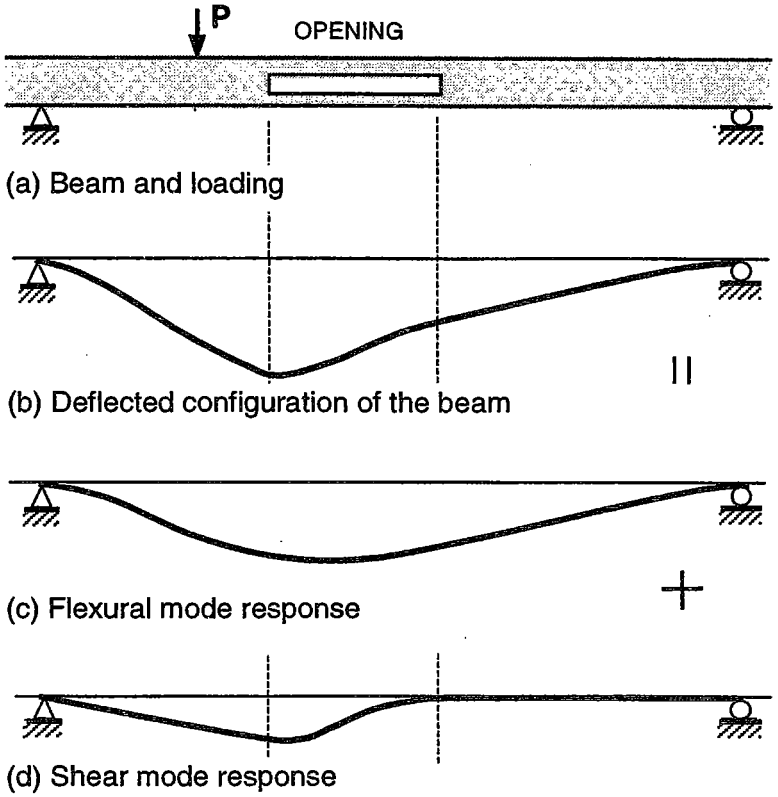

Figure 5.2 Deflection configuration of a typical beam containing an opening.

Similar observations can also be made from the test results by Barney et al. (1977). In the calculation of service load deflections for simply supported beams, Barney et al. accounted for the observed responses by adding the deflection due to the flexural action of the beam as a whole to that produced by shear forces at the opening segment. Basically the same approach was used by Mansur et al. (1991b) to predict the piecewise linear behavior of reinforced concrete continuous beams with large openings by performing successive elastic analyses to trace the formation of hinges until a mechanism was formed. Although the agreement of the analytical predictions with the test data generated was good, the method does not take the effect of the observed shear mode response into account in the analysis of the structure. Therefore, in the theoretical modeling of the opening segment, the effects of both flexural and shear stiffnesses must be taken into consideration.

In the method proposed by Mansur et al. (1992), the connecting chord members at an opening are replaced by an equivalent continuous medium. The beam may then be considered as a structural member comprising a number of uniform segments as shown in Fig. 5.3. For the opening segment, it is, however, necessary to draw equivalence of the flexural and shear stiffnesses, EI and GA, to represent the behavior of the actual box-type structure at the opening, in which E is the elastic modulus, I is the moment of inertia of the section, G is the modulus of rigidity, and A is the cross-sectional area of the section.

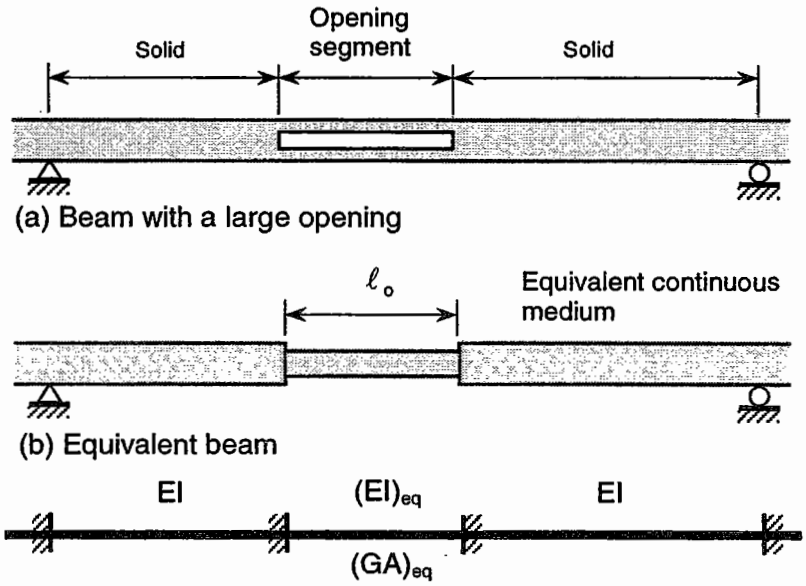

Figure 5.3 Equivalent segmented beam.

5.2.1 EQUIVALENT FLEXURAL STIFFNESS

The equivalent flexural stiffness $(EI)_{eq}$ of the continuous medium is based on the net section through the opening. Assuming that the two chords act as one unit and that the section is cracked in flexure, the moment of inertia I is calculated using the transformed area method. The modulus of elasticity E_c of the concrete is taken as that recommended by the ACI Code (1995).

5.2.2 EQUIVALENT SHEAR STIFFNESS

The equivalent shear stiffness, $(GA)_{eq}$, depends on the flexural stiffnesses of the connecting chord members and the effective length, ℓ_e, of the opening. It may be obtained by equating the vertical shearing deformation caused by a unit shearing force applied to the box structure to the corresponding value caused by shearing deformation of the equivalent continuous medium. Assuming that the points of contraflexure occur at midspan of the chord members during the loading process, the deflection Δ caused by a unit load as shown in Fig. 5.4(a) for the box structure is given by

$$\Delta = \frac{\ell_e^3}{12E_c(I_b + I_t)} \tag{5.1}$$

in which I_b and I_t are the moments of inertia for the bottom and top chords, respectively.

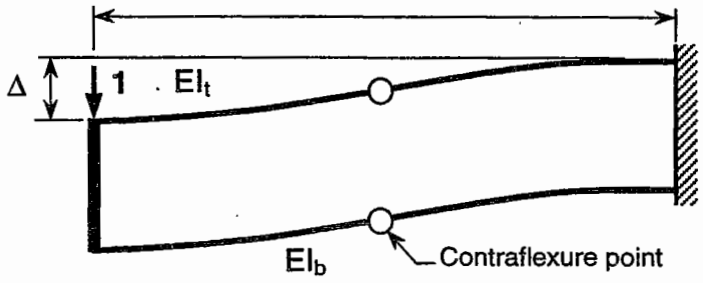

(a) Box structure representing the opening

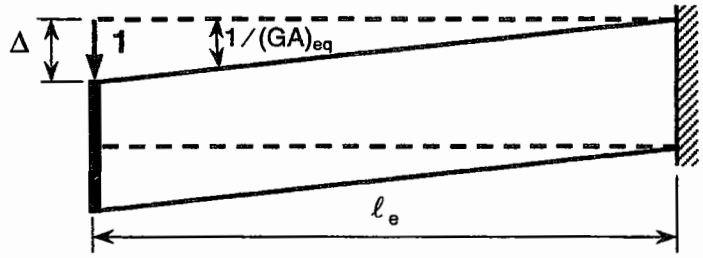

(b) Equivalent continuous medium

Figure 5.4 Derivation of equivalence for shearing rigidity.

The corresponding deflection caused by shearing deformation of the uniform continuous medium shown in Fig. 5.4(b) is

$$\Delta = \frac{\ell_e}{(GA)_{eq}} \tag{5.2}$$

The *GA* parameter of the equivalent continuous medium is then obtained from Eqs. (5.1) and (5.2) as

$$(GA)_{eq} = \frac{12E_c(I_b + I_t)}{\ell_e^2} \tag{5.3}$$

In the above derivation of the equivalent shear stiffness for the opening segment of the beam, an effective length, ℓ_e, of the opening has been used instead of its actual length, ℓ_o. The rationale of introducing this effective length is to account for the deflection due to the rotation when cracking occurs at the end of the chord members, which was not included in the vertical shearing deformation of the box structure in Eq. (5.1). It is assumed that ℓ_e is a function of the ratio of opening depth to overall depth of the beam, d_o/h. Using the available test data, the value of ℓ_e has been evaluated empirically (Mansur et al., 1992) as:

$$\ell_e = \frac{\ell_o}{1-\left(\frac{d_o}{h}\right)^{1.45}} \tag{5.4}$$

Later, with the incorporation of additional test data (Huang, 1992), the exponent for d_o/h has been revised as 1.5.

5.2.3 MEMBER STIFFNESS AND TRANSFER MATRIX

In order to account for shear deformations, the shear stiffness must be incorporated into the member stiffness matrix. The matrix S_M that includes the effects of shearing deformations for a beam member of length L may be derived from flexibility considerations (Weaver and Gere, 1980) as

$$S_M = \frac{EI}{1+g}\begin{bmatrix} \frac{12}{L^2} & \frac{6}{L^2} & -\frac{12}{L^2} & \frac{6}{L^2} \\ \frac{6}{L^2} & \frac{4}{L}\left(1+\frac{g}{2}\right) & -\frac{6}{L^2} & \frac{2}{L}(1-g) \\ -\frac{12}{L^2} & -\frac{6}{L^2} & \frac{12}{L^2} & -\frac{6}{L^2} \\ \frac{6}{L^2} & \frac{2}{L}(1-g) & -\frac{6}{L^2} & \frac{4}{L}\left(1+\frac{g}{2}\right) \end{bmatrix} \tag{5.5}$$

in which

$$g = \frac{6\,(EI)_{eq}}{\ell_e^2\,(GA)_{eq}} \tag{5.6}$$

Similarly, the transfer matrix T_{ML} for concentrated loading may be obtained as

$$T_{ML} = \frac{1}{1+g}\begin{bmatrix} -\frac{\beta^2}{L^3}\{3\alpha+\beta+2\beta(L/\beta)^2 g\} & \frac{6\alpha\beta}{L} \\ -\frac{\alpha\beta^2}{L^2}\{1+(L/\beta)g\} & \frac{\beta}{L^2}(2\alpha-\beta-2gL) \\ -\frac{\alpha^2}{L^3}\{\alpha+3\beta+2\alpha(L/\alpha)^2 g\} & -\frac{6\alpha\beta}{L} \\ \frac{\alpha^2\beta}{L^2}\{1+(L/\alpha)g\} & \frac{\alpha}{L^2}(2\beta-\alpha-2gL) \end{bmatrix} \tag{5.7}$$

in which α and β are the distances of the applied point load or moment in a member from the left and right supports, respectively, as shown in Fig. 5.5. The transfer matrix for other loading conditions can be derived using the standard procedures

described by Weaver and Gere (1980). It should be noted that the transfer matrix is unchanged by the inclusion of shear deformation for symmetrical loading such as a uniformly distributed load across the entire beam span.

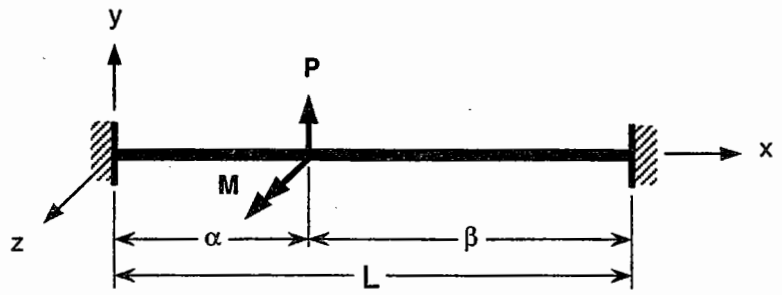

Figure 5.5 Concentrated load or moment on members.

5.2.4 ANALYSIS PROCEDURE

With the stiffness and transfer matrices modified as above to take into account of the effects of shearing deformations for the equivalent continuous medium, the usual procedure of most of the elastic methods of structural analysis can be employed. The Direct Stiffness Method (Weaver and Gere, 1980) may be chosen because it can be readily translated into a computer algorithm. The beam is treated as a non-prismatic member with two sections of different cross-sectional properties, that is, the solid section and the equivalent opening section as shown in Fig. 5.3(b). It is, therefore, necessary to introduce two extra joints, as shown in Fig. 5.3(c), for each opening added to the structure. For the solid segments of the beam, shearing deformation can be considered as negligible [that is, $g = 0$ in Eqs. (5.5) and (5.7)], and the flexural stiffness is based on the cracked transformed section. However, if a more accurate result is required, the shear stiffness, GA, of the solid section should be derived from concrete properties of the section. Thus, the problem of analyzing a beam with large openings eventually reduces to any regular continuous beam problem.

A computer program based on the Direct Stiffness Method has been developed for the analysis of continuous beams with web openings. The complete listing of the program, input and output files, and an analysis example are available elsewhere (Huang, 1992).

5.2.5 COMPARISON WITH TEST DATA

5.2.5.1 Details of Available Test Data

In order to test their method, Mansur et al. (1992) made a comparison of the theoretical predictions with the experimental data available in the literature. Test results available with full documentation of the information relevant to the analysis problem are those reported by Tan (1982), Lee (1989), and Huang (1992). The experiment conducted by Tan involved testing of fourteen simply supported beams, each containing a rectangular opening. Lee has reported tests on two series of

beams. The first series (Series B) consisted of three two-span continuous beams while five three-span continuous beams comprised the second series (Series C). The loading and support details of these beams are shown in Fig. 5.6. All these beams were rectangular in cross section, 200 mm wide and 400 mm deep. The major parameters included in these investigations were the length, depth, and eccentricity of the opening, and its location along the length of the beam. The experiments conducted by Huang (1992) included fifteen T-beams, and each beam was tested simulating either the midspan or the support region of a continuous beam.

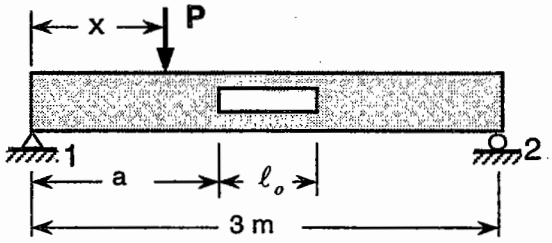

(a) Simply-supported beam (Tan, 1982)

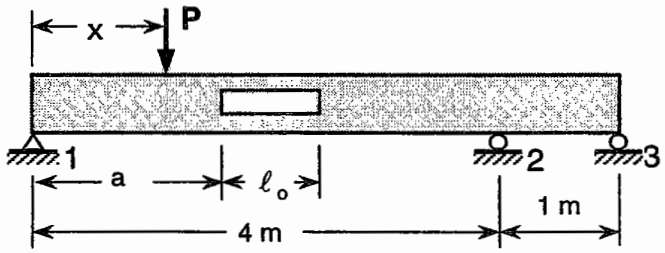

(b) Two-span continuous beam (Lee, 1989)

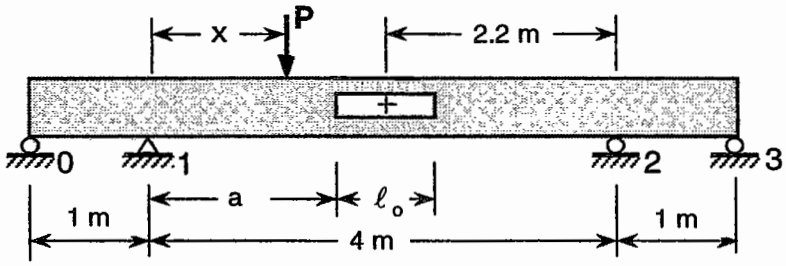

(c) Three-span continuous beam (Lee, 1989)

Figure 5.6 Loading and support details for available test beams.

5.2.5.2 Deflection at Service Load

In the serviceability design of a reinforced concrete structure, the maximum deflection under working loads is generally sought to ensure compliance with the code provisions. In the present analysis, service load is taken as the experimental ultimate load divided by a factor of 1.7. Since many uncertainties and approximations are involved in modeling reinforced concrete for the calculation of

deflection, an accuracy within ± 20% is usually considered satisfactory for all design purposes.

The method presented in the preceding section is used to calculate the maximum deflections of the beams tested by Tan (1982), Lee (1989), and Huang (1992) at the assumed service load level. In Fig. 5.7, these deflections are presented together with the corresponding experimental values. It may be seen that one of the beams recorded very small deflection; this may be due to some experimental fault. If this beam is excluded, then for the remaining 36 test data, the ratio of experimental to predicted deflections was found to range from 0.75 to 1.21 with an average of 0.95 and a coefficient of variation of 12%. Only five beams violated the acceptable accuracy of ± 20%, but it is only marginal. On an average, the method gives a conservative prediction of deflections at service load.

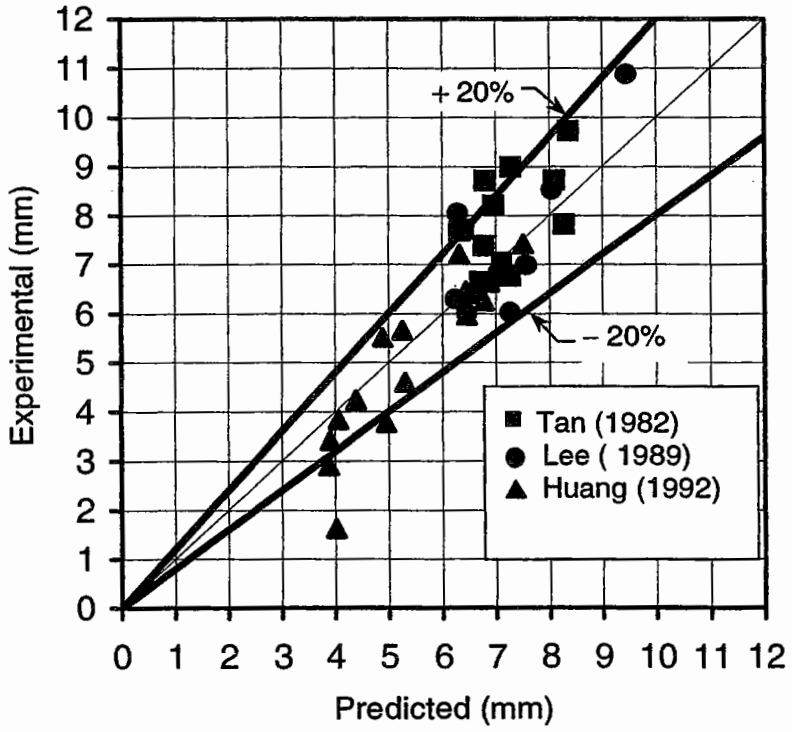

Figure 5.7 Comparison of deflections at calculated service load.

5.2.5.3 Redundant Support Reactions

For the continuous beams tested by Lee (1989), the measured reactions at the redundant supports, that is, at support 3 for series B and at supports 0 and 3 (see Fig. 5.6) for series C under the assumed service load are presented in Table 5.1. Also presented are the corresponding predicted values. It may be seen that the theoretical predictions are in good agreement with the available test data. Except for the reaction at support 3 for the three-span continuous beam C3, the ratio of

experimental-to-predicted deflections varies from 0.79 to 1.19, thus providing an useful second check for the validity and accuracy level of the method.

Table 5.1 Comparison between experimental and predicted support reactions for the continuous beams (Mansur et al., 1992).

Beam	Reaction at support 0*			Reaction at support 3*		
	Test, $R_{0,test}$ kN	Theory, $R_{0,theory}$ kN	$\frac{R_{0,test}}{R_{0,theory}}$	Test, $R_{3,test}$ kN	Theory, $R_{3,theory}$ kN	$\frac{R_{3,test}}{R_{3,theory}}$
B1	-	-	-	21	22.2	0.95
B2	-	-	-	32	28.0	1.14
B3	-	-	-	26	23.1	1.13
C1	62	78.1	0.79	26	21.8	1.19
C2	58	66.8	0.87	19	16.4	1.16
C3	72	76.3	0.94	15	10.4	1.44
C4	64	67.7	0.95	27	22.7	1.19
C5	50	63.4	0.79	**	4.6	**

* Refer to Fig. 5.6; ** Data not available

5.2.5.4 Redistribution of Internal Forces and Moments

In statically determinate structures, the shear force and bending moment diagrams are unique whether or not any opening exists because they are obtained from statical considerations alone. But in statically indeterminate structures, the distribution of shear forces and bending moments depends on the relative stiffnesses of various members. Since incorporation of openings reduces the stiffness of a beam, there will be a redistribution of shear forces and bending moments from that given by an elastic analysis ignoring the presence of opening as suggested by Barney et al. (1977). Mansur et al.'s (1991b) proposal of calculating the flexural stiffness of the opening segment on the basis of net section will also produce identical results as long as the neutral axis lies within the compression chord. It will, therefore, be interesting to evaluate the extent of such redistribution in light of the above analysis method.

The shear force and bending moment distributions at the assumed service load are calculated for two typical beams tested by Lee (1989) using Mansur et al.'s (1992) proposal and are compared with the test data in Fig. 5.8. It may be observed that the redistribution is rather significant. Such a redistribution will not only affect the ultimate strength of a beam but also the calculation of deflection at service load, and therefore must be taken into account in design.

Also presented in Fig. 5.8 are the results of the analysis presented herein. It will be seen that inclusion of the equivalent shear stiffness for the opening segment in the analysis of the beam gives a realistic picture of the redistribution of shear forces and bending moments observed experimentally.

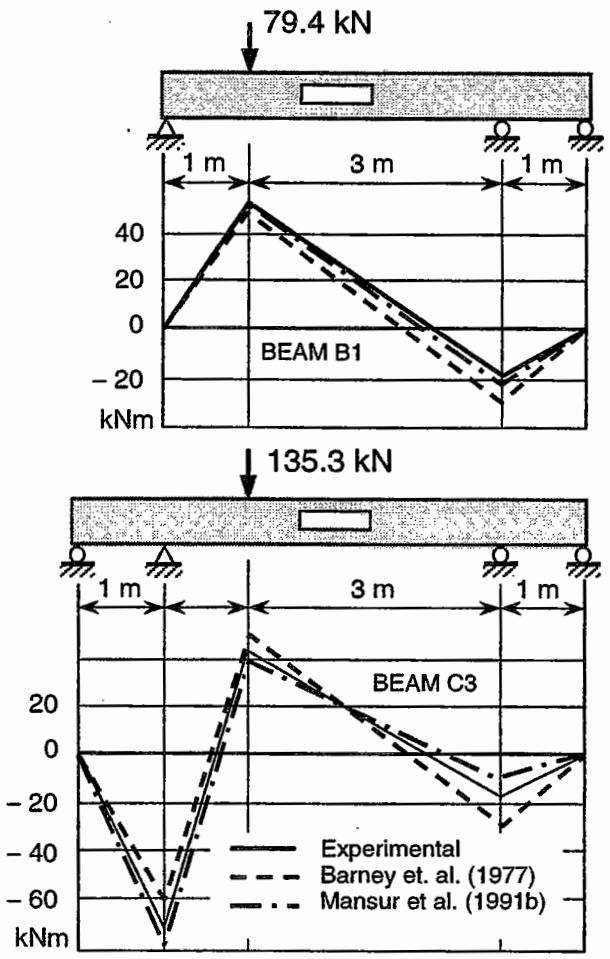

Figure 5.8 Redistribution of internal forces and moments in typical beams (Mansur et al., 1992).

5.3 DESIGN PROCEDURE AND RECOMMENDATIONS

5.3.1 GENERAL GUIDELINES

A review of literature on the behavior and strength of beams with web openings indicates that the following guidelines can be used to facilitate selection of the size and location of web openings (refer to Fig. 5.9):

1. For T-beams, openings should preferably be positioned flushed with the flange for ease in construction. In the case of rectangular beams, openings are commonly placed at mid-depth of the section, but they may be placed eccentrically with respect to the depth if situation dictates. Care must be exercised to provide sufficient concrete cover to the reinforcement for the chord members above and below the opening. The compression chord should also have sufficient concrete area to develop the ultimate

compression block in flexure and have sufficient depth to provide effective shear reinforcement.

2. Openings should not be located closer than half the beam depth, h, to the supports to avoid the critical region for shear failure and reinforcement congestion. Similarly, positioning of an opening closer than $0.5h$ to any concentrated loads should be avoided.
3. The depth of openings should be limited to 50% of the overall beam depth.
4. The factors that limit the length of an opening are the stability of the chord members, in particular the compression chord, and the serviceability requirement of deflection. It is preferable to use multiple openings providing the same passageway instead of using a single long opening.
5. When multiple openings are used, the post separating two adjacent openings should not be less than $0.5h$ or 100 mm, whichever is larger, to ensure that each opening behaves independently.

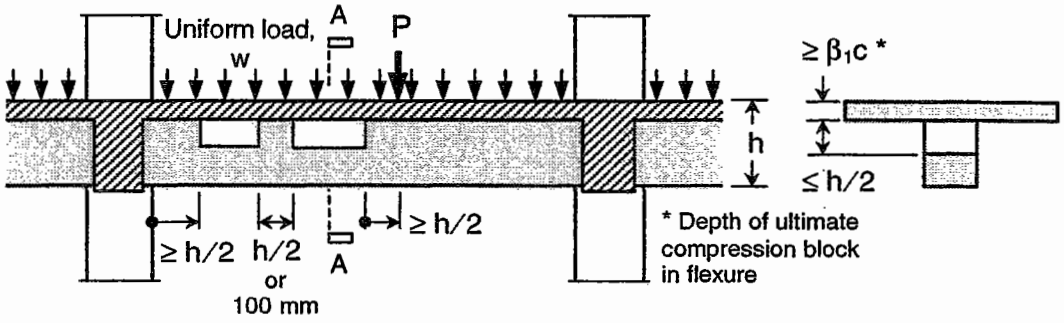

Figure 5.9 Guidelines for the location of web openings (Tan et al., 1996).

5.3.2 RECOMMENDED DESIGN PROCEDURE

In the design procedure proposed herein, the ACI Code (1995) has been followed throughout unless otherwise stated. In general, the design of reinforced concrete structures involves:

Structural analysis, whereby the structure is analyzed to determine the distribution of shear forces and moments due to ultimate loads. All possible loading combinations are considered, and the bending moment and shear force envelopes are determined accordingly.

(b) ***Strength design***, wherein the critical sections are designed for ultimate strength in bending, shear and torsion. The strength requirements are fulfilled throughout the whole structure.

(c) ***Serviceability design***, to ensure that the structure performs its intended functions satisfactorily under working loads.

5.3.2.1 Structural Analysis

In the case of a statically determinate beam, the shear force and bending moment envelopes can be obtained from statics. For continuous beams, the method given in the preceding section can be followed. According to the method, the member containing an opening is considered as a non-prismatic beam with different cross-sectional properties, as discussed earlier. Provided that the guidelines described above are complied with, the problem can be reduced to an ordinary continuous beam analysis by introducing two extra joints for each web opening. For this purpose, it is necessary to estimate the stiffnesses of the various segments comprising the member.

Stiffness of beam segments

Stiffness calculations may be based on the gross concrete section as permitted by the ACI Code (1995). The modulus of elasticity of concrete according to section 8.5.1 of the Code can be taken as:

$$E_c = 4730\sqrt{f'_c} \tag{5.8}$$

where f'_c is the cylinder compressive strength of concrete (in MPa) and the shear modulus may be taken as:

$$G = \frac{E_c}{2(1+\nu)} \tag{5.9}$$

where the Poisson's ratio, ν, for concrete is taken as 0.2 as recommended by BS 8110 (1997). In calculating the equivalent flexural stiffness of an opening segment, $(EI)_{eq}$, the moment of inertia based on the concrete section minus the void due to the opening should be used.

The equivalent shear stiffness for an opening segment can be obtained as (Mansur et al., 1992)

$$(GA)_{eq} = \frac{12\,E_c\,(I_{gt} + I_{gb})}{\ell_e^2} \tag{5.10}$$

where I_{gt} and I_{gb} are the gross moment of inertia for top and bottom chord members, respectively, and ℓ_e is the effective length of an opening which has been empirically established as (Tan et al., 1996):

$$\ell_e = \frac{\ell_o}{1 - \left(\frac{d_o}{h}\right)^{1.5}} \tag{5.11}$$

where ℓ_o, d_o, and h are the opening length, opening depth, and beam depth, respectively. The shearing deformation of the solid segments is generally ignored in beam design.

Bending moment and shear force envelopes

The beam can be analyzed for all possible load combinations by any elastic method to obtain the shear force and bending moment envelopes. Here, the Direct Stiffness Method (Weaver and Gere, 1980) is recommended because it can be easily modified to include shear deformations and be easily translated into a computer algorithm.

5.3.2.2 Design for Strength

Knowing the bending moment and shear force envelopes, the solid segments of the beam can be designed in the usual manner. The recommended design process for the opening segment is based on the observed Vierendeel truss behavior of chord members at an opening. That is, consistent with test results, contraflexure points are assumed at midspan of chord members, for which the axial load is obtained by dividing the beam moment at the center of the opening by the distance between the plastic centroids of the chord members. The shear force acting at the center of the opening is distributed between the chord members according to their relative flexural stiffnesses. Such an assumption has been found to give a realistic distribution of the applied shear (Barney et al., 1977) and simplifies the calculation. The moments at the ends of the chord member are then calculated from statics. The steps involved are summarized as follows.

Forces and moments in chord members

Determine the ultimate design bending moment, M_m, and shear force, V_m, at the middle of the opening segment from bending moment and shear force envelopes obtained from the global action, and calculate axial forces N_t and N_b (positive for compression) acting in the top and bottom chords, respectively, as:

$$N_t = \frac{M_m}{z} \tag{5.12}$$

$$N_b = -N_t \tag{5.13}$$

where z is the distance between the plastic centroids of the top and bottom chords.

Distribute the applied shear between the top and bottom chords in proportion to their gross flexural stiffness as:

$$V_t = V_m\left(\frac{I_{gt}}{I_{gt}+I_{gb}}\right) \tag{5.14}$$

$$V_b = V_m\left(\frac{I_{gb}}{I_{gt}+I_{gb}}\right) \tag{5.15}$$

where V_t and V_b are the shear forces carried by the top and bottom chords, respectively.

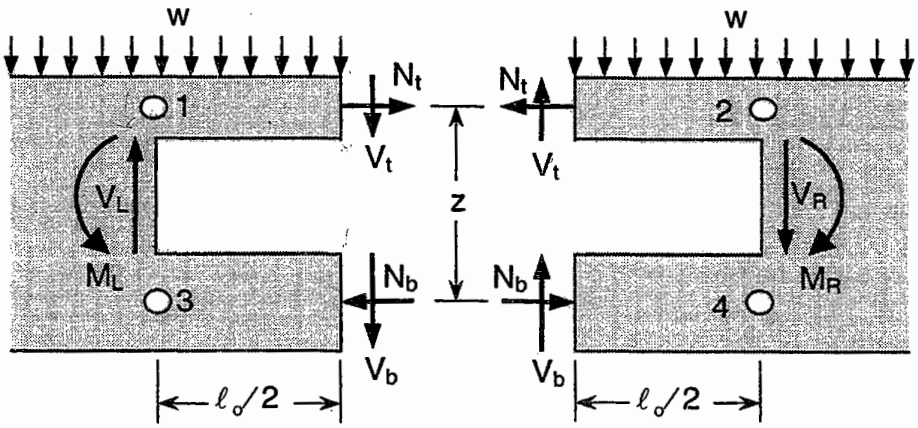

Figure 5.10 Free-body diagram of opening segment.

Calculate moments at the ends of the top and bottom chords from statics (refer to Fig. 5.10):

$$M_1 = -\frac{w\ell_o^2}{8} - \frac{V_t \ell_o}{2} \tag{5.16}$$

$$M_2 = -\frac{w\ell_o^2}{8} + \frac{V_t \ell_o}{2} \tag{5.17}$$

$$M_3 = -\frac{V_b \ell_o}{2} \tag{5.18}$$

$$M_4 = \frac{V_b \ell_o}{2} \tag{5.19}$$

where w is the uniformly distributed load acting directly on the top chord and M is the moment. The subscripts 1, 2, 3, and 4 designate the opening corners as shown in Fig. 5.10.

Stability of compression chord

When the section being analyzed is a T-beam, the effective width of flange in determining the properties and capacities of the compressive strut should not exceed the limits set by the ACI Code (1995) in section 8.10.2. Where the opening segment is subject to positive bending (for example, in the midspan region of a continuous beam), the compression (top) chord will be restrained by the continuity of the slab and, thus, may be considered as a non-sway frame member for which, according to section 10.12.2 of the Code, the effects of slenderness may be neglected when

$$\frac{k\ell_u}{r} < 34 - 12\frac{M_{1b}}{M_{2b}} \tag{5.20}$$

in which the effective length factor k is taken as 1, ℓ_u is the unsupported length of the compression chord, and r is the radius of gyration. The values of M_{1b} and M_{2b} can be taken as M_3 and M_1, respectively, with the signs as dictated by section 10.12.2 of the ACI Code. According to the Code, r can be taken as:

$$r = 0.3\, d_c \tag{5.21}$$

where d_c can be taken as the depth of the compression chord. However, when an opening segment is subject to negative bending (for example, in between the inflection points and the support of a continuous beam), the compression (bottom) chord should be considered as a non-sway frame member for which, according to section 10.13.2 of the ACI Code, the effects of slenderness may be neglected when

$$\frac{k\ell_u}{r} < 22 \tag{5.22}$$

If Eq. (5.20) or Eq. (5.22) is not satisfied, the moment magnification method as described in section 10.12 of ACI Code (1995) may be used to design the compression chord. However, it is suggested that the dimensions of the compression chord be revised so as to eliminate the effects of slenderness.

Design of longitudinal reinforcement for chord members

The longitudinal reinforcement in the top and bottom of the solid section adjacent to the opening should be continued throughout the opening segments. Additional reinforcement required to resist the combined moment and axial force in each chord member is designed and, as a trial, it could be such that each chord is symmetrically reinforced. With the reinforcement for the chord members so decided, the corresponding idealized column interaction diagrams can be constructed by the method of strain compatibility. The critical combinations of bending moment and axial load for the chord members as determined earlier are then plotted in the interaction diagrams. If all the combinations fall within the appropriate interaction diagrams, the reinforcement provided will be sufficient. Otherwise, a revision of reinforcement is necessary. Also, the flexural capacity of the top chord should be sufficient to support any direct external loading.

Design of shear reinforcement for chord members

The shear forces carried by the top and bottom chords are given by Eqs. (5.14) and (5.15), respectively. Knowing these forces, the required amount of reinforcement can be designed in a manner similar to reinforced concrete beams and slabs. However, according to section 11.3 of the ACI Code, the effects of axial forces in the chord members must be accounted for in design. For a T-beam where the opening is placed flushed with the flange, the top chord can be considered as a slab. Although the flange may be too shallow for effective placement of shear reinforcement, the shear stresses are usually low and, consequently, shear reinforcement would not usually be necessary in the top chord.

Design of post between openings

The post should be designed as a solid segment to carry the total applied shear as described in Art. 3.7 in Chapter 3. The contribution of the corner reinforcement at the two adjacent openings should be ignored.

5.3.2.3 Design for Serviceability

The two important serviceability requirements to be met are cracking and deflection.

Cracking

Assuming that the crack control requirements of the solid segments are met either by proper reinforcement detailing or by physical calculation, the following crack control provisions are recommended for the critical sections at corners of the opening. At each vertical edge of the opening, a combination of vertical stirrups and diagonal bars would be used with a shear concentration factor, η, of 2 such that at least 50% of the shear resistance is provided by the diagonal bars (Tan, 1982). Thus, for each side of the opening, the required area of vertical stirrups, A_v, is given by:

$$A_v = \frac{0.50\,(\eta V)}{\phi\, f_{yv}} \tag{5.23}$$

in which V, ϕ, and f_{yv} are the design shear, capacity reduction factor, and yield stress of stirrups, respectively. The vertical stirrups should be placed as close to the edge of the opening as permitted by the required concrete cover. The required area of diagonal reinforcement, A_d, is given as

$$A_d = \frac{0.50\,(\eta V)}{\phi\, f_{yd} \sin\alpha} \tag{5.24}$$

where f_{yd} is the yield stress and α is the angle of inclination of the diagonal bars to the beam axis. To avoid confusion during construction and to account for any possible load reversal, the same amount of diagonal reinforcement should be provided both at the top and bottom corners of the opening.

Deflections

The indirect way of satisfying the serviceability requirement of deflection by limiting the span-effective depth ratio is not valid for a beam with openings. Therefore, an estimate of the actual service load deflection is necessary. For this purpose, the method used for the analysis of the beam at ultimate load may be used. Since the reinforcement details are fully known, a conservative estimate of service load deflection may be obtained and checked against code requirements by using the cracked moment of inertia of various segments. The equivalent shear stiffness of the opening segment [Eq. (5.3)] can also be calculated using the cracked moment of inertia of the chord members.

EXAMPLE PROBLEM 5.1

A 3-span, continuous reinforced concrete T-beam containing a web opening in the interior span is shown in Fig. E5.1.1. This represents a typical feature of an office floor in which the air-conditioning ducts run along the corridor between two rows of office rooms. The beam carries a dead load G_k, including self-weight, of 14 kN/m and a uniformly distributed imposed load Q_k of 11.3 kN/m. The material properties are: f'_c = 30 MPa; f_y (longitudinal steel) = 460 MPa; and f_{yv} (stirrups) = 250 MPa. Provide a suitable design for the beam with particular emphasis on the opening segment of the beam.

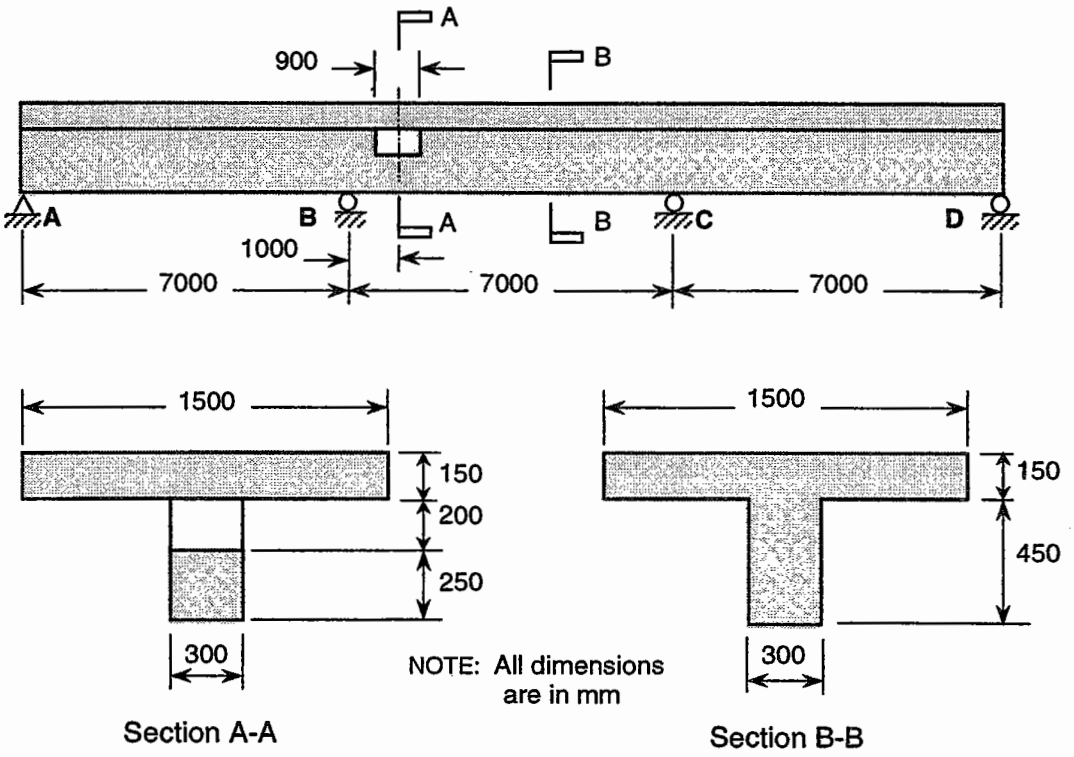

Figure E5.1.1 Three-span continuous beam with web opening in Example Problem 5.1.

SOLUTION

1. STRUCTURAL ANALYSIS

(a) Calculate stiffnesses of beam segments

From Eqs. (5.8) and (5.9), the modulus of elasticity and modulus of rigidity are

$$E_c = 26{,}000 \text{ MPa; and } G = 10{,}800 \text{ MPa}$$

Since the effective slab width as T-beam flange = 1500 mm (ACI Code, section

8.10.2), the gross moment of inertia of the solid section, opening section, top chord and bottom chord, respectively, are

$$I_{gs} = 1.03 \times 10^{10}\ \text{mm}^4;\ I_{go} = 9.81 \times 10^{9}\ \text{mm}^4;\ I_{gt} = 4.22 \times 10^{8}\ \text{mm}^4;$$
$$\text{and}\quad I_{gb} = 3.91 \times 10^{8}\ \text{mm}^4$$

Also, the effective length of opening and the cross-sectional area of the solid segment are given, respectively, as

$$\ell_e = 1114.5\ \text{mm [refer to Eq. (5.11)]; and } A_{so} = 3.6 \times 10^{5}\ \text{mm}^2$$

Hence, for the solid segment,

$$E_c I_{gs} = 2.67 \times 10^{14}\ \text{Nmm}^2; \text{ and } GA_{so} = 3.89 \times 10^{9}\ \text{N}$$

For the opening segment, the equivalent flexural stiffness is based on gross concrete section minus the void due to the opening and the equivalent shear stiffness is obtained by Eq. (5.10). Thus,

$$(EI)_{eq} = 2.54 \times 10^{14}\ \text{Nmm}^2; \text{ and } (GA)_{eq} = 2.03 \times 10^{8}\ \text{N}$$

(b) Obtain bending moment and shear force envelopes

The method of analysis described herein was used to analyze the beam for all possible factored load combinations (refer to Fig. E5.1.2). The equivalent segmented beams for the analysis are shown in Fig. E5.1.3, and the results are presented in Fig. E5.1.4 with 0% moment redistribution at ultimate.

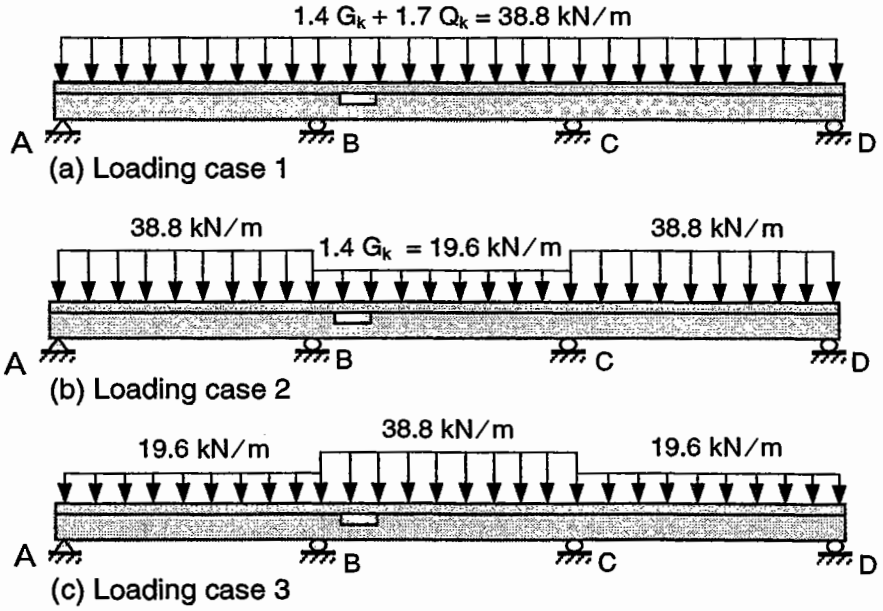

Figure E5.1.2 Loading combination.

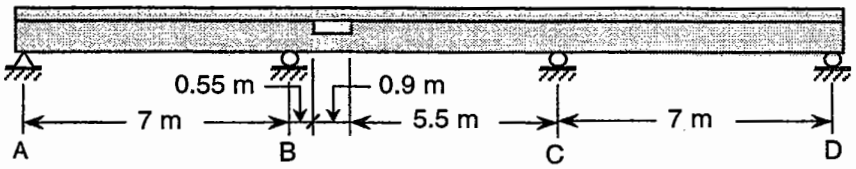

(a) Continuous beam with opening

NOTE:
J1, J2, ...Joints
1, 2, ...Members

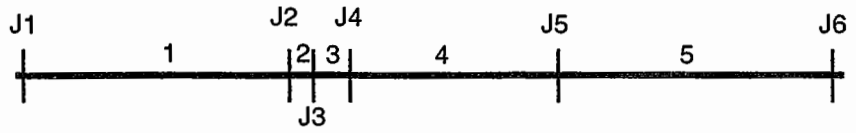

(b) Equivalent segmented beam for ultimate load analysis

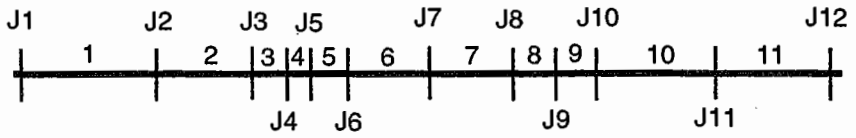

(c) Equivalent segmented beam for service load analysis

Figure E5.1.3 Equivalent segmented beam.

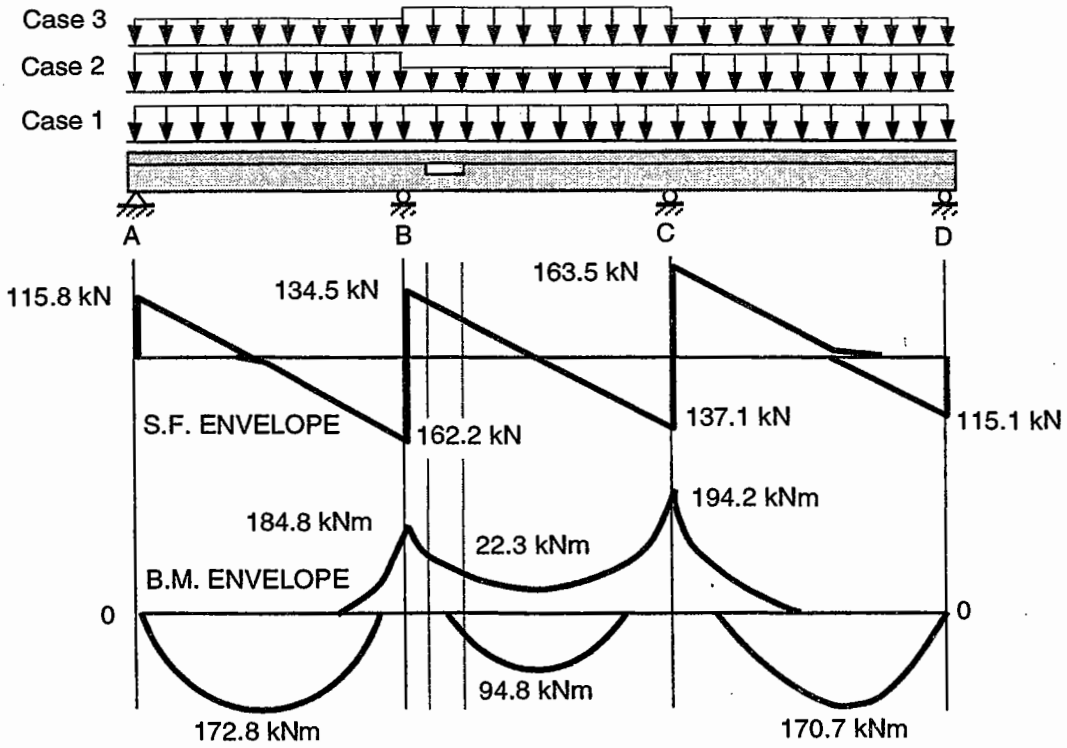

Figure E5.1.4 Shear force and bending moment envelopes.

2. DESIGN FOR STRENGTH

(a) Design of critical solid section

The critical solid sections were designed for bending and shear in the usual manner. Table E5.1.1 summarizes the final output.

Table E5.1.1 Summary of flexural design for critical solid sections.

Location	Moment (kNm)	Main reinforcement
Span AB	172.8	4T16 (bottom)
Support B	–184.8	12T10 (top)
Span BC	94.8, –22.3	8T10 (top); 4T16 & 2T10 (bottom)
Support C	–194.2	12T10 (top)
Span CD	170.7	4T16 (bottom)

Note: Shear reinforcement consisting of R8 at 200 mm spacing is to be provided throughout the beam.

(b) Design of the opening segment

For the opening segment, the axial loads and shear forces in chord members (refer to Fig. E5.1.2) are evaluated from the bending moment M_m and shear force V_m at the center of opening for each loading pattern using Eqs. (5.12) to (5.15) with z = 400 mm and are shown in Table E5.1.2. The secondary moments at the critical end sections, calculated by Eqs. (5.16) to (5.19), are shown in Table E5.1.3.

The opening segment is subject to negative bending. Therefore, the compression chord is considered as a non-sway frame member. Since $r = 0.3 \times 250 = 75$ mm [refer Eq. (5.21)] and $\ell_u = 900$ mm,

$$k\ell_u/r = 1 \times 900/75 = 12 < 22 \quad \text{[refer to Eq. (5.22)]}$$

Hence, the compression chord is satisfactory with regard to stability.

Table E5.1.2 Shear and axial forces at midspan of chord members.

Loading case	M_m (kNm)	V_m (kN)	V_t (kN)	V_b (kN)	$N_t = -N_b$ (kN)
1	– 69.7	95.7	49.8	45.9	174.3
2	– 81.8	48.3	25.1	23.2	204.5
3	– 23.2	95.7	49.8	45.9	58.0

Table E5.1.3 Moments at critical end sections of chord members.

Loading case	Top chord		Bottom chord	
	M_1 (kNm)	M_2 (kNm)	M_3 (kNm)	M_4 (kNm)
1	−22.0	14.1	−19.5	19.5
2	−8.4	5.6	−7.6	7.6
3	−23.0	15.1	−20.7	20.7

Longitudinal reinforcement: From Table E5.1.1, it is seen that the solid section adjacent to the opening is provided with 12 nos. of T10 bars (high-strength deformed bars of 10 mm in diameter) and 4 nos. of T16 (high-strength deformed bars of 16 mm in diameter). Hence, for symmetrical arrangement of reinforcement, provide the top chord with an additional 12 nos. of T10 bars at the bottom and the bottom chord with an additional 4 nos. of T16 bars at the top as a first trial.

For the tension chord, only the bending-tension interaction curves are needed while for the compression chord, the bending-compression interaction curves are required. The interaction curves are shown in Fig. E5.1.5 together with the bending moment-axial force combinations for the end sections of the chord members. Since all the points fall within the respective interaction diagrams, the amount of reinforcement provided is satisfactory.

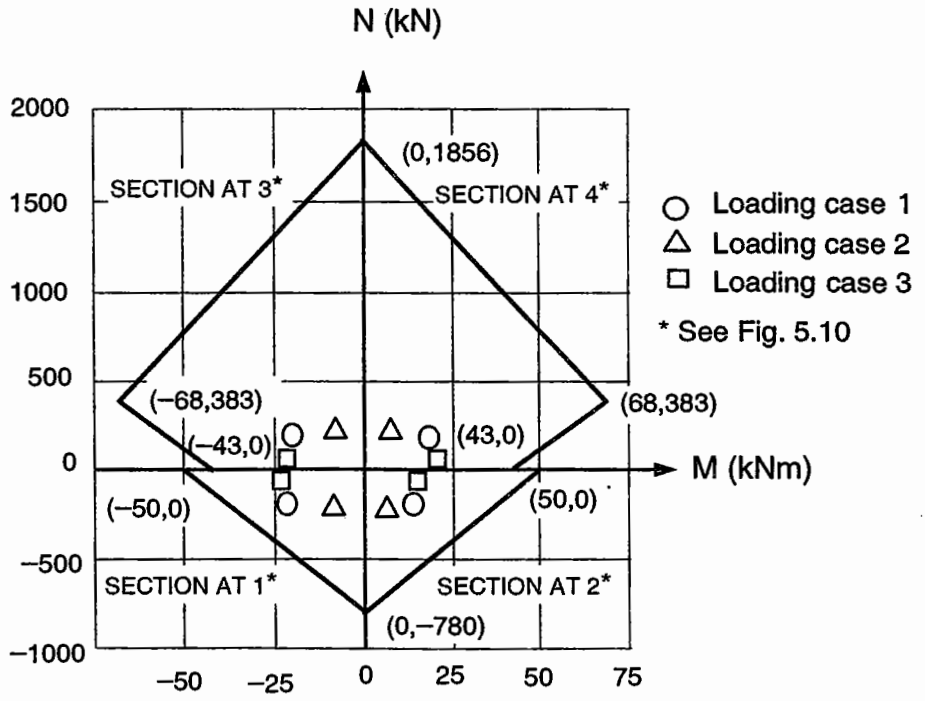

Figure E5.1.5 Linearized interaction diagrams for chord members.

The uniformly distributed loading is carried directly by the top chord over the opening segment and creates a midspan moment of $38.8 \times 0.9^2/24 = 1.31$ kNm. This is less than the pure bending moment capacity of 49.6 kNm for the top chord [refer to Fig. E5.1.5].

Shear reinforcement: *The* maximum shear of 95.7 kN at opening center occurs for loading cases 1 and 3 [refer to Fig. E5.1.4]. Therefore, from Table E5.1.2, the design shear is

$$V_t = 49.8 \text{ kN and } V_b = 45.9 \text{ kN}$$

The top chord is subject to combined bending and axial tension, thus the shear strength of concrete is [ACI Code, section 11.3.2.3]:

$$\phi V_c = 0.85 \times 0.17 \left[1 + 0.29 \frac{-174.3}{1500 \times 150}\right] \sqrt{30} \times 1500 \times 95 = 112.7 \text{ kN} > 49.8 \text{kN}$$

The top chord is treated as a slab and no links are required. The bottom chord is subject to combined bending and axial compression, thus the shear strength of concrete can be taken as [ACI Code (1995), section 11.3.1.2]:

$$\phi V_c = 0.85 \times 0.17 \left[1 + 0.073 \frac{58}{300 \times 120}\right] \sqrt{30} \times 300 \times 192 = 45.6 \text{ kN} < 45.9 \text{ kN}$$

The bottom chord is treated as a beam, therefore a minimum amount of links must be provided. The maximum spacing limit is $d/2 = 192/2 = 96$ mm [ACI Code, section 11.5.4.1]. Therefore, provide stirrups of M8 (mild steel bars of 8 mm diameter) at 90 mm spacing.

3. DESIGN FOR SERVICEABILITY

(a) Cracking

Crack control requirements of the solid segments are met by proper reinforcement detailing. For the opening segment, the maximum shear at the left edge occurs for loading case 1 and case 3. That is,

$$V_l = 95.7 + 38.8 \times 0.45 = 113.2 \text{ kN}$$

Assuming $\eta = 2$, $\alpha = 45^\circ$, f_{yd} and $f_{yv} = 460$ MPa, and 75% of the total shear is carried by the diagonal bars, the required areas of vertical stirrups and diagonal bars [refer to Eqs. (5.23) and (5.24)] are:

$$A_v = 0.25 \times 2 \times 113.2/(0.85 \times 460) = 145 \text{ mm}^2$$

$$A_d = 0.75 \times 2 \times 113.2/(0.85 \times 460 \sin 45^\circ) = 614 \text{ mm}^2$$

Therefore, provide 1 no. of T10 vertical stirrup (area of 157.1 mm^2) at 40 mm away from the edge of the opening and 4 nos. of T16 diagonal bars (area of 804 mm^2) at both top and bottom corners.

For the right edge of the opening,

$$V_r = 95.7 - 38.8 \times 0.45 = 78.2 \text{ kN}$$

Hence, the required areas of vertical stirrups and diagonal bars [refer to Eqs. (5.23) and (5.24)] are:

$$A_v = 0.25 \times 2 \times 78.2/(0.85 \times 460) = 100 \text{ mm}^2$$

$$A_d = 0.75 \times 2 \times 78.2/(0.85 \times 460 \sin 45^\circ) = 424 \text{ mm}^2$$

Therefore, provide 1 no. of T10 vertical stirrup (area of 157.1 mm^2) at 40 mm away from the edge of the opening and 4 nos. of T12 diagonal bars (area of 452.4 mm^2) at both top and bottom corners.

(b) Deflections

Short-term deflection: Assuming cracked moment of inertia for various segments, the beam is analyzed using the method suggested herein for a service load of $(G_k + Q_k)$ = 25.3 kN/m. The maximum deflection is found to occur in span AB at 2.98 m from support A with values of 10.3 mm, 5.7 mm, and 4.6 mm, respectively, due to the total load, dead load only, and live load only.

According to the ACI Code (1995), section 9.5.2.6, the allowable short-term deflection for floors not supporting or attached to nonstructural elements likely to be damaged by large deflections is $L/360 = 7000/360 = 19.4$ mm. Since the calculated service load deflection of 4.6 mm is less than this permissible value, the design may be considered satisfactory.

Long-term deflection: Assume that 20% of the live load is being sustained for a period of 5 years. Following the ACI Code, section 9.5.2.5, the additional long-term deflection due to shrinkage and creep may be determined by multiplying the immediate deflection caused by the sustained load, by a factor $\lambda = 2/(1 + 50\rho')$ where ρ' is the ratio of the compression steel at the location when maximum deflection occurs.

In the present case,

$$\rho' = 942/(300 \times 542) = 0.0058$$

Therefore,

$$\lambda = 2/(1 + 50 \times 0.0058) = 1.55$$

For a sustained load of (1.0 G_k + 0.2 Q_k) = 16.3 kN/m, the calculated maximum deflection is 6.6 mm.

Hence, the total long-term deflection is

$$\Delta_{long\text{-}term} = 10.3 + 1.55 \times 6.6 = 20.6 \text{ mm}$$

This amount is less than the allowable long-term deflection (ACI Code, section 9.5.2.6) of $L/240 = 7000/240 = 29.2$ mm. Hence, the design is acceptable.

4. REINFORCEMENT DETAILING

The reinforcement details for the solid segments of the beam should follow the normal detailing procedure for continuous beams. The opening segment requires additional reinforcement, and it should be detailed carefully keeping in mind the strength and crack control requirements. Fig. E5.1.6 shows the final arrangement of reinforcement for the opening segment for satisfactory performance of the beam in question.

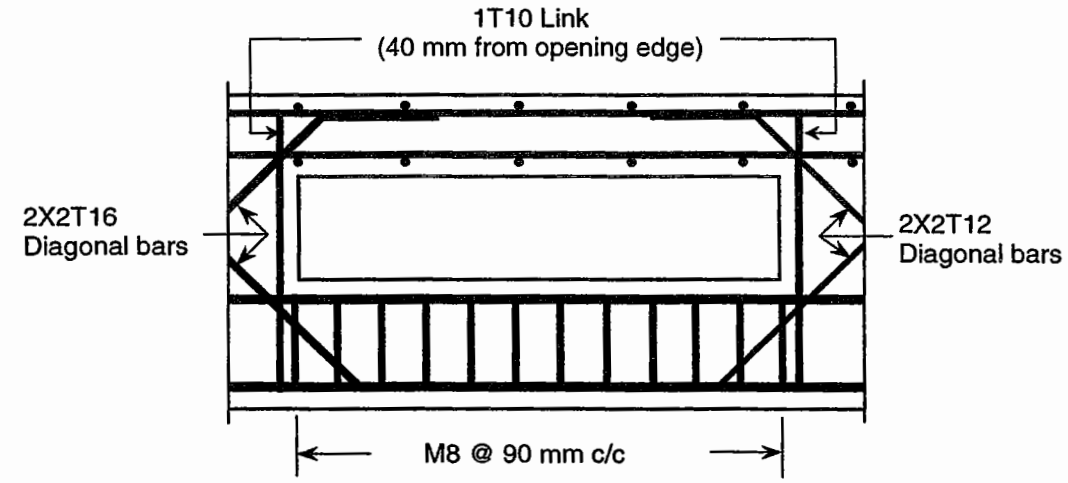

(a) Around the opening

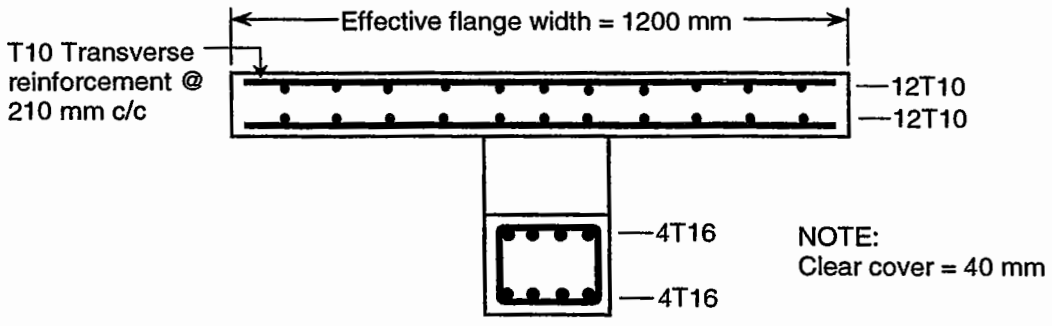

(b) Section through the opening

Figure E5.1.6 Reinforcement details at opening segment.

6
Effect of Prestressing

6.1 GENERAL INTRODUCTION

In general, large web openings can be accommodated in prestressed concrete members without sacrificing strength or violating serviceability requirements (Barney et al., 1977; Dinakaran and Dastry, 1984; Ragan and Warwaruk, 1967; Savage et al., 1996; Warwaruk, 1974).

As it is with reinforced concrete beams, prestressed beams with openings behave similar to Vierendeel trusses, with contraflexure points occurring at approximately the mid-length of the chord members. The shear at the center of an opening may be considered to be distributed between the top and bottom chords in proportion to the chords' stiffness, cross-sectional area, or a combination of these (Barney et al., 1977; Abdalla and Kennedy, 1995a, 1995b; Ragan and Warwaruk, 1967), depending on the extent of cracking of the chord members. Provided that the individual chord members are adequately designed against shear and direct compression or tension failures, the beam fails by the formation of a mechanism consisting of hinges at the ends of the chord members. This is similar to what was described for reinforced concrete beams in Chapter 3.

However, in the case of prestressed concrete, particular attention has to be given to the possibility of cracking around the opening at transfer of prestress. Stirrups should be provided in sufficient quantity on either side of an opening to control these cracks (Barney et al., 1977; Kennedy and Abdalla, 1992; Salam and Harrop, 1979).

In pretensioned beams, web openings should be placed away from the regions required for the development of full tendon force (Barney et al., 1977; Savage et al., 1996). Also, beams in which openings are placed in high shear regions do not perform as well as beams in which openings are located in regions of predominant flexural stresses (Salam and Harrop, 1979). However, beams with web openings do not deflect significantly more than those with solid webs if they have been properly reinforced, especially when the chord members have not cracked at transfer of prestress (Barney et al., 1977; Kennedy and Abdalla, 1992; Ragan and Warwaruk, 1967; Savage et al., 1996).

The effects of different opening parameters on deflections at service load, stress distribution in the vicinity of the opening at ultimate load, and the ultimate strength of prestressed concrete beams are shown in Table 6.1. In general, the horizontal location of the opening has the least effect, followed by the eccentricity, length, and depth of opening, in ascending order. The shear stresses and ultimate loads are more significantly affected by the presence of an opening than the normal stresses and the resulting beam deflections.

Table 6.1 Effect of different opening parameters on response of prestressed beams (Adalla and Kennedy, 1995a).

Parameters	Deflection at service load	Horizontal normal stresses at ultimate load	Shear stresses at ultimate load	Ultimate load
Horizontal location of opening	<10%	10-30%	10-30%	10-30%
Eccentricity of opening	<10%	10-30%	>30%	>30%
Length of opening	10-30%	>30%	>30%	>30%
Depth of opening	>30%	>30%	>30%	10-30%

<10% : not significant; 10-30% : significant; >30% : very significant

6.2 STRESS CONCENTRATION AND STRESS DISTRIBUTION

Finite element analysis carried out on simply-supported, precast pretensioned T-beams with multiple chamfered openings and tendons draped at quarter-points indicated several areas of stress concentrations in the beam, as shown in Fig. 6.1 (Savage et al., 1996).

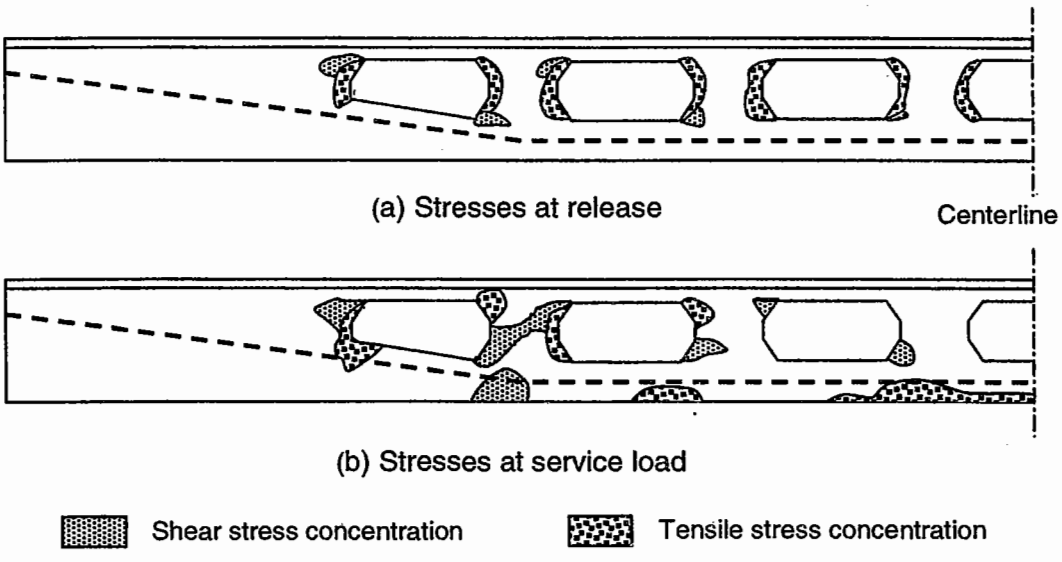

Figure 6.1 Locations of stress concentrations in prestressed beams with web openings (Savage et al., 1996).

At the time of transfer of the prestressing force, compressive stress concentration occurred near the draping points. Tensile stress concentration was observed on both sides of the openings while shear stress concentration was found at the top and bottom corners at the low- and high-moment ends of the opening, respectively, especially in the high shear region.

Under service loads, stress concentration occurred at the corners of the openings, below the post on either side of the opening at midspan and at the edge of the end openings toward the supports.

6.2.1 NORMAL STRESSES

Nonlinear finite-element analysis and tests (Abdalla and Kennedy, 1995a) on unbonded post-tensioned concrete beams indicated that, at the transfer stage, the normal stress distribution in the tension (bottom) chord of the opening is nearly rectangular, while that in the compression (top) chord is nearly triangular, as shown in Fig. 6.2(a). The stress distribution becomes more rectangular in shape as the depth of the tension chord member is decreased, while it becomes more triangular in shape as the depth of the compression chord member is increased.

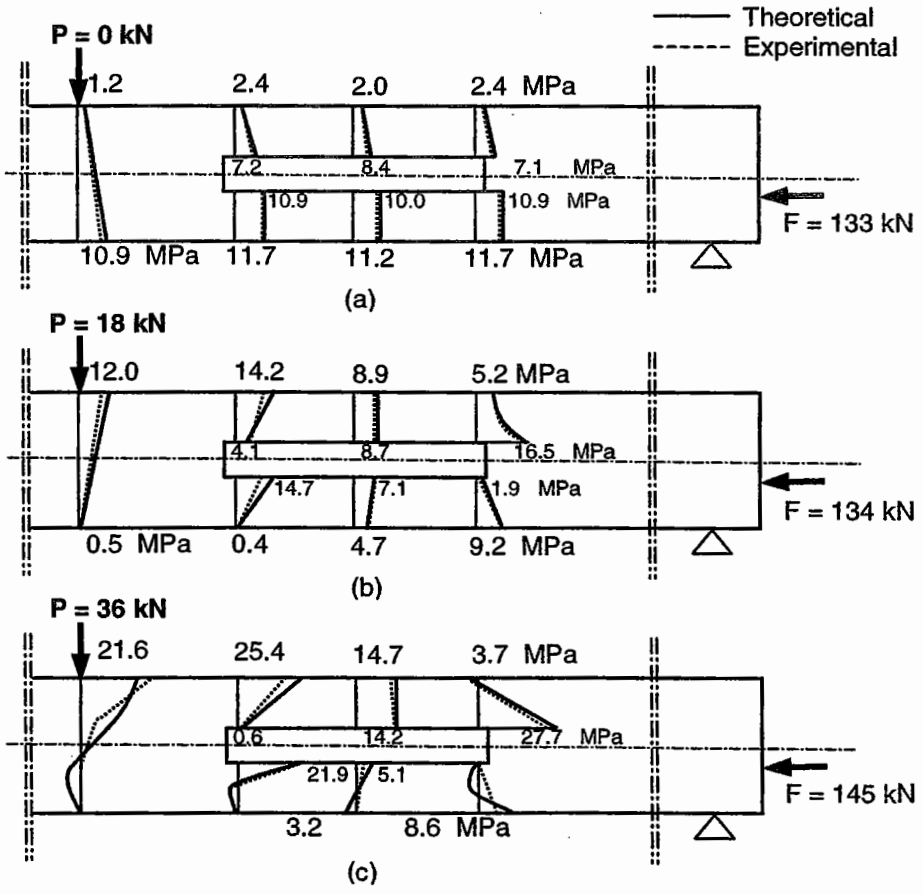

Figure 6.2 Typical normal stress distribution at opening for rectangular beams at (a) transfer stage; (b) service load stage; (c) ultimate stage (Abdalla and Kennedy, 1995a).

At the working and ultimate load stages [Fig. 6.2(b) and (c)], the shear forces induce secondary moments at the end of the chord members. These secondary moments cause cracking of the chord members, which in turn controls the normal stress distribution at ultimate load stage. At this stage, maximum compressive stresses occur on opposite faces at two ends of the compression chord, which together with the shear stresses would lead to shear compression failure of the chord member. The maximum tensile stresses occur in the tension chord member, also on opposite faces at the two ends of the member. Also, at these load stages, the normal stresses increase as the opening is moved near to the applied vertical load. The eccentricity of the opening also affects the normal stress distribution. Increasing the opening length results in higher secondary moments, which lead to higher stresses and a reduction in the cracking load of the beam.

6.2.2 SHEAR STRESSES

The shear stresses in the vicinity of the opening significantly affect the cracking and ultimate capacities of prestressed beams. As shown in Fig. 6.3(a), the prestressing force gives rise to shear stresses close to the opening corners, while the vertical load results in shear stresses in the chord members [Fig. 6.3(b) and (c)]. These shear stresses can cause direct shear failure in the chord members.

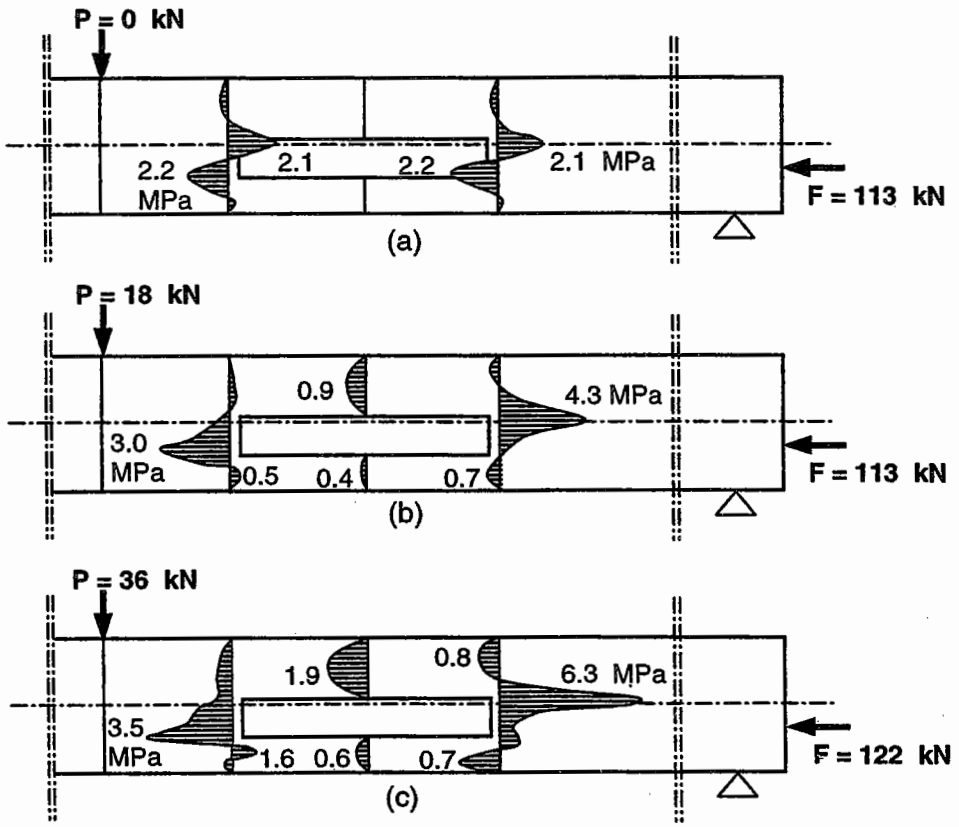

Figure 6.3 Typical shear stress distribution at opening. (a) Transfer stage; (b) Service load stage; (c) Ultimate stage (Abdalla and Kennedy, 1995a).

While the horizontal location and width of the opening have almost no effect on the shear stresses at the transfer stage, the vertical location and depth of the opening significantly affect these stresses. As the opening is moved vertically toward the line of action of the prestressing force or as the depth of the opening increases, the shear stresses around the opening would increase.

The distribution of shear between the compression and tension chords before cracking can be assumed to be in proportion to the square root of the product of area and moment of inertia of the chord members. However, after cracking, the tension chord suffers a reduction in shear capacity while the compression chord carries more shear. After the first crack appears, the shear force in the tension chord may be assumed to remain constant and any increase in the applied load requires an increase in the shear force carried by the compression chord. When the tension chord becomes fully cracked, the entire shear force at the opening may be assumed to be resisted by the compression chord.

6.3 TYPES OF CRACKING AND CRACK CONTROL

Five critical locations for potential cracking of prestressed concrete beams with openings are identified in Fig. 6.4. These are: (a) at the edges of the opening due to the prestressing force; (b) at the corners of the opening due to the framing action at the opening region; (c) in the chord members due to shear; (d) in the chord members due to flexural stresses that arise from secondary moments; and (e) in the tension chord member due to normal tensile stresses. The shear cracks and tension cracks can trigger the complete collapse of the beam.

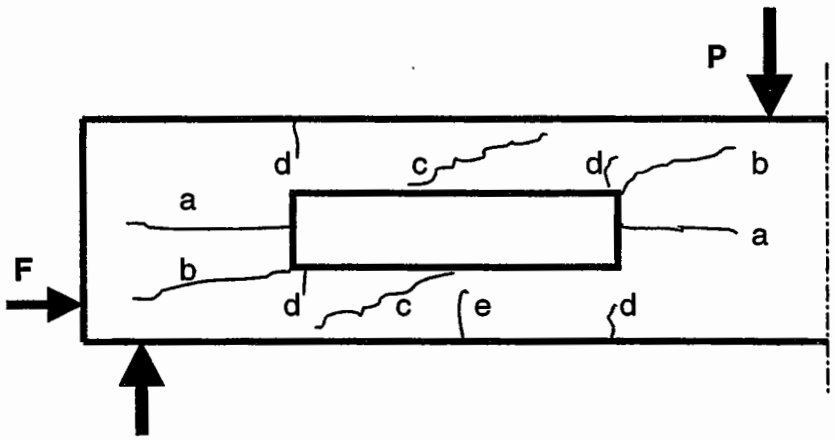

At transfer a: Cracking at mid-depth of opening

At service load stage
b: Cracking at opening corners
c: Shear cracking in chords
d: Flexural cracking in chords
e: Cracking of tension chord

Figure 6.4 Types of cracking around opening (Abdalla and Kennedy, 1995a).

The typical crack pattern for T-beams with openings at initial cracking, near the service load stage (70% of M_u), and at ultimate stage (M_u) is shown in Fig. 6.5. The initial cracks were caused by localized stresses [Fig. 6.1(a)] at the openings. The cracking also indicated Vierendeel truss-like end forces on the chords below some of the openings. As the load on the beam increased, the crack pattern changed from localized cracking to a more uniform cracking caused by the flexure of the overall T-beam.

At failure, there were flexural cracks across the middle half of the T-beam. In beams in which the shear reinforcement adjacent to the openings were not bent into the flange, shear cracks were observed to extend from the top corner of the opening to the underside of the flange, which then extend horizontally along the flange-web interface.

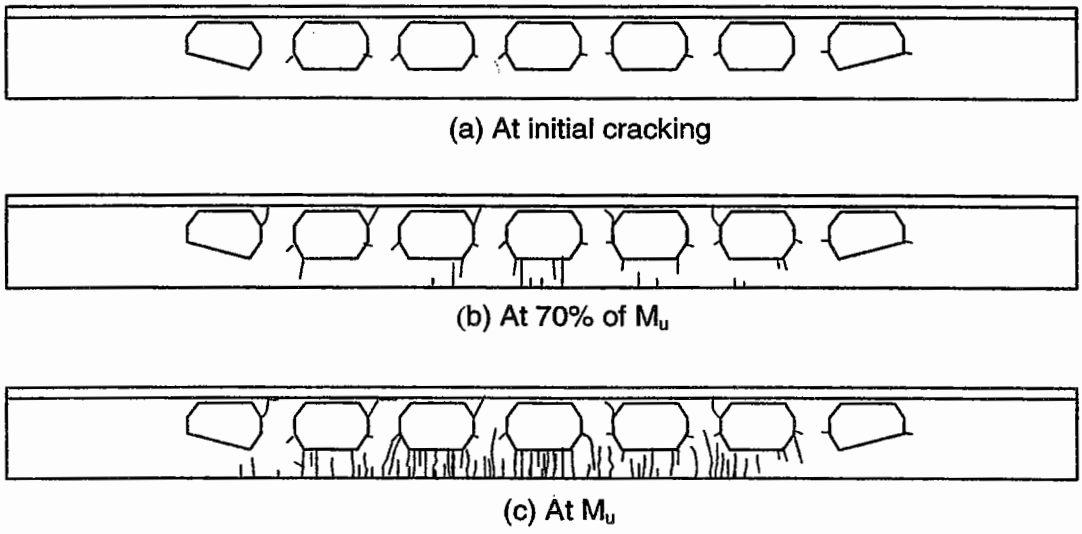

Figure 6.5 Crack development in T-beams with multiple openings (Savage et al., 1996).

6.3.1 CRACKING DUE TO PRESTRESSING FORCE AT TRANSFER STAGE

The prestressing force gives rise to vertical splitting tensile stresses at the opening edges, which cause horizontal cracks. The maximum stresses occur very close to the mid-depth of the opening as shown in Fig. 6.6(a), regardless of the position of the opening or the position of the prestressing force. They increase in magnitude as the opening is moved with respect to the beam depth toward the horizontal line of action of the prestressing force or as the depth of the opening is increased.

The distribution of vertical stress due to prestressing force along the centerline at both sides of the opening, is shown in Fig. 6.6 (b). Maximum vertical tensile stress occurs at the edge of the opening, and this reduces to zero within a distance x_t, defined as the length of tension field. The vertical stress becomes compressive for a distance x_c.

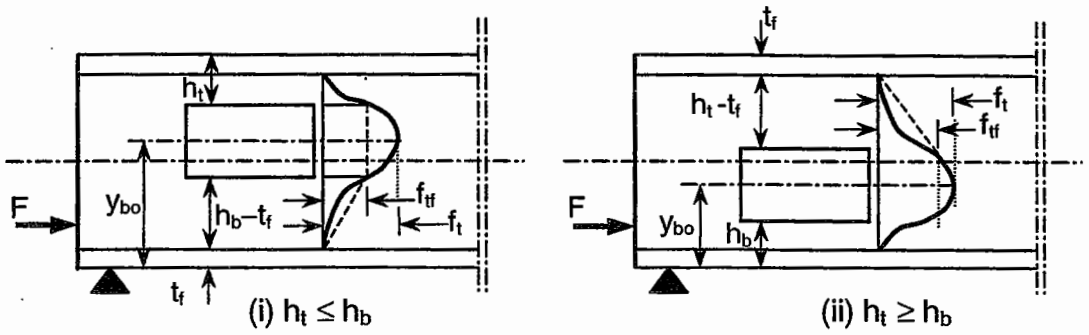

(a) Vertical tensile splitting stress distribution along edge of opening

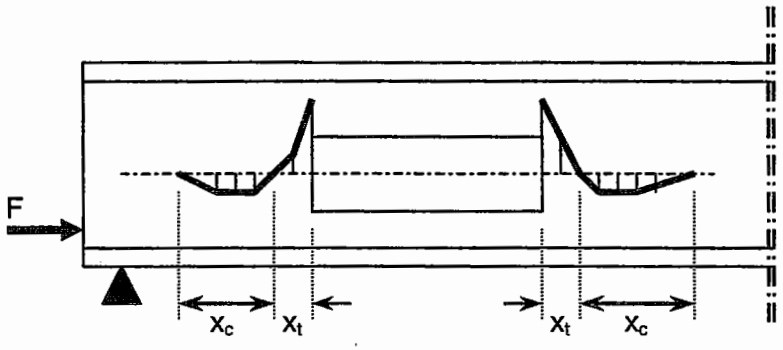

(b) Vertical stress distribution along centerline of opening

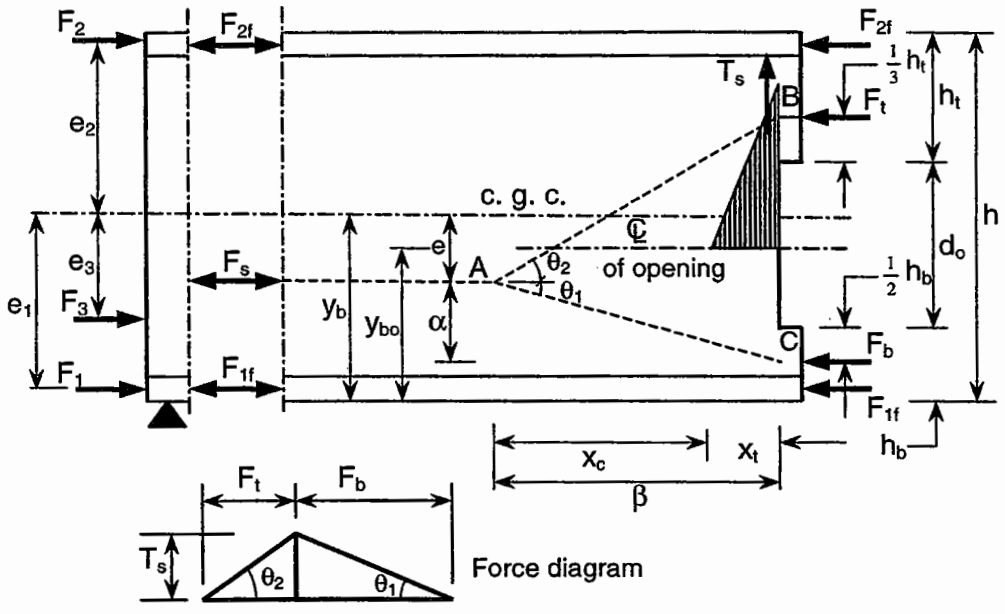

(c) Vertical tensile force at edge of opening

Figure 6.6 Development of vertical tensile force at an opening (Abdalla and Kennedy, 1995a).

The values of x_t and x_c may be taken as (Kennedy and El-Laithy, 1982)

$$x_t = 13\frac{h^2}{d_o y_{bo}} \tag{6.1a}$$

$$x_c = \frac{2hy_{bo}}{3d_o} \tag{6.1b}$$

in which h = depth of beam; y_{bo} = distance from center of opening to bottom edge of beam [Fig. 6.6(c)]; and the numerical coefficient 13 in Eq. (6.1a) is a dimensional constant in millimeters.

The vertical tensile stresses give rise to a vertical tensile splitting force, T_s, as shown in Fig. 6.6(c). For design purposes, the vertical tensile stress distribution can be assumed to be triangular. Thus, the maximum vertical tensile stress, f_t, due to the prestressing force can be calculated as

$$f_t = \frac{2T_s}{x_t b} \tag{6.2}$$

where b is the beam width.

The I-beam with a rectangular opening in Fig. 6.6(c) is subject to three prestressing forces F_1, F_2, and F_3, applied at the bottom flange, top flange, and web of the beam, respectively. The force causing the vertical tensile force at the opening, F_s, is the sum of three components. First, the prestressing force, F_3, applied directly to the web, with the second and the third components being the fractions of F_1 and F_2, whose diffusions into the web are interrupted by the presence of the web opening. It can be shown that

$$F_s = F_1\left(\frac{A_w}{A - A_{f2}}\right) + F_2\left(\frac{A_w}{A - A_{f1}}\right) + F_3 \tag{6.3}$$

in which A_w, A_{f1}, A_{f2}, and A are the areas of the web, bottom flange, top flange, and total cross section, respectively. The eccentricity of F_s from the center of gravity of the cross section, e, can be determined from statics as:

$$e = \left[F_1\left(\frac{A_w}{A - A_{f2}}\right)e_1 - F_2\left(\frac{A_w}{A - A_{f1}}\right)e_2 + F_3 e_3\right] / F_s \tag{6.4}$$

For a T-section, $A_{f1} = 0$ and $A_w = A - A_{f2}$,

$$F_s = F_1 + F_2\left(\frac{A_w}{A}\right) + F_3 \tag{6.5}$$

For a rectangular section, $A_{f1} = 0$, $A_{f2} = 0$, and $A_w = A$,

$$F_s = F_1 + F_2 + F_3 \tag{6.6}$$

The force F_s is assumed to be resisted by internal forces F_t and F_b in the top and bottom chords of the opening and that the diffusion of the force F_s is through the skeletal truss ABC. Assuming that the vertical splitting tensile force T_s acts at the edge of the opening and referring to the force diagram in Fig. 6.6(c), it is seen that $T_s = F_t(\gamma - \alpha)/\beta = F_b\,\alpha/\beta$, which results in

$$T_s = \frac{\alpha(\gamma - \alpha)}{\beta\gamma} F_s \tag{6.7}$$

where

$$\alpha = y_b - e - \frac{h_b}{2} \tag{6.8a}$$

$$\gamma = d_o + \frac{h_t}{3} + \frac{h_b}{2} \tag{6.8b}$$

$$\beta = x_t + x_c \tag{6.8c}$$

in which d_o = depth of opening; h_t = depth of top chord member; h_b = depth of bottom chord member; γ = vertical distance between the forces F_t and F_b; x_t = length of tension field; and x_c = length of compression field [Eq. (6.1)].

Before cracking, both the concrete and the reinforcement resist the vertical splitting tensile force and the total resisting tensile force is

$$T_r = \left\{\left(\frac{x_t b}{2}\right) + \left(\frac{x_t - d'}{x_t}\right)[(n-1)A_s]\right\} f_t \tag{6.9}$$

where A_s = cross-sectional area of closed stirrups at one edge of opening; n = modular ratio; x_t = length of tension field at opening edge, given by Eq. (6.1); b = beam width; d' = distance between opening edge and center of gravity of steel area uniformly distributed within distance x_t, which may be taken as equal to $0.5x_t$; and f_t = direct tensile strength of concrete, which may be taken as equal to $0.33\sqrt{f'_c}$.

Equating $T_s = T_r$ gives the area of vertical stirrups, A_s, required to resist the splitting stress at the transfer stage. If cracking is allowed at the transfer stage, then the stirrups should be designed to resist the total splitting tensile force. Because the splitting stress has a steep gradient, it is recommended that the design stress for the reinforcing steel be taken as one half the allowable stress f_s. That is,

$$A_s = \frac{2T_s}{f_s} \tag{6.10}$$

The required stirrups should be arranged within the distance x_t and be placed as close as possible to the opening edge.

The tensile stress, f_{tf}, at the corners of the opening can be estimated from f_t assuming a linear distribution as shown in Fig. 6.6(c). Thus,

$$f_{tf} = \left(\frac{h_b - t_f}{y_{bo} - t_f}\right) f_t \qquad \text{for } h_b \geq h_t \qquad (6.11)$$

$$f_{tf} = \left(\frac{h_t - t_f}{h - y_{bo} - t_f}\right) f_t \qquad \text{for } h_t \geq h_b \qquad (6.12)$$

where t_f is the flange thickness.

Using Eq. (6.2) and substituting $f_{tf} = 2T_f / x_t b$ in Eqs. (6.11) and (6.12), the maximum tensile force T_f at the four corners of the opening can be estimated as

$$T_f = \left(\frac{h_b - t_f}{y_{bo} - t_f}\right) T_s \qquad \text{for } h_b \geq h_t \qquad (6.13)$$

$$T_f = \left(\frac{h_t - t_f}{h - y_{bo} - t_f}\right) T_s \qquad \text{for } h_t \geq h_b \qquad (6.14)$$

This force T_f will be added to the force due to the vertical load so as to determine the total reinforcement required at the opening edges, as discussed in Art. 6.3.2. Eqs. (6.13) and (6.14) can be applied to rectangular beams by putting $t_f = 0$ in both equations and to T-beams by putting $t_f = 0$ in Eq. (6.13).

6.3.2 CRACKING AROUND THE OPENINGS AT SERVICE LOAD

At the service load stage, the beam is subject to both vertically applied loads as well as the effective prestressing force. Under such loadings, four different types of cracks can develop around the openings, as described in Fig. 6.4.

6.3.2.1 Cracking at Opening Corners

The vertical splitting stress due to prestressing force is shown in Fig. 6.6(a). It reaches a maximum near the mid-depth of the opening and remains relatively high with a value of f_{tf} given by Eqs. (6.11) or (6.12), at the corners of the opening. The stress, f_{tv}, due to the vertical load, on the other hand, has a distribution along a horizontal plane passing through the top opening corner at the high-moment end, changing from tension to compression at a distance x_t as shown in Fig. 6.7. At the lower corner, f_{tv} changes from compression to tension in the same distance x_t. Similar stress distributions occur at the other opening corners at the low-moment end.

Due to the combined action of f_{tf} and f_{tv}, the maximum splitting tensile stress shifts upward at the high-moment end of the opening and downward at the low-moment end of the opening. This can cause cracking of the opening corners, as shown in Fig. 6.4.

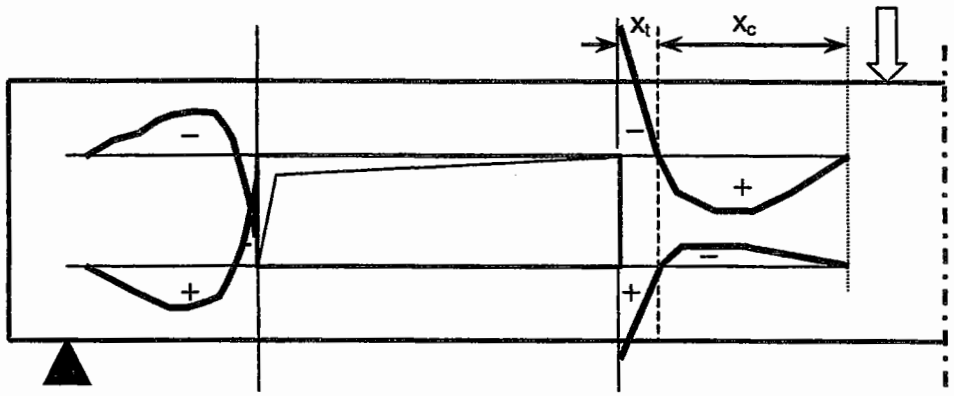

+ Compressive stresses
− Tensile stresses

Figure 6.7 Vertical tensile stresses f_{tv} at opening due to vertical load.

The maximum vertical splitting stress due to vertical load occurs at the opening corner related to the deeper chord. For example, if the top chord is deeper than the bottom chord, it will occur at the corner of opening that is at the high-moment end of the top chord. This is because the splitting stresses are due to secondary moments that result from the shear forces carried by the chords, as shown in Fig. 6.8.

As the deeper chord generally carries a larger amount of shear before cracking, it is subject to higher splitting stresses. Increasing the length of the opening increases the secondary moment at the opening edges and results in higher vertical splitting stresses at the opening corners. Increasing the depth of the opening significantly increases the vertical splitting stress at the upper and lower corners of the opening at the high-moment and low-moment ends, respectively.

The secondary moments at the opening chords are transferred to the solid segments at the opening edges by framing action. Assume that the width of the solid segments to be $(x_t + x_c)$, where x_t and x_c are as previously given in Eq. (6.1). Then, it can be seen that the secondary moment at each opening corner is resisted by a couple formed by two forces, T_v and C_v, where T_v is assumed to act at a distance $x_t / 3$ from the corner and C_v at the middle of the distance x_c. Thus, the tensile force T_v due to the vertical load can be calculated from

$$T_v = \frac{(M_s)_t}{\left(\frac{2x_t}{3} + \frac{x_c}{2}\right)} \tag{6.15}$$

in which $(M_s)_t$ is the secondary moment at the top chord of the opening. Assuming a triangular distribution for the vertical splitting stress, the maximum tensile stress due to vertical load only can be calculated as

$$f_{tv} = \frac{2T}{x_t b} \tag{6.16}$$

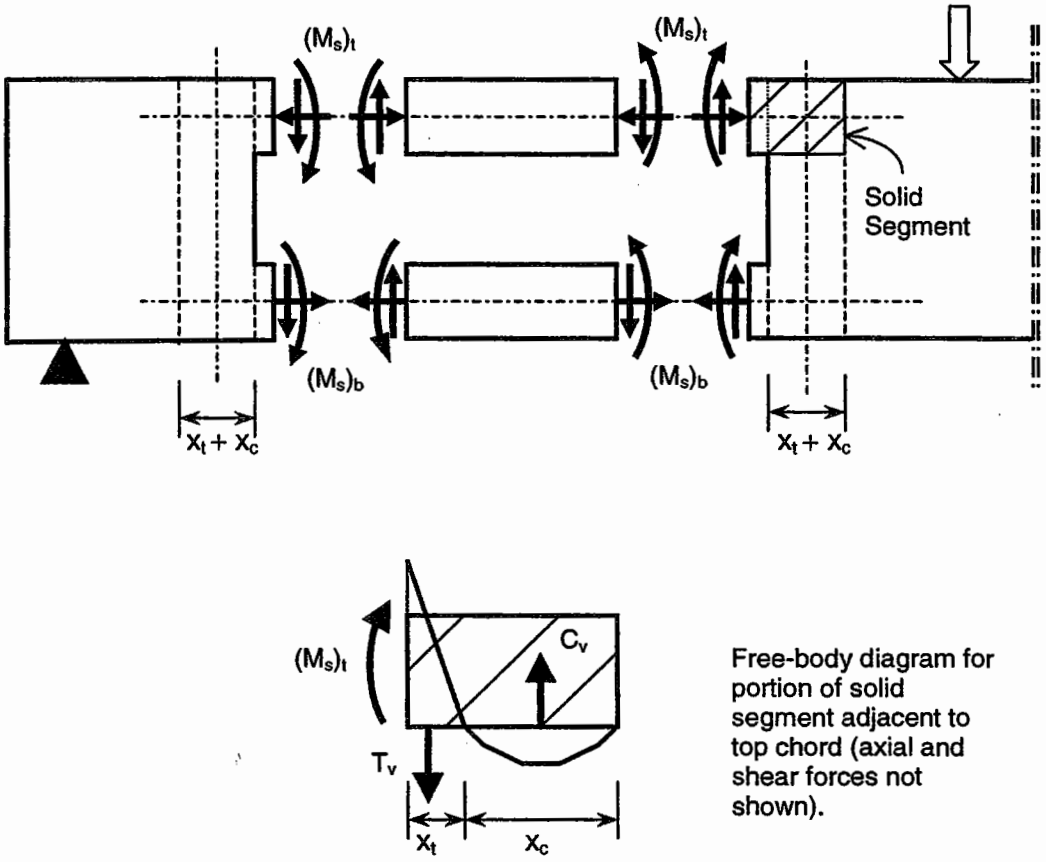

Figure 6.8 Framing action around opening.

The values of $(M_s)_t$ and $(M_s)_b$ at the top and bottom chords of the opening can be determined by considering Vierendeel truss behavior at the opening and assuming contraflexure points at mid-length of the chord members, as described in Chapter 3, Arts. 3.2 and 3.4. In this case, the shear force can be distributed between the chord members in proportion to their cross-sectional areas or flexural stiffnesses or, as suggested by Abdalla and Kennedy (1995b), in accordance to

$$\frac{V_b}{V} = \frac{\sqrt{A_{bw} I_b}}{\sqrt{A_{bw} I_b} + \sqrt{A_{tw} I_t}} \tag{6.17}$$

where V_b = shear force carried by bottom chord; V = total shear force at center of opening; $A_{bw} = bh_b$ = area of bottom web; $A_{tw} = bh_t$ = area of top web; I_b, I_t = moments of inertia of bottom and top chords about their centroidal axes, respectively. Eq. (6.17) is valid only when the tension chord is not cracked.

The larger of the values of $(M_s)_t$ and $(M_s)_b$ is used in Eq. (6.15) to determine the tensile force T_v at the opening edge due to the vertical load. The total tensile force due to the final prestressing force at the edge of the opening is $(T_v + T_f)$, where T_v and T_f are given by Eq. (6.15) and Eqs. (6.13) or (6.14), respectively; and T_s in the latter equations is given by Eq. (6.7) with F_s based on the effective prestressing forces. Eq. (6.9) is used to determine the required area of reinforcing steel to prevent cracking at the corners of the opening by substituting T_r by $(T_v + T_f)$. This area of reinforcement should be added to the reinforcement required to resist the shear stresses resulting from the external load on the beam.

The cracks at the opening corners are due to the splitting stress, f_{tf}, resulting from the prestressing force and to the splitting stress, f_{tv}, resulting from the external vertical load. As the tensile force generated from the combination of f_{tf} and f_{tv} is almost vertical, vertical steel reinforcement becomes more effective than inclined reinforcing steel in controlling corner cracking in prestressed beams with openings. This is unlike reinforced concrete beams where the resultant force is inclined more to the longitudinal axis, in which case inclined reinforcing steel would be more effective.

For beams with T- or I-sections, cracking at the opening corners may cause separation along the flange-web interface of the section. Therefore, the reinforcing steel should extend well into the flange with adequate anchorage length to resist such separation.

6.3.2.2 Shear Cracking in Chords

The prestressing force induces shear stresses close to the opening corners, while the applied vertical load produces shear stresses in the opening chords, as shown in Fig. 6.3. The vertical location and the depth of the opening affect the magnitude of these stresses significantly at the working stage before cracking. Excessive shear stresses in the chord members may cause shear cracks, as shown in Fig. 6.4. To avoid such cracking, the shear stresses must not exceed the allowable shear stress.

Before cracking, the ratio of the shear force carried by each chord member may be taken as being given by Eq. (6.17). After cracking of the chord members, the shear force carried by each chord depends on the level of cracking of that chord. If the tension force in the chord is less than $0.63A_b\sqrt{f'_c}$, the compression chord is assumed to carry a shear force equal to

$$V_t = V - V_{bcr} \tag{6.18}$$

where V_{bcr} is the shear force in the tension chord at cracking, calculated using Eq. (6.17). For design purpose, the tension (bottom) chord is assumed to carry a shear force calculated directly from Eq. (6.17). This results in a conservative design against shear failure in the chord members.

If the crack in the tension chord extends the full depth and the tension force in the chord exceeds $0.63A_b\sqrt{f'_c}$, it is reasonable to assume that the compression chord carries the total shear, that is,

$$\begin{aligned} V_t &= V \\ V_b &= 0 \end{aligned} \tag{6.19}$$

The calculated shear forces should be compared to the ultimate shear capacity, V_{ci}, of a concrete section subject to shear and prestressing forces, given by the ACI Code (1995) as

$$V_{ci} = 0.05\sqrt{f'_c}b_w d + 2\frac{M_{cr}}{\ell_o} \quad \geq \quad 0.14\sqrt{f'_c}b_w d \tag{6.20}$$

where M_{cr} = cracking moment of opening chord; f'_c = concrete strength in MPa; ℓ_o = opening length; b_w = width of web; and d = effective depth of chord member.

If the shear in either of the top or the bottom chord members exceeds V_{ci}, given by Eq. (6.20), vertical stirrups are required to resist the difference. In this case, the shear force carried by vertical stirrups is given by

$$V_s = V_c - V_{ci} \tag{6.21}$$

where V_c is the shear force in the chord member and V_{ci} is the shear force carried by the concrete in that chord.

The amount and arrangement of the vertical stirrups in the chords is determined in the usual way. Thus, the required cross-sectional area of the vertical stirrups is given by $A_v = V_s s/(f_{yv} d)$, where s is the spacing between stirrups, and f_{yv} is the yield strength of the stirrups.

6.3.2.3 Flexural Cracking in Chords

This type of cracking occurs due to the primary moment in the beam and the secondary moment in the chord members, which cause flexural tensile stresses at the upper and lower corners of the opening chords, at the high-moment and low-moment ends, respectively, as shown in Fig. 6.4. The secondary moments result from the shear forces in the chord members, which can be obtained as described in the previous article on cracking at the edge of opening. The maximum tensile stress f_{ts} in the tension (bottom) chord is obtained as

$$f_{ts} = -\frac{F_b}{A_b} + \frac{N}{A_b} + \frac{(M_s)_b y}{I_b} \tag{6.22}$$

where F_b = prestressing force in bottom chord; N = tensile force resulting from primary moment and equal to M_m / z in which M_m is the primary moment at the center of the opening and z is the vertical distance between the centroids of the chord members; $(M_s)_b$ = secondary moment in the tension chord; y = distance from center of gravity to the upper extreme fiber of the tension chord; A_b, I_b = area and

moment of inertia of transformed section consisting of area of concrete A_c and area of transformed steel $(n-1)A_s$ in the tension chord, in which n is the modular ratio.

By assuming an allowable flexural tensile stress as given by the design codes, the area of steel A_s required to prevent flexural cracking in the tension chord can be calculated from Eq. (6.22). Although flexural cracking is more likely to occur in the tension chord, it is noted that the presence of secondary moments at the edges of the opening may also cause cracking in the flange even if it is in the compression chord.

6.3.2.4 Cracking of Tension Chord

For relatively shallow chords, the crack may extend the full depth of the chord if the net axial stresses at the middle of the chord exceed the allowable tensile stress of the concrete. The condition for such cracking is given by

$$T = N - F_b \geq 0.63 A_g \sqrt{f'_c} \tag{6.23}$$

where N = tensile force resulting from primary moment and is equal to M_m / z in which M_m is the primary moment at the center of the opening and z is the vertical distance between the centroids of the chord members, and F_b is the prestressing force in the tension chord.

To prevent this type of cracking, longitudinal reinforcement should be provided. With such reinforcement, the resisting tensile strength of the tension chord becomes

$$T_r = 0.63\sqrt{f'_c}\,[A_c + (n-1)A_s] \tag{6.24}$$

The required area of steel A_s can be calculated by equating T_r of Eq. (6.24) to T of Eq. (6.23). The steel reinforcement should be placed equally near the top and bottom faces of the chord member.

EXAMPLE PROBLEM 6.1

The precast pretensioned double-T floor member shown in Fig. E6.1.1 has been designed to span 14 m in an office building and to carry a service live load of 2.4 kN/m^2 and a superimposed dead load of 0.72 kN/m^2. Four straight prestressing strands, each with a diameter of 12.9 mm (A_{ps} = 100 mm^2 per strand), ultimate strength, f_{pu} of 1860 MPa and modulus of elasticity, E_{ps} of 195 GPa, were placed in each leg at a depth of 510 mm. The strands were pretensioned to $0.7f_{pu}$. An opening measuring 1000 mm by 300 mm is to be provided in each web with its center at a distance of 4 m from one support. The following information is given:

Concrete strength at transfer, f_{ci} = 25 MPa;
Concrete strength at service load, f'_c = 35 MPa;
Prestress loss ratio, η = 0.8;
Modulus of elasticity of concrete, $E_c = 4730\sqrt{f'_c}$

Design the reinforcement required around the opening to resist cracking at the transfer stage and under service load condition.

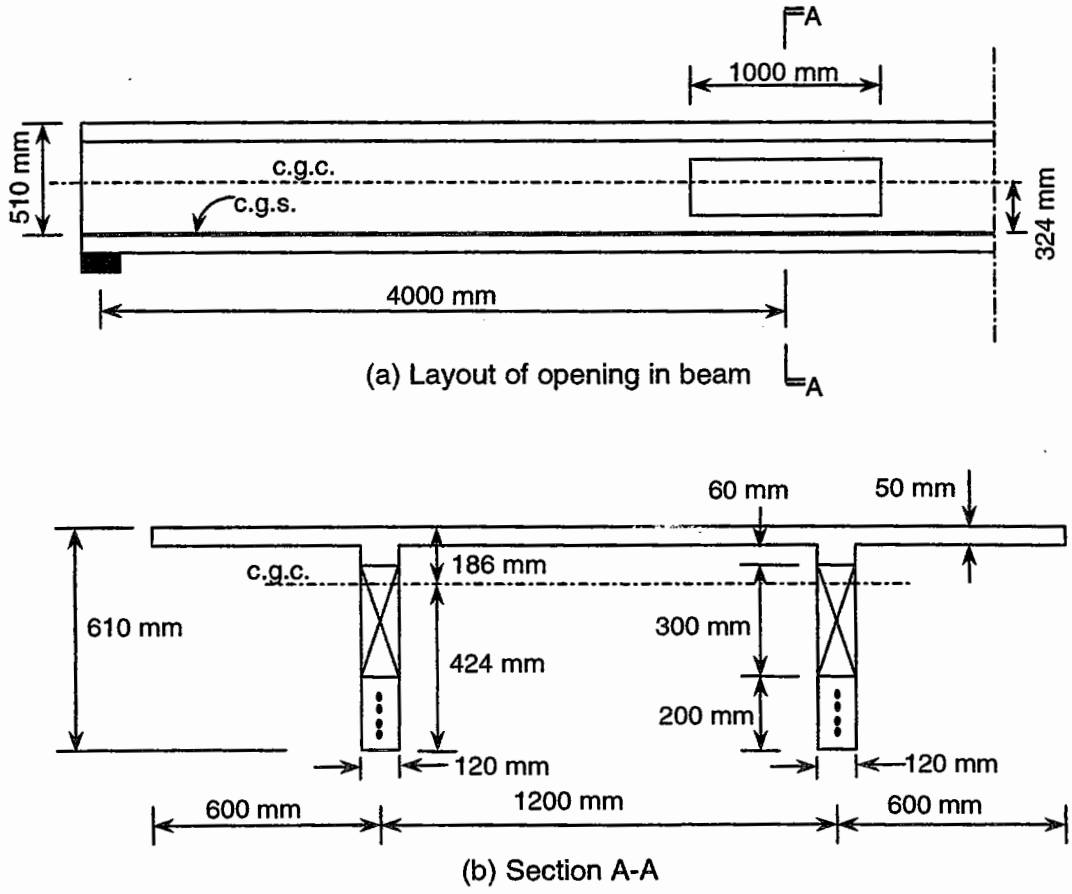

Figure E6.1.1 Precast pretensioned double-T beam with opening.

SOLUTION

(a) Design data

The self-weight of the double-T beam is 6.1 kN/m and the cross-sectional properties are

$$A_c = 254400 \text{ mm}^2; \; I = 8.40 \times 10^9 \text{ mm}^4$$
$$y_b = 424 \text{ mm; and } y_t = 186 \text{ mm}$$

Consider a single leg of the beam. The design service moment at midspan of the beam is $[w_D + w_{SD} + w_L]L^2/8 = [\frac{1}{2} \times 6.1 + 0.72 \times 1.2 + 2.4 \times 1.2] \times 14^2/8 = 166$ kNm, while the corresponding design ultimate moment is $[1.4\,(w_D + w_{SD}) + 1.7w_L]L^2/8 = [1.4(\frac{1}{2} \times 6.1 + 0.72 \times 1.2) + 1.7 \times 2.4 \times 1.2] \times 14^2/8 = 254$ kNm.

(b) Cracking due to prestressing only

From Eq. (6.5),

$$F_s = F_3 = A_{ps}\dot{f}_{pi} = 4 \times 100 \times 0.7 \times 1860 = 521 \text{ kN}$$

Since $y_b = 424$ mm, $e = d_{ps} - y_t = 510 - 186 = 324$ mm and $h_b = 200$ mm, then from Eq. (6.8),

$$\alpha = 424 - 324 - 200/2 \text{ mm} = 0 \text{ mm}$$

Therefore, from Eq. (6.7), $T_s = 0$. In this case, since the prestressing strands are placed with the c.g.s. coinciding with the centroid of the bottom chord member, no cracking at the opening is expected.

(c) Cracking under service load condition

The moment and the shear force at the center of the opening, respectively, are

$$M = 166\,[4\,(4/14)(1 - 4/14)] = 136 \text{ kNm}$$

$$V = [½ \times 6.1 + 0.72 \times 1.2 + 2.4 \times 1.2](14/2 - 4) = 20.4 \text{ kN}$$

Now, $A_{tw}/A_{bw} = h_t/h_b = 110/200 = 0.55$, $I_t = 34.1 \times 10^6$ mm^4, $I_b = 80 \times 10^6$ mm^4, therefore, $I_t/I_b = 34.1/80 = 0.426$. Hence, from Eq. (6.17)

$$V_b/V = 1/[1 + \sqrt{A_{tw}I_t/(A_{bw}I_b)}\,] = 1/\,[1 + \sqrt{(0.55 \times 0.426)}\,] = 0.674$$

$$V_b = 0.674 \times 20.4 = 13.7 \text{ kN}; \quad V_t = 20.4 - 13.7 = 6.7 \text{ kN}$$

The secondary moments are

$$(M_s)_b = 13.7 \times ½ = 6.9 \text{ kNm}$$

$$(M_s)_t = 6.7 \times ½ = 3.4 \text{ kNm}$$

Check for cracking at opening corners

From Eq. (6.1), since $h = 610$ mm, $d_o = 300$ mm, and $y_{bo} = d_o/2 + h_b = 300/2 + 200 = 350$ mm, then

$$x_t = 13 \times 610^2 / (300 \times 350) = 46 \text{ mm}$$

$$x_c = 2 \times 610 \times 350 / (3 \times 300) = 474 \text{ mm}$$

From Eq. (6.15),

$$T_v = 6.9 \times 10^3 / (2/3 \times 46 + ½ \times 474) = 25.7 \text{ kN}$$

From Eq. (6.10), assuming that cracking is allowed but to be controlled, the required area of reinforcement would be $A_s = 2T_v / f_s$ where f_s is the allowable steel stress. Assuming $f_s = 140$ MPa, then $A_s = 2 \times 25.7 \times 10^3 / 140 = 367$ mm^2. Thus, provide two T16 single-leg stirrups (402 mm^2) adjacent to the sides of the opening.

Check for shear cracking in chord members

The centroid of the top chord member is at a distance of 31 mm from the top extreme compressive fiber of the beam section. Therefore the distance between the centroids of the chord members is $z = 610 - 31 - 100 = 479$ mm. Since the moment at the center of the opening is $M_m = 136$ kNm, then the tension force in bottom chord member would be

$$N = M_m / z = 136 / 0.479 = 284 \text{ kN}$$

Also, the prestressing force in the bottom chord is

$$F_b = \eta (A_{ps} f_{pi}) = 0.8 \times 521 = 417 \text{ kN}$$

Therefore, the resultant axial force in the bottom chord is

$$T = N - F_b = 284 - 417 = -133 \text{ kN (compression)}$$

Hence, the bottom chord is not cracked and $V_b = 13.7$ kN and $V_t = 6.7$ kN, as calculated earlier.

For the top compression chord, from Eq. (6.20),

$$V_{ci} \geq 0.14\sqrt{35}\ (1200 \times 50) \times 10^{-3} = 49.7 \text{ kN} > V_t = 6.7 \text{ kN}$$

Similarly, for the bottom chord,

$$V_{ci} \geq 0.14\sqrt{35}\ (120 \times 200) \times 10^{-3} = 19.9 \text{ kN} > V_b = 13.7 \text{ kN}$$

Therefore, the chord members will not crack in shear at service load stage.

Check for flexural cracking in chords

Since $F_t = 0$ kN, and $F_b = 417$ kN, the maximum tensile stress in the tension chord is

$$\begin{aligned} f_{ts} &= -(F_b / A_b) + (N / A_b) + (M_s)_b y / I_b \\ &= -(417 \times 10^3 / 24{,}000) + (284 \times 10^3 / 24{,}000) + \\ &\quad 6.9 \times 10^6 \times 100 / (80 \times 10^6) = 3.08 \text{ MPa} \end{aligned}$$

The allowable flexural tensile stress is $0.5\sqrt{35} = 2.96$ MPa $< f_{ts}$.

Place a WWF (Welded wire fabric) U-shaped mesh with a 75 mm × 75 mm grid and bar diameter of 10 mm as shown in Fig. E6.1.2. Based on transformed section, and since $n = E_{ps}/E_c = 195 \times 10^{-3}/4730\sqrt{35} \approx 195/28 \approx 7$,

$$A_{b,t} = 120 \times 200 + 6 \times 6 \times 78.5 = 26{,}826 \text{ mm}^2$$

$$I_{g,t} = 120 \times 200^3/12 + 4 \times 6 \times 78.5 \times 75^2 = 90.6 \times 10^6 \text{ mm}^4$$

Thus,

$$\begin{aligned} f_{ts} &= -(F_b/A_{b,t}) + (N/A_{b,t}) + (M_s)_b\, y/I_{b,t} \\ &= -(417 \times 10^3/26{,}826) + (284 \times 10^3/26{,}826) + \\ &\quad 6.9 \times 10^6 \times 100/(90.6 \times 10^6) \\ &= -15.55 + 10.59 + 7.62 = 2.66 \text{ MPa} < 0.5\sqrt{35} = 2.96 \text{ MPa} \end{aligned}$$

Therefore, the welded wire fabric provided will prevent flexural cracking in the tension chord.

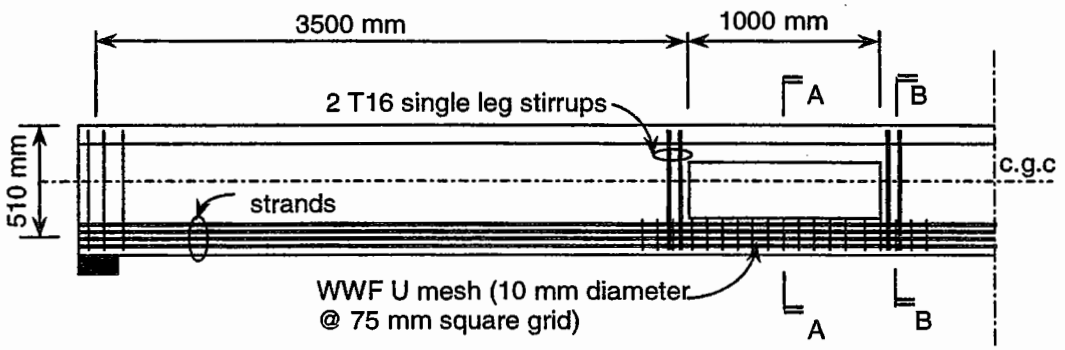

(a) Elevation

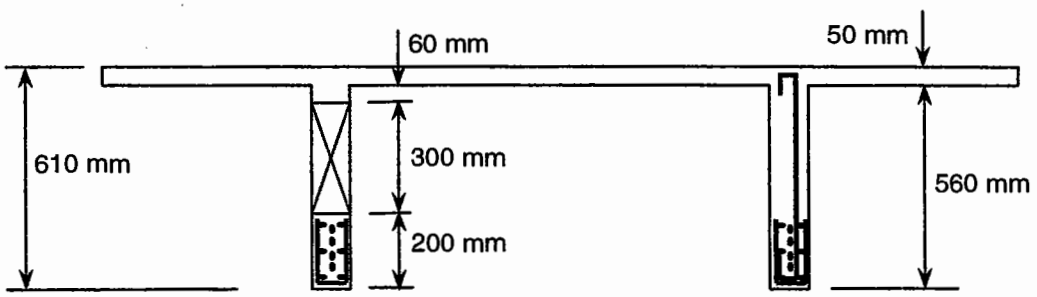

(b) Section A-A (b) Section B-B

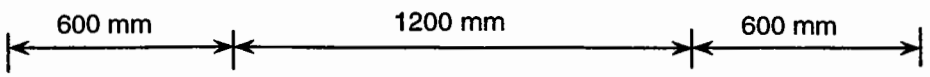

(b) Sections

Figure E6.1.2 Reinforcement details for crack control.

Check for cracking of tension chord:

Since $T = 284 - 417 = -133$ kN (compression), the bottom chord will not crack in direct tension under service load condition. The welded wire mesh provided as in Fig. E6.1.2 will further assist in preventing the cracking of this chord.

Note that Fig. E6.1.2 shows only the reinforcement that is required for crack control at transfer stage and service load stages. The beam, including the chord members, has to be further reinforced to carry the ultimate loads, as described in Art. 6.5.

6.4 DEFLECTIONS

Provided that the beam has been properly detailed as described in Art. 6.5.1, the influence of openings on deflections is minor (Ragan and Warwaruk, 1967; Barney et al., 1977; Dinakaran and Sastry, 1984). For loads up to the point of cracking, the deflection of a beam with web openings is practically identical to that without web openings. Due to the effect of prestressing, the service load deflection of a prestressed concrete beam, in general, is smaller than the corresponding reinforced concrete beam. However, It should be noted that cracking of the beams reduces the beam stiffness considerably and this, in turn, lead to an increase in beam deflection.

The effects of progressive cracking on the load-deflection response of prestressed concrete beams with web openings may be determined analytically by means of a truss model (Alves and Scanlon, 1985). Nevertheless, the recommended practice is to ensure that the tension chord does not crack under service loads. Provided that the chords remain crack-free, deflections may be checked using any recognized method of analysis for normal beams.

A simple method for the calculation of deflections of simply-supported beams is given in Art. 3.6. According to the method, the deflection of a beam with web openings, when the effect of prestressing is included, may be obtained as follows:

$$\delta = \delta_p + \delta_w + (\delta_v)_{opening1} + (\delta_v)_{opening2} + ... \tag{6.25}$$

where δ_p is the deflection (camber) due to the prestressing force and δ_w is the deflection due to applied loads, both calculated by ignoring the presence of any opening, and δ_v is the deflection caused by shear at the opening, which may be calculated as follows:

$$\delta_v = 2\frac{V\left(\frac{\ell_o}{2}\right)^3}{3E_c(I_c + I_t)} \tag{6.26}$$

where E_c is the modulus of elasticity of concrete, I_c and I_t are the moments of inertia of the compression chord and fully cracked tension chord, respectively, and ℓ_o is the length of opening.

6.5 DESIGN AND DETAILING FOR ULTIMATE STRENGTH

Several investigators (Barney et al., 1977; Abdalla and Kennedy, 1995a; Savage et al., 1996) have made recommendations for the design of prestressed concrete beams with web openings. Barney et al. dealt with prestressed, pretensioned beams having straight tendons. Abdalla and Kennedy's method is applicable to simply-supported, post-tensioned unbonded prestressed beams having a single opening with symmetrically reinforced rectangular chord members only, while the procedure of Savage et al. concerns uniformly loaded double tees with web openings.

The above design procedures can be generalized by the following provisions for prestressed concrete beams with web openings in terms of detailing requirements and ultimate strength check.

6.5.1 GENERAL DETAILING REQUIREMENTS AND RECOMMENDATIONS

It is a good practice to observe the following details (also see Fig. 6.9) while incorporating web openings in prestressed concrete beams.

1. Openings should preferably be placed in B-regions where flexural action is predominant, leaving sufficient concrete area on the compression side of the beam to develop the compression stress block at ultimate. They should be located in the web, at a minimum distance equal to the web depth from the end zone or from the vertically applied concentrated load, that is, away from the D-regions.
2. In flanged beams, a gap of 50 mm may be maintained between the top of the opening and the bottom of the flange for better transfer of stress from the flange to the web.
3. Corners of the opening should preferably be rounded off or chamfered.
4. For beams with more than one opening, the distance between two openings should be at least twice the length of the tension field, x_t, defined in Eq. (6.1), or half the opening length, or half the beam depth.
5. Vertical stirrups and / or diagonal bar reinforcement must be provided adjacent to openings in sufficient amount to carry at least twice the design ultimate shear force (see Art. 3.4). These reinforcement should be placed as close as possible to the opening edge and corners.
6. In pretensioned beams, openings must be located outside the required transmission or development length to avoid slip of the prestressing tendons.
7. Draping points for tendons should be located between the one-quarter point and the one-third point of a beam and be centered below a post between openings.
8. The strands should be placed with the centroid coinciding with the centroid of the bottom chord to counteract the localized tensile stresses due to bending.
9. If necessary, a prestressing strand may also be added in the compression chord to counteract localized tensile stress concentrations.

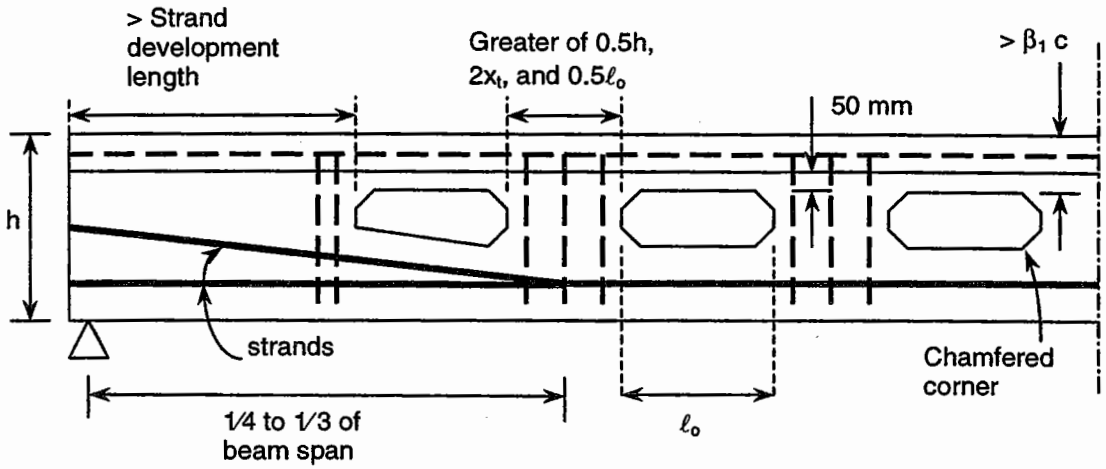

Figure 6.9 General recommendations for detailing of prestressed beams with web openings.

6.5.2 CHECK FOR ULTIMATE STRENGTH

In general, prestressed concrete beams with openings may fail in four different modes. These are (i) mechanism failure due to the formation of plastic hinges at the edge of the opening; (ii) shear failure of chord members; (iii) strut failure in compression chord; and (iv) failure of the tension chord member. Except for the mechanism mode, the other types involving local failure of the chord members, which are sudden and brittle in nature, are therefore undesirable. For design purpose, it would be prudent to design for mechanism failure, and check that this is not preceded by the other modes of failure. Thus, a procedure for the design of openings in prestressed concrete beams to carry the ultimate load can be considered as follows.

6.5.2.1 Design for Mechanism Failure

The method for reinforced concrete beams with openings, as described in Chapter 3, Art. 3.3, can be modified for prestressed concrete beams. It is assumed that for an applied load, the chord members deflect in double curvature with contraflexure points at the mid-length of the chord members.

Based on a simple beam mechanism of failure, the applied load at collapse, P_u, can be related to the moment of resistance of the section at the edge of the opening. Thus, referring to Fig. 3.3, it can be readily shown that for a plastic hinge forming at the high-moment and low-moment ends of the opening, the corresponding values of P_u are, respectively,

$$P_{u,H} = \frac{2M_{p,H}}{\left(a + \frac{\ell_o}{2}\right)} \tag{6.27}$$

and

$$P_{u,L} = \frac{2M_{p,L}}{\left(a - \frac{\ell_o}{2}\right)} \tag{6.28}$$

in which $M_{p,H}$ and $M_{p,L}$ = moment capacities of the high-moment and low-moment ends of the opening, respectively; and a = distance of the low-moment end of the opening from the support. The smaller of $P_{u,H}$ and $P_{u,L}$ given by Eqs. (6.27) and (6.28) is the collapse load.

The normal axial force in each chord is related to the moment at the center of the opening, M_m, by

$$N = \frac{M_m}{z} \tag{6.29}$$

where z = distance between the centroids of the two chords. At failure, the moment capacity will be equal to the capacity of each chord resisting local bending, overall bending, and axial load, that is, referring to Fig. 6.8

$$M_{p,H} = (M_s)_t + (M_s)_b + M_m \tag{6.30}$$

$$M_{p,L} = -(M_s)_t - (M_s)_b + M_m \tag{6.31}$$

Now, the values of $(M_s)_t$ and $(M_s)_b$ are related to the axial load N in the chords according to their strength (N-M) interaction diagram, typically shown in Fig. 3.7. Thus, assuming that $N > N_b$,

$$M_{p,H} = \left(\frac{N_o - \frac{M_m}{z}}{N_o - N_b}\right) M_b + \left(\frac{N'_o - \frac{M_m}{z}}{N'_o}\right) M_o + M_m \tag{6.32}$$

$$M_{p,L} = -\left(\frac{N_o - \frac{M_m}{z}}{N_o - N'_b}\right) M'_o - \left(\frac{N'_o - \frac{M_m}{z}}{N'_o}\right) M'_o + M_m \tag{6.33}$$

in which M_o and M'_o = ultimate moments of resistance of a section in positive and negative bending, respectively; N_o and N'_o = ultimate capacitites of a section in axial compression and tension, respectively; M_b and M'_b = moments of resistance of a balanced section at failure corresponding to positive and negative moments, respectively; and N_b and N'_b = axial compressive forces corresponding to M_b and M'_b, respectively.

Similar to the design of reinforced concrete beams with openings, explained in Art. 3.4.2, the iterative solution starts with a moment M_m based on an assumed applied load. Substituting the values of $M_{p,H}$ and $M_{p,L}$ from Eqs. (6.32) and (6.33) in

(6.27) and (6.28) will yield another estimate for the failure load P_u. This iteration is continued until the assumed applied load and the load resulting from the yield surface are sufficiently close to each other.

6.5.2.2 Check for Compression-Shear Failure

Prestressed beams with rectangular sections may collapse by compression-shear failure when the compression chord fails suddenly under the combined action of the compression force and secondary moments at the ends of the chord, caused by the primary moment and shear force, respectively. The compression-shear failure of the compression chord should be differentiated from the mechanism failure, which involves the formation of plastic hinges at the corners of the opening.

To estimate the ultimate load of the beam corresponding to compression-shear failure, it is assumed that the compression chord has symmetrical reinforcement and bends in double curvature with the contraflexure point at the middle of its length. The distribution of shear force is assumed to follow Eqs. (6.17) to (6.19). That is, before cracking, the chords carry shear according to the root ratio. After cracking occurs in the tension chord, the shear force in that chord remains constant and any increase in shear force is to be carried by the compression chord. When the tension chord becomes fully cracked, the compression chord carries the entire shear force.

For an assumed applied moment M_m at the center of the opening, N can be evaluated from Eq. (6.29). The secondary moment at the opening edges of the compression chord is determined from

$$(M_s)_t = V_t \frac{\ell_o}{2} \tag{6.34}$$

where V_t is the shear carried by the compression chord. Defining $e' = (M_s)_t / N$, it is seen from Eqs. (6.29) and (6.34) that

$$e' = \frac{V_t \ell_o z}{2 M_m} \tag{6.35}$$

According to Whitney (1940), the ultimate compression force N_u of the chord can be determined from

$$N_u = A_g \left[\frac{f'_c}{(3/\xi^2)(e'/h) + 1.18} + \frac{\rho_s f_y}{(2/\gamma)(e'/h) + 1} \right] \tag{6.36}$$

in which $A_g = bh$, $\rho_g = 2A_s / A_g$, $\gamma = (d - d') / h$, and $\xi = d / h$, where b, d, d', and h are the width, effective depth to tensile steel, depth of compression steel, and overall depth of the beam. With the value of e' from Eq. (6.35) and the normal force N_u from Eq. (6.36), the moment at the middle of the opening, M_m, causing a compression-shear failure can be calculated from $M_m = N_u z$. This value of M_m is compared to the initially assumed value. If there is significant difference between them, another iteration is carried out until the assumed moment and the calculated

moment are close to each other. The desired ultimate load is then calculated from the moment at center of opening based on static requirement.

For long compression chords, the effect of the slenderness ratio should also be taken into consideration, as explained in Art. 3.1. That is, the slenderness effect can be neglected if ℓ_o/r is less than 22, where r is the radius of gyration of the chord section. Otherwise, the moment $(M_s)_t$ in Eq. (6.34) should be magnified by a factor as specified by the ACI Code (1995).

6.5.2.3 Check for Shear Failure in Chord Member

The shear failure of chord members may occur due to high shear stresses. The design of reinforcement to prevent shear cracking and consequent shear failure in the chord members, which follows the normal procedure for solid beams, has been dealt with in Art. 6.3.2.

6.5.2.4 Check for Tension Failure of Chord Members

To prevent failure in the tension chord, longitudinal reinforcement must be provided with an area equal to

$$A_s = \frac{N_u - F_b}{\phi f_y} \tag{6.37}$$

where N_u is the tensile force, F_b is the effective prestressing force in the chord, f_y is the yield strength of longitudinal reinforcement, and ϕ is the capacity reduction factor, taken equal to 0.9. In addition, it is recommended that

$$\phi A_s f_y \geq 1.2 T_r \tag{6.38}$$

where T_r is given by Eq. (6.24), which translates Eq. (6.38) into

$$\frac{A_s}{A_c} = \frac{1.2\,(0.63\sqrt{f'_c})}{\phi f_y - 1.2\,[0.63\sqrt{f'_c}\,(\eta - 1)]} \tag{6.39}$$

References

Abdalla, H. and Kennedy, J.B. (1995a). Design of prestressed concrete beams with openings. *Proceedings, ASCE*, Vol. 121, No. 5, May, pp. 890-898.

Abdalla, H. and Kennedy, J.B. (1995b). Design against cracking at openings in prestressed concrete beams. *PCI Journal*, Vol. 40, No. 6, Nov.-Dec., pp. 60-75.

ACI Committee 318 (1995). *Building code requirements for reinforced concrete* (ACI 318-95) *and commentary* (ACI 318R-95). American Concrete Institute, Detroit, 369 pp.

ACI-ASCE Committee 426 (1973). The shear strength of RC members (ACI 426R-74)(Reapproved 1980). *Proceedings, ASCE*, Vol. 99, No. ST6, June, pp. 1168-1171.

Alves, T.M.J. and Scanlon, A. (1985). Deflection of prestressed concrete beams with openings. *Deflections of Concrete Structures*, Special Publication SP-86, American Concrete Institute, pp. 215-230.

Alwis, W.A.M. and Mansur, M.A. (1987). Torsional strength of R/C beams containing rectangular openings. *Journal of Structural Engineering, ASCE*, Vol. 113, No. 11, Nov., pp. 2248-2258.

Architectural Institute of Japan (1988). *AIJ standard for structural calculation of reinforced concrete structures.* (In Japanese).

Architectural Institute of Japan (1994). *AIJ structural design guidelines for reinforced concrete buildings*, 207 pp.

Barney, G.B., Corley, W.G., Hanson, J.M., and Parmelee, R.A. (1977). Behavior and design of prestressed concrete beams with large web openings. *PCI Journal*, Vol. 22, No. 6, Nov.-Dec., pp. 32-61.

Bower, J.E. (1966a). Elastic stresses around holes in wide-flange beams. *Journal of the Structural Division, ASCE*, Vol. 92, No. ST2, Apr., pp. 85-101.

Bower, J.E. (1966b). Experimental stresses in wide-flange beams with holes. *Journal of the Structural Division, ASCE*, Vol. 92, No. ST5, Oct., pp. 167-186.

British Standards Institution (1997). *Structural use of concrete*, BS 8110:Part 1:1997.

Collins, M.P., and Lampert, P. (1973). Redistribution of moments at cracking - the key to simpler torsion design? *Analysis of Structural Systems for Torsion*, Special Publication SP-35, American Concrete Institute, Detroit, pp. 343-383.

Collins, M.P., Walsh, P.F., Archer, F.E., and Hall, A.S. (1968). Ultimate strength of reinforced concrete beams subjected to combined loading. *Torsion of Structural Concrete* SP-18, American Concrete Institute, Detroit, pp. 379-402.

Cook, W.D. and Mitchell, D. (1988). Studies of disturbed regions near discontinuities in reinforced concrete members. *ACI Structural Journal*, Vol. 85, No. 2, Mar.-Apr., pp. 206-216.

Daniel, H.R. and McMullen, A.E.(1977). Torsion in concrete beams containing openings. *Journal of the Structural Division, ASCE*, V.103, ST3, Mar., pp. 607-617.

Dinakaran, V. and Sastry, M.K. (1984). Behavior of post-tensioned prestressed concrete T-beams with large web openings. *Indian Concrete Journal*, Vol. 58, No. 2, Feb., pp. 34-38.

Douglas, T.R. and Gambrell, S.C.(1974). Design of beams with off-center web openings. *Journal of the Structural Division, ASCE,* Vol. 100, No. ST6, June, pp. 1189-1203.

Elfgren, L., Karlson, I., and Losberg, A. (1974). Torsion-bending-shear interaction for concrete beams. *Journal of the Structural Division, ASCE*, Vol. 100, ST8, Aug., pp. 1657-1676.

Hanson, J.M. (1969). Square openings in webs of continuous joists. *PCA Research and Development Bulletin* RD 100.01D, Portland Cement Association, Stokie, Ill. pp. 1-14.

Heller, S.R., Jr. (1953). Reinforced circular holes in bending with shear. *Journal of Applied Mechanics, ASME*, Vol.2, June, pp. 279-285.

Hasnat, A. and Akhtaruzzaman, A.A. (1987). Beams with small rectangular opening under torsion, bending and shear. *Journal of Structural Engineering, ASCE*, Vol. 113, No. 10, Oct., pp. 2253-2270.

Hsu, T.T.C. (1968). Torsion of structural concrete - plain concrete rectangular sections. *Torsion of Structural Concrete*, Special Publication SP-18, American Concrete Institute, pp. 203-238.

Hsu, T.T.C. (1984). *Torsion of reinforced concrete*. Van Nostrand Reinhold Inc., New York, 544 pp.

Hsu, T.T.C. and Burton, K.T.(1974). Design of reinforced concrete spandrel beams. *Journal of the Structural Division, ASCE,* Vol. 100, ST1, Jan., pp. 209-299.

Hsu, T.T.C. and Hwang, C.S. (1977). Torsional limit design of spandrel beams. *ACI Journal*, Proceedings, Vol. 74, No. 2, Feb., pp. 71-79

Hsu, T.T.C. and Hwang, C.S. (1979). Discussion of "Torsion in spandrel beams" by M.A. Mansur and B.V. Rangan. *Journal of the Structural Division, ASCE*, Vol. 105, ST9, Sept., pp. 1858-1862.

Huang, L.M. (1989). Concrete beams with small openings under bending and shear. *MEng. Thesis*, National University of Singapore, 1989, 92pp.

Ichinose, T. and Yokoo, S. (1990). A shear design procedure of reinforced concrete beams with web openings. *Summaries of Technical Papers of Annual Meeting*, Architectural Institute of Japan (In Japanese), pp. 319-322.

Kennedy, J.B. and Abdalla, H. (1992). Static response of prestressed girders with openings. *Journal of Structural Engineering, ASCE,* Vol. 118, No. ST2, Feb., pp. 488-504.

Kennedy, J.B. and El-Laithy, A.M. (1982). Cracking at openings in prestressed beams at transfer. *Proceedings, ASCE*, Vol. 108, No. ST6, June, pp. 1250-1265.

Lee, Y.F. (1989). Strength and stiffness of continuous reinforced concrete beams with openings. *MEng. Thesis*, National University of Singapore, 137 pp.

Lessig, N.N. (1959). Determination of the load-bearing capacity of reinforced concrete elements with rectangular cross section subjected to flexure and torsion. Concrete and Reinforced Concrete Institute, Moscow, Work No. 5, pp. 5-28.

Lorensten, M. (1962). Holes in Reinforced Concrete Girders. *Byggmastaren*, Vol. 41, No. 7, July, pp. 141-152. (English translation from Swedish, XS6506, Portland Cement Association, Skokie, Ill, Feb. 1965.)

Mansur, M.A., (1983). Combined bending and torsion in reinforced concrete beams with rectangular opening. *Concrete International: Design and Construction*, Vol. 5, No. 11, Nov., pp. 51-58.

Mansur, M.A. (1988). Ultimate strength design of beams with large openings. *International Journal of Structures*, Vol. 8, No. 2, July-Dec., pp. 107-125.

Mansur, M.A. (1998). Effect of openings on the behaviour and strength of R/C beams in shear. *Cement and Concrete Composites*, Elsevier Science Ltd., Vol. 20, No. 6, pp. 477-486.

Mansur, M.A. (In Press). Design of R/C beams with small openings under combined loading. *ACI Structural Journal.*

Mansur, M.A. and Hasnat, A. (1979). Concrete beams with small openings under torsion. *Journal of the Structural Division, ASCE*, Vol. 106, ST11, Nov., pp. 2433-2447.

Mansur, M.A., Huang, L.M., Tan, K.H., and Lee, S.L. (1992). Deflections of reinforced concrete beams with web openings. *ACI Structural Journal*, Vol. 89, No. 4, July-Aug., pp. 381-389.

Mansur, M.A. and Paramasivam, P. (1984). Reinforced concrete beams with small opening in bending and torsion. *ACI Journal, Proceedings* Vol. 81, No. 2, Mar.-Apr., pp. 180-185.

Mansur, M.A., Paramasivam, P., and Lee, S.L. (1982).Torsion in reinforced concrete beams containing circular opening. *International Journal of Structures*, Vol. 2, No. 3, July-Sept., pp. 89-98.

Mansur, M.A. and Rangan, B.V. (1978). Torsion in spandrel beams. *Journal of the Structural Division, ASCE*, Vol. 104, ST7, July, pp. 1061-1075.

Mansur, M.A. and Tan, K.H. (1989). Strength of R/C beams with large openings under combined torsion, bending and shear. *Proceedings of the International Conference on Highrise Buildings*, 25-27 Mar., Nanjing, China, pp. 380-385.

Mansur, M.A., Tan, K.H., and Lee, S.L. (1984). Collapse loads of R/C beams with large openings. *Journal of Structural Engineering, ASCE*, Vol. 110, No.11, Nov., pp. 2602-2610.

Mansur, M.A., Tan, K.H., and Lee, S.L. (1985). Design method for reinforced concrete beams with large openings. *ACI Journal, Proceedings* Vol. 82, No.4, July-Aug., pp. 517-524.

Mansur, M.A., Lee, Y.F., Tan, K.H., and Lee, S.L. (1991). Tests on R/C continuous beams with openings. *Journal of Structural Engineering, ASCE*, Vol. 117, No. 6, June, pp. 1593-1606.

Mansur, M.A., Tan, K.H., Lee, Y.F., and Lee, S.L. (1991). Piecewise linear behavior of R/C beams with openings. *Journal of Structural Engineering, ASCE*, Vol. 117, No. 6, June, pp. 1607-1621.

Mansur, M.A., Tan, K.H., and Weng, W. (In Press). Effects of creating an opening in existing beams. *ACI Structural Journal.*

Mansur, M.A., Ting, S.K., and Lee, S.L. (1983a). Torsion tests of R/C beams with large openings. *Journal of the Structural Division, ASCE*, Vol. 109, ST8, Aug., pp. 1780-1791.

Mansur, M.A., Ting, S.K., and Lee, S.L. (1983b). Ultimate torque of R/C beams with large openings. *Journal of the Structural Division, ASCE*, Vol. 109, ST8, Aug., pp. 1887-1902.

McMullen, A.E., and Daniel, H.R. (1975). Torsional strength of longitudinally reinforced beams containing an opening. *ACI Journal, Proceedings,* Vol. 72, No. 8, Aug., pp. 415-420.

Merchant, W. (1967). Structural failures: case notes and general comments. *Proceedings of the Institution of Civil Engineers*, London, Vol. 36, Mar., pp. 512-513.

Michell, D., and Collins, M.P. (1976). Detailing for torsion. *ACI Journal, Proceedings* Vol. 73, No. 9, Sept., pp. 506-511.

Nasser, K.W., Acavalas, A., and Daniel, H.R. (1967). Behavior and design of large openings in reinforced concrete beams. *ACI Journal, Proceedings,* Vol. 64, No. 1, Jan., pp. 25-33.

Nielsen, M.P. (1984), *Limit Analysis and Concrete Plasticity.* Prentice-Hall, Inc. USA, 420 pp.

Nilson, A.H. (1997). *Design of concrete structures*. McGraw-Hill, New York (Twelfth Edition), 780 pp.

Prager, W. (1959). *An introduction to plasticity*. Addison-Wesley Publishing Co., Inc., Reading, Massachusetts, pp. 11-14.

Prentzas, E.G. (1968). Behaviour and reinforcement of concrete beams with large rectangular apertures. *Ph.D. Thesis*, University of Sheffield, U.K., Sept., 230 pp.

Ragan, H.S. and Warwaruk, J. (1967). Tee members with large web openings. *PCI Journal*, Vol. 12, No. 4, Aug., pp. 52-65.

Salam, S. A. (1977). Beams with openings under different stress conditions. *Proceedings of 3rd Conference on Our World in Concrete and Structures, CI-Premier*, Singapore, 25-26 Aug., pp. 259-267.

Salam, S.A. and Harrop, J. (1979). Prestressed concrete beams with transverse circular holes. *Journal of the Structural Division, ASCE*, V.105, ST3, Mar., pp. 635-652.

Savage, J.M., Arumugasaamy, P., Tadros, M.K., Einea, A., and Fischer, L. (1994). Precast prestressed concrete double Tees with web openings. *FIP - XIIth International Congress*, Washington, May 29 – June 2, pp. C48-C54.

Savage, J.M., Tadros, M.K., Arumugasaamy, P., and Fischer, L.G. (1996). Behavior and design of double Tees with web openings. *PCI Journal*, Vol. 41, No. 1, Jan.-Feb., pp. 46-61.

Savin, G.N. (1951). *Stress concentration around holes*. Pergamon Press, New York, 1961 (a translation of the Russian original of 1951).

Schlaich, J., Schäfer, K., and Jennewein, M. (1987). Toward a consistent design of structural concrete. *PCI Journal*, Vol. 32, No. 3, May-June, pp. 74-150.

Siao, W.B. and Yap S.F. (1990). Ultimate behaviour of unstrengthened large openings made in existing concrete beams, *Journal of the Institution of Engineers*, Singapore, Vol. 30, No. 3, May/June, pp. 51-57.

Somes, N.F. and Corley, W.G. (1974). Circular openings in webs of continuous beams. *Shear in Reinforced Concrete*, Special Publication SP-42, American Concrete Institute, Detroit, pp. 359-398.

Standards Association of Australia (1974). *SAA concrete structures code*, AS 1480-74. Sydney, 1974, 101 pp.

Tan, K.H. (1982). Ultimate strength of reinforced concrete beams with rectangular openings under bending and shear. *MEng. Thesis*, National University of Singapore, 1982, 163 pp.

Tan, K.H. and Mansur, M.A. (1996). Design procedure for reinforced concrete beams with large web openings. *ACI Structural Journal*, Vol. 93, No. 4, July-Aug., pp. 404-411.

Tan, K.H., Mansur, M.A., and Huang, L.M. (1996). Reinforced concrete T-beams with large web openings in positive and negative moment regions. *ACI Structural Journal*, Vol. 93, No. 3, May-June, pp. 277-289.

Thurlimann, B. (1978). Plastic analysis of reinforced concrete beams. *Plasticity in Reinforced Concrete,* Introductory Report of IABSE COLLOQUIUM COPENHAGEN, pp. 71-90.

Thurlimann, B. (1979). Torsional strength of reinforced and prestressed concrete beams - CEB Approach. *Concrete Design: U.S. and European Practices*, Special Publication SP-59, American Concrete Institute, Detroit, pp. 117-143.

Warwaruk, J. (1974). Behavior of prestressed concrete T-beams with large rectangular web openings. *Shear in Reinforced Concrete*, Special Publication SP-42, American Concrete Institute, Detroit, Vol. 1, pp. 399-423.

Weaver, W., Jr. and Gere, J.M. (1980). *Matrix analysis of framed structures*. 2nd Edition, Van Nostrand Reinhorn, New York, 491 pp.

Weng W. (1998). Concrete beams with small openings under bending and shear. *MEng. Thesis*, National University of Singapore, 1998, 92 pp.

Whitney, C.S. (1940). Plastic theory of RC design. *Proceedings, ASCE*, Vol. 66, No. 12, pp. 1749-1780.

Index

A

Aggregate interlock, 31, 96
Allowable crack widths, 120
Allowable stresses, 195
Analysis:
- collapse load, 136
- elastic, 4, 162
- for bending, 7, 80
- for shear, 28, 94
- for torsion, 40, 135
- linear elastic, 161

Anchorage, 56
Arch action, 28-30
Arch mechanism, 29, 31, 94
Assessment, structural, 61
Axial load, 209

B

Balanced failure, 82
Beam action, 29
Beam, prestressed, 187
Beam-type behavior, 3
Beam-type failure, 52
Bending:
- combined with shear, 12-37, 77
- combined with shear and torsion, 41, 158
- combined with torsion, 50, 152
- lateral, 134, 151, 153
- pure, 4, 71

Bernoulli's hypothesis, 8, 29, 97
B-region, 28, 97

C

Capacity (strength) reduction factor, 18, 53, 57, 106, 211
Centroid, plastic, 84
Chord members:
- compression, 9, 105
- tension, 106, 201

Collapse load (analysis), 86, 136
Collapse (failure) mechanism, 80, 208
Collapse (failure) modes, 82
Compression field, 194
Compression member, 81, 97, 153, 158
Continuous beams, 61, 161, 167, 168
Contraflexure, points of, 78, 134, 187
Concrete:
- direct tensile strength, 195
- effective compressive strength, 30
- in-filled, 61
- plain, 38

Cores (coring), 60-61
Corner reinforcement, 87, 120, 177
Crack control, 6, 22, 119, 151, 177, 191, 205
Crack widths (cracking), 63, 65, 72, 120, 177, 191
Cracking (failure) pattern:
- bending, 7, 74, 78, 79, 127
- shear, 15, 63-64
- torsion, 40, 133

Cracking, types of, 191
Critical (opening) length, 140, 145
Cross-members, 135

D

Deflection (deformation), 66, 84, 124, 168, 177
  bending (flexural), 125, 163
  configuration, 163
  lateral, 134
  prestressed beams, 206
  shear, 125, 206
Design:
  approaches, 16
  considerations, 6
  guidelines, 171, 207
  for serviceability, 177
  for ultimate strength, 100
Detailing:
  prestressed beams, 207
  torsion, 56
Development (transmission) length, 207
Diagonal:
  compression, 12, 32
  cracks, 63
  reinforcement, 20, 22-23, 35, 87
  tension, 12, 19-20
Direct stiffness method, 126, 167
Distribution:
  of shear force, 21, 91, 100, 191, 198-199
  of torsion, 145
Double-T beams, 201
Dowel action, 16, 41
Draping points, 207
D-region, 29, 97
Ducts:
  layout, 1-2

E

Effective compressive strength, 29
Effective length, 164, 173
Effect of opening, 9:
  depth (size), 14, 35, 67, 80, 92, 120, 124, 133, 148, 188
  eccentricity, 80, 92, 120, 124, 133, 149, 188, 191
  length, 80, 92, 120, 124, 131, 133, 147, 188
  location (moment-to-shear ratio), 13-14, 67, 80, 92, 120, 124, 188
Effect of prestressing, 187
Elastic stress, 4
Envelopes, 174
Equilibrium, 8
Equivalent:
  flexural stiffness (rigidity), 164, 173
  shear, 46, 54
  shear stiffness, 164, 173
  moment, 52

F

Fabric (mesh), welded wire, 205
Failure:
  beam-type, 19-20, 51
  frame-type, 19-21, 51, 55
  modes, torsion, 40-46, 132
  primary compression, 54
  shear, 208, 211
  shear-compression, 46, 54, 210
  strut, 208
  tension, 211
Failure mechanism (*see* mechanism)
Failure modes (*see* collapse modes)
Failure pattern (*see* cracking pattern)
Fiber-reinforced polymer, 61
Flexural analysis, 7-10
Flexural:
  cracking, 200
  failure, 7-10
  stiffness (rigidity), 158, 161, 174
  strength, nominal, 9
Flexural strength theory, 7-9
Frame-type failure, 20, 51, 55
Framing action, 198

G

Grid frame, 131
Grout, non-shrink, 61
Guidelines (recommendations) (*see* Design)

H

Hinges, plastic, 78, 82, 100, 134
Holes, 61
Horizontal cracks, 192

I

I-beams, 194
Inclined cracking, 16
Interaction diagram (chart), 81, 105, 106
Interface, flange-web, 192, 199

J

Joist, 13

L

Large openings, 71-211
Lateral shear, 56
Light-weight concrete, 170
Limit analysis, 80, 138
Limit design, 150
Load reversal, 23
Load, service (working), 63, 120, 161, 168, 172, 189, 192
Load stage:
  service, 189, 192, 196
  transfer, 189
  ultimate, 189
Long-term deflection, 184
Lower bound approach (solution), 86, 141

M

Mechanism, failure (collapse), 80, 136, 163, 208
Member stiffness, 166
Mesh (fabric), welded wire, 205
Modulus of elasticity, 173
Modulus of rigidity, 163
Modulus of rupture, 38
Moment:
  magnified, 155
  primary, 200
  secondary, 101, 197, 200
Moment of inertia, 163
Moment redistribution, 161

N

Nodes, 97
Normal stresses, 189

O

Openings:
  circular, 4, 127
  classification, 3
  corners, 3, 207
  multiple, 127, 188
  rectangular, 5
  unreinforced, 78
Opening corner, 207
Opening length:
  critical, 140
  effective, 164, 173

P

Pipes, 1-3
Plastic capacity, 138
Plastic centroid, 84
Plastic flow rule, 83, 138
Plastic hinge method, 100
Plastic hinges (*see* Hinges)
Plasticity truss model, (*see* truss model)
Plates, externally bonded, 63
Posts, 127, 172, 177, 189
Prestressing, 187
Primary compression failure, 54

R

Radius of gyration, 73, 176
Reactions, support, 169
Redistribution, moment (force), 161, 170
Reinforcement:
  diagonal, 20
  effective, 6
  longitudinal, 176
  minimum shear, 19
Reinforcement arrangement (schemes), 15, 33
Repair (strengthening), 61-62, 65, 67

S

Secondary moment (*see* moment)
Service load (*see* load)
Serviceability design, 172, 177
Shear:
  failure, 13, 15
  lateral, 55
  maximum, 19, 22
  size effects, 26, 96
  strength, 13
  vertical, 58
Shear-compression failure (*see* failure)
Shear concentration factor, 23, 121, 177
Shear cracking, 199
Shear force distribution, 91-92
Shear reinforcement, 19, 176
Shear stresses, lateral, 145
Short-term deflection, 184

Size effect, shear, 26, 96
Skew-bending
  failure, 38-40, 134
  theory, 37, 40
Slenderness effect, 73, 75-76, 87, 175
Small openings:
  combined bending and shear, 12
  pure bending, 7-12
  shear, 12-23
  torsion, 51-56
Space-truss model, 37-39
Spacing, stirrup, 19
Spandrel beams, 150
Splitting stresses, 192, 197
Stability, compression chord, 175
Stiffness, 66
  flexural, 163
  matrix, 166
  post-cracking, 67
  shear, 163
Strain compatibility analysis (method), 81, 105
Strength:
  analysis, 9
  shear, 16
  torsion, 135, 140
Strength design, 172
Strength reduction factor (*see* capacity reduction factor)
Strengthening (*see* repair)
Stress concentration, 4, 189
Stress distribution, 4, 188
Stresses:
  bending, 4
  elastic, 4
  principal, 37
  shear, 190
  splitting tensile, 192, 197
  tangential, 4
Structural analysis, 172
Structures:
  statically determinate, 6
  statically indeterminate, 6, 149
Strut-and-tie method (model), 97, 115
St. Venant's concept, 38

T

T-beams, 61, 99, 108, 171, 188, 194
Tension failure, 211
Tension field, 192
Tension chord member (*see* chord member)
Tension member, 81, 97, 153, 158
Throat section, 40
Torsion (torque), 37-61, 131-159
  beam-type failure, 52
  design, 51, 149
  detailing, 56
  failure modes, 37-47
  frame-type failure, 55
  primary compression failure, 54
  pure, 51, 132, 150
  shear-compression mode, 54
Torsional ductility, 150
Torsional shear stress, 38
Torsional web reinforcement, 150
Transfer matrix, 166
Transfer stage, 189
Truss action (mechanism), 29, 32-33, 94
Truss model (method):
  45-degree, 16, 18
  plasticity, 28-37, 80, 94, 115
  space, 37

U

Ultimate strength, 208
  shear, 13, 68
  flexure, 7-12
  torsion, 40
Under-reinforced, 8
Upper bound approach (solution), 85, 138

V

Vertical shearing deformation, 164
Vierendeel truss (panel), 3, 78, 162, 187, 198
Virtual work, 85, 140

W

Web-reinforcement, torsional, 150
Whitney, stress block, 8

Y

Yield condition, 80, 137
Yield surface (plane):
  combination, 83
  piecewise linear, 82